ABSTRACT

Title of dissertation: CODING AND SCHEDULING IN
ENERGY HARVESTING COMMUNICATION SYSTEMS

Omur Ozel, Doctor of Philosophy, 2014

Dissertation directed by: Professor Şennur Ulukuş
Department of Electrical and Computer Engineering

Wireless networks composed of energy harvesting devices will introduce several transformative changes in wireless networking: energy self-sufficient, energy self-sustaining, perpetual operation; and an ability to deploy wireless networks at hard-to-reach places such as remote rural areas, within the structures, and within the human body. Energy harvesting brings new dimensions to the wireless communication problem in the form of intermittency and randomness of available energy. In such systems, the communication mechanisms need to be designed by explicitly accounting for the energy harvesting constraints. In this dissertation, we investigate the effects of intermittency and randomness in the available energy for message transmission in energy harvesting communication systems. We use information theoretic and scheduling theoretic frameworks to determine the fundamental limits of communications with energy harvesting devices.

We first investigate the information theoretic capacity of the single user Gaussian energy harvesting channel. In this problem, an energy harvesting transmitter with an unlimited sized battery communicates with a receiver over the classical

AWGN channel. As energy arrives randomly and can be saved in the battery, codewords must obey cumulative stochastic energy constraints. We show that the capacity of the AWGN channel with such stochastic channel input constraints is equal to the capacity with an average power constraint equal to the average recharge rate. We provide two capacity achieving schemes: save-and-transmit and best-effort-transmit. In the save-and-transmit scheme, the transmitter collects energy in a saving phase of proper duration that guarantees that there will be no energy shortages during the transmission of code symbols. In the best-effort-transmit scheme, the transmission starts right away without an initial saving period, and the transmitter sends a code symbol if there is sufficient energy in the battery, and a zero symbol otherwise. Finally, we consider a system in which the average recharge rate is time-varying in a larger time scale and derive the optimal offline power policy that maximizes the average throughput, by using majorization theory.

Next, we remove the battery from the model to understand the impact of stochasticity in the energy arrival on the communication rate. We consider the single user AWGN channel in the zero energy storage case. We observe that the energy arrival is a channel state and channel state information is available at the transmitter only. We determine the capacity in this case using Shannon strategies. We, then, extend the capacity analysis to an additive Gaussian multiple access channel where multiple users with energy harvesting transmitters of zero energy storage communicate with a single receiver. We investigate the achievable rate region under static and stochastic amplitude constraints on the users' channel inputs. Finally, we consider state amplification in a single user AWGN channel with an

energy harvesting transmitter to analyze the trade-off between the objectives of decoding the message and estimating the energy arrival sequence.

Next, we specialize in the finite battery regime in the energy harvesting channel. We focus on the case of side information available at the receiver side. We determine the capacity of an energy harvesting channel with an energy harvesting transmitter and battery state information available at the receiver side. This is an instance of a finite-state channel and the channel output feedback does not increase the capacity. We state the capacity as maximum directed mutual information from the input to the output and the battery state. We identify sufficient conditions for the channel to have stationary input distributions as optimal distributions. We also derive a single-letter capacity expression for this channel with battery state information at both sides and infinite-sized battery at the transmitter. Then, we determine the capacity when energy arrival side information is available at the receiver side. We first find an n-letter capacity expression and show that the optimal coding is based on only current battery state s_i. We, next, show that the capacity is expressed as maximum directed information between the input and the output and prove that the channel output feedback does not increase the capacity.

Then, we consider security aspects of communication in energy harvesting systems. In particular, we focus on a wiretap channel with an energy harvesting transmitter where a legitimate pair of users wish to establish secure communication in the presence of an eavesdropper in a noisy channel. We characterize the rate-equivocation region of the Gaussian wiretap channel under static and stochastic amplitude constraints. First, we consider the Gaussian wiretap channel with a

static amplitude constraint on the channel input. We prove that the entire rate-equivocation region of the Gaussian wiretap channel with an amplitude constraint is obtained by discrete input distributions with finite support. We also prove the optimality of discrete input distributions in the presence of an additional variance constraint. Next, we consider the Gaussian wiretap channel with an energy harvesting transmitter with zero energy storage. We prove that single-letter Shannon strategies span the entire rate-equivocation region and obtain numerically verifiable necessary and sufficient optimality conditions.

In the remaining parts of this dissertation, we consider optimal transmission scheduling for energy harvesting transmitters. First, we consider the optimization of single user data transmission with an energy harvesting transmitter which has a limited battery capacity, communicating over a wireless fading channel. We consider two objectives: maximizing the throughput by a deadline, and minimizing the transmission completion time of the communication session. We optimize these objectives by controlling the time sequence of transmit powers subject to energy storage capacity and causality constraints. We, first, study optimal offline policies. We introduce a *directional water-filling* algorithm which provides a simple and concise interpretation of the necessary optimality conditions. We show the optimality of the directional water-filling algorithm for the throughput maximization problem. We solve the transmission completion time minimization problem by utilizing its equivalence to its throughput maximization counterpart. Next, we consider online policies. We use dynamic programming to solve for the optimal online policy that maximizes the average number of bits delivered by a deadline under stochastic

fading and energy arrival processes with causal channel state feedback. We also propose near-optimal policies with reduced complexity, and numerically study their performances along with the performances of the offline and online optimal policies.

Then, we consider a broadcast channel with an energy harvesting transmitter with a finite capacity battery and M receivers. We derive the optimal offline transmission policy that minimizes the time by which all of the data packets are delivered to their respective destinations. We obtain structural properties of the optimal transmission policy using a dual problem and determine the optimal total transmit power sequence by a directional water-filling algorithm. We show that there exist $M-1$ cut-off power levels such that each user is allocated the power between two corresponding consecutive cut-off power levels subject to the availability of the allocated total power level. Based on these properties, we propose an iterative algorithm that gives the globally optimal offline policy.

Finally, we consider parallel and fading Gaussian broadcast channels with an energy harvesting transmitter. Under offline knowledge of energy arrival and channel fading variations, we characterize the transmission policies that achieve the boundary of the maximum departure region in a given interval. In the case of parallel broadcast channels, we show that the optimal total transmit power policy that achieves the boundary of the maximum departure region is the same as the optimal policy for the non-fading broadcast channel, which does not depend on the priorities of the users, and therefore is the same as the optimal policy for the non-fading scalar single user channel. The optimal total transmit power can be found by a directional water-filling algorithm while optimal splitting of the power among

the parallel channels is performed in each epoch separately. In the case of fading broadcast channels, the optimal power allocation depends on the priorities of the users. We obtain a modified directional water-filling algorithm for fading broadcast channels to determine the optimal total transmit power allocation policy.

CODING AND SCHEDULING IN ENERGY HARVESTING COMMUNICATION SYSTEMS

by

Omur Ozel

Dissertation submitted to the Faculty of the Graduate School of the
University of Maryland, College Park in partial fulfillment
of the requirements for the degree of
Doctor of Philosophy
2014

Advisory Committee:
Professor Şennur Ulukuş, Chair/Advisor
Professor Anthony Ephremides
Professor Nuno Martins
Professor Prakash Narayan
Professor Radu Balan

To curiosity.

ACKNOWLEDGEMENT

I gratefully thank my advisor Professor Şennur Ulukuş for giving me the opportunity to work together and develop my doctoral dissertation. The past five years I spent doing research under her supervision have been full of learning. Her passion to ask and learn is definitely contagious and it has been very helpful for my research. This dissertation is, indeed, composed of answers to a sequence of curious questions that emanated from our frequent discussions. I have learnt from her not only the skills necessary to do research, but also critical thinking and professional attitude necessary to work as a scientist and engineer. I gratefully thank for her guidance, support, care and advice.

I sincerely thank Professor Aylin Yener for giving me the chance to do research together and hosting me in WCAN Lab. at Penn State several times. These visits and following video conferences proved to yield very productive results. Performing research together with Professor Yener has widened my view and enhanced my professional development in my doctoral studentship. Working on many aspects of energy harvesting communications with Professors Ulukuş and Yener has been a remarkable and rewarding intellectual experience.

I sincerely thank Professors Anthony Ephremides, Nuno Martins, Prakash Narayan and Radu Balan for serving in my dissertation committee and providing valuable feedback on my work. Additionally, I would like to thank all UMD faculty members whose courses I had a chance to attend, including Professor Patrick M. Fitzpatrick, Professor Peter Cramton and Professor Andre Tits. I extend my thanks

to Professor Andre Tits for making it possible for me to teach in the Signals and Systems course as a future faculty fellow. It was an invaluable teaching experience.

Very special thanks to Dr. Jing Yang and Kaya Tutuncuoglu due to our separate and altogether collaborations in many research problems, some of which are covered in this dissertation. I thank Jing and Kaya for their friendliness, collegiality and readiness to discuss the problems. A good portion of what I learned in my doctoral study was through my collaborations with them. I would like to thank Kaya due also to hosting me in Penn State several times. I extend my appreciation to Dr. Ersen Ekrem and Berk Gurakan due to our separate joint works, which enabled me to apply my knowledge on energy harvesting communications to other related scenarios. I also thank Khurram Shahzad for our work together on energy harvesting communications. Additionally, I would like to thank Dr. Pulkit Grover for useful discussions on possible new directions in energy harvesting communications.

I thank all friends; including Dr. Ravi Tandon, Dr. Osman Yagan, Dr. Ersen Ekrem, Dr. Jing Yang, Dr. Beiyu Rong, Dr. Raef Bassily, Dr. Himanshu Tyagi, Dr. Jianwei Xie, Berk Gurakan, Pritam Mukherjee, Praneeth Boda, Ahmed Arafa, Karim Banawan, Abdulrahman Baknina and Yi-Peng Wei for the nice environment we shared in the office and in the campus.

Finally, I pay my sincerest thanks and regards to my parents, my brother and my extended family for caring about my education, supporting me in my decisions and cheering for me in the good times.

Table of Contents

List of Figures

Chapter 1

Introduction

1.1 Overview

Energy harvesting devices offer several significant advantages over conventional grid-powered and non-rechargeable battery-powered devices [1–3]. These advantages include energy self-sufficient, energy self-sustaining operation with lifetimes limited only by the lifetimes of their hardware. Circuits and devices side of engineering has been contributing to the development of energy harvesting devices for decades. However, on the communications, networking and systems side of engineering, the focus has been on energy-aware communication system design, in the form of optimum average-power constrained communications, and energy-efficient networking. Only recently, communications subject to explicit energy harvesting conditions has garnered attention. In this dissertation, we consider the communication problem in energy harvesting systems subject to explicit energy harvesting conditions. We focus on wireless networking applications where nodes, e.g., sensor nodes, can harvest energy from nature through various different sources, such as solar cells, vibration absorption devices, water mills, thermoelectric generators, microbial fuel cells, etc. We use information theory and scheduling theory as the mathematical frameworks to study the communication of these devices.

In energy harvesting communication systems, energy that becomes available

for data transmission can be modeled as an exogenous recharge process and arriving energy can be saved in a battery before consumption. In such a scenario, incremental energy is harvested by the transmitter during the course of data transmission from the exogenous recharge process at random times and in random amounts. In addition, the wireless communication channel fluctuates randomly due to fading. These together lead to a need for designing new transmission strategies that can best take advantage of and adapt to the random energy arrivals as well as channel variations in time. In this dissertation, our main objective is to investigate the implications of stochasticity and intermittency of the available energy for data transmission using information theoretic and scheduling theoretic frameworks. These frameworks yield complementary insights about data transmission with an energy harvesting transmitter.

In information theory, channel capacity has been extensively studied under different constraints on the energy of the channel input symbols. It is well known due to Shannon's original work [4] that the capacity achieving input distribution is Gaussian with variance equal to the power constraint in an average power constrained additive white Gaussian noise (AWGN) channel. Smith [5, 6] considers amplitude constraints in addition to average power constraints and concludes that the capacity achieving input distribution has all the mass distributed over finite number of points on the real line. Moreover, Shamai and Bar-David [7] extend Smith's result to amplitude constrained quadrature Gaussian channel and show that the optimal input distribution is concentrated on a finite number of uniform phase circles within the amplitude constraint.

To the best of our knowledge, information theoretic formulation of communication in energy harvesting systems has not been considered before our work in [8, 9]. In contrast, there have been many motivating works in the networking literature before our work. In [10], Lei *et. al.* address replenishment in one hop transmission. Formulating transmission strategy as a Markov decision process, [10] uses dynamic programming techniques for optimization of the transmission policy under replenishment. In [11], Gatzianas *et. al.* extend classical wireless network scheduling results to a network with users having rechargeable batteries. Each battery is considered as an energy queue, and data and energy queues are simultaneously updated where interaction of these queues are determined by a rate versus power relationship. Stability of data queues is studied using Lyapunov techniques. A back pressure algorithm is proposed that takes both data and energy queues into consideration and it is shown to achieve the stability region of the average power constrained system as the battery capacity goes to infinity. In [12, 13], in a similar energy harvesting setting, a dynamic power management policy is proposed and is shown to stabilize the data queues. In each frame, energy spent is equal to the average recharge rate. Moreover, under a linear approximation, some delay-optimal schemes are proposed. In [14, 15], optimal packet scheduling that minimizes the transmission completion time has been derived. Additionally, an earlier line of research considered the problem of energy management in communications satellites [16, 17].

Motivated by the works in the networking literature, we first consider the information theoretic capacity of a single user AWGN channel with an energy harvesting transmitter and an unlimited energy storage. The input dependence and memory

due to the battery and the stochasticity in the energy arrivals require a major shift in terms of the power constraint imposed on the channel input compared to those in the existing literature. We investigate the impact of stochastic energy arrivals on reliable communication rates. In particular, we augment an energy buffer with unlimited energy storage to the classical AWGN channel and determine the information theoretically achievable rates.

Next, we remove the battery from the model to understand the impact of stochasticity in the energy arrival only on the communication rates. We study the channel capacity of the single user AWGN channel in the zero energy storage case. We observe that the available energy in this case could be treated as a channel state where channel state information is available at the transmitter only. This enables us to characterize the capacity using Shannon strategies [18]. We, then, extend the capacity analysis with zero energy storage to an additive Gaussian multiple access channel where multiple users communicate with a single receiver. We investigate the achievable rate region under static and stochastic amplitude constraints on the users' channel inputs. Finally, we consider state amplification [19, 20] in a single user AWGN channel with energy harvesting transmitters. In a state-dependent channel, the objective of decoding the message conflicts with the objective of estimating the realizations of the state sequence. Characterization of this trade-off in an energy harvesting communication system provides an understanding of the value of energy as a state.

In accordance with the view of energy as a state of the channel, we next consider the scenario when side information is available at the receiver and we specialize

in the finite battery case in a single user channel. In particular, our treatment hinges on the view of the energy level in the battery or the energy arrival as the state of the channel. In practice, battery energy level and energy arrival could be partially or fully available at the receiver side in scenarios where the energy source of the circuits of the transmitter and the receiver share an electrical connection or have strong dependence. We first provide an overview of achievable rates with no side information at the receiver. Then, we derive capacities when battery state information and energy arrival information are available at the receiver as side information.

Next, we consider security aspects of communication in energy harvesting systems. In particular, we focus on a wiretap channel with an energy harvesting transmitter. In a wiretap channel, a legitimate pair of users wish to establish secure communication in the presence of an eavesdropper in a noisy channel [21]. In general, there is a trade-off between the rate of the message and the equivocation of the message at the eavesdropper and it is characterized by the rate-equivocation region. The rate-equivocation region for the Gaussian wiretap channel was characterized in [22] under an average power constraint for the channel input. We characterize the rate-equivocation region of the Gaussian wiretap channel under static and stochastic amplitude constraints, which are typical characteristics of energy harvesting communications systems.

In the remaining parts of the dissertation, we consider optimal transmission scheduling for energy harvesting transmitters. Assuming transmission epochs sufficiently long to achieve information theoretically possible rates and rate regions, we obtain optimal transmission schemes in single user and multi-user scenarios. Build-

ing on the works in [14, 15, 23], we start with the optimal transmission scheduling problem over the fading channel. We solve for the optimal throughput over a finite horizon and minimum transmission completion time when fading and energy arrival information are available at the transmitter a priori. Then, we build on [24] and analyze transmission completion time minimization problem over an M-user AWGN broadcast channel when the transmitter has finite battery. We finally extend the solution of the optimal transmission scheduling problem to parallel and fading Gaussian broadcast channels. In each channel model, we obtain structural properties of the optimal transmission schemes and provide algorithmic solutions.

1.2 Outline

In Chapter 2, we consider the setting where energy arrives at the transmitter as a discrete-time stochastic process, and unused energy is saved in a battery of unlimited size [8, 9]. The energy arrival (or recharge) process has the same discrete time index as the channel use. The problem is posed as the design of a codebook that complies with instantaneous energy constraints at each channel use. The channel input in each channel use is constrained by the amount of energy in the battery, which evolves stochastically throughout the communication. The recharge process together with the past code symbols determine the allowable range of inputs in each channel use. We show that the capacity is equal to the capacity of the AWGN channel with an average power constraint equal to the average recharge rate. Therefore, a large battery can smooth out the uncertainties in the transmission energy without need to

design complicated codes to alleviate the uncertainty about the energy. This result extends to the capacity regions of multiple access, broadcast, interference, relay and wiretap channels with energy harvesting users having unlimited batteries [8, 9].

We start by showing that the capacity of the AWGN channel with an average power constraint equal to the average recharge rate is an upper bound for the capacity in the energy harvesting system. Then, we develop the *save-and-transmit* scheme that achieves this upper bound and hence the capacity. In the *save-and-transmit* scheme, zero code symbols are sent in a portion of the total block length, which becomes negligible as the block length gets large. The goal of this portion of the total block length where no signal is transmitted is to *save* energy to ensure that there will always be sufficient amount of energy to transmit the remaining code symbols, with probability approaching one. Next, we provide an alternative capacity achieving scheme termed the *best-effort-transmit* scheme. In this scheme, whenever available energy in the battery is sufficient to send the code symbol, it is put to the channel, while a zero symbol is put to the channel if there is not enough energy in the battery. This leads to a mismatch between the encoder and the decoder in the sense that some of the code symbols in the codeword are replaced with zeros. However, we show that the mismatch can be made negligible, and therefore this scheme can achieve rates arbitrarily close to the capacity.

In Chapter 3, we consider the same energy harvesting communication setting with zero energy storage at the transmitter [25]. Hence, the code symbol energy in a channel use is constrained to the energy arrived in that channel use. Arriving energy is known by the transmitter causally, right before the code symbol is decided.

Therefore, the code sequence is a function of the observed energy arrival. This is an instance of a state-dependent channel with an i.i.d. state process and causal state information at the transmitter. In this context, we investigate the role of energy arrival as a channel state in different channel models and using different objectives. The channel capacity can be found as the capacity of an extended input channel obtained by applying Shannon strategy [18]. The extended input is a collection of inputs designed for each possible energy arrival. Each component of the extended input is constrained in energy by the specific amount of energy arrival. This is a generalization of the amplitude constrained Gaussian channel in Smith's work [5, 6] where the capacity achieving input distribution is proved to be discrete with finite support. In general, it is challenging to extend Smith's result to the case of multi dimensional inputs [26]. We derive necessary and sufficient optimality conditions for the input distribution in the extended input channel, parallel to [5, 6, 26]. These conditions enable numerically verifiable conditions for the optimality of an input distribution. Even though we could not provide a mathematical proof, our numerical results show that the capacity achieving input distribution has finite support in the extended input channel.

Next, we address the achievable rate region of the Gaussian multiple access channel (MAC) with energy harvesting transmitters in the zero energy storage regime. We first consider the static amplitude constrained Gaussian MAC. We use the single-letter characterization of the MAC to prove that the boundary of the capacity region is achieved by discrete input distributions when the amplitude constraints are static [27]. This result extends Smith's result to the Gaussian MAC.

Then, we consider stochastic amplitude constraints on the inputs of the users. A capacity characterization for the state-dependent MAC is not available in the literature; however, Shannon strategies provide an achievable rate region. We study optimal Shannon strategies and numerically study necessary optimality conditions in the MAC setting [27]. Our numerical studies indicate that optimal distributions are discrete distributions with finite support.

Then, we consider state amplification in single user energy harvesting communication systems [28]. In many energy harvesting sensor applications, the receiver may aim at *extracting energy state information* from the received signal as well as *decoding the message*. We explore the interaction of these two objectives by studying the state amplification problem in the zero battery and infinite battery cases. In this problem, encoder performs the encoding to convey the information of the energy arrival and the message simultaneously. The receiver aims to list decode the sequence of energy arrivals from the signal it receives. Our goal is to characterize the trade-off between these two objectives. This trade-off is characterized by determining the region of rate versus entropy reduction. In the zero battery case, Shannon strategies achieve the boundary of this region due to [20]. We determine numerically verifiable necessary and sufficient conditions for optimal Shannon strategies over the AWGN channel. Additionally, we determine the exact characterization of this region when the transmitter has unlimited energy storage. Using a combination of block Markov encoding and best-effort-transmit scheme, we find that the boundary of the trade-off region is simply a line in the unlimited energy storage case.

In Chapter 4, we consider energy harvesting communication systems with

finite-sized batteries. As an initial step, we provide an overview of approaches for the finite battery case that were presented in [29–31]. Next, we propose a timing based achievable scheme similar to that in [30–32] for a noiseless channel with $E_{max} > 1$. We provide a simulation-based method to evaluate the achievable rates using [33]. Then, we focus on the case of side information available at the receiver side [34, 35]. We determine the capacity of an energy harvesting channel with an energy harvesting transmitter and battery state information available at the transmitter and receiver sides [34]. This is an instance of a finite-state channel and the channel output feedback does not increase the capacity. We state the capacity as maximum directed mutual information from the input to the output and the battery state. We identify sufficient conditions for the channel to have stationary input distributions as optimal distributions. We also derive a single-letter capacity expression for this channel with battery state information at both sides and infinite-sized battery at the transmitter. Then, we determine the capacity of an energy harvesting channel with an energy harvesting transmitter and energy arrival side information available at the transmitter and receiver sides [35]. We first find an n-letter capacity expression and show that the optimal coding is based on only current battery state s_i. Next, we show that the capacity is expressed as maximum directed information between the input and the output. Moreover, we prove that the channel output feedback does not increase the capacity.

In Chapter 5, we focus on the security aspects of energy harvesting communications. First, we consider the Gaussian wiretap channel with a static amplitude constraint on the channel input [36]. We show that the entire rate-equivocation

region of the Gaussian wiretap channel with an amplitude constraint is obtained by discrete input distributions with finite support. We prove this result by considering the existing single-letter description of the rate-equivocation region, and showing that discrete distributions with finite support exhaust this region. Our result highlights an important difference between the peak power (amplitude) constrained and the average power (variance) constrained cases: Although, in the average power constrained case, both the secrecy capacity and the capacity can be achieved simultaneously [22], our results show that in the peak power constrained case, in general, there is a trade-off between the secrecy capacity and the capacity, in the sense that, both may not be achieved simultaneously. We also show that under sufficiently small amplitude constraints the possible trade-off between the secrecy capacity and the capacity does not exist and they are both achieved by the symmetric binary distribution. Finally, we prove the optimality of discrete input distributions in the presence of an additional variance constraint [37].

Next, we investigate the role of stochastic energy arrivals in secure communications context by considering the Gaussian wiretap channel with an energy harvesting transmitter of zero energy storage [38]. In this case, the code symbols are subject to stochastic amplitude constraints which are observed by the transmitter causally. Viewing the available energy at the transmitter as a channel state, the setting becomes a state-dependent wiretap channel with causal state information at the transmitter only. We first prove that single-letter Shannon strategies span the entire rate-equivocation region. Then, we find the boundary of the rate-equivocation region by optimizing over single-letter Shannon strategies. However,

corresponding optimization problems are challenging to solve explicitly: The links of the constructed wiretap channel are not additive noise channels and the inputs are amplitude constrained. We determine numerically verifiable necessary and sufficient optimality conditions. Our numerical results show that optimal input distributions are discrete with finite support.

In the remaining parts of this dissertation, we consider optimal transmission scheduling for energy harvesting transmitters. In Chapter 6, we obtain optimal transmission policies to maximize the throughput and minimize the transmission completion time, under channel fluctuations and energy variations [39]. In particular, we consider two related optimization problems. The first problem is the maximization of the number of bits (or throughput) transmitted by a deadline T. The second problem is the minimization of the time (or delay) by which the transmission of B bits is completed. We solve the first problem under deterministic (offline) [40] and stochastic (online) [41] settings, and we solve the second problem in the deterministic setting. We start by considering the first problem in a static channel under offline knowledge. The solution calls for a new algorithm, termed *directional water-filling*. Taking into account the causality constraints on the energy usage, i.e., the energy can be saved and used in the future, the algorithm allows energy flow only to the right. In the algorithmic implementation of the solution, we utilize *right permeable taps* at each energy arrival point. This solution serves as a building block for the fading case. Specifically, we show that a directional water-filling algorithm that adapts to both energy arrivals and channel fade levels is optimal. Next, we consider the second problem, i.e., the minimization of the time by

which transmission of B bits is completed. We use the solution of the first problem to solve this second problem. This is accomplished by mapping the first problem to the second problem by means of the *maximum departure curve*. This completes the identification of the optimal offline policies in the fading channel. Next, we consider the online problem. We address online scheduling for maximum throughput by the deadline T in a setting where fading level changes and energy arrives as random processes in time. Assuming statistical knowledge and causal information of the energy and fading variations, we solve for the optimal online power policy by using dynamic programming [42, 43]. To address the high complexity required by the dynamic programming solution, we propose simple online algorithms that perform near-optimal.

In Chapter 7, we consider a broadcast channel with an energy harvesting transmitter with a *finite capacity battery* and M receivers [44]. It was shown previously in [24] that, under the assumption of an infinite-sized battery, the time sequence of the optimal total power in a broadcast channel increases monotonically as in the single user case in [14, 15]. Moreover, it was shown that there exists a *cut-off* power level for the power shares of the strong and weak users; strong user's power share is always less than or equal to this cut-off level and when it is strictly less than this cut-off level, weak user's power share is zero. The structure of the optimal policy in [24] is contingent upon the availability of an infinite capacity battery. Therefore, the added challenge in the finite capacity battery case is to accommodate every bit of the incoming energy by carefully managing the transmission power and users' power shares according to the times and amounts of the harvested energy. We find that

in the finite battery regime as well, the determination of the total transmit power can be separated from the determination of the shares of the users without losing optimality. We first obtain the structural properties of the optimal policy by means of a dual problem, namely, the maximization of the region of bits served for the receivers by a fixed time T, i.e., the *maximum departure region.* We show that, similar to the battery unlimited case, we have a *cut-off* property in the optimal power shares. However, different from the battery unlimited case, the transmit power is not monotonically increasing. The solution method in [24] uses the rate domain. However, when there is a battery capacity constraint, the resulting no-energy-overflow constraint gives a non-convex constraint for the optimization problem in the rate domain. Therefore, we formulate the problem in the power domain in this chapter. We show that the total power in each epoch must be the same as the total power in the single user channel, which, in turn, can be found by the directional water-filling algorithm developed in Chapter 6. We then find the optimal shares of the users from the total power in closed form via a single-variable optimization problem, completing the characterization of the optimal solution of the dual problem. We then use the structure of this dual problem, in particular the cut-off property and the optimality of directional water-filling to solve the transmission completion time minimization problem.

In Chapter 8, we extend the transmission scheduling problem with an energy harvesting transmitter to parallel and fading AWGN broadcast channels [45]. In particular, we consider an energy harvesting transmitter that sends data to two receivers over parallel and fading broadcast channels. Arriving energy is stored in

a finite-sized battery. Data to be sent to the receivers are assumed to be available at the data buffers before the transmission starts. As the users utilize the common resources, which are the harvested energy and the wireless communication medium, there is a trade-off between the performances of the users. We characterize this trade-off by obtaining the maximum departure region by a deadline T and determine the optimal offline policies that achieve the boundary of the maximum departure region. Although power allocation problem in traditional systems with non-rechargeable batteries subject to average power constraints in parallel and fading broadcast channels are solved using identical techniques, offline scheduling with rechargeable batteries in these two channel models are considerably different. We first consider offline scheduling for energy harvesting transmitters over parallel broadcast channels [46]. We show that the optimal total transmit power policy that achieves the boundary of the maximum departure region is the same as the optimal policy for the non-fading scalar broadcast channel, which does not depend on the priorities of the users, and therefore is the same as the optimal policy for the non-fading scalar single user channel. The power is split to each parallel channel separately in each epoch. We then consider offline scheduling for energy harvesting transmitters over fading broadcast channels [47]. We show that in the optimal policy that achieves the boundary of the maximum departure region, energy allocation in each epoch is determined by a directional water-filling algorithm that is specific to the fading broadcast channel. In particular, water level in between two energy arrivals is calculated by using the water-filling scheme described in [48] or the greedy power allocation in [49]. If the water level is higher on the right, no energy

is transferred; otherwise some energy is transferred to the future. Unlike the case of parallel broadcast channels, in the case of fading broadcast channels, the total transmit power policies achieving different points on the boundary of the maximum departure region depend on the priorities of the users.

In Chapter 9, we provide conclusions of this dissertation.

Chapter 2

The Gaussian Energy Harvesting Channel with Unlimited Energy Storage

2.1 Introduction

In this chapter, we consider the information theoretic capacity of the AWGN channel with an energy harvesting transmitter that has unlimited energy storage. Energy arrives at the transmitter as a discrete-time stochastic process, and unused energy is saved in a battery of unlimited size. The energy arrival (or recharge) process has the same discrete time index as the channel use. Therefore, the energy in the battery is updated as follows: First, it is increased by the energy arrival and then it is decreased by the energy of the transmitted code symbol. The problem is posed as the design of a codebook that complies with instantaneous energy constraints at each channel use. The channel input in each channel use is constrained by the amount of energy in the battery, which evolves stochastically throughout the communication. Therefore, this model generalizes classical deterministic amplitude constraint on the channel input. The recharge process together with the past code symbols determine the allowable range of inputs in each channel use.

We prove that the capacity of the Gaussian energy harvesting channel with unlimited energy storage is equal to the capacity with an average power constraint

equal to average recharge rate. We start by showing that the capacity of the AWGN channel with an average power constraint equal to the average recharge rate is an upper bound for the capacity in the energy harvesting system. Then, we develop the *save-and-transmit* scheme that achieves this upper bound and hence the capacity. In the *save-and-transmit* scheme, zero code symbols are sent in a portion of the total block length, which becomes negligible as the block length gets large. The goal of this portion of the total block length where no signal is transmitted is to *save* energy to ensure that there will always be sufficient amount of energy to transmit the remaining code symbols, with probability approaching one. Next, we provide an alternative capacity achieving scheme termed the *best-effort-transmit* scheme. In this scheme, whenever available energy in the battery is sufficient to send the code symbol, it is put to the channel, while a zero symbol is put to the channel if there is not enough energy in the battery. This leads to a mismatch between the encoder and the decoder in the sense that some of the code symbols in the codeword are replaced with zeros. However, we show that the mismatch can be made negligible, and therefore this scheme can achieve rates arbitrarily close to the capacity.

We note that after the publication of our results in [8, 9, 25], another paper appeared [50] which reported similar results.

2.2 The Capacity with Unlimited Energy Storage

System model is a scalar AWGN channel characterized by the input X, output Y, additive noise N with unit normal distribution $\mathcal{N}(0,1)$ and a battery (see Figure

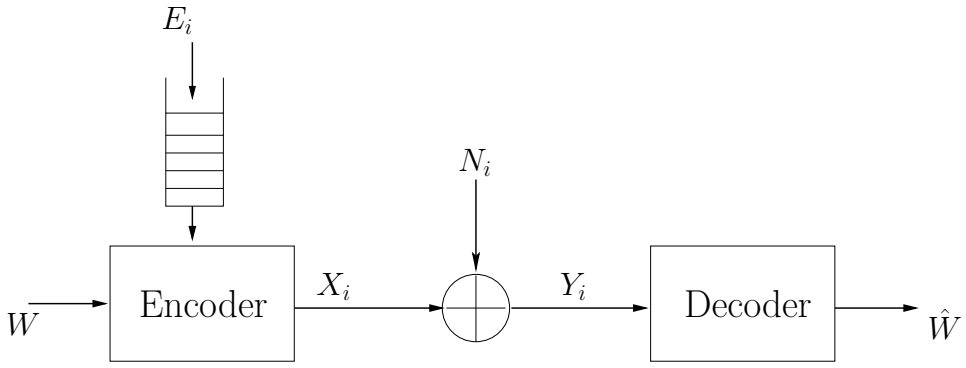

Figure 2.1: AWGN channel with an energy harvesting transmitter.

2.1). Input and output alphabets are taken as real numbers. Energy enters the system from a power source that supplies E_i units of energy in the ith channel use where $E_i \geq 0$. $E_1, \ldots, E_n$ is the time sequence of supplied energy in n channel uses. E_i is an i.i.d. sequence with average value P, i.e., $E[E_i] = P$, for all i.

E_{max} units of energy can be stored in the battery and the existing energy in the battery can be retrieved without any loss. For convenience, we assume that the energy stored and depleted from the battery are for only communication purposes (e.g., we do not consider the energy required for processing). Moreover, our focus here is on the case where $E_{max} = \infty$ and hence energy overflow does not occur and incoming energy can always be saved in the battery. This assumption is especially valid for the current technology in which batteries have very large energy storage capacities compared to the rate of harvested energy flow: $E_{max} \gg P$. The battery is initially empty and energy needed for communication of a message is obtained from the arriving energy during the transmission of the corresponding codeword subject to causality. In particular, E_i units of energy is added to the battery and X_i^2 units of energy is depleted from the battery in the ith channel use. This is illustrated in

Figure 2.2.

This brings us to the following cumulative power constraints on the channel inputs based on the causality of energy usage:

$$\sum_{i=1}^{k} X_i^2 \leq \sum_{i=1}^{k} E_i, \qquad k = 1, \ldots, n \tag{2.1}$$

Note that the constraints in (2.1) are upon the support set of the random variables X_i. The first constraint restricts the support set of X_1 to $[-\sqrt{E_1}, \sqrt{E_1}]$. The second constraint is $X_1^2 + X_2^2 \leq E_1 + E_2$. In general, letting S_i denote $[\sum_{j=1}^{i-1}(E_j - X_j^2)]^+$, in channel use i, the symbol X_i is subject to the constraint $X_i^2 \leq E_i + S_i$.

The input constraints in (2.1) introduce memory (in time) in the channel inputs. Randomness in E_i makes the problem similar to fading channels in that the state of recharge process (i.e., low or high E_i) affects instantaneous quality of communication. Moreover, this time variation in the recharge process allows opportunistic control of transmit energy as in fading channels. However, recharged energy can be saved in the battery for future use unlike a fading state. In fact, we will see that, this nature of energy arrivals renders saving energy in the battery more advantageous for later use when a peak occurs in the recharge process, as opposed to opportunistically *riding* the peaks.

Codebook $\mathcal{C}^n = (n, 2^{nR_n}, \epsilon_n)$ is defined by the code length n, the code size 2^{nR_n} and the probability of error ϵ_n. The messages in the set $\{1, \ldots, 2^{nR_n}\}$ are equally likely. Encoding function is $f_k^n : \{1, \ldots, 2^{nR_n}\} \to \mathcal{X}$, $k = 1, \ldots, n$ and the decoding function is $\phi^n : \mathcal{Y}^n \to \{1, \ldots, 2^{nR_n}\}$. Here, encoding and decoding are

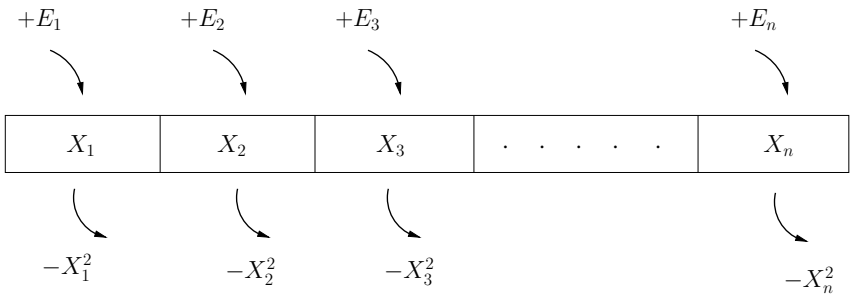

Figure 2.2: Illustration of the battery dynamics of the transmitter.

performed independent of energy information. In fact, energy information at the encoder/decoder does not improve the capacity as will be apparent in the following sections. There are two separate causes of error. The first one is that a codeword does not satisfy the input constraints at a particular channel use. In this case, the transmitter experiences an energy shortage to transmit the codeword and this event is counted as an error event. The second cause of error is the decoding error at the receiver. If the received signal is decoded to a message that is different from the message sent, then an error occurs. Accordingly, the error event is defined as the union of two events: $\varepsilon^n = \varepsilon_1^n \cup \varepsilon_2^n$ where ε_1^n is the energy shortage event, and ε_2^n is the decoding error event. The overall probability of error is $\epsilon_n = \Pr(\varepsilon^n)$.

2.2.1 Main Result

We will invoke the general capacity formula of Verdu and Han [51]. For fixed n, let F^n be the joint cumulative distribution function of the random variables $\{X_i\}_{i=1}^n$ and let $\mathcal{F}^n$ be the set of n variable joint cumulative distribution functions that satisfy the constraints in (2.1). Since the AWGN channel is an information-stable

channel [51], the capacity of the channel in Figure 2.1 with constraints in (2.1) is:

$$C = \lim_{n\to\infty} \max_{F^n \in \mathcal{F}^n} \frac{1}{n} I(X^n; Y^n) \tag{2.2}$$

In general, for an AWGN channel, the capacity achieving input distribution is in the form of a product of marginal distributions (independent distribution) [51]. However, note that the power constraints in our problem create dependence among the random variables. The constraint on X_{i+1} is dependent on the given values of X_j, $j \leq i$. Though in a classical AWGN channel independent processes achieve higher mutual information than the ones with the same marginal distribution but with correlation [51], the capacity that we seek in this problem does not let the process be independent. This problem falls in the family of problems of finding capacity under dependence constraints on code symbols which is by itself interesting and less studied.

An upper bound for C is the corresponding AWGN capacity with average power constrained to average recharge rate P, as $\frac{1}{n}\sum_{i=1}^{n} X_i^2 \leq \frac{1}{n}\sum_{i=1}^{n} E_i$ and by the i.i.d. nature of E_i, invoking the strong law of large numbers [52], $\frac{1}{n}\sum_{i=1}^{n} E_i \to P$ with probability one. Therefore, each codeword satisfying the constraints in (2.1) automatically satisfies $\lim_{n\to\infty} \frac{1}{n}\sum_{i=1}^{n} X_i^2 \leq P$ with probability one. However, the reverse is not true. If a codeword satisfies the average power constraint, it does not necessarily satisfy the constraints in (2.1). Hence, the channel capacity under the energy constraints in (2.1) is bounded by the following for almost all realizations of

the energy arrival process:

$$C \leq \frac{1}{2}\log\left(1+P\right) \tag{2.3}$$

Our main result in this chapter is that the upper bound in (2.3) can be achieved, as stated in the following theorem.

Theorem 2.1 *The capacity of an AWGN channel with channel inputs constrained by i.i.d. energy arrival sequence* $\{E_i\}_{i=1}^{\infty}$*,* $E[E_i] = P$ *and an infinite-sized battery is equal to the classical AWGN capacity with average power constraint* P

$$C = \frac{1}{2}\log\left(1+P\right) \tag{2.4}$$

In the next two sections, we develop two different achievability schemes that achieve the capacity given in Theorem 2.1.

2.2.2 Save-and-Transmit Scheme

While designing the codebook and the encoding/decoding rule, a first approach could be to optimize the codebook design subject to the input constraints in (2.1) so that the occurrence of the error event ε_1^n is eliminated from the beginning. Instead, we propose a scheme that implements a *save-and-transmit* principle which averages out the randomness in energy arrivals first, and then performs channel coding to counter errors due to the randomness in the channel.

In the save-and-transmit scheme, data transmission is performed in two phases: first the saving phase where the battery is fueled with energy and then the trans-

mission phase where information carrying code symbols are sent. Therefore, we will consider the sequence of codes with code length n such that the first $h(n) \in o(n)$ symbols of each codeword are zero and the remaining $n - h(n)$ code symbols are the information carrying symbols, where $o(n)$ denotes the class of functions that scale slower than n. We particularly consider $h(n) \in o(n)$ such that $h(n) \to \infty$ and $n - h(n) \to \infty$ as $n \to \infty$. The reason for considering $o(n)$ functions for the saving period is to allow sufficient number of channel uses for the data transmission period so that no loss is incurred in achievable rates.

In the first $h(n)$ symbols, no energy is spent for communication and battery energy is increased. In the remaining $n - h(n)$ channel uses, information carrying symbols which are chosen as independent random variables from the (capacity achieving) Gaussian distribution with mean zero and variance P_{avg} are transmitted. That is, for $k = 1, \ldots, h(n)$, we have $f_k^n(m) = 0$ for all $m \in \{1, \ldots, 2^{nR_n}\}$. For $k = h(n) + 1, \ldots, n$, $f_k^n(m)$ is selected as independent samples of a zero-mean and variance P_{avg} Gaussian random variable for all $m \in \{1, 2, \ldots, 2^{nR_n}\}$.

We note that save-and-transmit scheme does not use any information of the recharge process $\{E_i\}_{i=1}^{\infty}$. Irrespective of the realization of $\{E_i\}_{i=1}^{\infty}$, we introduce $h(n) \in o(n)$ amount of delay to save energy and then transmit with average power $P_{avg} < P$. We aim to prove that there exists $h(n) \in o(n)$, that can guarantee sufficient energy savings to prevent any energy shortages in the transmission phase, which, in turn, implies that the energy shortage probability $\varepsilon_1^{(n)}$ and probability of decoding error $\varepsilon_2^{(n)}$ both go to zero and rates arbitrarily close to the upper bound in (2.3) are achieved.

For $h(n) \to \infty$, by the strong law of large numbers, at time index $h(n)$, about $h(n)P$ amount of energy is saved in the battery with high probability. We argue that if $P_{avg} < P$, in the remaining $n - h(n)$ channel uses, this saved energy together with energy entering the system is sufficient to provide the energy needed for data transmission (see Figure 2.3). We will formalize this argument in the following lemma.

Lemma 2.1 *Assume $h(n) \in o(n)$ with $\lim_{n\to\infty} h(n) = \infty$. The save-and-transmit scheme satisfies the input constraints in (2.1) with probability arbitrarily close to one provided that $P_{avg} < P$.*

A proof of Lemma 2.1 is provided in Appendix 2.5.2. Lemma 2.1 says that in the save-and-transmit scheme if $P_{avg} < P$, a saving period $h(n) \in o(n)$ with $h(n) \to \infty$ is sufficient to collect an initial amount of energy to prevent energy shortages during the transmission phase. The proof requires an application of the strong law of large numbers along with the tail behavior of sums of i.i.d. random variables. For instance, we can select $h(n) = \log(n)$ as $\log(n) \in o(n)$ and $\log(n) \to \infty$ and by Lemma 2.1, it is guaranteed that the probability of any energy shortages goes to zero. The achievable rate for this scheme with decoding error approaching zero is [51]

$$\lim_{n\to\infty} \frac{1}{n} I(\mathbf{X}^n; \mathbf{Y}^n) = \lim_{n\to\infty} \frac{1}{n} \sum_{j=h(n)+1}^{n} I(X_j; Y_j) \tag{2.5}$$

$$= \lim_{n\to\infty} \frac{n - h(n)}{2n} \log\left(1 + P_{avg}\right) \tag{2.6}$$

$$= \frac{1}{2} \log\left(1 + P_{avg}\right) \tag{2.7}$$

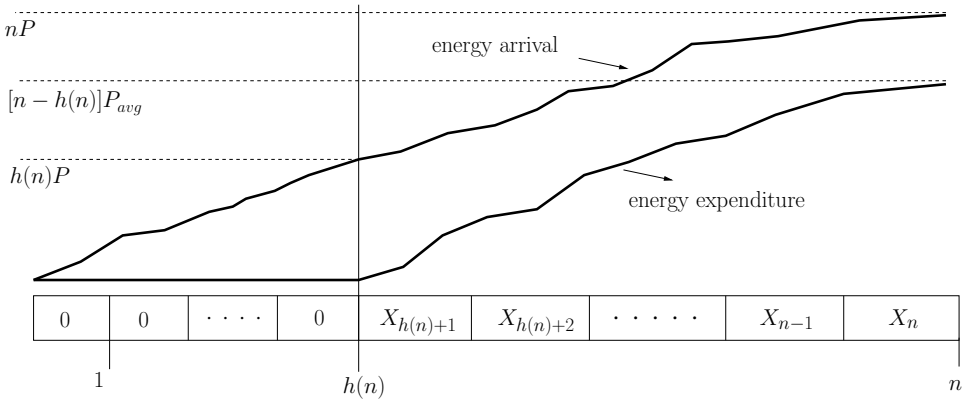

Figure 2.3: Illustration of the save-and-transmit scheme.

Since $\log(.)$ is continuous, $R < \frac{1}{2}\log(1+P)$ can be achieved by choosing $P_{avg} = P-\epsilon$ and therefore the capacity in Theorem 2.1 is achievable by the save-and-transmit scheme.

Using the advantage of having a battery to buffer energy, the save-and-transmit scheme first eliminates the uncertainty in the energy arrivals, and then copes with the uncertainty in the channel by means of appropriate channel coding. The actual data transmission starts with an $o(n)$ delay and the capacity with average power constrained to the average recharge rate can be achieved.

2.2.2.1 The Case of $P_{avg} = P$

We have seen that the save-and-transmit scheme can achieve rates arbitrarily close to the capacity by saving energy in the first $h(n) \in o(n)$ channel uses and then transmitting with zero-mean Gaussian distributed codewords of power $P-\epsilon$. Although this scheme proves the desired capacity result, in this section we consider the case of $P_{avg} = P$. This is a technically challenging case where the average energy entering

the battery is exactly the same as the average energy exiting the battery. We will establish that the capacity could be achieved with the save-and-transmit scheme even when $P_{avg} = P$. However, we have to modify the scheme and the assumptions on the statistics of energy arrivals. In particular, in this case, the saving period $h(n) = \log(n)$ is not sufficient to guarantee that the energy constraints are satisfied with probability one. That is, the hypothesis in Lemma 2.1 should be refined for this particular case. To see this, assume that $P_{avg} = P$ and consider $h(n) = \sqrt{n}$. Note that $\sqrt{n} = \omega(\log(n))$ where $\omega(\log(n))$ denotes the class of functions f such that for all $k \geq 0$ there exists sufficiently large n that satisfies $f(n) > k \log(n)$. In this case, as shown in Appendix 2.5.3, we have

$$\lim_{n\to\infty} \Pr\left(\sum_{i=1}^{n} X_i^2 > \sum_{i=1}^{n} E_i\right) = \Phi\left(\frac{P}{a}\right) \tag{2.8}$$

where, assuming that E_i has a finite-variance σ_E^2, a is given as $a^2 \triangleq \sigma_E^2 + 2P^2$ (see Appendix 2.5.3), and $\Phi(x)$ is the cumulative distribution function of a unit normal random variable, i.e., $\Phi(x) = \int_x^\infty \frac{1}{\sqrt{2\pi}} e^{-\frac{\tau^2}{2}} d\tau$. Hence, if $h(n) = \sqrt{n}$, energy shortages occur with a non-zero probability. In fact, with $h(n) = \log(n)$, as also shown in Appendix 2.5.3,

$$\lim_{n\to\infty} \Pr\left(\sum_{i=1}^{n} X_i^2 > \sum_{i=1}^{n} E_i\right) = \Phi(0) = \frac{1}{2} \tag{2.9}$$

and hence energy shortages occur with probability higher than $\frac{1}{2}$ when $h(n) = \log(n)$. After these pessimistic results, it is of question whether we can find $h(n) \in$

$o(n)$ that guarantees that no energy shortages occur in the $P_{avg} = P$ case. Clearly, such $h(n)$ must scale at least as fast as $\sqrt{n}$.

We are able to find a family of $h(n) \in o(n)$ under some mild regulatory assumptions on the probability distribution of the energy arrivals, as stated in the following lemma.

Lemma 2.2 *Suppose that E_i, the energy arrival random variable, satisfies $E[e^{E_i^\gamma}] < \infty$ for some $0 < \gamma < 1$. Then, the save-and-transmit scheme satisfies the constraints in (2.1) with probability arbitrarily close to one for $h(n) = n^{\frac{1}{\alpha}}(\log(n))^{\frac{1}{\gamma}}$, where $1 < \alpha \leq 2$.*

A proof of Lemma 2.2 is provided in Appendix 2.5.4. It is based on a recent strong law for sums of i.i.d. random variables that is originally proved in [53] and the fact that $E[e^{|X_i|^{2\gamma}}] < \infty$ for the Gaussian distributed X_i in the assumed range of γ. Lemma 2.2 says that under mild conditions on the energy harvesting process E_i, there exists $h(n)$ that scales faster than $\sqrt{n}\log(n)$ such that we can save sufficient amount of initial energy in the saving phase to guarantee that there will be no energy shortages during the transmission phase even when the average energy exiting the system P_{avg} (codebook power) exactly equals the average energy entering the system P (recharge rate). For example, if $E[e^{\sqrt{E_i}}] < \infty$ is satisfied, then $h(n) = \sqrt{n}\,(\log(n))^2$ guarantees no energy shortages during the transmission. We note that $E[e^{\sqrt{E_i}}] < \infty$ is true for a large class of random variables including bounded support, exponential and χ^2 distributed random variables. Since $h(n) = n^{\frac{1}{\alpha}}\,(\log(n))^{\frac{1}{\gamma}} \in o(n)$ for $1 < \alpha \leq 2$ and $0 < \gamma < 1$, the saving period does not result in any loss in the

achievable rate, and thus, the save-and-transmit scheme achieves the capacity for the case of $P_{avg} = P$.

2.2.3 Best-Effort-Transmit Scheme

The input constraints in (2.1) impose that the codewords must satisfy the energy constraint in every channel use. However, it is possible to achieve a reliable communication rate even if code symbols satisfy the energy constraints in *almost* every channel use except possibly a finite number of them. Therefore, transmission of data in two phases may not be necessary. In this section, we propose an alternative *single-phase* scheme that attains the capacity using Gaussian codewords subject to the availability of energy in the battery. We call this new scheme the *best-effort-transmit* scheme.

Let $X^n = (X_1, X_2, \ldots, X_n)$ be a codeword of length n where X_i is the code symbol to be transmitted in channel use i and the codebook be $\mathcal{C}^n$. The codebook that the two parties agree upon is determined by generating independent Gaussian distributed random samples with mean zero and variance P_{avg}, i.e., $\mathcal{C}^n$ is a randomly generated codebook. Let $S(i)$ be the battery energy just before the ith channel use starts. In the best-effort-transmit scheme, the code symbol X_i can be put to the channel if $S(i) \geq X_i^2$. Otherwise, the transmitter puts a code symbol 0 to the channel as battery does not have sufficient energy to transmit symbol X_i. Hence,

the battery energy is updated according to the following rule:

$$S(i+1) = S(i) + E_i - X_i^2 \mathbf{1}(S(i) \geq X_i^2) \tag{2.10}$$

The energy updates in (2.10) are analogous to the queue updates in classical slotted systems [11]. Unlike in classical queuing in data networks, the energy queue is desired to be unstable so that there is always sufficient energy to transmit code symbols.

We say that the symbol X_i is infeasible if there is not sufficient energy to send X_i, that is, $S(i) < X_i^2$. Note that the codewords in the best-effort-transmit scheme are allowed to violate the energy constraints in (2.1); however, the actual channel inputs always satisfy the energy feasibility constraints in (2.1) in all channel uses. Therefore, there is no error due to energy shortages in the codewords and we only account for the decoding error at the receiver in the best-effort-transmit scheme. The input to the channel is $X_i \mathbf{1}(S(i) \geq X_i^2)$. Consequently, the codeword in the codebook may be different from what is actually transmitted. That is, in the transmitted codeword, some of the symbols in the actual codeword in the codebook are replaced with zeros. This causes a mismatch between the encoder and the decoder. Occurrences of such mismatches are determined by the dynamics of the available energy in the battery, which, in turn, is determined by the energy arrival and channel input processes. We are able to show that the resulting mismatch is negligible and communication with rates arbitrarily close to $\frac{1}{2}\log(1+P)$ is possible. We start with the following key observation, which is proved in Appendix 2.5.1.

Lemma 2.3 *In the best-effort-transmit scheme, if $P_{avg} < P$, for almost all realizations of the energy arrival process $\{E_i\}_{i=1}^n$ and the codebook $\mathcal{C}^n$, the code symbols are infeasible only at finitely many channel uses as n grows to infinity.*

In an AWGN channel, with a codebook generated with i.i.d. Gaussian samples with variance P_{avg}, rates arbitrarily close to $\frac{1}{2}\log(1 + P_{avg})$ can be achieved with probability of decoding error approaching zero [54]. The achievability is based on random coding and joint typical decoding, which checks whether the received vector is jointly typical with a codeword from the codebook, and the associated joint asymptotic equipartition property (AEP). In the best-effort-transmit scheme, there are mismatches between the codewords in the codebook and the actual transmitted codewords. However, if the average power of the codewords, P_{avg}, is smaller than the average recharge rate, $E[E_i] = P$, in view of Lemma 2.3, such mismatches are only finitely many, as the number of channel uses goes to infinity. This enables us to use joint typicality decoding at the receiver to reliably decode the message. This is true essentially because the joint AEP (see [54, Theorem 7.6.1]) is based on laws of large numbers which are unaffected by finite number of alterations, as the number of samples goes to infinity. More specifically, we prove that in the best-effort-transmit scheme if $P_{avg} < P$ and joint typicality decoder is used at the receiver, the probability of decoding error goes to zero as the block length n gets large. The following lemma provides the desired step to prove this result.

Lemma 2.4 *Let x^n be an arbitrary codeword in the codebook $\mathcal{C}^n$ and y^n be the corresponding received signal in the best-effort-transmit scheme. Let A_ϵ^n denote the*

set of jointly typical sequence tuples with respect to $p(x,y) = p(x)p(y|x)$ *where* $p(x) = \mathcal{N}(0, P_{avg})$ *and* $p(y|x) = \mathcal{N}(x,1)$*. Assume* $P_{avg} < P$*. The following statements hold for almost all realizations of the energy arrival process* $\{E_i\}_{i=1}^{n}$*:*

1. $Pr((x^n, y^n) \in A_\epsilon^n | E_1, \ldots, E_n) \to 1$ *as* $n \to \infty$

2. *Let* $\tilde{x}^n \neq x^n$ *be another codeword in* $\mathcal{C}^n$*. For sufficiently large* n*, we have*

$$Pr((\tilde{x}^n, y^n) \in A_\epsilon^n | E_1, \ldots, E_n) \leq 2^{-n(I(X;Y)-3\epsilon)} \tag{2.11}$$

where $I(X;Y)$ *is the mutual information between single-letter random variables* X *and* Y *jointly distributed as* $p(x,y)$*.*

Proof of Lemma 2.4 directly follows from Lemma 2.3 and [54, Theorem 7.6.1]. In particular, whenever $P_{avg} < P$, for almost all realizations of the energy arrival process $\{E_i\}_{i=1}^{\infty}$ and codewords in the codebook, there exists a finite number $N > 0$ such that none of the code symbols with index $i > N$ in any codeword are altered due to the insufficiency of the battery energy. Therefore, given $E_1, \ldots, E_n$ and codeword x^n with $n \gg N$, the last $n - N$ received symbols of y^n are the channel responses to the last $n - N$ code symbols of x^n. As n gets large, the effect of the first N received symbols becomes negligible and hence the received signal is jointly typical with the transmitted codeword for all $\epsilon > 0$ and sufficiently large n. In view of [54, Theorem 7.6.1], Lemma 2.4 holds.

We note that the message, channel noise sequence and energy arrival sequence are mutually independent. Consequently, we combine Lemma 2.4, [54, Theorem

7.6.1] and the achievability part of [54, Theorem 7.7.1] and conclude that if $P_{avg} < P$ and the receiver uses a joint typicality decoder, then in the best-effort-transmit scheme the probability of decoding error vanishes as n grows to infinity for almost all realizations of the energy arrival process. Finally, as the probability of decoding error approaches zero in a randomly designed codebook $\mathcal{C}^n$, there must exist a codebook such that the probability of decoding error approaches zero for almost all realizations of the energy arrival process. Since rate $R = \frac{1}{2}\log(1 + P_{avg})$ is achievable under an average power constraint $P_{avg} < P$, we have the desired result:

Theorem 2.2 *Rates arbitrarily close to* $\frac{1}{2}\log(1 + P)$ *are achievable in the best-effort transmit scheme.*

2.2.4 Discussion

We now comment on the two capacity achieving schemes. In the save-and-transmit scheme, the available channel uses are divided into two phases. The saving phase duration $h(n)$ is selected as $o(n)$ with $\lim_{n\to\infty} h(n) = \infty$ and this, along with the unlimited sized battery, allows averaging out the uncertainty in the available energy. Remaining $n - h(n)$ channel uses are used for channel coding with an average power constraint equal to the average recharge rate. Although for a fixed block length n, there is a non-zero probability that available energy in the battery is not sufficient to put the designed code symbol into the channel, this probability approaches zero as n gets large. The save-and-transmit scheme does not use the information about the amount of available energy in the battery at any given time. In contrast, the best-

effort-transmit scheme uses this information: Whenever battery energy is sufficient to send the designed code symbol, that code symbol is put to the channel, and if the energy in the battery falls short of sending the designed code symbol, a zero symbol is put to the channel. The best-effort-transmit scheme interacts with the battery energy level and adapts the transmission so that the message is reliably transmitted. It is clear that the extra information that the best-effort-transmit scheme uses brings no advantage in terms of the achievable rates. However, this information enables the transmitter start transmission of the message right away and codewords are infeasible in at most finitely many channel uses. In the save-and-transmit scheme, the saving period $h(n)$ has to grow to infinity for eradicating any energy shortages throughout the data transmission, which is a consequence of the lack of interaction between the channel input and the battery energy level.

We note that both save-and-transmit and best-effort-transmit schemes need unlimited sized batteries. It is more obvious that the save-and-transmit scheme needs an unlimited sized battery, since the battery energy needs to go to infinity in the saving phase as the block length gets large. The fact that the best-effort-transmit scheme also needs an unlimited sized battery is less obvious. While the best-effort-transmit scheme starts transmission right away, since $P_{avg} < P$, eventually, the battery energy goes to infinity. In fact, this is the reason that energy shortages occur only in finitely many channel uses. Essentially, after a large enough channel use index, the battery has so much energy that no energy shortages occur.

It is also worth noting that stochastic energy levels at the transmitter connects the problem considered here to the problem of communicating over state-dependent

channels with state information available at the transmitter only, where the state is the energy arrival sequence [25]. Although the availability of the state information at the transmitter and/or receiver boosts the capacity of state-dependent channels in general [25], the capacity of the AWGN channel with an energy harvesting transmitter with an unlimited battery does not change whether the energy arrival information is available at the transmitter/receiver or not. In fact, in the save-and-transmit and best-effort-transmit schemes, neither the transmitter nor the receiver needs to know the energy arrival information.

Moreover, we note that memory may affect the capacity of state-dependent channels in general [55]; however, the capacity of the AWGN channel with an energy harvesting transmitter with an unlimited battery is invariant to the memory in the energy arrival process, so long as the energy arrival process is stationary and ergodic. That is, an i.i.d. energy arrival process and a non-i.i.d. energy arrival process with the same average arrival rate will yield the same capacity so long as the non-i.i.d. energy arrival process is stationary and ergodic. Clearly, the converse argument in (2.3) is still valid in this case since the sample mean of the energy arrival process has the same limiting property. Furthermore, the save-and-transmit and best-effort-transmit schemes achieve the capacity in this case on the grounds that laws of large numbers hold for stationary and ergodic class of random processes [52]. In particular, Lemmas 2.1, 2.3 and 2.4 generalize to this class of energy arrival processes after simple modifications in their proofs.

Finally, we remark that the save-and-transmit and best-effort-transmit schemes and the capacity results presented in this chapter can be straightforwardly general-

ized to a single user fading or MIMO channel, or various multi-user channel models, such as the multiple access channel, broadcast channel, interference channel, relay channel, and wiretap channel, etc., with energy harvesting transmitters, as long as the transmitters are equipped with unlimited sized batteries. With save-and-transmit and best-effort-transmit schemes, we can achieve the rates that are achievable with corresponding average power constraints.

2.3 Optimal Power Management in a Large Time Scale

We have seen that energy harvesting systems can achieve classical AWGN capacity if the recharge process is i.i.d. and the block length is sufficiently large. However, the recharge process can deviate from its i.i.d. characteristic in a large time scale. In particular, the mean value of the recharge process may vary after a long duration that is sufficient to decode the transmitted message. In the classical example of sensor nodes fueled with solar power, mean recharge rate changes depending on the time of the day. As an example, the mean recharge rate may vary in one-hour frames and the sensor may be on for twelve hours a day, in which case, a careful management of energy expenditure in each frame will be required to optimize the average performance during the day.

Consider L time frames (see Figure 2.4). The duration of each frame is T_s. For each frame $i = 1, \ldots, L$, the average recharge rate is P_i and Q_i units of power is allocated for data transmission. Hence, in frame i, $P_i T_s$ units of energy enters the system and $Q_i T_s$ units of energy is spent. T_s is sufficiently large so that

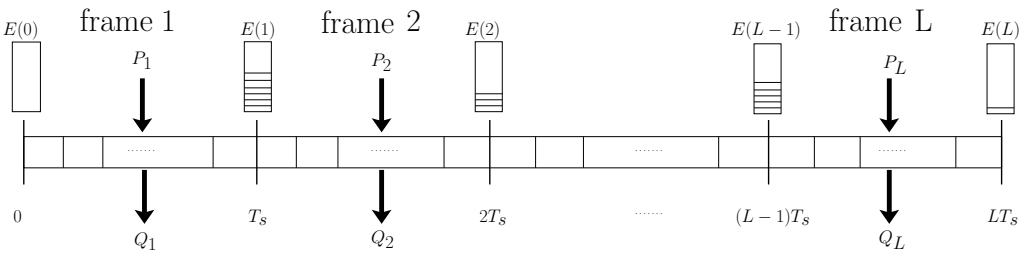

Figure 2.4: L large time frames. Each frame is sufficiently long to achieve AWGN capacity with average power constrained to the allocated power in that frame.

$T_s \frac{1}{2} \log(1 + Q_i)$ bits are reliably sent in this duration. Assuming zero initial energy in the battery and unlimited battery storage capacity, the causality constraint on the energy expenditure due to the energy arrivals is

$$\sum_{i=1}^{\ell} Q_i \leq \sum_{i=1}^{\ell} P_i, \qquad \ell = 1, \ldots, L \tag{2.12}$$

The designer knows the mean recharge rates P_i for all i and calculates Q_i before the communication and adjusts the average power of codewords in frame i to Q_i during transmission[1]. We allocate a transmit power to each frame subject to causality constraint so that average throughput in L frames is maximized:

$$\begin{aligned} \max \quad & \frac{1}{L} \sum_{i=1}^{L} \frac{1}{2} \log(1 + Q_i) \\ \text{s.t.} \quad & \sum_{i=1}^{\ell} Q_i \leq \sum_{i=1}^{\ell} P_i, \qquad \ell = 1, \ldots, L \end{aligned} \tag{2.13}$$

A first observation about the optimization problem in (2.13) is that any power vector with $\sum_{i=1}^{L} Q_i < \sum_{i=1}^{L} P_i$ is strictly suboptimal because log(.) is a monotone

[1]Changing the average power of codewords requires using different codebooks in each frame. However, scaling a common codebook by frame power Q_i works as well. This can also be interpreted as a codebook with dynamic power allocation [55] in slow time variation.

increasing function. Hence, the constraint in (2.13) for $\ell = L$ can be cast as an equality. We will refer to power vectors satisfying (2.13) as *feasible* in the following. We denote the solution of the optimization problem in (2.13) as $\mathbf{Q}^* = [Q_1^*, \ldots, Q_L^*]$. The rest of this section is devoted to characterizing the optimal power vector $\mathbf{Q}^*$.

We will solve the optimization problem in (2.13) by using tools from majorization theory and Schur-convexity [56]. We start with the following definition.

Definition 2.1 *Let* $\mathbf{x} = [x_1, \ldots, x_n]$ *and* $\mathbf{y} = [y_1, \ldots, y_n]$ *be two* n *dimensional non-negative vectors and let* $x_{(j)}$ *denote the* j*th largest component of* $\mathbf{x}$*. Then,* $\mathbf{x}$ *is said to be majorized by* $\mathbf{y}$*, denoted by* $\mathbf{x} \preceq \mathbf{y}$*, if*

$$\sum_{j=1}^{k} x_{(j)} \leq \sum_{j=1}^{k} y_{(j)}, \qquad k = 1, \ldots, n-1 \tag{2.14}$$

$$\sum_{j=1}^{n} x_j = \sum_{j=1}^{n} y_j \tag{2.15}$$

The majorization relation measures how spread a vector is from its mean value. It can be shown that [56] any n dimensional vector $[x_1, \ldots, x_n]$ majorizes the constant n dimensional vector with each coordinate equal to $\frac{\sum_i x_i}{n}$. If a function $f(x_1, \ldots, x_n)$ is *Schur-convex* then $[x_1, \ldots, x_n] \preceq [y_1, \ldots, y_n]$ implies $f(x_1, \ldots, x_n) \leq f(y_1, \ldots, y_n)$. If $-f$ is Schur-convex, then f is Schur-concave. The following result [56] will be useful.

Lemma 2.5 *If* $f(x_1, \ldots, x_n) = \sum_{i=1}^{L} g(x_i)$ *where* $g(x)$ *is convex, then* f *is Schur-convex.*

The objective function in (2.13) is Schur-concave since log(.) is concave. Therefore,

the solution of the optimization problem in (2.13) is the transmit power vector $\mathbf{Q}^*$ which is the most majorized feasible power vector, i.e., $\mathbf{Q}^*$ is the optimal transmit power vector if $\mathbf{Q}^* \preceq \mathbf{Q}$ for all feasible $\mathbf{Q}$. Thus, we need to find the most majorized feasible transmit power vector.

In order to understand how the most majorized feasible power vector may look like, we first consider the simplest scenario. Suppose that cLT_s amount of energy is available in the battery for some non-negative constant c and the recharge process is zero. In this case, the uniform power vector $Q_i = c$ is majorized by every other feasible vector. For the original problem, if the constant vector $Q_i = \frac{\sum_{j=1}^{L} P_j}{L}$ is feasible, then it is majorized by any other feasible vector. However, the constant vector may not be in the feasible set. This is due to the causality of energy arrivals: while energy can be spread to future to equalize powers as much as possible, if large amounts of energy arrive in later frames they cannot be spread to earlier frames to equalize the powers.

We now generalize the intuition obtained from the previous discussion for an arbitrary energy arrival case. In particular, we adapt the idea of allocating power as constant as possible for the general case taking the causality constraints into consideration using an energy curve approach. This approach has appeared in the context of energy minimal transmission in [57] where authors characterize energy minimal policy in a delay limited scenario as the tightest line below the data arrival curve. Later in the context of energy harvesting systems, similar structural properties have been observed in the policies with minimum transmission completion time in [14, 15]. We will obtain the optimal power management vector as the tightest

line below the cumulative energy arrivals. First, we define the cumulative energy arrivals as

$$e(i) = \sum_{j=1}^{i} P_j, \qquad i = 1, \ldots, L \tag{2.16}$$

and by convention $e(0) = 0$. Since the power vector should be made as constant as possible, it is determined such that its cumulative energy expenditure is the tightest piecewise linear curve below $e(i)$. Therefore, the algorithm divides the frames into K constant power bands $L_k+1 \leq i \leq L_{k+1}$, $k = 1, \ldots, K$. In particular, the optimal power vector Q_i^* is constant over $L_k + 1 \leq i \leq L_{k+1}$, $k = 1, \ldots, K$. By convention, $L_1 = 0$, $L_{K+1} = L$ and the remaining L_k are determined as follows:

$$L_k = \arg \min_{i \in \{L_{k-1}+1, \ldots, L\}} \frac{e(i) - e(L_{k-1})}{i - L_{k-1}} \tag{2.17}$$

As we find the tightest line below the energy arrival curve, Q_i^* takes the constant value $\frac{e(L_{k+1})-e(L_k)}{L_{k+1}-L_k}$ over the kth band $L_k+1 \leq i \leq L_{k+1}$. We claim that the following power vector is optimal:

$$Q_i^* = \frac{e(L_k) - e(L_{k-1})}{L_k - L_{k-1}}, \qquad i = L_{k-1} + 1, \ldots, L_k \tag{2.18}$$

To prove optimality, we show in the next theorem that Q_i^* obtained via this procedure is the most majorized feasible transmit power vector.

Theorem 2.3 $\mathbf{Q}^*$ *defined through (2.17) and (2.18) is the most majorized feasible*

power vector.

A proof of the Theorem 2.3 is provided in Appendix 2.5.5 which uses direct verification of the majorization conditions in (2.14) and (2.15). Since the objective function is Schur-concave, by Theorem 2.3, $\mathbf{Q}^*$ in (2.18) is the optimal power vector.

An illustration of the operation of the optimum power management algorithm is presented for a four frame case in Figure 2.5. Lines are drawn from the cumulative energy point $(i, e(i))$ to the future points $(j, e(j))$ for all $j > i$ and the one with the minimum slope is chosen which has the index j^*. The corresponding slope is the allocated power for all frames between i and j^*. In the depicted example, there are $L = 4$ frames and $P_1 = 1$, $P_2 = 2$, $P_3 = 1.3$ and $P_4 = 0.8$. We start with calculating the slopes by connecting $(0, 0)$ to $(j, e(j))$ for $j > 0$, which are $\frac{1}{1}$, $\frac{1+2}{2}$, $\frac{1+2+1.3}{3}$ and $\frac{1+2+1.3+0.8}{4}$. We observe that the minimum slope is obtained by connecting $(0, 0)$ to $(1, e(1))$. Hence, the optimal power level in frame 1 is $Q_1^* = 1$. We next determine power levels for $i > 1$, which are larger than $Q_1^* = 1$. Proceeding similarly, by connecting $(1, e(1))$ to $(j, e(j))$ for $j > 1$, the minimum slope is obtained by connecting $(1, e(1))$ and $(4, e(4))$ and hence the optimal power levels are $Q_i^* = \frac{2+1.3+0.8}{3} = 1.37$ for $2 \leq i \leq 4$. There are $K = 2$ constant power bands where $L_1 = 0, L_2 = 1, L_3 = 4$.

2.3.1 Numerical Results

The optimum power management algorithm takes the arrival rate vector $[P_1, \ldots, P_L]$ and outputs the optimal power vector $[Q_1^*, ..., Q_L^*]$. We let the arrival rates of energy

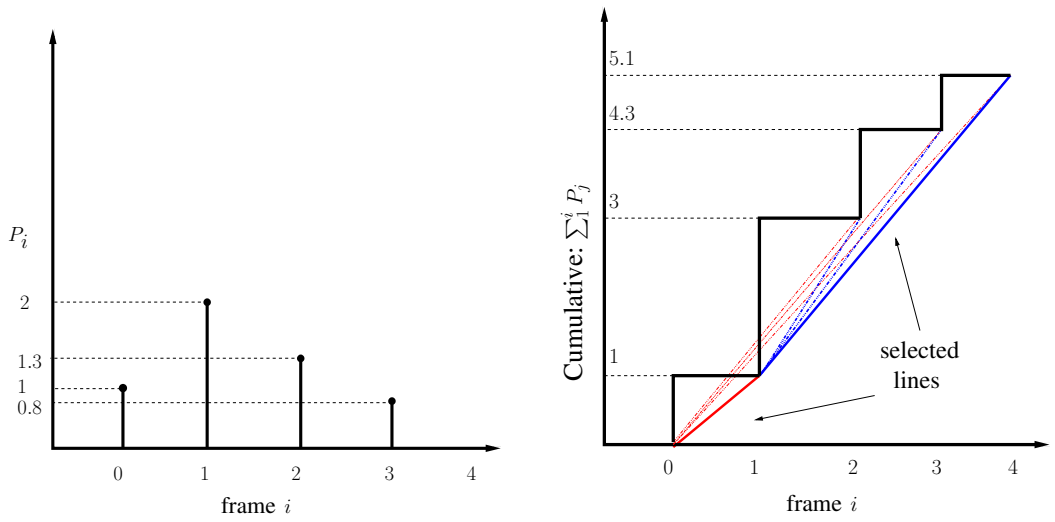

Figure 2.5: Operation of the algorithm that finds optimal power management.

in all frames, P_i, follow an i.i.d. exponential distribution. A benchmark algorithm is simply no power management algorithm, i.e., $Q_i = P_i$. In this simple scheme, the energy arrival rate in each frame is taken as the communication power in that frame. This scheme yields an average throughput

$$T_{lb} = \frac{1}{L}\sum_{i=1}^{L}\frac{1}{2}\log\left(1+P_i\right) \tag{2.19}$$

which is a lower bound. However, if the designer has the information of arrival rates in future frames, then the optimal power management algorithm can improve the average throughput. It is clear that an upper bound for the average throughput is

$$T_{ub} = \frac{1}{2}\log\left(1+\frac{1}{L}\sum_{i=1}^{L}P_i\right) \tag{2.20}$$

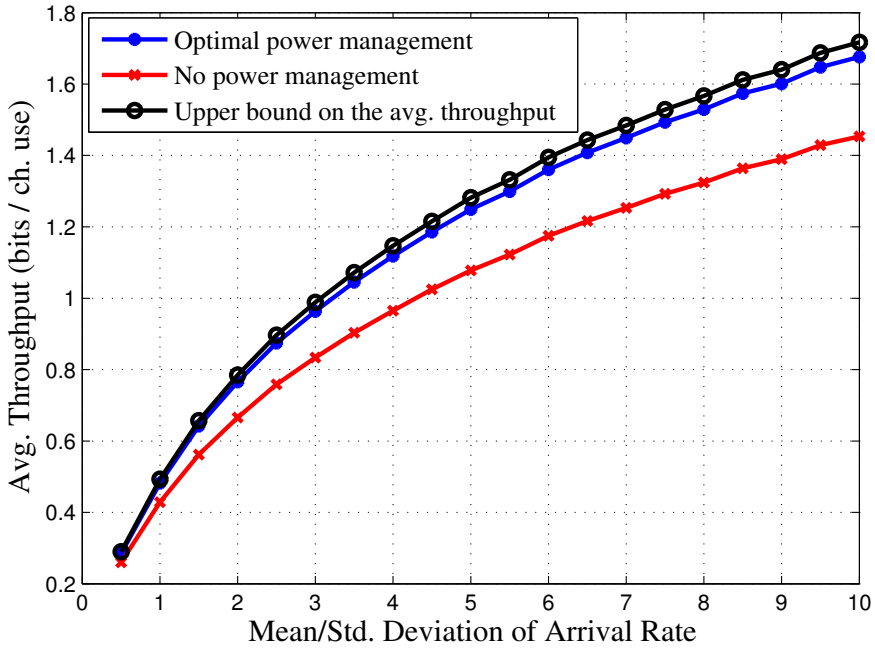

Figure 2.6: Average throughput versus mean/standard deviation of the arrival rate for $L = 20$ frames.

which assumes that $\sum_{i=1}^{L} P_i$ is available at the beginning, and therefore can be spread evenly over all time.

The comparison of the performances of the optimal power management algorithm with the upper bound T_{ub} and the lower bound T_{lb} (no power management) is given in Figure 2.6 for $L = 20$ frames. We observe that as the variance of the arrival rates increases, the advantage of optimal power management becomes more apparent with respect to no power management. Another observation is that the difference between the upper bound and the average throughput with optimal power management also increases as the standard deviation of the arrival rate is increased. Hence, the causality constraint becomes more restrictive as the variation in the arrival rate is increased.

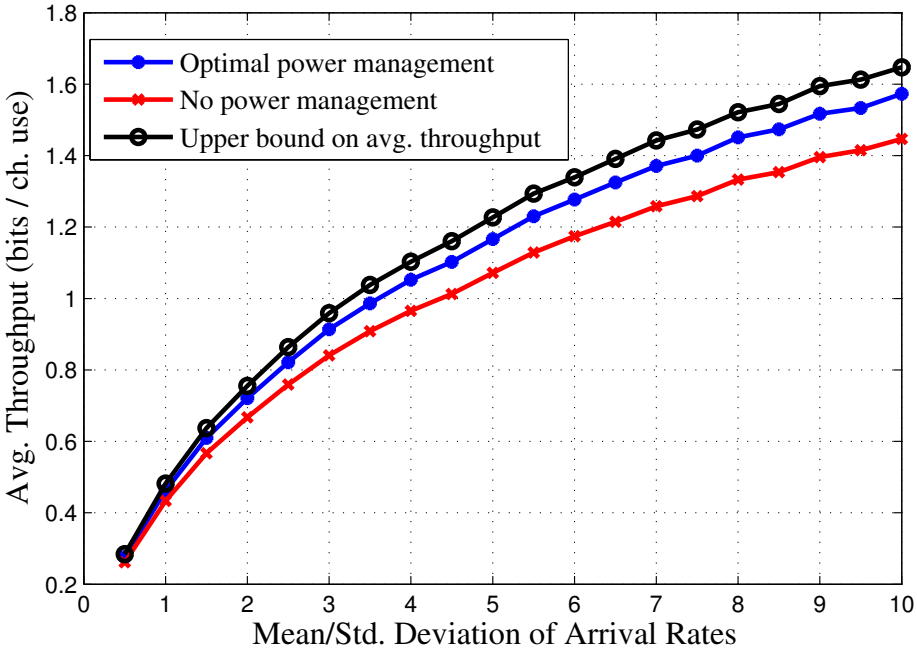

Figure 2.7: Average throughput versus mean/standard deviation of the arrival rate for $L = 5$ frames.

The comparison of the performances of the optimal power management with the upper bound T_{ub} and the lower bound T_{lb} (no power management) is given in Figure 2.7 for a $L = 5$ frame system. We observe that the upper bound and the average throughput with the optimal power management scheme are strictly smaller for $L = 20$ frames. This difference becomes more apparent when the variance of the arrival rates is higher. The upper bound has smaller value because arrival rates cannot be averaged sufficiently in $L = 5$ frames. Moreover, since $L = 5$ frames is not long enough to react to peaks in the arrival rate by saving and spreading the energy for future frames, average throughput with the optimal power management scheme is smaller in this case.

2.4 Conclusion

In this chapter, we established the capacity of the AWGN channel under stochastic energy harvesting where an unlimited sized battery buffers communication energy between an uncontrolled recharge process and the transmitter. This nature of the energy arrivals yields an unprecedented power constraint on each code symbol. Remarkably, communication rates can be reliably achieved at the capacity of the average power constrained AWGN channel. We first presented a save-and-transmit scheme in which data transmission occurs in two phases. In the first phase energy is collected and in the second phase data is transmitted. Next, we provided an alternative best-effort-transmit scheme that achieves the capacity without utilizing an initial saving phase. Finally, we extended our model to time-varying recharge rates in large time scales, and obtained optimal offline power management for maximum average throughput.

2.5 Appendix

2.5.1 Proof of Lemma 2.3

Let $P_{avg} = P - \epsilon$ and note that $E_i - X_i^2 - \epsilon$ is a zero-mean sequence. By the strong law of large numbers, only finitely many of the events $\left\{\frac{1}{n}\sum_{i=1}^{n}(E_i - X_i^2 - \epsilon) < -\delta\right\}_{n=1}^{\infty}$ occur for any $\delta > 0$. Selecting $\delta = \epsilon$, this is equivalent to the assertion that for only finitely many of the indices $\sum_{i=1}^{n}(E_i - X_i^2) < 0$. Note that $\sum_{i=1}^{n}(E_i - X_i^2 1(S(i) \geq X_i^2)) \geq \sum_{i=1}^{n}(E_i - X_i^2)$. This implies that $\sum_{i=1}^{n}(E_i - X_i^2 \mathbf{1}(S(i) \geq X_i^2)) < 0$ occurs

for only finitely many of the indices. Therefore, code symbols are infeasible, i.e., there is a shortage of energy in the battery, only in finitely many channel uses.

2.5.2 Proof of Lemma 2.1

In view of the instantaneous energy constraints in (2.1) in each channel use, in order to prove the statement of the lemma, we need to show that for any $\epsilon > 0$ and sufficiently large n:

$$\Pr\left(\bigcup_{k=1}^{n}\left\{\sum_{i=1}^{k} E_i < \sum_{i=1}^{k} X_i^2\right\}\right) \leq \epsilon \tag{2.21}$$

In the saving phase, $X_i = 0$ for $i = 1, \ldots, h(n)$, and hence, $\left\{\sum_{i=1}^{k} E_i < \sum_{i=1}^{k} X_i^2\right\} = \emptyset$ for the saving phase. For convenience, we use the index s for the saving phase, i.e., $s = 1, \ldots, h(n)$ and the index t for the transmission phase, i.e., $t = 1, \ldots, n - h(n)$. We have $E[E_t] = P$, $E[X_t^2] = P_{avg}$ and $P_{avg} < P$. Note that E_s, $s = 1, \ldots, h(n)$ and E_t, $t = 1, \ldots, n-h(n)$, are independent. Thus, we need to show that for sufficiently large n:

$$\Pr\left(\bigcup_{k=1}^{n-h(n)}\left\{\sum_{s=1}^{h(n)} E_s + \sum_{t=1}^{k} E_t < \sum_{t=1}^{k} X_t^2\right\}\right) \leq \epsilon \tag{2.22}$$

By the strong law of large numbers [52], we have as $n \to \infty$

$$\frac{1}{n-h(n)}\left(\sum_{t=1}^{n-h(n)} E_t - \sum_{t=1}^{n-h(n)} X_t^2\right) \longrightarrow P - P_{avg}, \text{ w.p. } 1 \tag{2.23}$$

since $n - h(n) \to \infty$ as $n \to \infty$. Then, (2.23) implies for any $\delta > 0$

$$\lim_{m\to\infty} \Pr\left(\bigcup_{k=m}^{\infty}\left\{\left|\frac{\sum_{t=1}^{k} E_t - X_t^2}{k} - (P - P_{avg})\right| > \delta\right\}\right) = 0 \tag{2.24}$$

Choosing $\delta = P - P_{avg}$, there exists sufficiently large k_0 such that

$$\Pr\left(\bigcup_{k=k_0}^{\infty}\left\{\sum_{t=1}^{k} E_t < \sum_{t=1}^{k} X_t^2\right\}\right) < \epsilon' \tag{2.25}$$

Therefore, since $\sum_{s=1}^{h(n)} E_s \geq 0$, for all $n - h(n) \geq k_0$, (2.25) implies

$$\Pr\left(\bigcup_{k=k_0}^{n-h(n)}\left\{\sum_{s=1}^{h(n)} E_s + \sum_{t=1}^{k} E_t < \sum_{t=1}^{k} X_t^2\right\}\right) < \epsilon' \tag{2.26}$$

To reach (2.22), it remains to show that $\Pr\left(\bigcup_{k=1}^{k_0-1}\left\{\sum_{s=1}^{h(n)} E_s + \sum_{t=1}^{k} E_t < \sum_{t=1}^{k} X_t^2\right\}\right)$ can be made arbitrarily small by selecting n sufficiently large. We first apply the union bound:

$$\Pr\left(\bigcup_{k=1}^{k_0-1}\left\{\sum_{s=1}^{h(n)} E_s + \sum_{t=1}^{k} E_t < \sum_{t=1}^{k} X_t^2\right\}\right) \leq \sum_{k=1}^{k_0-1} \Pr\left(\left\{\sum_{s=1}^{h(n)} E_s + \sum_{t=1}^{k} E_t < \sum_{t=1}^{k} X_t^2\right\}\right) \tag{2.27}$$

By weak law of large numbers [52], for every $\kappa > 0$, $\delta > 0$ and sufficiently large n

$$\Pr\left(\left|\frac{1}{h(n)}\sum_{s=1}^{h(n)} E_s - P\right| > \delta\right) < \kappa \tag{2.28}$$

Define the event $A_{\delta,n} = \left\{\left|\frac{1}{h(n)}\sum_{s=1}^{h(n)} E_s - P\right| > \delta\right\}$. Conditioning on $A_{\delta,n}$ and using

the law of total probability, and in view of the independence of E_s and E_t, we have for any $\kappa > 0$, $\delta > 0$ and sufficiently large n

$$\begin{aligned}
&\Pr\left(\left\{\sum_{s=1}^{h(n)} E_s + \sum_{t=1}^{k} E_t < \sum_{t=1}^{k} X_t^2\right\}\right) \\
&\quad = \Pr\left(\left\{\sum_{s=1}^{h(n)} E_s + \sum_{t=1}^{k} E_t < \sum_{t=1}^{k} X_t^2 \Big| A_{\delta,n}^c\right\}\right) \Pr\left(A_{\delta,n}^c\right) \\
&\qquad + \Pr\left(\left\{\sum_{s=1}^{h(n)} E_s + \sum_{t=1}^{k} E_t < \sum_{t=1}^{k} X_t^2 \Big| A_{\delta,n}\right\}\right) \Pr\left(A_{\delta,n}\right) \qquad (2.29) \\
&\quad \le \Pr\left(\left\{h(n)(P-\delta) + \sum_{t=1}^{k} E_t < \sum_{t=1}^{k} X_t^2\right\}\right) + \kappa \qquad (2.30) \\
&\quad \le \epsilon'' \qquad (2.31)
\end{aligned}$$

Note that neither $\sum_{t=1}^{k} E_t$ nor $\sum_{t=1}^{k} X_t^2$ depends on n. Using (2.31) in (2.27), for sufficiently large n we have

$$\Pr\left(\bigcup_{k=1}^{k_0-1}\left\{\sum_{s=1}^{h(n)} E_s + \sum_{t=1}^{k} E_t < \sum_{t=1}^{k} X_t^2\right\}\right) \le \epsilon''' \qquad (2.32)$$

Then, using (2.26) and (2.32), combined with the union bound, we get

$$\Pr\left(\bigcup_{k=1}^{n-h(n)}\left\{\sum_{s=1}^{h(n)} E_s + \sum_{t=1}^{k} E_t < \sum_{t=1}^{k} X_t^2\right\}\right) \le \epsilon' + \epsilon''' \triangleq \epsilon \qquad (2.33)$$

which is what we need in (2.22). ■

2.5.3 Calculation of (2.8) and (2.9)

For convenience, we use $s = 1, \ldots, h(n)$ for the saving phase and $t = 1, \ldots, n - h(n)$ for the transmission phase as in Appendix 2.5.2. Since $X_s = 0$ for $s = 1, \ldots, h(n)$, we have

$$\Pr\left(\sum_{i=1}^{n} X_i^2 > \sum_{i=1}^{n} E_i\right) = \Pr\left(\sum_{t=1}^{n-\sqrt{n}} Z_t > \sum_{s=1}^{\sqrt{n}} E_s\right) \tag{2.34}$$

where $Z_t = X_t^2 - E_t$ and thus $E[Z_t] = 0$ for $t = 1, \ldots, n - \sqrt{n}$. Let the event $B_{\delta,n}$ be $B_{\delta,n} \triangleq \left\{\left|\frac{1}{\sqrt{n}}\sum_{s=1}^{\sqrt{n}} E_s - P\right| > \delta\right\}$. By the law of total probability, we have:

$$\begin{aligned}\Pr\left(\sum_{t=1}^{n-\sqrt{n}} Z_t > \sum_{s=1}^{\sqrt{n}} E_s\right) = &\Pr\left(\sum_{t=1}^{n-\sqrt{n}} Z_t > \sum_{s=1}^{\sqrt{n}} E_s \middle| B_{\delta,n}\right) \Pr(B_{\delta,n}) \\ &+ \Pr\left(\sum_{t=1}^{n-\sqrt{n}} Z_t > \sum_{s=1}^{\sqrt{n}} E_s \middle| B_{\delta,n}^c\right) \Pr(B_{\delta,n}^c)\end{aligned} \tag{2.35}$$

Note that we have

$$\Pr\left(\sum_{t=1}^{n-\sqrt{n}} Z_t > \sqrt{n}(P+\delta)\right) \leq \Pr\left(\sum_{t=1}^{n-\sqrt{n}} Z_t > \sum_{s=1}^{\sqrt{n}} E_s \middle| A_{\delta,n}^c\right) \tag{2.36}$$

$$\leq \Pr\left(\sum_{t=1}^{n-\sqrt{n}} Z_t > \sqrt{n}(P-\delta)\right) \tag{2.37}$$

From the central limit theorem [52], for n i.i.d. samples of a random variable D_i with zero-mean and variance d^2, we have

$$\lim_{n\to\infty} \Pr\left(\frac{1}{\sqrt{n}}\sum_{i=1}^{n} D_i > x\right) = \Phi\left(\frac{x}{d}\right) \tag{2.38}$$

where $\Phi(x) = \int_x^\infty \frac{1}{\sqrt{2\pi}} e^{-\frac{\tau^2}{2}} d\tau$. In view of the fact that $\frac{1}{\sqrt{n}} \sum_{i=1}^{\sqrt{n}} D_i \to 0$ almost surely as $n \to \infty$, we have

$$\lim_{n\to\infty} \Pr\left(\frac{1}{\sqrt{n}} \sum_{i=1}^{n-\sqrt{n}} D_i > x \right) = \Phi\left(\frac{x}{d}\right) \tag{2.39}$$

Applying (2.39) for Z_t, $t = 1, \ldots, n - \sqrt{n}$, we get

$$\lim_{n\to\infty} \Pr\left(\sum_{t=1}^{n-\sqrt{n}} Z_t > \sqrt{n}P \right) = \Phi\left(\frac{P}{a}\right) \tag{2.40}$$

where we assume that the variance of Z_t is finite and equal to a^2. We can have this, for instance, when E_t has finite variance, σ_E^2. In this case, as X_t is Gaussian and independent of E_t, we have $a^2 \triangleq E[Z_t^2] = \sigma_E^2 + 2P^2$. As a consequence, $\lim_{n\to\infty} \Pr\left(\sum_{t=1}^{n-\sqrt{n}} Z_t^2 > \sqrt{n}(P \pm \delta) \right) = \Phi(\frac{P\pm\delta}{a})$. Since $\Phi(x)$ is continuous in x, in view of (2.36)-(2.37), we have

$$\lim_{\delta\to 0^+} \lim_{n\to\infty} \Pr\left(\sum_{t=1}^{n-\sqrt{n}} Z_t^2 > \sum_{s=1}^{\sqrt{n}} E_s \Big| A_{\delta,n}^c \right) = \Phi\left(\frac{P}{a}\right) \tag{2.41}$$

By the weak law of large numbers [52], $\lim_{n\to\infty} \Pr(A_{\delta,n}^c) = 1$ for all $\delta > 0$ and evaluating (2.35) as $\delta \to 0^+$, we get

$$\lim_{n\to\infty} \Pr\left(\sum_{i=1}^{n} X_i^2 > \sum_{i=1}^{n} E_i \right) = \lim_{n\to\infty} \Pr\left(\sum_{t=1}^{n-\sqrt{n}} Z_t > \sqrt{n}P \right) \tag{2.42}$$

$$= \Phi\left(\frac{P}{a}\right) \tag{2.43}$$

which is (2.8).

When $h(n) = \log(n)$, as in the above derivation, this probability becomes

$$\lim_{n\to\infty} \Pr\left(\sum_{i=1}^{n} X_i^2 > \sum_{i=1}^{n} E_i\right) = \lim_{n\to\infty} \Pr\left(\sum_{t=1}^{n-\log(n)} Z_t > \log(n)P\right) \tag{2.44}$$

$$= \lim_{n\to\infty} \Phi\left(\frac{P}{a}\sqrt{\frac{\log(n)}{\sqrt{n}}}\right) \tag{2.45}$$

$$= \Phi(0) \tag{2.46}$$

$$= \frac{1}{2} \tag{2.47}$$

which is (2.9).

2.5.4 Proof of Lemma 2.2

We need to show the following result for sufficiently large n:

$$\Pr\left(\bigcup_{k=1}^{n}\left\{\sum_{i=1}^{k} E_i < \sum_{i=1}^{k} X_i^2\right\}\right) \leq \epsilon \tag{2.48}$$

We have again $\left\{\sum_{i=1}^{k} E_i < \sum_{i=1}^{k} X_i^2\right\} = \emptyset$ for $k = 1, \ldots, h(n)$. As $E[X_i^2] = E[E_i] = P$ in the transmission phase, we cannot proceed by using the strong law of large numbers. Recall that in the proof of Lemma 2.1, the strong law of large numbers is invoked in (2.25) by choosing $\delta = P - P_{avg}$; however, in this case, since $P - P_{avg} = 0$, $\delta = P - P_{avg} = 0$ is not allowed as a selection. Our proof for the $P = P_{avg}$ case uses a stronger version of Marcinkiewicz-Zygmund type strong law of large numbers that is originally proved in [53]. In particular, we use Corollary 2.16 in [53], which

we state next for completeness.

Theorem 2.4 (Corollary 2.16 in [53]) *Let $\{X_i\}$ be a sequence of i.i.d. random variables with $E[X_i] = 0$ and let $\{a_{ni}, 1 \leq i \leq n, n \geq 1\}$ be a triangular array of constants satisfying $A_\alpha = \limsup_{n\to\infty} A_{\alpha,n} < \infty$ where $A_{\alpha,n} = \frac{1}{n}\sum_{i=1}^{n} |a_{ni}|^\alpha$ for some $1 < \alpha \leq 2$. Let $T_n = \sum_{i=1}^{n} a_{ni}X_i$, $n \geq 1$, and let $b_n = n^{\frac{1}{\alpha}}(\log(n))^{\frac{1}{\gamma}}$. Moreover, for some $h > 0$ and $\gamma > 0$, we assume $E[e^{h|X|^\gamma}] < \infty$. Then,*

$$\lim_{n\to\infty} \frac{|T_n|}{b_n} = 0, \qquad a.s. \tag{2.49}$$

As in Appendix 2.5.2, we use the index s for the saving phase, i.e., $s = 1, \ldots, h(n)$ and the index t for the transmission phase, i.e., $t = 1, \ldots, n - h(n)$. We start by noting that the condition in (2.48) is equivalent to the following for all $\epsilon > 0$ and sufficiently large n:

$$\Pr\left(\bigcup_{k=1}^{n-h(n)} \left\{\sum_{t=1}^{k} Z_t > \sum_{s=1}^{h(n)} E_s\right\}\right) \leq \epsilon \tag{2.50}$$

where $Z_t = X_t^2 - E_t$. Note that the random variables $\{E_s\}_{s=1}^{h(n)}$ are independent of $\{Z_t\}_{t=1}^{n-h(n)}$ and $E[Z_t] = 0$, while $E[E_i] = P$. In order to show (2.50), we replace $T_k = \sum_{t=1}^{k} Z_t$ where we take the triangular array in Theorem 2.4 as $a_{ni} = 1$. Note that this agrees with $A_\alpha < \infty$ requirement as this selection leads to $A_\alpha = 1$ for any α.

By the weak law of large numbers [52], for every $\epsilon > 0$, $\delta > 0$ and sufficiently large n

$$\Pr\left(\left|\frac{1}{h(n)}\sum_{s=1}^{h(n)} E_s - P\right| > \delta\right) < \epsilon \tag{2.51}$$

Define the event $C_{\delta,n} = \left\{\left|\frac{1}{h(n)}\sum_{s=1}^{h(n)} E_s - P\right| > \delta\right\}$. Conditioning on $C_{\delta,n}$ and using the law of total probability in a similar fashion to the corresponding steps in Appendices 2.5.2 and 2.5.3, we have for any $\epsilon > 0$, $\delta > 0$ and sufficiently large n

$$\Pr\left(\bigcup_{k=1}^{n-h(n)}\left\{\sum_{t=1}^{k} Z_t > \sum_{s=1}^{h(n)} E_s\right\}\right) \leq \Pr\left(\bigcup_{k=1}^{n-h(n)}\left\{\sum_{t=1}^{k} Z_t > h(n)(P-\delta)\right\}\right) + \epsilon \tag{2.52}$$

Therefore, we need to show that for any $\delta > 0$, $\epsilon' > 0$ and sufficiently large n

$$\Pr\left(\bigcup_{k=1}^{n-h(n)}\left\{\sum_{t=1}^{k} Z_t > h(n)(P-\delta)\right\}\right) < \epsilon' \tag{2.53}$$

Now, we let $h(n) = n^{\frac{1}{\alpha}}(\log(n))^{\frac{1}{\gamma}}$ for some $1 < \alpha \leq 2$ and $\gamma > 0$. Moreover, we note that $E[e^{|Z_t|^\gamma}] < \infty$ for $0 < \gamma < 1$. To see this, we first note $Z_t = X_t^2 - E_t$ and $X_t^2 > 0$, $E_t > 0$. Hence, we get $|Z_t|^\gamma \leq X_t^{2\gamma} + E_t^\gamma$ for $0 < \gamma < 1$ and hence $e^{|Z_t|^\gamma} \leq e^{X_t^{2\gamma}} e^{E_t^\gamma}$. Since X_t is zero mean Gaussian with variance P, $E[e^{X_t^{2\gamma}}] < \infty$ for $0 < \gamma < 1$. That is, the hypothesis $E[e^{E_t^\gamma}] < \infty$ implies $E[e^{|Z_t|^\gamma}] < \infty$, which is a

requirement for Theorem 2.4. Therefore, by Theorem 2.4, we have

$$\lim_{n\to\infty} \frac{|\sum_{t=1}^{n} Z_t|}{h(n)} = 0, \qquad \text{w.p.1} \tag{2.54}$$

(2.54) implies for any $\bar{\delta} > 0$

$$\lim_{n\to\infty} \Pr\left(\bigcup_{k=n}^{\infty} \left\{\left|\sum_{t=1}^{k} Z_t\right| > h(k)\bar{\delta}\right\}\right) = 0 \tag{2.55}$$

Therefore, for any $\epsilon > 0$, there exists sufficiently large k_0 such that (c.f. (2.25))

$$\Pr\left(\bigcup_{k=k_0}^{\infty} \left\{\left|\sum_{t=1}^{k} Z_t\right| > h(k)\bar{\delta}\right\}\right) < \epsilon \tag{2.56}$$

In particular, we have for $n - h(n) \geq k_0$ and $\bar{\delta} = P - \delta$

$$\Pr\left(\bigcup_{k=k_0}^{n-h(n)} \left\{\left|\sum_{t=1}^{k} Z_t\right| > h(n)(P-\delta)\right\}\right) < \epsilon \tag{2.57}$$

where we use the fact that $h(k) < h(n)$ for all $k = k_0, \ldots, n - h(n)$. In order to show (2.53), it remains to prove that for sufficiently large n

$$\Pr\left(\bigcup_{k=1}^{k_0-1} \left\{\left|\sum_{t=1}^{k} Z_t\right| > h(n)(P-\delta)\right\}\right) < \epsilon \tag{2.58}$$

Using the union bound, we have

$$\Pr\left(\bigcup_{k=1}^{k_0-1} \left\{\left|\sum_{t=1}^{k} Z_t\right| > h(n)(P-\delta)\right\}\right) \leq \sum_{k=1}^{k_0-1} \Pr\left(\left|\sum_{t=1}^{k} Z_t\right| > h(n)(P-\delta)\right) \tag{2.59}$$

We note that $\Pr\left(|\sum_{t=1}^{k} Z_t| > h(n)(P-\delta)\right) \to 0$ as $h(n) \to \infty$. Hence, (2.58) holds for sufficiently large n.

Therefore, under the hypothesis of Lemma 2.2, probability of energy shortage goes to zero as n gets large. This establishes Lemma 2.2. ■

2.5.5 Proof of Theorem 2.3

First, we observe that the transmit power vector $\mathbf{Q}^*$ defined in (2.17) and (2.18) has monotonically increasing entries, i.e., $Q_1^* \leq Q_2^* \leq \ldots \leq Q_L^*$. This is true, because otherwise, we could construct a line with a smaller slope that connects two energy arrival points and this would contradict the definition of the algorithm in (2.17) and (2.18).

Let $\{L_1, \ldots, L_{K+1}\}$ be the indices of constant power bands $\{L_k - L_{k+1}\}$ and let $\mathbf{Q} = [Q_1, \ldots, Q_L]$ be any feasible power vector. We will show that $\mathbf{Q}^* \preceq \mathbf{Q}$ by verifying that all of the conditions in (2.14) are satisfied. Note that the condition in (2.15) is satisfied by definition of feasibility.

Since the algorithm produces monotone increasing powers, $Q_{(j)}^* = Q_L^*$, $j = 1, \ldots, L - L_K$. In particular, $Q_{(1)}^* = \max_i Q_i^* = Q_L^*$ and as $\mathbf{Q}$ is feasible, we have

$$\sum_{j=1}^{L_k} Q_j \leq \sum_{j=1}^{L_k} Q_j^*, \qquad k = 1, \ldots, K \tag{2.60}$$

Moreover, by feasibility we have the equality $\sum_{j=1}^{L} Q_j = \sum_{j=1}^{L} Q_j^*$. Hence, (2.60)

and the equality implies

$$\sum_{j=L_k+1}^{L} Q_j^* \leq \sum_{j=L_k+1}^{L} Q_j, \qquad k = 1, \ldots, K \tag{2.61}$$

Applying (2.61) at $k = K$

$$Q_{(1)}^* = \frac{\sum_{j=L_K+1}^{L} Q_j^*}{L - L_K} \leq \frac{\sum_{j=L_K+1}^{L} Q_j}{L - L_K} \leq \frac{\sum_{j=1}^{L-L_K} Q_{(j)}}{L - L_K} \tag{2.62}$$

By rearranging the terms,

$$(L - L_K)Q_{(1)}^* = \sum_{j=1}^{L-L_K} Q_{(j)}^* \leq \sum_{j=1}^{L-L_K} Q_{(j)} \tag{2.63}$$

Since $Q_{(j)}$ is ordered and $Q_{(j)}^* = Q_{(1)}^*$ for $j = 1, \ldots, L - L_K$, we have the following

$$\sum_{j=1}^{\ell} Q_{(j)}^* \leq \sum_{j=1}^{\ell} Q_{(j)}, \quad \ell = 1, \ldots, L - L_K \tag{2.64}$$

The remaining conditions are verified similarly. Again since the algorithm yields monotone increasing powers, for $j = L - L_K + 1, \ldots, L - L_{K-1}$, $Q_{(j)}^* = Q_{(L-L_K+1)}^*$. By applying (2.61) at $k = K - 2$, we have

$$(L_K - L_{K-1})Q_{(L-L_K+1)}^* + (L - L_K)Q_{(1)}^* = \sum_{j=1}^{L-L_{K-1}} Q_{(j)}^* \tag{2.65}$$

$$\leq \sum_{j=1}^{L-L_{K-1}} Q_{(j)} \tag{2.66}$$

Then, we must have

$$\sum_{j=1}^{\ell} Q^*_{(j)} \leq \sum_{j=1}^{\ell} Q_{(j)}, \quad \ell = L - L_K + 1, \ldots, L - L_{K-1} \tag{2.67}$$

Repeating this argument, we verify all conditions required to get (2.14) for $\mathbf{Q}^*$ and $\mathbf{Q}$ in places of $\mathbf{x}$ and $\mathbf{y}$. ■

Chapter 3

Gaussian Energy Harvesting Channels with Zero Energy Storage: The Case of Energy as a Channel State

3.1 Introduction

In this chapter, we focus on channels with energy harvesting transmitters and zero energy storage. The energy arrival is observed by the transmitter causally, right before the code symbol is decided. Hence, the code symbol energy in a channel use is constrained to the energy arrived in that channel use. This is an instance of a state-dependent channel with causal information at the transmitter and the state of the channel is the energy arrival.

We first consider the single user AWGN channel with energy harvesting transmitters of zero energy storage. It is known due to [18] that the capacity is achieved by Shannon strategies. In particular, the capacity of this channel is expressed as a single-letter optimization problem over the extended inputs where each input is constrained in energy by the corresponding energy arrival. Even though it is a convex problem, corresponding optimization problem is hard to solve due to the continuous alphabet inputs. We obtain numerically verifiable necessary and sufficient optimality conditions for the input distributions.

Then, we consider the capacity region of the Gaussian MAC with energy har-

vesting transmitters of zero energy storage. We prove that when the energy arrivals are deterministic, the boundary of the capacity region is achieved by discrete input distributions of finite support. In the stochastic amplitude constrained case, we provide achievable rate regions by Shannon strategies and provide numerical performance comparisons.

Finally, we revisit the single user AWGN channel with zero energy storage setting and we consider the state amplification problem. In many energy harvesting sensor applications, the receiver may aim at extracting energy state information from the received signal as well as decoding the message. From an information theoretic point of view, the interaction of these two objectives is investigated by considering the state amplification problem [20]. We determine the trade-off between these two objectives in the zero energy storage and unlimited energy storage regimes.

3.2 Single User Gaussian Energy Harvesting Channel with Zero Energy Storage

The system model is shown in Figure 3.1. $E_1, \ldots, E_n$ is the i.i.d. energy arrival sequence where $E_i \in \mathcal{E}$ and $|\mathcal{E}|$ is finite. At each channel use, the transmitter observes E_i and generates a channel input X_i that satisfies $X_i^2 \leq E_i$, i.e., the code symbol is amplitude constrained to (the square root of) the observed energy. Therefore, the major effect of energy arrivals is the time variation in the amplitude constraint that the code symbol should obey at each channel use. As the transmitter can observe the energy arrival causally, the resulting system is a state-dependent

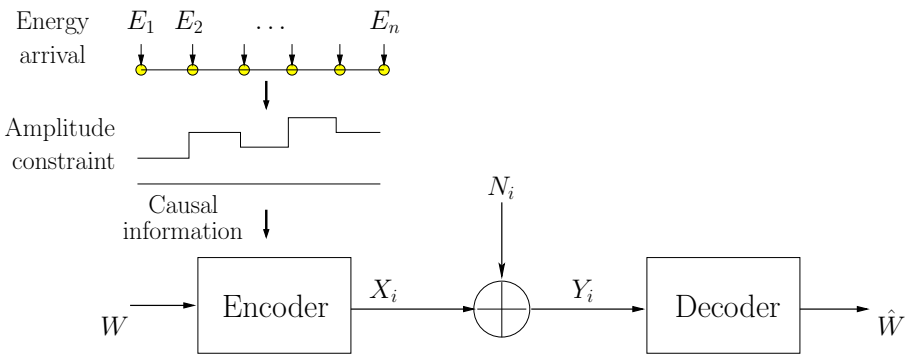

Figure 3.1: The AWGN channel with zero energy storage.

channel with causal state information at the transmitter and no state information at the receiver. The state of the channel is the amount of energy available at each channel use. At each state, the channel conditioned on the realized state is an AWGN channel with an input amplitude constraint equal to the square root of the arrived energy.

The channel capacity of the static amplitude constrained AWGN channel was first studied by Smith in [5] where it is proved that the capacity achieving input distribution has a finite support set. This line of research has later been extended in [7, 58–60] for various channels including quadrature-amplitude constrained AWGN channel and Rayleigh and Ricean fading channels. In [26], the finiteness of the support set of the capacity achieving distribution for conditionally Gaussian channels with bounded inputs, which encompasses a large class of practical channels, is proved. In particular, optical channels and fading MIMO channels with and without state information at the receiver are encompassed in the finiteness result of [26]. Moreover, [61] reports finiteness of the capacity achieving distribution for the quantized output AWGN channel. Also in [62], capacity achieving input distribution for

a duty cycle constrained system is shown to have countably infinite mass points with finite number of points in each bounded interval. In [63], new sufficient conditions for the noise distribution are provided for the optimality of discrete channel inputs in an amplitude constrained additive noise channel.

The capacity and optimal coding for a state-dependent channel with causal state information at the transmitter and no state information at the receiver was characterized by Shannon in [18]. In [18], Shannon proved that the capacity of the state-dependent channel with causal state information available at the transmitter only is equal to the capacity of an equivalent channel which has an input alphabet extended by the cardinality of the state alphabet. In the capacity achieving coding scheme, the codewords are matrices rather than vectors, whose number of columns is the block length and the number of rows is the cardinality of the state alphabet. At each channel use, the code symbol that corresponds to the observed state is put to the channel. In the sequel, we refer to this coding scheme as the *Shannon strategy*.

The problem that we wish to address in this section has two main characteristics:

- amplitude constraints due to available energy, and
- a state-dependent channel due to different energy arrivals where the state is naturally known to the transmitter but not to the receiver.

We obtain the capacity by applying the Shannon strategy to the time-varying amplitude constrained channel and optimizing the input distribution of the resulting extended alphabet channel. In particular, we extend the alphabet of the channel

in accordance with the amplitude constraints and construct an equivalent channel which has the number of inputs equal to the cardinality of the alphabet of energy arrivals. Each input variable is constrained in amplitude by the square root of the corresponding amount of energy.

Next, we numerically study the considered setting. We compare the capacity with several upper bounds such as the capacity of the AWGN channel with state information available at both sides and the capacity of the AWGN channel with unlimited energy storage. The numerical results indicate that capacity achieving input distributions are discrete with finite support. Additionally, we observe from numerical results that the capacity with unlimited energy storage is considerably higher than the capacity with zero energy storage, indicating the usefulness of collecting energy.

3.2.1 Capacity of the Gaussian Energy Harvesting Channel with Zero Energy Storage

Before we address the stochastic amplitude constrained case, let us start with the AWGN channel with a static amplitude constraint. The channel capacity under the amplitude constraint A is [5]

$$C_{Sm}(A) = \max_{F \in \mathcal{F}} I_F(X;Y) \tag{3.1}$$

where $\mathcal{F}$ is the space of input probability distribution functions whose support sets are constrained to $[-A, A]$. The subscript Sm refers to Smith [5].

Now, we start with the original setting. Let E be the energy random variable with the alphabet $\mathcal{E} = \{e_1, \ldots, e_M\}$. $\{E_k\}_{k=1}^{\infty} \in \mathcal{E}$ is an i.i.d. process with probability that $E_k = e_i$ is equal to p_i for all k. The realizations of the energy arrivals $\{E_1, \ldots, E_n\}$ are observed by the transmitter causally and the code symbol must comply with the observed energy constraint at each channel use:

$$|X_k| \leq \sqrt{E_k}, \qquad k = 1, \ldots, n \tag{3.2}$$

The receiver has no information about the energy arrivals. This is a state-dependent channel with causal state information at the transmitter only [18]. The code sequence is determined as a function of the observed amplitude constraint sequence and the channel capacity is

$$C = \max_{p_T(t)} I(T; Y) \tag{3.3}$$

where $T = [T_1, \ldots, T_M]$ is an extended channel input related with the output as

$$p_{Y|T}(y|t) = \sum_{i=1}^{M} p_i \phi(y - t_i) \tag{3.4}$$

where $\phi(.)$ is the zero mean unit variance Gaussian density and $|T_i| \leq \sqrt{E_i}$. For simplicity, we assume that the energy arrival process takes two different values, e_1 and e_2 with probabilities p_1 and $p_2 = 1 - p_1$. The analysis in the sequel is valid for any finite value of $|\mathcal{E}|$.

We now determine necessary and sufficient optimality conditions for the opti-

mal input distribution $F^*_{T_1,T_2}$. The space of joint probability distribution functions over $[-\sqrt{e_1}, \sqrt{e_1}] \times [-\sqrt{e_2}, \sqrt{e_2}]$ is:

$$\Omega \triangleq \left\{ F : \int_{-\sqrt{e_1}}^{\sqrt{e_1}} \int_{-\sqrt{e_2}}^{\sqrt{e_2}} dF(t_1, t_2) = 1 \right\} \tag{3.5}$$

The capacity in (3.3) is:

$$C = \max_{F \in \Omega} I_F(T; Y) \tag{3.6}$$

with

$$I_F(T; Y) = \int_{-\sqrt{e_1}}^{\sqrt{e_1}} \int_{-\sqrt{e_2}}^{\sqrt{e_2}} \int_{-\infty}^{\infty} f(y|t_1, t_2) \log \left(\frac{f(y|t_1, t_2)}{f(y; F)} \right) dy dF \tag{3.7}$$

where

$$f(y|t_1, t_2) = p_1 \phi(y - t_1) + p_2 \phi(y - t_2) \tag{3.8}$$

$$f(y; F) = \int_{-\sqrt{e_1}}^{\sqrt{e_1}} \int_{-\sqrt{e_2}}^{\sqrt{e_2}} f(y|t_1, t_2) dF(t_1, t_2) \tag{3.9}$$

The main difference between the static amplitude constrained and the time-varying amplitude constrained problems resides in the fact that the channel between T and Y is not an additive channel. Hence $f(y; F)$ is not obtained through a convolution integral and $h(Y|T = (t_1, t_2))$ is not a constant, it takes different values at different (t_1, t_2).

We note that $I_F(T; Y)$ is a concave functional of $F \in \Omega$. Moreover, Ω is a

convex and compact space in the weak topology. Finally, $I_F(T;Y)$ is strictly concave and weakly differentiable in Ω with the mutual information density $i(t_1,t_2;F)$ such that the derivative at $G \in \Omega$ is

$$\frac{d}{dF} I_G(T;Y) = \int_{-\sqrt{e_1}}^{\sqrt{e_1}} \int_{-\sqrt{e_2}}^{\sqrt{e_2}} i(t_1,t_2;F) dG(t_1,t_2) - I_F(T;Y) \tag{3.10}$$

In particular, the mutual information density is

$$i(t_1,t_2;F) = \int_{-\infty}^{\infty} \log\left(\frac{f(y|t_1,t_2)}{f(y;F)}\right) f(y|t_1,t_2) dy \tag{3.11}$$

These claims are parallel to those in [5, 26, 58, 63] and can be proven by following the steps in [58, Appendix]. The convexity and compactness of Ω as well as the concavity and weak differentiability of $I_F(T;Y)$ guarantee the uniqueness of the solution of the optimization problem in (3.6). This enables us to have the following necessary and sufficient optimality conditions for the input distribution [58]:

Theorem 3.1 *Let $F^* \in \Omega$ and let $\mathcal{S}_{F^*}$ indicate the support set of F^*. Then, F^* is optimal if and only if*

$$i(t_1,t_2;F^*) \leq C, \ \forall (t_1,t_2) \in [-\sqrt{e_1},\sqrt{e_1}] \times [-\sqrt{e_2},\sqrt{e_2}] \tag{3.12}$$

$$i(t_1,t_2;F^*) = C, \ \forall (t_1,t_2) \in \mathcal{S}_{F^*} \tag{3.13}$$

where $C = I_{F^*}(T;Y)$.

3.2.2 Numerical Results

We note that the optimality conditions in Theorem 3.1 are numerically verifiable for any fixed input distribution. In particular, any input distribution can be set and the resulting mutual information density can be calculated numerically. We provide an example in Figure 3.2. In this illustration, we consider a binary energy arrival process with $e_1 = 4$ and $e_2 = 1$ and $p_1 = 0.5$. We set the input distribution as a symmetric binary distribution at $(\sqrt{e_1}, \sqrt{e_2})$ and $(-\sqrt{e_1}, -\sqrt{e_2})$. We observe in Figure 3.2 that the resulting mutual information density satisfies the optimality condition in Theorem 3.1. Therefore, we conclude that in this example the symmetric binary distribution at $(\sqrt{e_1}, \sqrt{e_2})$ and $(-\sqrt{e_1}, -\sqrt{e_2})$ is the optimal input distribution. Even though we were unable to prove that optimal input distributions always have finite support, we observe in our numerical experiments that this holds.

In the case of on-off energy arrivals with the probability that E units of energy is harvested with p_{on}, we have

$$f(y|t_2) = (1 - p_{on})\phi(y) + p_{on}\phi(y - t_2) \tag{3.14}$$

Note that similar to the static amplitude constrained AWGN channel [5], if $\sqrt{E}$ is small, the support set of $F^*_{T_2}$ is symmetric binary with two mass points located at $\pm\sqrt{E}$. For $p_{on} = 1$, the problem reduces to Smith's amplitude constrained AWGN capacity problem. In this case, if $\sqrt{E} \leq 1.66$, then symmetric binary distribution for T_2 is optimal and if $\sqrt{E} > 1.66$, optimal distribution of T_2 has more than two mass points [64]. For $p_{on} \neq 1$, the channel between T and Y is different from an AWGN

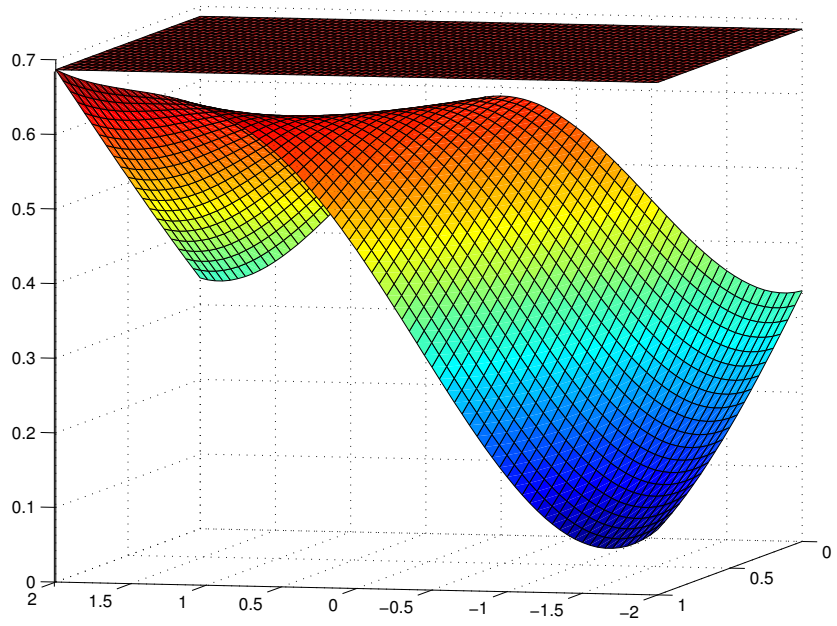

Figure 3.2: Illustration of the mutual information density corresponding to the optimal input distribution when $e_1 = 4$, $e_2 = 1$, $p_1 = 0.5$.

channel; hence, the optimizing distribution is different. To capture this effect, we define a function of p_{on} as follows

$$U(p_{on}) = \max\{x \in \mathbb{R} : g(t_2, x) \leq g(x, x),\ \forall t_2 \in [-x, x]\}$$

where $g(t_2, x)$ is the mutual information density $i(x, t_2; F)$ evaluated at the binary symmetric distribution with two equiprobable mass points located at $-x$ and x. In view of the conditions in Theorem 3.1, $U(p_{on})$ is the highest amplitude constraint under which the binary symmetric distribution is optimum when the energy arrival probability is p_{on}. The function $U(p_{on})$ is monotonically decreasing with p_{on} as shown in Figure 3.3. As p_{on} is decreased, the number of channel uses the nature

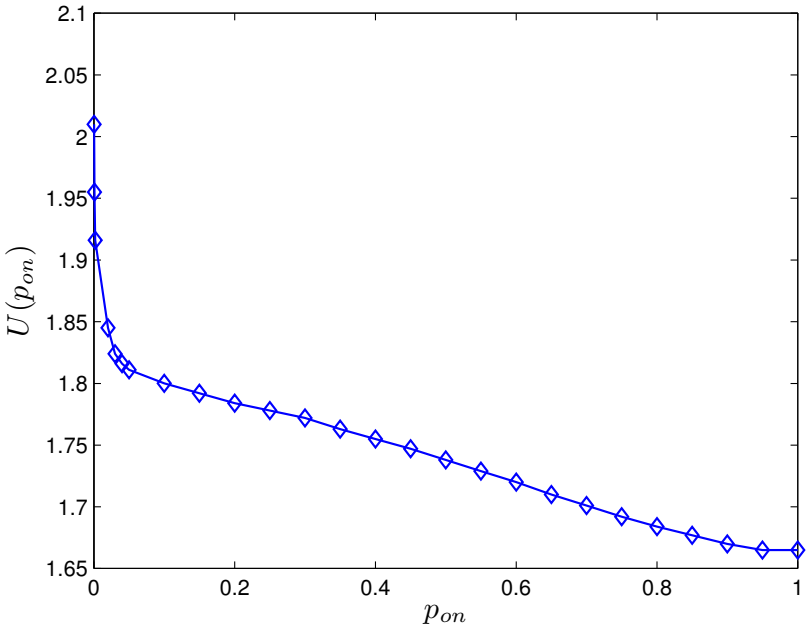

Figure 3.3: $U(p_{on})$ function for the AWGN channel with unit noise power.

allows the transmitter to send a non-zero data symbol decreases and this leads to smaller capacity. We observe in Figure 3.3 that as p_{on} is increased, binary input distribution becomes optimal for a smaller range of amplitude constraints, leading $U(p_{on})$ to be monotonically decreasing.

If perfect information of the energy arrival is available at both the transmitter and the receiver, a multiplexed coding strategy achieves the maximum possible rate and we obtain the capacity in this case as [65]

$$C_{si@both} = \sum_{i=1}^{|\mathcal{E}|} p_i C_{Sm}(\sqrt{e_i}) \tag{3.15}$$

In Figures 3.4 and 3.5, we compare the channel capacity under the on-off energy arrival when the state information is available at the transmitter causally with the

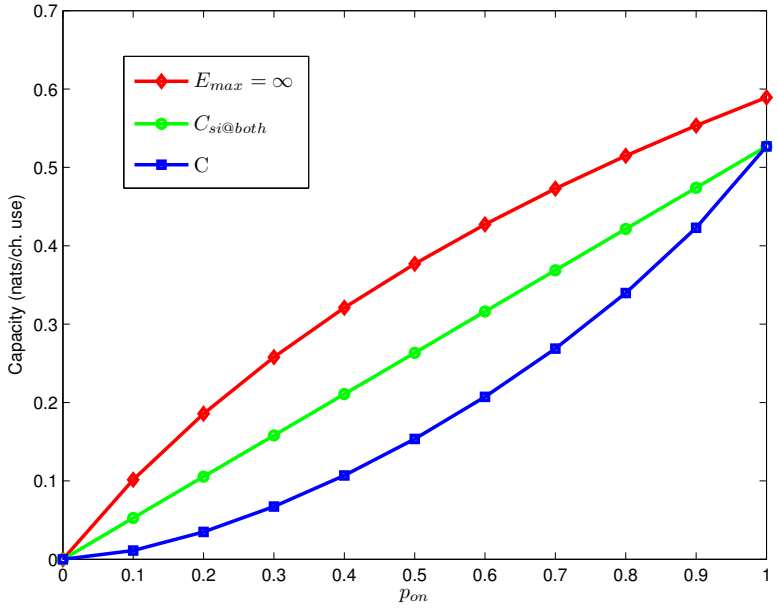

Figure 3.4: Capacity versus p_{on} for $E = 2.25$, i.e., $\sqrt{E} = 1.5$.

capacity when the state (energy arrival) information is available at both sides. We also plot the channel capacity when the battery size is unlimited, i.e., $E_{max} = \infty$, as in [8, 9]. The capacity in this case is $\frac{1}{2}\log(1 + p_{on}E)$. In Figure 3.4, we observe the differences in the capacities for different values of p_{on} when $\sqrt{E} = 1.5$. The capacity achieving input distribution is binary for all p_{on} in this case since $\sqrt{E} = 1.5 < 1.66$. In Figure 3.5, we plot the capacities for different E for a fixed p_{on}. Note that the capacity achieving input distribution changes as E is increased. We show the ranges over which the capacity achieving input distribution is binary, ternary and quaternary in Figure 3.5. In particular, the capacity achieving distribution for (3.15) is the capacity achieving distribution with a constant amplitude constraint $\sqrt{E}$. We observe that the transition from binary to ternary for $C_{si@both}$ occurs at $E = (1.66)^2$ while it occurs for the capacity C with causal state information at the transmitter at

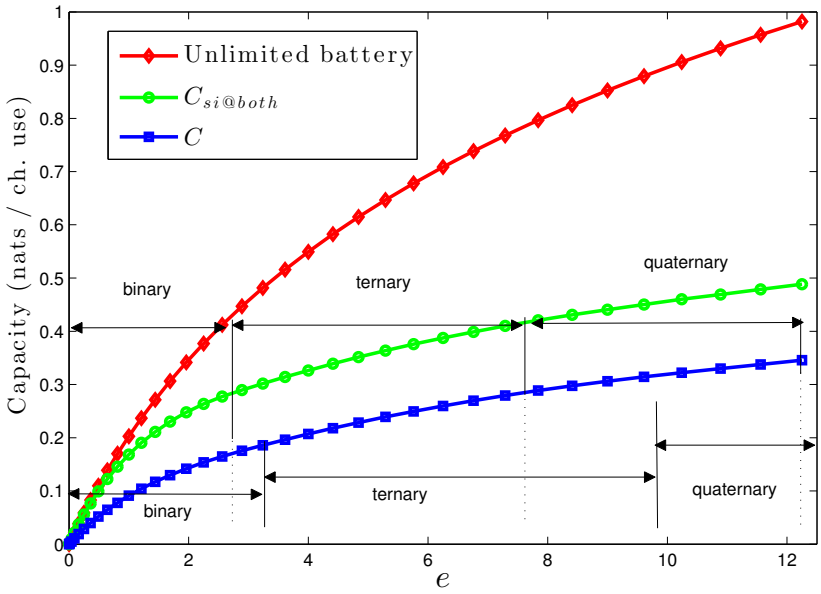

Figure 3.5: Capacity versus E when p_{on}=0.5.

$E = (U(p_{on})|_{p_{on}=0.5})^2 = (1.74)^2$. We also observe that as E gets large, the capacity with an unlimited battery is significantly larger than the capacities with no battery, with or without the state information at the receiver.

3.3 Gaussian Energy Harvesting Multiple Access Channel

We consider two energy harvesting transmitters sending messages over an AWGN MAC as shown in Figure 3.6. Exogenous energy sources supply E_{1i} and E_{2i} amounts of energies to users 1 and 2, respectively, at the ith channel use and upon observing the arrived energy, users send a code symbol whose energy is constrained to the currently available energy. The channel input and output are related as

$$Y_i = X_{1i} + X_{2i} + N_i, \quad i = 1, \ldots, n \tag{3.16}$$

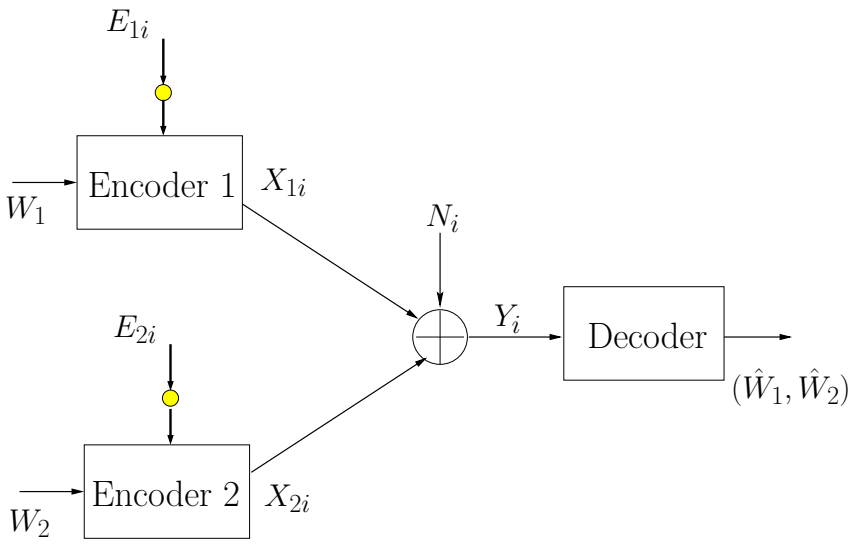

Figure 3.6: The Gaussian MAC with energy harvesting transmitters of zero energy storage.

where X_{1i} and X_{2i} are the channel inputs of users 1 and 2, respectively, and Y_i is the channel output at the ith channel use. N_i is the i.i.d. Gaussian noise distributed as $\mathcal{N}(0,1)$. $E_{11},\ldots,E_{1n}$ and $E_{21},\ldots,E_{2n}$ are i.i.d. (in time) energy arrival sequences which are independent of the messages of the users. The code symbol energy at the ith channel use is constrained according to the exogenous energy arrival. In particular, users 1 and 2 observe E_{1i} and E_{2i} and generate channel inputs X_{1i} and X_{2i} that satisfy $X_{1i}^2 \leq E_{1i}$ and $X_{2i}^2 \leq E_{2i}$, i.e., each code symbol is amplitude constrained to (the square root of) the observed energy.

In this section, we extend our work in the previous section to a MAC where the channel inputs are constrained to possibly correlated time-varying amplitude constraints. We first investigate the case of static amplitude constraints in the MAC setting. The literature on static amplitude constraints has generally covered the single user case [5, 26, 58, 59, 63] for various channels. Reference [66] considers

a MAC with static amplitude constrains and shows that under small amplitude constraints, every point on the boundary of the capacity region is achieved by binary input distributions. The recent independent and concurrent work [67] addresses the sum capacity of the Gaussian MAC with peak power constraints.

The variations in the available energy at the transmitter links the problem of data transmission with an energy harvesting transmitter to the problem of data transmission over state-dependent channels: The energy level at the transmitter is a state that is available to only the transmitter. Single user and multiple access state-dependent channels have been well investigated [55, 68–72]. Specifically, when causal state information at the transmitters is available, Shannon strategies are capacity achieving for the single user state-dependent channels and provide an achievable region for the state-dependent MAC [68–72].

In this section, we first consider the Gaussian MAC with static amplitude constraints and show that the boundary of the capacity region is achieved by discrete input distributions of finite support. We, then, consider a MAC where transmitters are energy harvesting with no battery and provide an achievable region by Shannon strategies applied by each user. We provide numerical illustrations.

3.3.1 Capacity Region of the Gaussian MAC with Static Amplitude Constraints

In this section, we consider the two-user Gaussian MAC with amplitude constrained inputs $|X_1| \leq A_1$ and $|X_2| \leq A_2$. The Gaussian MAC has the conditional density

$p(y|x_1, x_2) = \phi(y - x_1 - x_2)$ where x_1 and x_2 are the channel inputs of users 1 and 2, respectively, y is the channel output and $\phi(\tau) = \frac{1}{\sqrt{2\pi}} e^{-\frac{\tau^2}{2}}$ is the zero-mean unit-variance Gaussian density. The feasible (i.e., amplitude constrained) marginal input distributions are given, respectively, as

$$\Omega_1 = \left\{ F_{X_1} : \int_{-A_1}^{A_1} dF_{X_1} = 1 \right\} \tag{3.17}$$

$$\Omega_2 = \left\{ F_{X_2} : \int_{-A_2}^{A_2} dF_{X_2} = 1 \right\} \tag{3.18}$$

where F_{X_1} and F_{X_2} are the cumulative distribution functions. Given F_{X_1} and F_{X_2}, the following region is achievable [54]:

$$R_1 \leq I(X_1; Y|X_2) \tag{3.19}$$

$$R_2 \leq I(X_2; Y|X_1) \tag{3.20}$$

$$R_1 + R_2 \leq I(X_1, X_2; Y) \tag{3.21}$$

Note that the mutual information terms $I(X_1, X_2; Y)$, $I(X_1; Y|X_2)$ and $I(X_2; Y|X_1)$ are functionals defined from $\Omega_1 \times \Omega_2$ to $\mathbb{R}^+ \cup \{0\}$. The capacity region of the MAC with input amplitude constraints is the convex hull of the union of the pentagons [54] in the form of (3.19)-(3.21).

Since the capacity region is convex [54], the pair of input distributions (F_{X_1}, F_{X_2}) that achieves the boundary of the capacity region are found by solving optimization problems that are parametrized by the slope of the supporting hyperplanes (see Figure 3.7). In particular, the sum-rate optimal pair of distributions that achieves the

time-sharing points between B and C in Figure 3.7 is the solution of the following functional optimization problem:

$$\max_{F_{X_1}\in\Omega_1, F_{X_2}\in\Omega_2} I(X_1, X_2; Y) \tag{3.22}$$

The boundary on the left of the sum-rate optimal points between A and B in Figure 3.7 is achieved by a pair (F_{X_1}, F_{X_2}) that is the solution of the following problem for some $\mu < 1$

$$\max_{F_{X_1}\in\Omega_1, F_{X_2}\in\Omega_2} (1-\mu) I(X_2; Y|X_1) + \mu I(X_1, X_2; Y) \tag{3.23}$$

Similarly, the boundary on the right of the sum-rate optimal points between C and D in Figure 3.7 is achieved by the solution of the following problem for some $\mu > 1$

$$\max_{F_{X_1}\in\Omega_1, F_{X_2}\in\Omega_2} (\mu-1) I(X_1; Y|X_2) + I(X_1, X_2; Y) \tag{3.24}$$

In the sequel, we will focus on the solution of (3.24) since (3.22) is a special case of (3.24) for $\mu = 1$ and the solution of (3.23) follows from symmetry. For convenience, we define the following:

$$\widehat{Y} = X + N \tag{3.25}$$

$$\widetilde{Y} = X_1 + \widetilde{N} \tag{3.26}$$

$$\bar{Y} = X_2 + \bar{N} \tag{3.27}$$

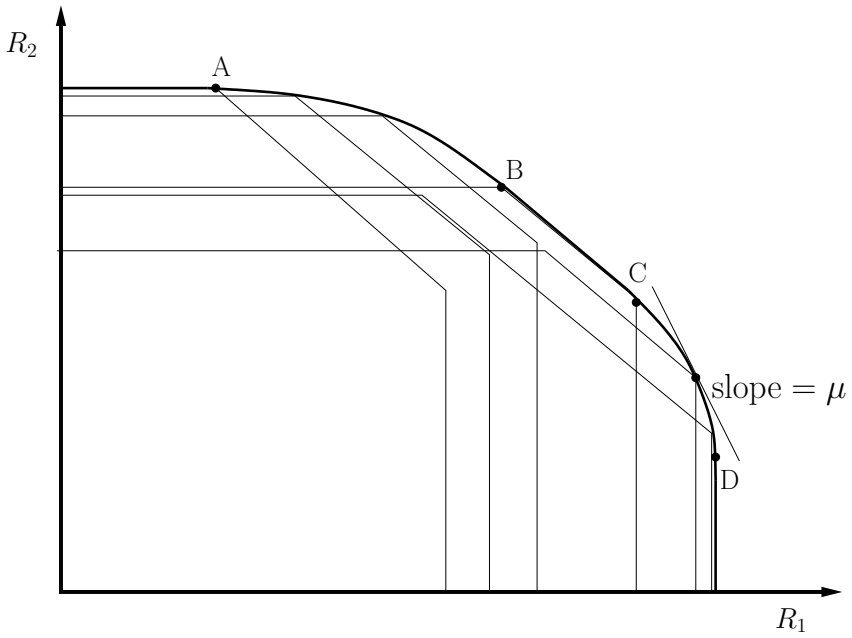

Figure 3.7: The capacity region of Gaussian MAC with amplitude constraints.

where $\widetilde{N} = X_2 + N$ for fixed X_2 and $\bar{N} = X_1 + N$ for fixed X_1. X in (3.25) can be either X_1 or X_2. We therefore note that $I(X_1; Y|X_2) = I(X_1; \widehat{Y})$ and $I(X_2; Y|X_1) = I(X_2; \widehat{Y})$. Moreover, $I(X_1, X_2; Y)$ can be equivalently expressed as $I(X_2; \bar{Y}) + I(X_1; \widehat{Y})$ and as $I(X_1; \widetilde{Y}) + I(X_2; \widehat{Y})$.

We now provide several facts about the objective function and the feasible set in (3.24). The proofs of these facts follow from arguments similar to those in [26, 63] and therefore are skipped here for brevity. We first note that Ω_1 and Ω_2 are convex and sequentially compact function spaces. $I(X_1, X_2; Y)$ is a continuous functional of the tuple (F_{X_1}, F_{X_2}) on $\Omega_1 \times \Omega_2$ and is strictly concave in F_{X_1} given F_{X_2} and vice versa. $I(X_1; Y|X_2) = I(X_1; \widehat{Y})$ and $I(X_2; Y|X_1) = I(X_2; \widehat{Y})$ are strictly concave functionals of only F_{X_1} and only F_{X_2}, respectively. $I(F_{X_1}, F_{X_2})$, an alternative notation for $I(X_1, X_2; Y)$, is Frechet differentiable in both F_{X_1} and F_{X_2}. We use the

relation $I(X_1, X_2; Y) = I(X_2; \bar{Y}) + I(X_1; \widehat{Y})$. Given F_{X_1}, $I(X_1; \widehat{Y})$ is fixed and the derivative of $I(F_{X_1}, F_{X_2})$ with respect to F_{X_2} in the direction of F'_{X_2} is equal to the derivative of $I(X_2; \bar{Y})$, which is [5]:

$$\begin{aligned}\lim_{\theta \to 0} \frac{1}{\theta} \left[I(F_{X_1}, \theta F'_{X_2} + (1-\theta) F_{X_2}) - I(F_{X_1}, F_{X_2}) \right] \\ = \int_{-A_2}^{A_2} h_{\bar{Y}}(x_2; F_{X_1}, F_{X_2}) dF'_{X_2} - h_{\bar{Y}}(F_{X_1}, F_{X_2})\end{aligned} \tag{3.28}$$

where $h_{\bar{Y}}(x_2; F_{X_1}, F_{X_2})$ is the entropy density of $\bar{Y}$ generated by F_{X_1} and F_{X_2}:

$$h_{\bar{Y}}(x_2; F_{X_1}, F_{X_2}) = -\int_{\mathbb{R}} p_{\bar{N}}(y - x_2; F_{X_1}) \log \left(p_{\bar{Y}}(y; F_{X_1}, F_{X_2}) \right) dy$$

where $p_{\bar{N}} = \int_{-A_1}^{A_1} \phi(y - x_1) dF_{X_1}$ is the density of $\bar{N}$ given F_{X_1} and $h_{\bar{Y}}(F_{X_1}, F_{X_2})$ is the entropy of $p_{\bar{Y}}(y; F_{X_1}, F_{X_2})$. Similarly, we can express the derivative of $I(F_{X_1}, F_{X_2})$ given F_{X_2} with respect to F_{X_1} in the direction of any other distribution in Ω_1. $h_{\widetilde{Y}}(x_1; F_{X_1}, F_{X_2})$ is defined similarly given F_{X_2}:

$$h_{\widetilde{Y}}(x_1; F_{X_1}, F_{X_2}) = -\int_{\mathbb{R}} p_{\widetilde{N}}(y - x_1; F_{X_2}) \log \left(p_{\widetilde{Y}}(y; F_{X_1}, F_{X_2}) \right) dy \tag{3.29}$$

where $p_{\widetilde{N}} = \int_{-A_2}^{A_2} \phi(y - x_2) dF_{X_2}$. Finally, we define

$$h_{\widehat{Y}}(x; F_X) = -\int_{\mathbb{R}} \phi(y - x) \log \left(p_{\widehat{Y}}(y; F_X) \right) dy \tag{3.30}$$

where X can be either X_1 or X_2.

Note that in general the problem in (3.24) is not a convex optimization prob-

lem since the independence of X_1 and X_2 causes non-convexity. In particular, the objective function in (3.24) is not concave if it is viewed as a functional of tuples (F_{X_1}, F_{X_2}). On the other hand, it is a strictly concave functional of the joint distribution of (X_1, X_2) but the space of joint distributions generated by independent X_1 and X_2 marginal distributions is not a convex space. Therefore, finding the optimal F_{X_1} and F_{X_2} is challenging.

Note that since the objective function in (3.24) is strictly concave in marginal distributions, the solution of (3.24), denoted as $(F^*_{X_1}, F^*_{X_2})$, necessarily satisfies the KKT optimality conditions. In particular, given $F^*_{X_1}$, the directional derivative of the objective function with respect to F_{X_2} at $F^*_{X_2}$ in any direction must be less than or equal to zero with equality at $F^*_{X_2}$. Note that since $I(X_1; Y|X_2)$ does not depend on X_2 for fixed F_{X_1}, the derivative of the objective function in (3.24) with respect to F_{X_2} in the direction of F'_{X_2} is equal to the derivative in (3.28) and it should be less than or equal to zero for all $F'_{X_2} \in \Omega_2$:

$$\int_{-A_2}^{A_2} h_{\bar{Y}}(x_2; F^*_{X_1}, F^*_{X_2}) dF'_{X_2} \leq h_{\bar{Y}}(F^*_{X_1}, F^*_{X_2}) \tag{3.31}$$

One can show that (3.31) is equivalent to [5]:

$$h_{\bar{Y}}(x_2; F^*_{X_1}, F^*_{X_2}) \leq h_{\bar{Y}}(F^*_{X_1}, F^*_{X_2}), \quad x_2 \in [-A_2, A_2] \tag{3.32}$$

$$h_{\bar{Y}}(x_2; F^*_{X_1}, F^*_{X_2}) = h_{\bar{Y}}(F^*_{X_1}, F^*_{X_2}), \quad x_2 \in S_{F^*_{X_2}} \tag{3.33}$$

where $S_{F^*_{X_2}}$ denotes the support set of $F^*_{X_2}$. Similarly, the corresponding condition

for the directional derivative with respect to F_{X_1} in the direction of F'_{X_1} given $F^*_{X_2}$ yields

$$\int_{-A_1}^{A_1} \left[(\mu-1)h_{\widehat{Y}}(x_1; F^*_{X_1}) + h_{\widetilde{Y}}(x_1; F^*_{X_1}, F^*_{X_2})\right] dF'_{X_1}$$
$$\leq (\mu-1)h_{\widehat{Y}}(F^*_{X_1}) + h_{\widetilde{Y}}(F^*_{X_1}, F^*_{X_2}) \tag{3.34}$$

for all $F'_{X_1} \in \Omega_1$ and we have the equivalent conditions

$$(\mu-1)h_{\widehat{Y}}(x_1; F^*_{X_1}) + h_{\widetilde{Y}}(x_1; F^*_{X_1}, F^*_{X_2})$$
$$\leq (\mu-1)h_{\widehat{Y}}(F^*_{X_1}) + h_{\widetilde{Y}}(F^*_{X_1}, F^*_{X_2}), \quad x_1 \in [-A_1, A_1] \tag{3.35}$$
$$(\mu-1)h_{\widehat{Y}}(x_1; F^*_{X_1}) + h_{\widetilde{Y}}(x_1; F^*_{X_1}, F^*_{X_2})$$
$$= (\mu-1)h_{\widehat{Y}}(F^*_{X_1}) + h_{\widetilde{Y}}(F^*_{X_1}, F^*_{X_2}), \quad x_1 \in S_{F^*_{X_1}} \tag{3.36}$$

Note that for given $F^*_{X_1}$, $I(X_1; Y|X_2)$ does not depend on F_{X_2}; however, for given $F^*_{X_2}$, both terms in the objective function (3.24) depend on F_{X_1}.

Next, we show that the necessary optimality conditions in (3.32)-(3.33) and (3.35)-(3.36) imply that the solution of (3.24), which is guaranteed to exist due to the continuity of the objective function and the compactness of the input distribution space, must be a discrete distribution. We first show that the conditions in (3.32)-(3.33) imply that $F^*_{X_2}$ is discrete. Note that given $F^*_{X_1}$, (3.32)-(3.33) are optimality conditions for finding the capacity of the single user channel between X_2 and $\bar{Y} = X_2 + \bar{N}$. We claim that for *any* $F^*_{X_1} \in \Omega_1$, $p_{\bar{N}}(y) = \int \phi(y - x_1) dF^*_{X_1}$ is in the class of noise densities in [63] for which the optimal input distribution is discrete under an

amplitude constraint. Specifically, we verify the conditions i-iv in [63]: $p_{\bar{N}}(y) > 0$ for all $y \in \mathbb{R}$ and $E[|Z|^2] < \infty$. Moreover, $p_{\bar{N}}(z) = \int \phi(z - x_1) dF^*_{X_1}$ is analytic over the whole complex plane $\mathbb{C}$. It suffices to use the analyticity of $p_{\bar{N}}(z)$ over the region $|\Im(z)| < \delta$ for some $\delta > 0$. We next define:

$$L(|\Re(z)|) \triangleq \frac{1}{\sqrt{2\pi}} e^{-\frac{1}{2}(|\Re(z)|^2 + A_2^2 + 2A_2|\Re(z)|)} \tag{3.37}$$

$$U(|\Re(z)|) \triangleq \frac{1}{\sqrt{2\pi}} e^{-\frac{1}{2}((|\Re(z)|)^2 - 2A_2|\Re(z)| - \delta^2)} \tag{3.38}$$

One can show that $0 < L(|\Re(z)|) \leq |p_Z(z)| \leq U(|\Re(z)|)$ for all $z \in \mathbb{C}$ with $|\Im(z)| < \delta$ and $|\Re(z)| > k$ where k is sufficiently large. Moreover, for this selected k, $-\int_k^\infty U(\tau) \log(U(\tau))\, d\tau < \infty$ and $\int_{x+k}^\infty \frac{U^3(\tau - x)}{L^2(\tau)} d\tau$ for all $x \in \mathbb{R}$. This proves that the support set of $F^*_{X_2}$ is a discrete set for any given *arbitrary distribution* $F^*_{X_1}$ in Ω_1.

Now, we prove that conditions in (3.35)-(3.36) imply that $F^*_{X_1}$ is discrete given $F^*_{X_2}$ in Ω_2. To this end, we assume $S_{F^*_{X_1}}$ is infinite and reach a contradiction. By Bolzano-Weirestrass Theorem, $S_{F^*_{X_1}}$ has an accumulation point. Note that $\int \phi(y - x_1) \log\left(p_{Y|X_2}(y; F^*_{X_1})\right) dy$ and $\int p_{\widetilde{N}}(y - x_1) \log\left(p_{\widetilde{Y}}(y; F^*_{X_1}, F^*_{X_2})\right) dy$ are analytic functions of x_1 and they have extension over the whole complex plane $\mathbb{C}$. By identity theorem of complex analysis and the optimality condition in (3.34), we have

$\forall x_1 \in \mathbb{C}$ and in particular $\forall x_1 \in \mathbb{R}$:

$$(\mu-1)\int_{\mathbb{R}} \phi(y-x_1)\log\left(p_{\widehat{Y}}(y;F^*_{X_1})\right)dy + \int_{\mathbb{R}} p_{\widetilde{N}}(y-x_1)\log\left(p_{\widetilde{Y}}(y;F^*_{X_1},F^*_{X_2})\right)dy = D \tag{3.39}$$

where $D = -(\mu-1)h_{\widehat{Y}}(F^*_{X_1}) - h_{\widetilde{Y}}(F^*_{X_1},F^*_{X_2})$. However, (3.39) causes a contradiction. Note that $p_{\widehat{Y}}(y;F^*_{X_1})$ is a well defined density function and hence $\log\left(p_{\widehat{Y}}(y;F^*_{X_1})\right) \to -\infty$ as $y \to \infty$. Consequently, $\int_{\mathbb{R}} \phi(y-x_1)\log\left(p_{\widehat{Y}}(y;F^*_{X_1})\right)dy$ also diverges to $-\infty$ as x_1 gets large since the window of $\phi(y-x_1)$ integrates over large y values if x_1 is selected sufficiently large. Since $p_{\widetilde{N}}(y) = \int_{-A_2}^{A_2} \phi(y-x_2)dF_{X_2}$ shows the same windowing property as the Gaussian pdf $\phi(.)$ in view of the fact that A_2 is finite, we have $\int_{\mathbb{R}} p_{\widetilde{N}}(y-x_1)\log\left(p_{\widetilde{Y}}(y;F^*_{X_1},F^*_{X_2})\right)dy \to -\infty$ as $x_1 \to \infty$. This contradicts (3.39). Therefore, we have the following theorem:

Theorem 3.2 *$S_{F^*_{X_1}}$ and $S_{F^*_{X_2}}$ are finite sets.*

Theorem 3.2 states that rate tuples on the boundary of the capacity region of the Gaussian MAC with amplitude constraints is achieved by discrete input distributions of finite support. In [66, Proposition 3], Verdú observed that if the output distributions p_Y, $p_{Y|X_1}$ and $p_{Y|X_2}$ are all unimodal, which holds if amplitude constraints are sufficiently small, then the capacity region is the pentagon generated by independent equiprobable binary input distributions located at $\pm A_1$ and $\pm A_2$. Recently, independent and concurrent work in [67] showed that the sum capacity of the Gaussian MAC is achieved by discrete distributions. Theorem 3.2 generalizes

Smith's result for a single user AWGN channel [5] to an AWGN MAC, and the results in [66, 67] to the entire region.

3.3.2 Achievable Rate Region for the Gaussian Energy Harvesting MAC with Zero Energy Storage

In this section, we consider the Gaussian MAC where the energy required for data transmission is maintained by an exogenous joint energy arrival process and users have no battery to save energy. For convenience, we consider only two users and assume that the energy harvesting processes at both users take binary values $\mathcal{E}_1 = \{e_{11}, e_{12}\}$ and $\mathcal{E}_2 = \{e_{21}, e_{22}\}$. However, our analysis can be generalized for any finite value of $|\mathcal{E}_1|$ and $|\mathcal{E}_2|$. The joint energy arrival process is i.i.d. in time with $P(E_{1i} = e_{1k}, E_{2i} = e_{2l}) = p_{kl}$ for all i where $\sum_{k,l} p_{kl} = 1$. $p_1 = \sum_l p_{1l}$ is the marginal probability that e_{11} arrives at user 1 and $p_2 = \sum_k p_{k1}$ is the marginal probability that e_{21} arrives at user 2.

The amplitude constraints on x_1 and x_2 are time-varying according to the energy arrival process. Users 1 and 2 have messages $w_1 \in \mathcal{W}_1$ and $w_2 \in \mathcal{W}_2$, respectively. As the energies available for users at each channel use vary as an i.i.d. process and is independent of the messages of the users w_1, w_2, the resulting channel is an instance of a state-dependent MAC with causal state information at the users where the state is the available energy of users. In particular, we can associate four different states (k, l), $k, l = 1, 2$ where at each state (k, l), we have $|X_1| \leq \sqrt{e_{1k}}$ and $|X_2| \leq \sqrt{e_{2l}}$.

Capacity region of state-dependent MAC is still unknown; however, Shannon strategies provide an achievable region [69]. In particular, let the state information at the users be S_{U_1} and S_{U_2}, respectively, which are in general dependent. Let deterministic functions of S_{U_1} and S_{U_2} be $T_1 = f_1(S_{U_1})$ and $T_2 = f_2(S_{U_2})$. Then, the following rate region is achievable:

$$R_1 \leq I(T_1; Y|T_2) \tag{3.40}$$

$$R_2 \leq I(T_2; Y|T_1) \tag{3.41}$$

$$R_1 + R_2 \leq I(T_1, T_2; Y) \tag{3.42}$$

Achievability of the region in (3.40)-(3.42) follows from [69, Section IV]. Note that the state of the channel in the energy harvesting MAC problem has two components (the energy arrivals at the two users) as in [71] and only one or both components of the state may be available to the users. In the following, we study achievable rate regions using Shannon strategies under the availability of one or both of the components of the energy state to the users.

- **Joint Energy Arrival Information Available at Both Users**

  When the state information (e_{1k}, e_{2l}) is available to both users perfectly, full state information of the multiple access channel is available at the users. Let $T_{kl}^{(1)}$ and $T_{kl}^{(2)}$ denote the code symbols generated by users 1 and 2, respectively, upon observing that the joint energy arrival $(E_1, E_2) = (e_{1k}, e_{2l})$, $k, l = 1, 2$, occurred. The conditional density of the extended MAC with inputs $T_{kl}^{(1)}$ and

$T_{kl}^{(2)}$ and output Y is:

$$p(y|t_{kl}^{(1)}, t_{kl}^{(2)}) = \sum_{kl} p_{kl}\phi(y - t_{kl}^{(1)} - t_{kl}^{(2)}) \tag{3.43}$$

where $|T_{kl}^{(1)}| \leq \sqrt{e_{1k}}$ and $|T_{kl}^{(2)}| \leq \sqrt{e_{2l}}$. For $k, l = 1, 2$, $\{T_{kl}^{(1)}\}$ and $\{T_{kl}^{(2)}\}$ are jointly distributed and $\{T_{kl}^{(1)}\}$ are independent of $\{T_{kl}^{(2)}\}$. The region in (3.40)-(3.42) evaluated for $T_1 = T_{kl}^{(1)}$ and $T_2 = T_{kl}^{(2)}$ is achievable. Achievability of this region also follows from [70, Theorem 3]. Moreover, [70, Theorem 3] provides an outer bound for the capacity region by allowing cooperation between the users.

- **Each User Has Its Own Energy Arrival Information**

Now, we consider the scenario in which user 1 does not know the energy arrival of user 2 and vice versa. This scenario can be viewed as a state-dependent MAC with partial state information at the transmitter as in [69] or with only a component of the state available to each user as in [71]. However, note that the components of the states may not be independent unlike [71]. Let $T_k^{(1)}$ and $T_l^{(2)}$ denote the code symbols generated by users 1 and 2, respectively, upon user 1's observation that $E_1 = e_{1k}$, $k = 1, 2$, occurred and user 2's observation that $E_2 = e_{2l}$, $l = 1, 2$ occurred. The resulting extended input alphabet with inputs $T_k^{(1)}$ and $T_l^{(2)}$ and output Y has the following conditional density

$$p(y|t_k^{(1)}, t_l^{(2)}) = \sum_{kl} p_{kl}\phi(y - t_k^{(1)} - t_l^{(2)}) \tag{3.44}$$

where $|T_k^{(1)}| \leq \sqrt{e_{1k}}$, $k = 1, 2$ and $|T_l^{(2)}| \leq \sqrt{e_{2l}}$, $l = 1, 2$. $T_1^{(1)}, T_2^{(1)}$ are jointly distributed and they are independent of the other jointly distributed pair $T_1^{(2)}$ and $T_2^{(2)}$. The rate region evaluated at $T_1 = T_k^{(1)}$ and $T_2 = T_l^{(2)}$ in (3.40)-(3.42) is achievable. We note that if energy arrivals of the users E_1 and E_2 are independent, then the users have independent channel state information and the sum-rate yielded by Shannon strategies is the sum-rate capacity from [69, Theorem 4].

In both cases, the boundary of the achievable region is found by solving optimization problems as in (3.22)-(3.24) by replacing the sum rate and individual rate constraints accordingly.

For both of the possible available information cases, the general shape of the achievable rate region is as in Figure 3.7. At points D and A, users 1 and 2, respectively, achieve maximum single user rates with Shannon strategies $C_{Sh}^{(1)}$ and $C_{Sh}^{(2)}$. To illustrate, $C_{Sh}^{(1)}$ is the maximum mutual information between the input and output of the following extended input channel:

$$p(y|t_1, t_2) = p_1\phi(y - t_1) + (1 - p_1)\phi(y - t_2) \tag{3.45}$$

where $|t_1| \leq \sqrt{e_{11}}$, $|t_2| \leq \sqrt{e_{12}}$. p_1 is the marginal probability that e_{11} arrives. We note that $C_{Sh}^{(1)}$ or $C_{Sh}^{(2)}$ can always be achieved by letting $X_2 = 0$ or $X_1 = 0$ for any energy arrival, i.e., by creating no interference for the other user.

Note that in the MAC setting, individual users may achieve higher rates than $C_{Sh}^{(1)}$ or $C_{Sh}^{(2)}$. The potential boost in single user rates can be provided by the other

user's help: If the energy arrivals of the users are correlated or one user knows the other user's energy state information, then that user may convey the energy state information to the receiver using block Markov encoding [71] and the receiver then decodes the other user's message given this state information. This way, a user may better help the other one than just creating no interference.

3.3.3 Numerical Results

In this section, we numerically study the optimal input distributions and the resulting capacity or achievable regions.

- **Static Amplitude Constraints**

  First, we focus on small amplitude constraints. We numerically observe that for the unit noise variance, if $A_1 \leq 1.3$ and $A_2 \leq 1.3$, the unimodality condition in [66, Proposition 3] holds and binary input distributions are optimal. We numerically verify[1] that indeed binary distributions are optimal for $A_1 \leq 1.6$ and $A_2 \leq 1.6$.

  We let $A_1 = 1.3$ and $A_2 = 2$. The single user capacity under $A_1 = 1.3$ is achieved by symmetric binary distribution at ± 1.3 and the single user capacity under $A_2 = 2$ is achieved by ternary distribution located at 0 and ± 2. We observe in our numerical study[2] that the optimal input distribution for user 1 is always binary for any $\mu \geq 0$ and this enables us to determine the capacity

[1] We numerically verify the necessary optimality conditions in (3.32)-(3.33) and (3.35)-(3.36) for the binary distribution.

[2] By numerically studying (3.32)-(3.33) and (3.35)-(3.36), we observe that for any X_2 distribution, binary distribution on X_1 maximizes $I(X_1; X_1 + X_2 + N)$.

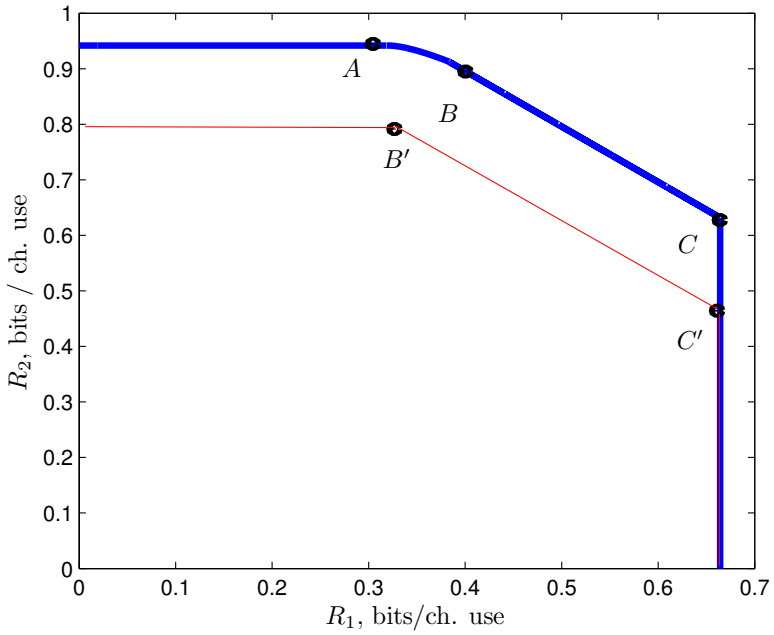

Figure 3.8: The capacity regions of Gaussian MAC under amplitude constraints $A_1 = 1.3$, $A_2 = 1.6$ (the smaller region) and $A_1 = 1.3$ and $A_2 = 2$ (the larger region).

region for this particular case. However, the optimal input distribution for user 2 varies: for $\mu = 1$, i.e., for the maximum sum-rate, binary input distribution is optimal. For some $\mu < 1$, ternary input distribution is optimal.

We plot the resulting capacity region with $A_1 = 1.3$ and $A_2 = 2$ in Figure 3.8 and compare it with the capacity region with $A_1 = 1.3$ and $A_2 = 1.6$. We observe that the latter capacity region is a pentagon and the optimal distributions are binary for both users. When the amplitude constraint of user 2 is increased, the capacity region becomes curved.

- **On-Off Energy Arrivals**

  Next, we consider binary on-off energy arrivals with $e_{11} = 0$, $e_{12} = 1$, $e_{21} = 0$

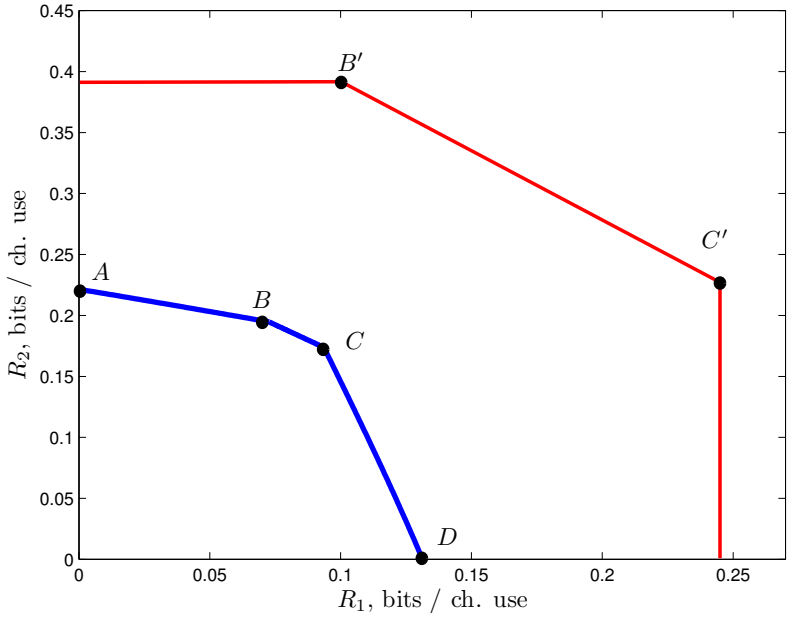

Figure 3.9: The achievable region (the smaller region) and an outer bound (the larger region) for the Gaussian MAC under on-off energy arrivals with causal individual energy state information at the users.

and $e_{22} = 2.25$. $p_{kl} = 0.25$ for all $k, l = 1, 2$, i.e., the energy arrivals of the users are independent. We plot in Figure 3.9 (the smaller region) the achievable rate region under only individual energy state information. We observe that the single user rates $C_{Sh}^{(1)}$ and $C_{Sh}^{(2)}$ are achievable only if the other user's rate is zero. We also observe that the optimal sum-rate is achieved by binary input distributions. Note that since the energy arrivals of the users are independent, by [69, Theorem 4] the sum-rate capacity is the optimal sum-rate achieved by Shannon strategies. Next, we plot in Figure 3.9 (the larger region) the capacity region when energy state information is available to the transmitters and the receiver, which is an outer bound for the case of state information at only the transmitters. Note that this region is obtained by averaging the regions

constrained by amplitude constraints due to each energy arrival over the joint energy arrival process. There is a large gap between the achievable region and the outer bound. This is partly because the naive Shannon strategy does not take advantage of block Markov encoding [71]. However, there is strong evidence from the numerical results in Section 3.2 that the achievable rates under energy state information at only the transmitters may be significantly lower than those under energy state information at both sides. We also observe in our numerical study that the cooperative outer bound in [70, Theorem 3] yields a looser outer bound.

3.4 Energy State Amplification in the Single User Gaussian Energy Harvesting Channel

In this section, we revisit the single user AWGN channel with an energy harvesting transmitter in Section 3.2. In particular, the channel input and output are related as

$$Y_i = X_i + N_i \tag{3.46}$$

where X_i is the channel input, Y_i is the channel output, and N_i is the i.i.d. zero-mean unit-variance Gaussian noise, in the ith channel use. $E_1, \ldots, E_n$ is the i.i.d. energy arrival sequence which is independent of the message. The code symbol energy at the ith channel use is constrained according to the exogenous energy arrival and the

availability of a battery (energy buffer) at the transmitter. In particular, if there is no battery at the transmitter, the transmitter observes E_i and generates a channel input X_i that satisfies $X_i^2 \leq E_i$, i.e., the code symbol is amplitude constrained to (the square root of) the observed energy. In the other extreme, if the transmitter has an unlimited battery, some portion of the arriving energy can be stored in the battery and the code symbol energy at the ith channel use is constrained to the energy in the battery at the beginning of the ith channel use.

In Chapter 2 and Section 3.2, the sole purpose of the transmitter is to convey the message which is independent of the energy arrival process. However, the transmitter may help the receiver get some information about the energy arrival process at the transmitter. In this section, we analyze the interaction between the message transmission rate and the receiver's information about the energy arrival process at the transmitter. In particular, there is a trade-off between these two objectives in view of the connection of this setting with state-dependent channels with causal state information at the transmitter. This trade-off has been well studied for state-dependent channels with causal or noncausal state information at the transmitter [19, 20, 73–75] where the information the receiver can learn about the state is measured by different metrics.

We use *entropy reduction* metric used in [20] and characterize the fundamental trade-off between the *entropy reduction* Δ of transmitter's energy arrivals at the receiver and the message transmission rate R in an energy harvesting communication system with causal energy state information at the transmitter only. When the transmitter has no battery, we find the optimal (R, Δ) trade-off points using

Shannon strategies. When the transmitter has an unlimited battery, we show that the optimal trade-off region has a simple form. Specifically, no information about the energy arrival process at the transmitter can be obtained at the receiver when the system is operated at the highest message rate. Finally, we propose an uncoded state amplification scheme that splits the energy between message transmission and entropy reduction.

3.4.1 Energy State Amplification with Zero Energy Storage

In this section, we revisit the energy harvesting transmitter with zero energy storage over an AWGN channel. For simplicity of exposition, we consider a binary energy arrival process with alphabet $\mathcal{E} = \{e_1, e_2\}$ and probabilities $P(E_i = e_1) = p_{e_1}$ and $P(E_i = e_2) = p_{e_2}$ for all i.

As the energy at each channel use varies as an i.i.d. process and is independent of the message $w \in \mathcal{W}$, the resulting channel is a state-dependent channel with causal state information at the transmitter. The transmitter helps the receiver estimate the energy arrived at the transmitter's side while sending a message $w \in \mathcal{W}$ at the same time where $|\mathcal{W}| = 2^{nR}$. The receiver forms a list $L_n(Y^n) \subset \mathcal{E}^n$ of possible energy arrival sequences upon receiving the sequence Y^n. Before receiving Y^n, the size of the list is $2^{nH(E)}$, the size of the typical set of energy arrival sequences. Upon receiving Y^n, the list size drops to $|L_n(Y^n)|$. Hence, the energy arrival sequence

uncertainty reduction rate is

$$\Delta = \frac{1}{n}(H(E^n) - \log_2 |L_n(Y^n)|) \tag{3.47}$$

A $(2^{nR}, 2^{n\Delta}, n)$ code is composed of an encoder map $X^n : \mathcal{W} \times \mathcal{E}^n \to \mathcal{R}^n$ where $X_i = \mathcal{W} \times \mathcal{E}^i \to \mathcal{R}$, $i = 1, \ldots, n$ since only causal information of energy arrivals is available. In particular, $|X_i(w, E_i)| \leq \sqrt{E_i}$ for all $w \in \mathcal{W}$ and $E_i \in \mathcal{E}$. The receiver performs two decoding operations after receiving the sequence Y^n: decoding the message $w \in \mathcal{W}$ and list decoding the energy arrival sequence $\{E_i\}_{i=1}^n$. A rate-entropy reduction pair (R, Δ) is achievable if there exists a sequence of $(2^{nR}, 2^{n\Delta}, n)$ codes with probabilities of message and list decoding errors converging to zero as the block length is increased. The optimal trade-off region $\mathcal{R}$ is the closure of all achievable (R, Δ) pairs.

We first note that $\mathcal{R}$ is a convex region [20]. In view of [20, Theorem 2] and replacing the auxiliary variable U with Shannon strategy (T_1, T_2) where T_i is the channel input when energy E_i is observed, the region $\mathcal{R}$ is characterized as

$$R \leq I(T_1, T_2; Y) \tag{3.48}$$

$$\Delta \leq H(E) \tag{3.49}$$

$$R + \Delta \leq I(X, E; Y) \tag{3.50}$$

for some (T_1, T_2) with amplitude constraints $|T_1| \leq \sqrt{E_1}$, $|T_2| \leq \sqrt{E_2}$ and

$$p(y|t_1, t_2) = p_{e_1}\phi(y - t_1) + p_{e_2}\phi(y - t_2) \tag{3.51}$$

where $\phi(y) = \frac{1}{\sqrt{2\pi}} e^{-\frac{y^2}{2}}$. We denote the interval $[-\sqrt{e_i}, \sqrt{e_i}]$ as $\mathcal{T}_i$, $i = 1, 2$. The received signal has pdf $p(y)$

$$p(y) = \int_{\mathcal{T}_1} \int_{\mathcal{T}_2} \left(p_{e_1}\phi(y - t_1) + p_{e_2}\phi(y - t_2)\right) dF_{T_1,T_2}(t_1, t_2)$$

If the goal of the encoder is only to transmit messages and not to assist the receiver to list decode the energy arrival sequence, the maximum achievable rate C_0 is:

$$C_0 = \max_{F_{T_1,T_2} \in \Omega} I(T_1, T_2; Y) \tag{3.52}$$

where the set of feasible distributions is

$$\Omega = \left\{ F : \int_{\mathcal{T}_1} \int_{\mathcal{T}_2} dF(t_1, t_2) = 1 \right\} \tag{3.53}$$

On the other extreme, if the goal of the encoder is only to *amplify* the arrived energy, optimal reduction in the entropy is

$$\Delta^* = \min\{H(E), \max_{F_{T_1,T_2} \in \Omega} I(X, E; Y)\} \tag{3.54}$$

Note that $I(X, E; Y) = h(Y) - \frac{1}{2}\log_2(2\pi e)$, that is, $h(Y|X, E)$ is equal to the

entropy of the Gaussian noise.

3.4.2 Optimal Input Distributions

As $\mathcal{R}$ is a convex region and due to its characterization in (3.48)-(3.50), one can show after algebraic rearrangements that the boundary of $\mathcal{R}$ is obtained by solving the following optimization problems for all $\mu \geq 0$:

$$\max_{F_{T_1,T_2} \in \Omega} \mu I(T_1, T_2; Y) + h(Y) \tag{3.55}$$

The problem in (3.55) is a convex functional optimization problem. As a first step, we note that the space of feasible distributions Ω is a convex and compact set and the objective function in (3.55) is concave in the input distribution in the weak topology. Next, we obtain an optimality condition in terms of the mutual information density, the entropy density and the support set of the optimal input distribution. In particular, the mutual information density and entropy density are given, respectively, as

$$i(t_1, t_2; F) = \int_{-\infty}^{\infty} \log_2 \left(\frac{f(y|t_1, t_2)}{f(y; F)} \right) f(y|t_1, t_2) dy \tag{3.56}$$

$$h(t_1, t_2; F) = -\int_{-\infty}^{\infty} \log_2 \left(f(y; F) \right) f(y|t_1, t_2) dy \tag{3.57}$$

As we emphasized in Section 3.2, Ω is convex and compact; $I(T_1, T_2; Y)$ and $h(Y)$ are both concave and weakly differentiable functionals of F. Therefore, we have the following necessary and sufficient optimality conditions for the optimal input

distribution:

Theorem 3.3 *For the optimal input distribution F^*, we have*

$$\mu i(t_1, t_2; F^*) + h(t_1, t_2; F^*) \leq \mu I(F^*) + h(F^*), \quad \forall (t_1, t_2) \in \mathcal{T}_1 \times \mathcal{T}_2 \tag{3.58}$$

$$\mu i(t_1, t_2; F^*) + h(t_1, t_2; F^*) = \mu I(F^*) + h(F^*), \quad \forall (t_1, t_2) \in \mathcal{S}_{F^*} \tag{3.59}$$

where $\mathcal{S}_{F^*}$ is the support set of F^*.

3.4.3 Energy State Amplification with Unlimited Energy Storage

In this section, we consider the state amplification problem with an energy harvesting transmitter that has an unlimited battery. At each channel use, the energy arrival replenishes, while the code symbol energy reduces, the battery energy. Hence, the code symbol at the beginning of a channel use is constrained by the current energy level in the battery:

$$\sum_{i=1}^{k} X_i^2 \leq \sum_{i=1}^{k} E_i, \qquad k = 1, \ldots, n \tag{3.60}$$

We assume that the transmitter has only causal information; however, it will be clear that the trade-off region is invariant under causal or noncausal information. At the ith channel use, transmitter has the observations $E_1, \ldots, E_i$ and determines the code symbol accordingly. State amplification problem in this setting is to characterize the achievable information rate R and entropy reduction Δ of the energy arrival sequence at the receiver side under the code symbol constraints in (3.60).

We determined in Chapter 2 that the maximum rate of information achievable under the input constraints in (3.60) and causal or noncausal information of the energy arrival information is

$$C_\infty = \frac{1}{2}\log_2\left(1 + \mathbb{E}[E_i]\right) \tag{3.61}$$

In addition, the entropy reduction is bounded by the entropy of the energy arrival process as $\Delta \leq H(E)$. It remains to determine the bound on $R + \Delta$:

$$\begin{aligned} n(R+\Delta) &\leq I(W;Y^n) + I(E^n;Y^n) + n\epsilon_n && (3.62)\\ &\leq I(W;Y^n|E^n) + I(E^n;Y^n) + n\epsilon_n && (3.63)\\ &\leq I(W,E^n;Y^n) + n\epsilon_n && (3.64)\\ &\leq I(X^n,E^n;Y^n) + n\epsilon_n && (3.65)\\ &\leq \sum_{i=1}^{n} I(X_i,E_i;Y_i) + \epsilon_n && (3.66) \end{aligned}$$

where (3.63) is due to the independence of the message W and the energy arrival E and conditioning reduces entropy, (3.65) is due to the data processing inequality and the fact that X_i is a function of W and $E_1,\ldots,E_i$, and (3.66) is due to the memoryless property of the AWGN channel. We note that $I(X_i,E_i;Y_i) = h(Y_i) -$

$\frac{1}{2}\log_2(2\pi e)$. Hence, we get:

$$R + \Delta \leq \frac{1}{n}\sum_{i=1}^{n} h(Y_i) - \frac{1}{2}\log_2(2\pi e) \tag{3.67}$$

$$\leq \frac{1}{n}\sum_{i=1}^{n} \frac{1}{2}\log_2\left(2\pi e \mathbb{E}[Y_i^2]\right) - \frac{1}{2}\log_2(2\pi e) \tag{3.68}$$

$$\leq \frac{1}{2}\log_2(1 + \mathbb{E}[E_i]) \tag{3.69}$$

where (3.68) is due to the fact that Gaussian distribution maximizes entropy, and (3.69) is due to the concavity of $\log_2(1+x)$ and since $\sum_{i=1}^{n}\mathbb{E}[Y_i^2] \leq n\mathbb{E}[E_i] + n$, which follows from the constraints in (3.60).

On the other hand, the bound in (3.69) is achievable by a combination of the best-effort-transmit scheme (or the save-and-transmit scheme) in Chapter 2 with the random binning in [20]. In particular, we consider a block-by-block encoding scheme of B blocks; each block is of n channel uses. We consider a single i.i.d. Gaussian codebook with average power $\mathbb{E}[E_i] - \epsilon$ composed of $2^{n\frac{1}{2}\log_2(1+\mathbb{E}[E_i]-\epsilon)}$ codewords with block length n. In each block, we allocate $0 \leq R \leq \frac{1}{2}\log_2(1 + \mathbb{E}[E_i] - \epsilon)$ bits for the message transmission and remaining $\Gamma = \frac{1}{2}\log_2(1 + \mathbb{E}[E_i] - \epsilon) - R$ bits for state amplification. Hence, we have 2^{nR} bins each composed of $2^{n\Gamma}$ sequences, i.e., we divide the index interval $[1 : 2^{n\frac{1}{2}\log_2(1+\mathbb{E}[E_i]-\epsilon)}]$ into 2^{nR} intervals $[w2^{n\Gamma} : (w+1)2^{n\Gamma}]$, $w = 1, \ldots, 2^{nR} - 1$ where w is a message index. In the first block, an arbitrary codeword independent of the energy arrival sequence is sent. The transmitter observes the energy arrival sequence $E_1, \ldots, E_n$, maps it to one of $2^{n\Gamma}$ indices independent of the message w. Then, according to the chosen message index

w, the codeword to be sent is determined. The transmitter uses the best-effort-transmit scheme: if the energy of the code symbol X_i in the ith channel use is higher than the energy in the battery E_{b_i} (i.e., $X_i^2 > E_{b_i}$), then a zero symbol is put; otherwise, the code symbol X_i is sent as it is. The codeword $X_1, \ldots, X_n$ is sent with only finitely many mismatches as $X_i^2 > E_{b_i}$ occurs only in finitely many channel uses and this causes no error in the decoding of the sent codeword [8, 9]. As $X_1, \ldots, X_n$ is decoded at the receiver side with vanishing probability of error, the receiver recovers the message index w and the bin index for the observed energy arrival sequence as the block length n gets larger. If we allow B increase and $\epsilon \to 0$, we have $R + \Delta \leq \frac{1}{2} \log_2 (1 + \mathbb{E}[E_i])$.

Theorem 3.4 *In an energy harvesting transmitter with an unlimited battery, the optimal* (R, Δ) *region is:*

$$\Delta \leq H(E) \tag{3.70}$$

$$R + \Delta \leq \frac{1}{2} \log_2 (1 + \mathbb{E}[E]) \tag{3.71}$$

We observe in Theorem 3.4 that the optimal trade-off region in the unlimited battery case is expressed explicitly in a simple form and the maximum entropy reduction Δ^* is

$$\Delta^* = \min \left\{ H(E), \frac{1}{2} \log_2 (1 + \mathbb{E}[E]) \right\} \tag{3.72}$$

We also observe that in the unlimited battery case, the entropy reduction is zero

when the transmitter operates at the information transmission capacity C_∞. In this case, the received sequence Y^n is almost independent of the energy arrival profile E^n even though the message transmission is enabled by the energy E^n. Therefore, the unlimited sized energy queue acts as an information hider [76] and the receiver can get no information about the energy arrival sequence if the message transmission is performed at the capacity. Finally, the (R, Δ) region in Theorem 3.4 remains unchanged if the transmitter had noncausal information of the energy arrivals.

3.4.4 An Uncoded State Amplification Scheme

In this section, we propose a suboptimal uncoded state amplification scheme based on the power splitting scheme in [19]. Pure state amplification in the energy harvesting communication context is just putting a code symbol of energy equal to the observed energy. The transmitter puts the channel symbol $\sqrt{e_1}$ when e_1 is observed and $-\sqrt{e_2}$ when e_2 is observed. This scheme corresponds to the deterministic auxiliary selection at $(T_1, T_2) = (\sqrt{e_1}, -\sqrt{e_2})$. We denote the entropy reduction in the uncoded transmission as Δ_{uc}.

$$\Delta_{uc} = h(Y) - \frac{1}{2}\log_2(2\pi e) \tag{3.73}$$

where $p(y) = p_{e_1}\phi(y - \sqrt{e_1}) + p_{e_2}\phi(y + \sqrt{e_2})$. Note that the message transmission rate in this uncoded state amplification scheme is zero. In addition, all energy is utilized immediately after it is observed and hence the existence of a battery does not affect the performance.

Next, we propose an energy splitting scheme for simultaneous information transmission and entropy reduction. Upon observing energy e_i, αe_i is allocated for state amplification and $(1-\alpha)e_i$ is allocated for message transmission where $0 \leq \alpha \leq 1$. The transmitter puts αe_1 when e_1 is observed and $-\alpha e_2$ when e_2 is observed with the goal of entropy reduction. The remaining energy is allocated for message transmission. When the transmitter has no battery, the channel is

$$Y_i = X_i + \alpha E_i + N_i \tag{3.74}$$

where $|X_i| \leq \sqrt{(1-\alpha)e_1}$ if e_1 is observed and $|X_i| \leq \sqrt{(1-\alpha)e_2}$ if e_2 is observed. Hence, we find the optimal input distribution of the following channel:

$$p(y|\bar{t}_1, \bar{t}_2) = p_{e_1}\phi(y - \bar{t}_1 - \sqrt{\alpha e_1}) + p_{e_2}\phi(y - \bar{t}_2 + \sqrt{\alpha e_2}) \tag{3.75}$$

where $|\bar{t}_i| \leq \sqrt{(1-\alpha)e_i}$. For given α, the message transmission rate R is the capacity of the channel in (3.75) and the resulting Δ is the maximum entropy reduction subject to the message transmission rate R. These values are found by evaluating the region for the original channel in (3.48)-(3.50) at $(t_{1i}, t_{2i}) = (\bar{t}^*_{1i}, \bar{t}^*_{2i}) + (\alpha\sqrt{e_1}, -\alpha\sqrt{e_2})$ with probabilities $\bar{p}^*_i$ where $(\bar{t}^*_{1i}, \bar{t}^*_{2i})$ are the mass points in which the capacity achieving distribution for (3.75) is located with probabilities $\bar{p}^*_i$.

When the transmitter has unlimited energy storage, the energy that is allocated for message transmission can be saved in the battery and using the save-and-

transmit or best-effort-transmit scheme, the following maximum rate is achievable:

$$\begin{aligned} &\max \;\; I(T_1, T_2; Y) \\ &\text{s.t.} \;\; \mathbb{E}[p_{e_1} T_1^2 + p_{e_2} T_2^2] \leq (1-\alpha)\mathbb{E}[E] \end{aligned} \tag{3.76}$$

where T_1, T_2 and Y are related by the extended input channel relation in (3.75). In this case, we resort to $T_1 = T_2$ with a Gaussian distribution of zero mean and variance $(1-\alpha)\mathbb{E}[E]$. The resulting (R, Δ) pair is

$$(R, \Delta) = (I(X; X + \alpha E + N), I(\alpha E; X + \alpha E + N))$$

where $X \sim \mathcal{N}(0, (1-\alpha)\mathbb{E}[E])$.

3.4.5 Numerical Results

In this section, we provide numerical results of the optimal trade-off region $\mathcal{R}$ as well as the proposed suboptimal uncoded state amplification scheme under a binary energy arrival process with no battery and unlimited battery. In particular, $e_1 = 1$, $e_2 = 2.25$ with $p_{e_1} = 0.8$, so that the energy arrival has entropy $H(E) = 0.7219$ bits. The channel capacity with no battery and with unlimited battery are calculated as $C_0 = 0.5369$ bits and $C_\infty = \frac{1}{2}\log_2(1 + \mathbb{E}[E]) = 0.5850$ bits, respectively. We observe that in the no battery case, the symmetric binary distribution of (T_1, T_2) located at $(\sqrt{E_1}, \sqrt{E_2})$ and $(-\sqrt{E_1}, -\sqrt{E_2})$ maximizes $I(T_1, T_2; Y)$ and $h(Y)$ simultaneously. Therefore, the trade-off region generated by this symmetric binary distribution is

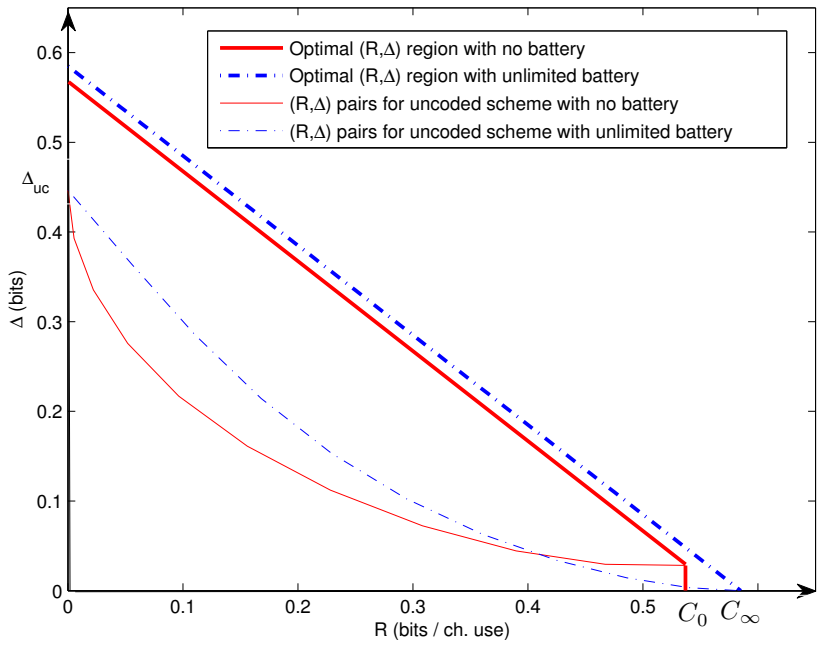

Figure 3.10: (R, Δ) regions with optimal and suboptimal schemes.

the optimal trade-off region. We calculate the maximum entropy reduction in this case as $\Delta^* = 0.5652$ bits. In the unlimited battery case, the boundary of the optimal (R, Δ) region is the line $R + \Delta = 0.5850$ and in particular, $\Delta^* = 0.5850$ bits as $H(E) > 0.5850$. Note that Δ^* is higher in the unlimited battery case though battery *blurs* the energy arrival information. This is due to the fact that higher rates can be achieved with an unlimited battery. Moreover, note that lossless recovery of the state sequence at the receiver is not possible for no battery and unlimited battery cases since Δ^* is less than $H(E)$ in both cases. We plot the resulting trade-off regions and the points achievable by the proposed uncoded state amplification scheme in Figure 3.10. Note that in the case of no battery if $I(T_1, T_2; Y)$ and $h(Y)$ are maximized at different discrete distributions of (T_1, T_2), then the optimal (R, Δ)

region is a union of many regions.

We calculate the entropy reduction in the uncoded transmission case as $\Delta_{uc} = 0.4466$ bits. As the energy splitting variable α is varied, we observe that the achieved (R, Δ) points travel from one edge to the other strictly interior to the optimal regions under no energy storage and unlimited energy storage cases. Therefore, in this case, *digitizing* the state sequence by means of channel codewords is optimal and analog state amplification has suboptimal performance. Additionally, we observe that with zero energy storage at the transmitter, even if the message transmission is performed at the capacity, there is a non-zero energy arrival information leakage to the receiver. In contrast, the receiver gets no information about the energy arrival process if transmitter has an unlimited battery and message transmission is performed at the capacity.

3.5 Conclusion

In this chapter, we considered the capacity of the AWGN channel with an energy harvesting transmitter and zero energy storage. The energy arrivals impose amplitude constraints on the code symbol at each channel use. Since the energy arrivals are channel state for this channel that is available causally at the transmitter only, the capacity is achieved by Shannon strategies. Optimal input distributions are challenging to obtain due to the continuous alphabet of AWGN channel. We provided numerically verifiable optimality conditions for this channel and our numerical results showed that, for the examples we considered, optimal input distributions are

discrete with finite support.

We extended the capacity analysis to the Gaussian MAC with energy harvesting transmitters of zero energy storage. We first considered MAC with static amplitude constraints and proved that the boundary of the capacity region is achieved by input distributions of finite support. Next, we considered discrete time-varying amplitude constraints. We investigated achievable rate regions by Shannon strategies.

Next, we characterized the trade-off region between entropy reduction Δ of the energy arrivals and the message transmission rate R in a communication system with an energy harvesting transmitter with no or unlimited battery. Shannon strategies achieve the boundary of the region in the no battery case. In the unlimited energy storage case, we showed that the optimal trade-off region can be expressed explicitly in a simple form and its boundary is achieved by a combination of best-effort-transmit and random binning schemes. We proposed an uncoded state amplification scheme and showed via a numerical example that digitizing the energy state performs significantly better than the uncoded scheme.

In [77], state amplification and state masking problems are studied for the finite energy storage regime. In particular, the interactions of these two objectives have been studied for the noiseless binary channel. In the case of one unit energy storage, achievable schemes based on timing based encoding are proposed and numerically evaluated.

Chapter 4

The Energy Harvesting Channel with Finite Energy Storage and Side Information

4.1 Introduction

In this chapter, we consider the finite battery regime in the energy harvesting channel and provide capacity results for the case when side information is available at the receiver. When there is no side information at the receiver, we obtained single-letter characterizations for the channel capacity in the extreme cases of unlimited energy storage and zero energy storage, in Chapters 2 and 3, respectively. However, a simple channel capacity expression in the general finite battery regime does not exist in the current literature. We first provide an overview of the approaches presented in [29–32] for the finite battery regime. We extend the achievable scheme in [30–32] to a noiseless channel with $E_{max} > 1$. We provide a simulation-based method to evaluate the achievable rates of this scheme.

Next, we determine the capacity of this channel for a discrete memoryless setting with an arbitrary finite battery size, when battery state information is available at both sides. We model energy arrivals as multiples of a fixed quanta, and obtain a physical layer which has a discrete alphabet based on this quanta. Consequently, we obtain a finite-state Markov channel where the state process interacts

with the channel input. We determine the capacity of this finite-state Markov channel when battery state information is available at both the transmitter and the receiver. Since the battery state information is available at the receiver, the information flows through both the physical channel and the battery. That is, the channel uncertainty in this case is due both to the error the physical channel introduces and to the uncertainty in the energy arrival process. In view of [78], in this case, the output feedback does not increase capacity. Thus, we express the capacity as the maximum directed information between the input and the physical channel output and the battery state. Moreover, utilizing the results reported in [79], we find sufficient conditions for which the optimal input distribution is stationary and the capacity is expressed in a simpler form in terms of stationary probabilities of the battery states. We also find a single-letter capacity expression for the infinite-sized battery case in which the finite-state results in [78, 79] are no longer valid.

Then, we determine the capacity of this channel when energy arrival is available at the receiver as side information. Unlike the case of battery state information at the receiver side, resulting channel is not a Markov channel when energy arrival side information is available at the receiver. We determine the capacity in this case as the limit of an n-letter maximum information rate. This expression reveals two crucial characteristics regarding the best achievable rate when energy arrival information is made available to the receiver: It suffices to use only current battery energy level in the encoding to achieve capacity. Reference [29] conjectures that for an energy harvesting channel with only the transmitter side energy arrival information, coding based only on the current battery energy level is optimal. Our results

show that when both the transmitter and the receiver have the energy arrival information, coding based only on the current battery energy level is optimal. Secondly, non-causal knowledge of energy arrivals at the transmitter does not improve the best achievable rate. Our work also relates to the recent work [80], [81]. In particular, bounds for the capacity with and without energy arrival side information are studied in [80]. Moreover, when the energy arrivals are deterministic as in [81], the receiver automatically has the energy arrival information and hence our results apply to the setting in [81]. Finally, we determine that the capacity expression is equivalently expressed as the maximum directed mutual information between the channel input and the channel output and energy. This enables us to show that additional channel output feedback does not increase the capacity.

4.2 System Model

We consider a communication channel with an energy harvesting transmitter. The battery in the transmitter can store at most E_{max} units of energy. Input symbols belong to the set $\{0, 1, \ldots, K\}$. Each symbol k has k-unit energy cost. When channel input X_i is transmitted in the ith channel use, the receiver gets Y_i. The stochastic relation $p(y|x)$ between the input and the output is determined by the underlying physical channel.

At each channel use, the transmitter both harvests energy and transmits a symbol. The order of harvesting and transmission in a channel use is as follows: S_i denotes the energy available in the battery at channel use i. The transmitter

observes the available battery energy S_i and transmits a symbol X_i. The energy of this symbol is constrained by the battery energy: $X_i \leq S_i$. After sending the symbol, the transmitter harvests energy. Energy arrivals (harvesting) is modeled as an i.i.d. process with $E_i \in \{0, 1, \ldots, |\mathcal{E}|\}$ and $\Pr[E_i = e] = q_e$ for $e \in \{0, 1, \ldots, |\mathcal{E}|\}$. Incoming energy E_i is first stored in the battery, if there is space, before it is used for transmission. Since the battery has finite size, energies may overflow and get wasted. The battery state is updated as:

$$S_{i+1} = \min\{S_i - X_i + E_i, E_{max}\} \tag{4.1}$$

In view of (4.1) and the physical channel model, the battery level S_i and the channel output Y_i evolve according to the following joint distribution:

$$p(s_{i+1}, y_i|x_i, s_i) = p(y_i|x_i)p(s_{i+1}|x_i, s_i) \tag{4.2}$$

4.3 Achievable Schemes With Battery State Information Available at the Transmitter Only

In this section, we consider the case when battery state information is available at the transmitter only. The full characterization of the capacity for this case with a finite-sized battery is an open problem in general. In the following, we provide an overview of the recent approaches in this problem [29–32].

4.3.1 Achievable Schemes by Shannon Strategies

A natural achievable scheme for the energy harvesting channel with only transmitter side information is obtained by Shannon strategies [18] as emphasized in [29]. The model in (4.2) fits well with the finite-state channel model of [33] with input controlled state. Let U_i denote the Shannon strategy. For an i.i.d. U_i, we have

$$p(y_i, u_i, s_{i+1}|s_i) = p(y_i, s_{i+1}|u_i, s_i)p(u_i) \tag{4.3}$$

where

$$p(y_i, s_{i+1}|u_i, s_i) = p(s_{i+1}|u_i, s_i)p(y_i|u_i(s_i)) \tag{4.4}$$

where $p(y_i|u_i(s_i))$ is due to the physical channel and $p(s_{i+1}|u_i, s_i)$ can be expressed in terms of the energy arrival process statistics and the battery size E_{max}. Then, with $p(u_i)$ fixed, the rate $R_{p(u_i)} = \lim_{n\to\infty} \frac{1}{n} I(U^n; Y^n)$ is achievable [29]. The rate $R_{p(u_i|u_{i-1})}$ can be calculated by the simulation-based method in [33]. We can then get the best achievable rate by optimizing over the probability $p(u_i)$. This method can be applied for a Markovian u_i of any order [29].

4.3.2 Binary Energy Harvesting Channel with Unit Sized Battery

In the special case of noiseless binary channel and unit-sized battery, references [30–32] shows that the channel is equivalent to an i.i.d. additive geometric-noise timing channel with causal information of the noise available at the transmitter. This

equivalence enables a single-letter capacity expression with an auxiliary random variable. In particular, equivalent timing channel is:

$$T = V + Z \tag{4.5}$$

where Z represents the waiting time for energy to arrive and V is the time to release the arriving energy and T is the total duration spent in one timing channel use. In [30–32], the capacity expression is found as the average number of bits sent in the timing channel per average time cost:

$$C = \max_{p(u),v(u,z)} \frac{I(U;T)}{E[T]} \tag{4.6}$$

4.3.3 Timing-Channel Based Achievable Schemes for $E_{max} > 1$

Next, we observe that the approach in [30–32] is still suitable when battery size is larger than one, and develop an achievable scheme based on the timing channel in [30–32]. The key to this scheme is the fact that the additive noise in the timing channel, which is causally available to the transmitter, has memory and input dependence in a suitable form, allowing us to determine a new class of achievable schemes combining the method in [33] and Shannon strategies in [18]. We calculate the achievable rate by using the simulation-based method in [33]. We numerically evaluate and compare the capacity and achievable rates with and without battery state information at the receiver.

Assume that the input is binary and the channel is noiseless, i.e., $p(y_i|x_i) =$

$\delta(y_i - x_i)$. Moreover, energy arrival is binary with $\Pr[E_i = 1] = q$. In this case, encoding and decoding can be performed over the number of channel uses between two 1s and we obtain the following timing channel (see [30–32]):

$$T_n = V_n + Z_n \tag{4.7}$$

where T_n is the number of channel uses between two 1s in the received signal, V_n is the number of channel uses the transmitter chooses to wait to transmit a 1 after the first energy availability, and Z_n is the number of channel uses until the battery has at least one unit energy. The transmitter has causal information of the noise Z_n before deciding V_n. Unlike the case with unit-sized battery as in [30–32], the noise process Z_n is not i.i.d. when battery size is larger than one.

In order to fit the model to those considered in [33], we need to include, as an additional state, the available energy in the battery B_n when Z_n is observed. Therefore, the state of this channel is the augmented random variables (Z_n, B_n). Let U_n denote an auxiliary i.i.d. random sequence. Then, we have:

$$p(z_{n+1}, b_{n+1}, t_n, u_n | z_n, b_n) = \delta(t_n - f(u_n, z_n, b_n)) p(z_{n+1}, b_{n+1}, u_n | z_n, b_n) \tag{4.8}$$

where $f(u_n, z_n, b_n)$ is a function that determines the Shannon strategy. Moreover, we have:

$$p(z_{n+1}, b_{n+1}, u_n | z_n, b_n) = p(z_{n+1}, b_{n+1} | u_n, z_n, b_n) p(u_n) \tag{4.9}$$

Here, $p(z_{n+1}, b_{n+1}|u_n, z_n, b_n)$ is determined by the energy arrival process statistics only. Specifically, if energy arrives during the waiting time $V_n = f(U_n, Z_n, B_n)$, next noise level is $Z_{n+1} = 0$ and B_{n+1} is found depending on the battery size.

In view of (4.8), the following rate is achievable and it can be evaluated by the method in [33]:

$$R = \lim_{n\to\infty} \frac{\frac{1}{n} I(U^n; T^n)}{\frac{1}{n}\sum_{i=1}^{n} E[T_i]} \tag{4.10}$$

We note that this achievable scheme is possibly sub-optimal as it does not update the strategy after the observation of a new energy arrival allocated in the battery. This constitutes a possible direction for improving the achievable scheme.

4.4 Capacity of the Energy Harvesting Channel with Battery State Information at the Receiver

In this section, we focus on the case when battery state information is available at the receiver side as shown in Figure 4.1. Since S_i is a state for this channel that is available at both the transmitter and the receiver, information flows through both the physical channel $p(y|x)$ as well as the battery state. The uncertainty is introduced due to both physical channel and the energy arrival process. Note that even when the channel is noiseless, uncertainty of the battery energy at the transmitter side makes it challenging for the receiver to decode the messages of the transmitter as the state has memory and input dependence.

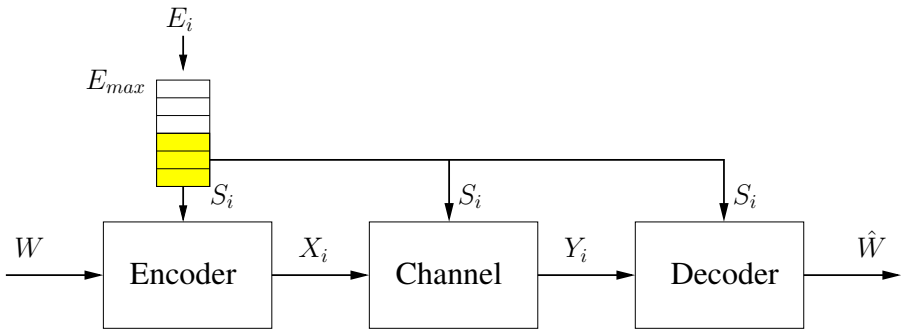

Figure 4.1: The channel with an energy harvesting transmitter with a finite-sized battery. The battery state information is available at both sides.

4.4.1 Main Result

Let us define two variables $Y_{1i} \triangleq S_{i+1}$ and $Y_{2i} \triangleq Y_i$ and express the model in (4.2) in terms of the new definitions as:

$$p(y_{1i}, y_{2i}|x_i, y_{1(i-1)}) \tag{4.11}$$

That is, $y_{1(i-1)}$ acts as a state, which is available at the transmitter and the receiver. The model in (4.11) was previously studied in [78, Section VIII]. Since the channel in (4.11) is connected in the sense of [78, Definition 3], the channel capacity is independent of the initial state and is characterized as in the following theorem (see also [78, Appendix VIII]).

Theorem 4.1 *The channel capacity for (4.11) is:*

$$C = \lim_{N\to\infty} \max_{p(x_i|y_{1(i-1)})} \frac{1}{N} \sum_{i=1}^{N} I(X_i; Y_{1i}, Y_{2i}|Y_{1(i-1)}) \tag{4.12}$$

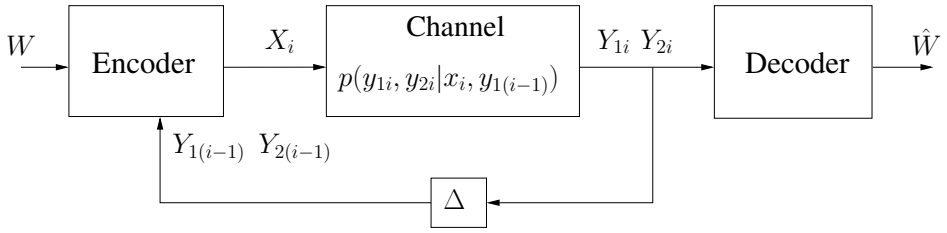

Figure 4.2: Virtual channel model with feedback. Presence of the feedback of Y_2 does not affect the capacity.

Note that the expression in (4.12) is the maximum directed information from the input X to the outputs Y_1, Y_2 for the channel in (4.11). Computation of (4.12) is possible by, e.g., the algorithm in [82], which is a combination of Blahut-Arimoto algorithm and dynamic programming.

In view of [78, Theorem 19], feedback of the channel output Y_2 does not increase the capacity (see also [83]). We note that the channel model (4.11) with the feedback of Y_2, as shown in Figure 4.2, also matches with the model in [79]. It is shown in [79] that under some technical conditions, the capacity is achieved by stationary input distributions and it can be expressed in terms of the stationary probability of the outputs Y_1 and Y_2. Specifically, the channel transition probability must satisfy strong irreducibility and strong aperiodicity conditions in [79]. Our goal is to extend the results in [79] for the channel in (4.11). To this end, we first state the following lemma. We provide the proof in Appendix 4.8.1.

Lemma 4.1 *Let $\{M_{1i}\}$ and $\{M_{2i}\}$ be strongly irreducible and strongly aperiodic Markov chains with a common input X_i. If $M_{1i} \to X_i \to M_{2i}$ holds, joint Markov process $\{M_{1i}, M_{2i}\}$ is also strongly irreducible and strongly aperiodic.*

Lemma 4.1 states that two strongly irreducible and strongly aperiodic Markov chains driven by a single input is jointly strongly irreducible and strongly aperiodic if they are conditionally independent given the input. Note that this conditional independence is satisfied by the energy harvesting model in (4.2) and (4.11). We are now ready to prove the following theorem. We provide the proof of this theorem in Appendix 4.8.2.

Theorem 4.2 *Assume that the channel $p(y_{1i}|x_i, y_{1(i-1)})$ is strongly irreducible and strongly aperiodic and let the channel $Q_k = p(y_{1i}, y_{2i}|x_i, y_{1(i-1)} = k)$ have a rank $|\mathcal{X}|$ transition matrix for any given $y_{1(i-1)} = k$. Moreover, assume that $Y_{1i} \to X_i \to Y_{2i}$ holds with $p(y_{2i}|x_i) > 0$ for all y_{2i} and x_i. Then, the capacity of the channel in (4.11) is:*

$$C = \max_{p(x|\tilde{y}_1)} \sum_{k=1}^{|\mathcal{Y}_1|} \pi_k I(X; Y_1, Y_2|\tilde{Y}_1 = k) \tag{4.13}$$

where $\tilde{Y}_1$ denotes the one-unit delayed feedback of Y_1.

We remark that the condition $p(y_i|x_i) > 0$ in Theorem 4.2 can be relaxed. Even if we allow $p(y|x) = 0$ for some x, y, Theorem 4.2 can be established following the lines in [78, Appendix VIII] and applying it in [79]. On the other hand, this condition holds for practical channel models, such as the binary symmetric channel with non-zero or non-one cross-over probability, and modulo additive noise channels with noise support set equal to the input alphabet.

Corollary 4.1 *If the battery state is strongly irreducible and strongly aperiodic, the*

capacity with battery state information at the transmitter and receiver, C_{SI}, is:

$$C_{SI} = \max_{p(x|\tilde{s})} \sum_{i=1}^{B} \pi_i I(X; Y, S|\tilde{S} = i) \tag{4.14}$$

where $\tilde{S}$ is the current battery state and S is the next battery state.

We note the similarity of the capacity expression in (4.14) and that of Goldsmith-Varaiya expression in [65] for the capacity of fading channels with side information. Even though the channel state has input dependence, in (4.14) the stationary probability of the state averages out the mutual information as in Goldsmith-Varaiya expression. A recent work [84] reported a similar capacity expression for this channel with side information at both sides. We note that the expression in (4.14) is different from that in [84, Theorem 1]. Specifically, the expression in [84, Theorem 1] does not involve battery state as an output in the mutual information and yields lower values.

We also remark that the strongly irreducible condition is satisfied in the current energy harvesting model under some further physical conditions. In order to enable edge formation between all state pairs (see [79, Definition 2]), we need to add non-zero energy leakage probability to the battery dynamics which may or may not depend on the particular energy state. We also need that the energy arrivals can take values in the set $\{0, 1, \ldots, E_{max}\}$ with non-zero probability.

4.4.2 Capacity with Battery State Information at the Receiver and Unlimited Energy Storage

We now determine the capacity with side information and infinite-sized battery. Note that the results we have derived so far in Theorems 4.1 and 4.2 are not applicable in this case as they follow from results in [78, 79] which hold only when the cardinality of the state is finite. We state the capacity result in the following theorem and we provide the proof in Appendix 4.8.3.

Theorem 4.3 *The capacity of the energy harvesting channel with battery state information at the transmitter and receiver and with an infinite-sized battery at the transmitter is*

$$C = \max_{p(x), E[X] \leq P_{avg}} I(X; Y, \hat{S}) \tag{4.15}$$

where P_{avg} is the average energy recharge rate $E[E_i]$ and the channel between X and $\hat{S}$ is an additive noise channel and the noise is the energy arrival variable E:

$$\hat{S} = X - E \tag{4.16}$$

and $\hat{S} \to X \to Y$.

Theorem 4.3 implies that in the infinite-sized battery case, the transmitter does not need to use the battery state information in the encoding and a single-letter code suffices to achieve the capacity. However, note that the receiver uses the

battery state information to obtain the output $\hat{S}_i$.

4.5 Capacity of the Energy Harvesting Channel with Energy Arrival Information at the Receiver

In this section, we study a communication channel with an energy harvesting transmitter where *energy arrival information is available at the receiver* in addition to the transmitter as shown in Figure 4.3. In particular, we consider the same energy harvesting channel described in Section 4.2 with the additional assumption that energy arrival information is available at the receiver.

The energy arrival E_i is available at the receiver. In view of (4.1) and the physical channel model, the energy arrival E_i and the channel output Y_i evolve according to the following joint distribution:

$$p(e_i, y_i|x^i, e^{i-1}) = p(e_i)p(y_i|x_i), \qquad x_i \leq s_i \tag{4.17}$$

where s_i is the battery energy level at the ith channel use. We note that the product form $p(y_i|x_i)p(e_i)$ in (4.17) suggests that the channel and the energy arrivals are independent; however, due to the constraint $x_i \leq s_i$, there is a time correlation in the transmitted input sequence, i.e., the battery imposes memory constraint in the channel input sequence.

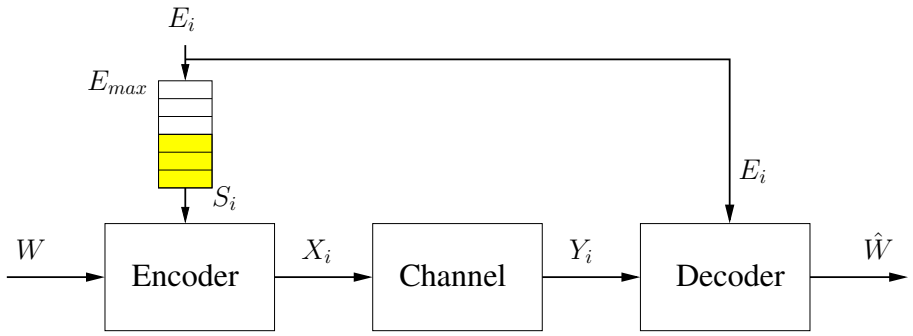

Figure 4.3: The channel with an energy harvesting transmitter with a finite-sized battery. The energy arrival information is available at both sides.

4.5.1 Main Result

We state the main result of this section in the following theorem and we provide the proof in Appendix 4.8.4:

Theorem 4.4 *The capacity of the energy harvesting channel with energy arrival side information at the receiver in addition to the transmitter is:*

$$C = \lim_{n\to\infty} \max_{p(x_i|s_i)} \frac{1}{n} I(X^n; Y^n|E^n) \tag{4.18}$$

Moreover, the capacity is invariant to the availability of non-causal knowledge of energy arrivals.

Next, we provide the following corollary and relegate its proof to Appendix 4.8.5:

Corollary 4.2 *The following rate R is achievable with energy arrival side informa-*

tion at both sides:

$$R = \lim_{n\to\infty} \max_{p(x_i|s_i)} \frac{1}{n} \sum_{i=1}^{n} I(X_i; Y_i|S_i) \tag{4.19}$$

We, next, comment on the capacity expression in (4.18) and achievable rate in (4.19). Note that the capacity achieving input sequence is obtained by using an input distribution at channel use i, $p(x_i|s_i)$, that depends only on the current battery level s_i. In fact, this could be viewed as an extension of [55, Theorem 3] where current state information is sufficient for encoding; however, realization of the whole energy arrival sequence is needed for decoding. Battery state information is inherently available at the transmitter; therefore, this is a feasible encoding scheme. However, note that the battery state information is not available at the receiver side. That is, even when the battery state information is not available at the receiver, the rate R in (4.19) and possibly higher rates are achievable. The conditioning on the battery state S_i in the mutual information in (4.19) should not be interpreted as the battery state information being available at the receiver. In fact, when the battery state information is available at the receiver, the capacity is found as in Section 4.4.

4.5.2 Solution of (4.19) via Dynamic Programming

The optimization problem in (4.19) can be solved by dynamic programming for fixed n. Assume s_n is fixed and calculate the value function for all $s_n \in \{0, \ldots, E_{max}\}$ as

follows:

$$J_n(s_n) = \max_{p(x_n|s_n)} I(X_n; Y_n|S_n = s_n) \tag{4.20}$$

Then, calculate the value function for $i = 1, \ldots, n-1$:

$$J_i(s_i) = \max_{p(x_i|s_i)} I(X_i; Y_i|S_i = s_i) + \sum_{s_{i+1}=0}^{E_{max}} p(s_{i+1}|s_i) J_i(s_{i+1}) \tag{4.21}$$

Note that $p(s_{i+1}|s_i)$ is calculated as:

$$p(s_{i+1}|s_i) = \sum_{e_i, x_i, s_{i+1}} p(s_{i+1}|s_i, x_i, e_i) p(e_i) p(x_i|s_i) \tag{4.22}$$

Since $s_{i+1} = \min\{(s_i - x_i + e_i)^+, E_{max}\}$ is a deterministic function, $p(s_{i+1}|s_i, x_i, e_i)$ is just an indicator function.

4.5.3 The Channel with Output Feedback

In this section, we consider the capacity of the channel under study when the channel output feedback is also present at the transmitter. In particular, we consider the channel in (4.17) with the feedback of the channel output Y_i. Since E_{i-1} is known by the transmitter, e_i and y_i could be viewed as the output of the channel in (4.17) which is fed back to the transmitter with unit delay as shown in Figure 4.4. It is well-known that in non-anticipative systems feedback does not increase capacity [85]. We will establish this result for our particular energy harvesting channel.

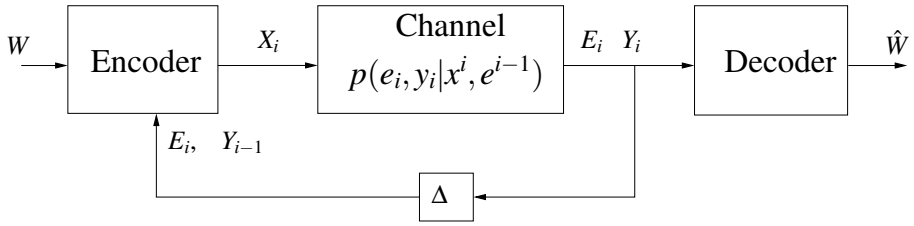

Figure 4.4: Virtual channel model with feedback. Presence of the channel output feedback Y does not affect the capacity.

We first note that the n-letter mutual information in (4.18) is the maximum directed information from the input X^n to the output Y^n given the energy arrivals E^n:

$$I(X^n;Y^n|E^n) = \sum_{i=1}^{n} I(X^n;Y_i|Y^{i-1},E^n) \tag{4.23}$$

$$= \sum_{i=1}^{n} I(X^i;Y_i|Y^{i-1},E^n) + I(X_{i+1}^n;Y_i|X^i,Y^{i-1},E^n) \tag{4.24}$$

$$= \sum_{i=1}^{n} I(X^i;Y_i|Y^{i-1},E^n) \tag{4.25}$$

$$= I(X^n \to Y^n|E^n) \tag{4.26}$$

where (4.25) is due to the fact that the Markov chain $Y_i \leftrightarrow (X^i, Y^{(i-1)}, E^n) \leftrightarrow X_{i+1}^n$ holds for all i. This Markov chain holds in view of the fact that X_{i+1}^n is determined as a function of message W, X^i and E^i. Therefore, Y_i is independent of X_{i+1}^n given $X^i, Y^{(i-1)}, E^n$. This renders the term $I(X_{i+1}^n;Y_i|X^i,Y^{i-1},E^n) = 0$. See also [86, Proposition 4.2.2].

Next, we observe that X^i is independent of E_i in view of the fact that E_i is an i.i.d. sequence and the constraint set for X^i is determined by E^{i-1}. Therefore,

we have the following:

$$I(X^n;Y^n|E^n) = \sum_{i=1}^{n} I(X^i;Y_i|Y^{i-1},E^n) \tag{4.27}$$

$$= \sum_{i=1}^{n} I(X^i;Y_i|Y^{i-1},E^{i-1}) \tag{4.28}$$

$$= \sum_{i=1}^{n} I(X^i;Y_i,E_i|Y^{i-1},E^{i-1}) \tag{4.29}$$

$$= I(X^n \to Y^n, E^n) \tag{4.30}$$

Since the limit $\lim_{n\to\infty} \frac{1}{n} \sup_{p(x^n)\in\mathcal{F}(E^n)} I(X^n;Y^n|E^n)$ exists, we conclude that the limit $\lim_{n\to\infty} \frac{1}{n} \sup_{p(x^n)\in\mathcal{F}(E^n)} I(X^n \to Y^n, E^n)$ also exists. In other words, the directed mutual information spectrum of the channel in (4.17) consists of a single point only. Note that the channel in (4.17) falls into the most general category of channels with feedback in [86]. In view of the general capacity formula for channels with feedback in [86, Theorem 4.4.1] and the fact that $\lim_{n\to\infty} \frac{1}{n} I(X^n \to Y^n, E^n)$ exists, we conclude that this limit is the capacity of the channel in (4.17) with feedback.

Theorem 4.5 *When energy arrival side information is causally available at the transmitter and the receiver in the discrete memoryless energy harvesting channel, the channel output feedback does not increase the capacity.*

We finally remark that in the case of an infinite-sized battery, the capacity is not affected by the presence of energy arrival side information at the receiver side, see also [9, Section IV]. Moreover, in view of Theorem 4.5, the presence of channel output feedback does not affect the capacity either.

4.6 Numerical Results

In this section, we evaluate the capacity and achievable rates with and without receiver side information. In the timing-based achievable scheme, we use an extended version of the auxiliary selection in [30] as follows. Let $U \in \{0, 1, \ldots, N-1\}$. Then, V as a function of U and Z is [30–32, 34]:

$$V = \begin{cases} U - Z + 1, & U \geq Z \\ (U - Z \bmod M) + 1, & U < Z \end{cases} \tag{4.31}$$

where $M < N$. Note that this particular scheme does not use B_n information available at the transmitter. We choose M and $p(u)$ in the simulation and calculate the achievable rate.

In Figure 4.5, we plot the achievable rates by the best i.i.d. [29–32] and the best first order Markovian [29] Shannon strategies and the timing-based achievable scheme when the channel is noiseless binary, $E_{max} = 2$ and the battery state information is available only at the transmitter. We also plot the capacity with battery state information at both sides for $E_{max} = 2$ and $E_{max} = \infty$. Note that when $E_{max} = \infty$, the availability of the battery state information at the receiver does not increase the capacity for the noiseless channel. We observe that the timing-based achievable scheme performs better than zeroth and first order Markovian Shannon strategies.

In Figure 4.6, we plot the achievable rates and the capacity without and with receiver side information, respectively, in a binary symmetric channel with crossover

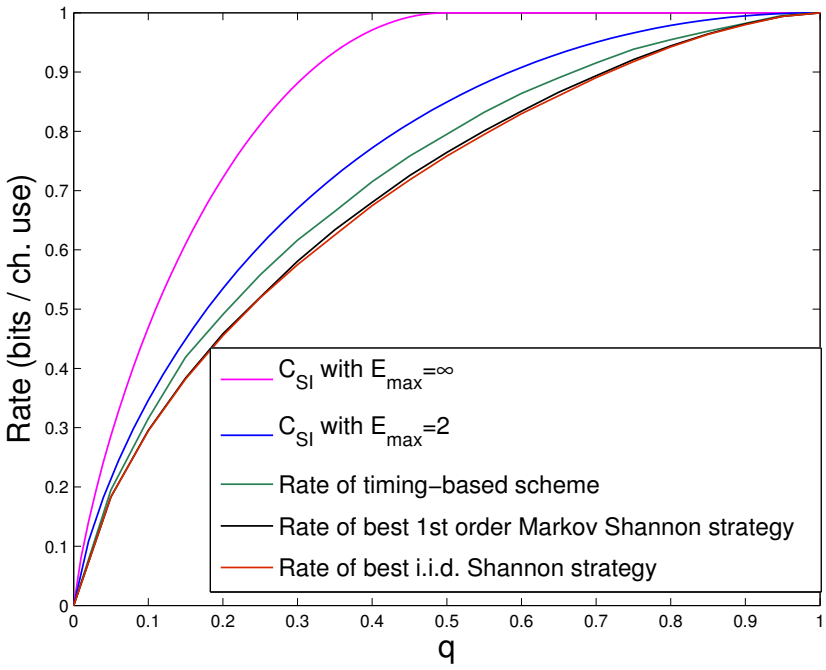

Figure 4.5: The capacity with battery state information at the receiver side and achievable rates with side information at the transmitter only in the noiseless binary channel. The plot is with respect to the energy arrival probability q.

probability p_e for $E_{max} = 2$ and $q = 0.5$ with respect to p_e. We also plot the capacity for $E_{max} = \infty$.

Next, we evaluate the capacity bounds C_n and achievable rates with and without energy arrival side information at the receiver. We consider a binary symmetric channel with crossover probability p_e. We select $E_{max} = 1$ and i.i.d. energy arrivals with $P[E_i = 1] = 0.5$. In Figure 4.7, we plot the achievable rates with and without receiver side information. We also include plots of the capacity for $E_{max} = \infty$. The achievable rate with energy side information at the transmitter only is calculated by using the method reported in [29, 30]. Moreover, we plot capacities with battery state information at the receiver using [34]. Note that capacity with energy side in-

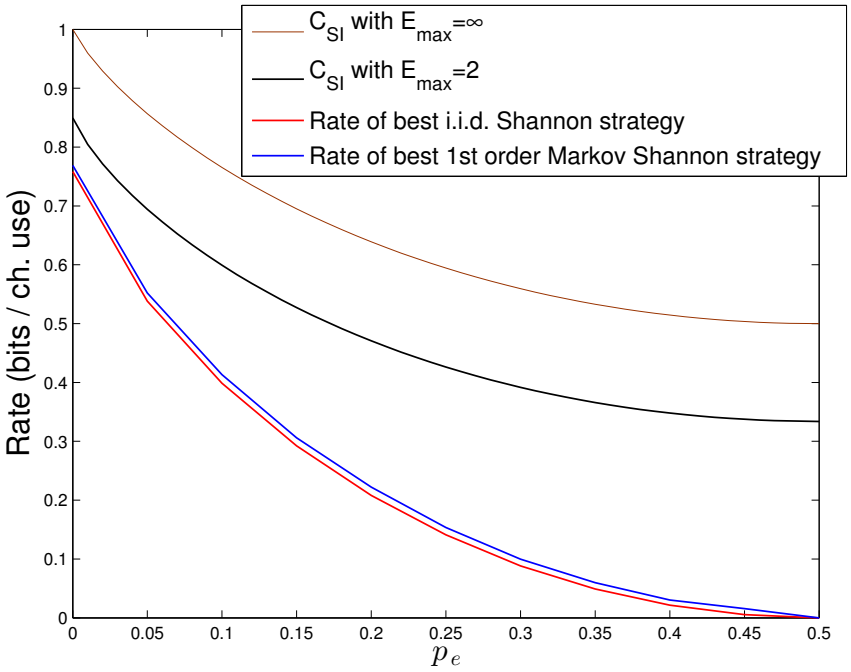

Figure 4.6: The capacity with battery side information at the receiver side and achievable rates with side information only at the transmitter in a BSC(p_e). The plot is with respect to the channel crossover probability p_e for $q = 0.5$.

formation and battery side information match when channel is noiseless. Moreover, we observe that C_n for $n = 7$ yields a tighter bound as it lies below the capacity with battery state information at the receiver for most p_e values.

4.7 Conclusion

In this chapter, we considered the finite battery regime in the energy harvesting channel and provided capacity results in the presence of side information at the receiver side. We first provided an overview of current approaches for this problem. We extended the achievable scheme in [30] to a noiseless channel with $E_{max} > 1$. We provided a simulation-based method to evaluate the achievable rates using [33].

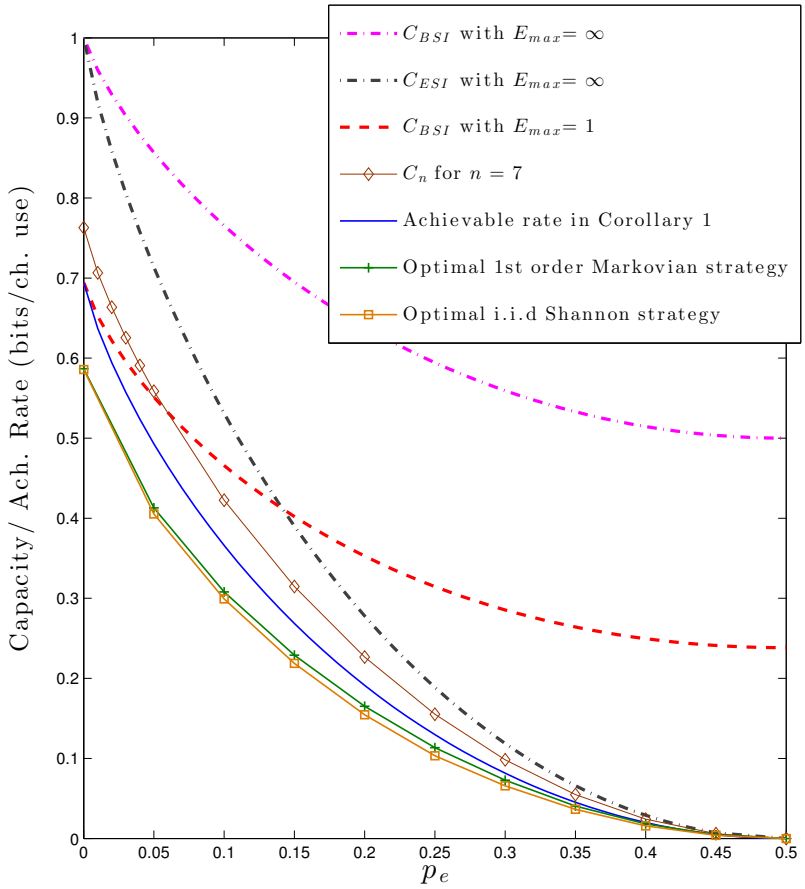

Figure 4.7: The capacities with energy arrival and battery side information at the receiver side and achievable rates with side information only at the transmitter in a BSC(p_e). The plot is with respect to the channel crossover probability p_e for $P[E_i = 0] = 0.5 = P[E_i = 1]$.

Next, we determined the capacity of an energy harvesting channel with an energy harvesting transmitter and battery state information available at the transmitter and receiver sides. This is an instance of a finite-state channel and the channel output feedback does not increase the capacity. We stated the capacity as maximum directed mutual information from the input to the output and the battery state. We identified sufficient conditions for the channel to have stationary input distributions as optimal distributions. We also derived a single-letter capacity expression for this

channel with battery state information at both sides and infinite-sized battery at the transmitter. Then, we determined the capacity of an energy harvesting channel with an energy harvesting transmitter and energy arrival side information available at the transmitter and receiver sides. We first found an n-letter capacity expression and showed that the optimal coding is based on only current battery state s_i. Finally, we showed that the capacity is expressed as maximum directed information between the input and the output and proved that the channel output feedback does not increase the capacity.

4.8 Appendix

4.8.1 Proof of Lemma 4.1

Since $M_{1i} \to X_i \to M_{2i}$ holds, we have:

$$p(m_{1i}, m_{2i}|x_i, m_{1(i-1)}, m_{2(i-1)}) = p(m_{1i}|x_i, m_{1(i-1)})p(m_{2i}|x_i, m_{2(i-1)}) \tag{4.32}$$

In view of (4.49), any path from the joint state (m_1, m_2) to $(\tilde{m}_1, \tilde{m}_2)$ requires $\{M_{1i}\}$ to travel from m_1 to $\tilde{m}_1$ and $\{M_{2i}\}$ from m_2 to $\tilde{m}_2$, respectively. Therefore, all possible paths from (m_1, m_2) to $(\tilde{m}_1, \tilde{m}_2)$ is a Cartesian product of all paths from m_1 to $\tilde{m}_1$ in $\{M_{1i}\}$ and from m_2 to $\tilde{m}_2$ in $\{M_{2i}\}$. Whenever $\{M_{1i}\}$ and $\{M_{2i}\}$ are individually strongly irreducible, there exists a path from any m_1 to $\tilde{m}_1$ in $\{M_{1i}\}$ and from m_2 to $\tilde{m}_2$ in $\{M_{2i}\}$ and therefore, there exits a path from any (m_1, m_2) to $(\tilde{m}_1, \tilde{m}_2)$ in $\{M_{1i}, M_{2i}\}$, which proves that $\{M_{1i}, M_{2i}\}$ is also strongly irreducible.

Similarly, due to the Cartesian product property, lengths of paths from any (m_1, m_2) to $(\tilde{m}_1, \tilde{m}_2)$ are common multiples of lengths of paths from m_1 to $\tilde{m}_1$ in $\{M_{1i}\}$ and lengths of paths from m_2 to $\tilde{m}_2$ in $\{M_{2i}\}$. Therefore, all possible lengths of paths from (m_1, m_2) to itself must have greatest common divisor 1 and $\{M_{1i}, M_{2i}\}$ is strongly aperiodic as otherwise either $\{M_{1i}\}$ or $\{M_{2i}\}$ is not strongly aperiodic.

4.8.2 Proof of Theorem 4.2

In view of Lemma 4.1, the hypothesis in [79, Theorem 6] are satisfied for the channel $p(y_{1i}, y_{2i}|x_i, y_{1(i-1)}, y_{2(i-1)})$. In particular, by [79, Lemma 6], the rank condition we stated in the theorem implies that the technical condition in the hypothesis in [79, Theorem 6] is satisfied. Therefore, the capacity C is:

$$\begin{aligned}\max_{p(x|\tilde{y}_1,\tilde{y}_2)} \sum_{k_1}\sum_{k_2} \pi_{k_1,k_2} I(X; Y_1, Y_2|\tilde{Y}_1 = k_1, \tilde{Y}_2 = k_2) \\ = \max_{p(x|\tilde{y}_1,\tilde{y}_2)} \sum_{k_1} \pi_{k_1} \sum_{k_2} \pi_{k_2|k_1} I(X; Y_1, Y_2|\tilde{Y}_1 = k_1) \qquad (4.33)\end{aligned}$$

where (4.33) follows from the fact that the channel in (4.11) does not have dependence on $\tilde{Y}_2$. In (4.33), the input distributions are selected based on the past channel outputs, i.e., $p(x|\tilde{y}_1 = k_1, \tilde{y}_2 = k_2)$. Now, consider the marginal distribution of X given $\tilde{Y}_1 = k_1$:

$$p(x|\tilde{y}_1 = k_1) = \sum_{k_2=1}^{|\mathcal{Y}_2|} p(x|\tilde{y}_1 = k_1, \tilde{y}_2 = k_2)\pi_{k_2|k_1} \qquad (4.34)$$

By Jensen's inequality and the concavity of mutual information we have:

$$\sum_{k_2} \pi_{k_2|k_1} I(X; Y_1, Y_2|\tilde{Y}_1 = k_1)|_{p(x|\tilde{y}_1=k_1,\tilde{y}_2=k_2)} \leq I(X; Y_1, Y_2|\tilde{Y}_1 = k_1)|_{p(x|\tilde{y}_1=k_1)} \quad (4.35)$$

To complete the proof, it remains to show that this adjustment does not change π_{k_1}, i.e., the marginal stationary distribution of Y_1. This fact follows from the Markov chain $Y_{1i} \to X_i \to Y_{2i}$.

4.8.3 Proof of Theorem 4.3

The receiver can form i.i.d. realizations of the channel $p(\hat{s}, y|x)$ by taking the difference $\hat{S}_i = S_{i+1} - S_i$ at each channel use. Hence, the capacity of the channel $p(\hat{s}, y|x)$ with input constraint $E[X] \leq P_{avg}$ is achievable by using the best-effort-transmit or save-and-transmit schemes in [9].

The converse is as follows: Let the received sequence in $n+1$ channel uses be Y^{n+1}, S^{n+1} and we discard Y_{n+1} which causes no loss of optimality as n goes to infinity:

$$(n+1)R - H(W|Y^n, S^{n+1}) = I(W; Y^n, S^{n+1}) \quad (4.36)$$

$$= H(Y^n, S^{n+1}) - H(Y^n, S^{n+1}|W) \quad (4.37)$$

$$= H(S_1) + \sum_{i=1}^{n} H(Y_i, S_{i+1}|Y^{i-1}, S^i) - \sum_{i=1}^{n} H(Y_i, S_{i+1}|W, Y^{i-1}, S^i) \quad (4.38)$$

$$\leq \sum_{i=1}^{n} H(Y_i, S_{i+1}|S_i) - \sum_{i=1}^{n} H(Y_i, S_{i+1}|X_i, W, Y^{i-1}, S^i) \quad (4.39)$$

$$= \sum_{i=1}^{n} H(Y_i, S_{i+1} - S_i|S_i) - \sum_{i=1}^{n} H(Y_i|X_i) - \sum_{i=1}^{n} H(S_{i+1} - S_i|X_i) \tag{4.40}$$

$$\leq \sum_{i=1}^{n} H(Y_i, \hat{S}_i) - \sum_{i=1}^{n} H(Y_i|X_i) - \sum_{i=1}^{n} H(\hat{S}_i|X_i) \tag{4.41}$$

$$= \sum_{i=1}^{n} I(X_i; Y_i, \hat{S}_i) \tag{4.42}$$

$$\leq n \max_{p(x), E[X] \leq P_{avg}} I(X; Y, \hat{S}) \tag{4.43}$$

where (4.39) follows from the facts that conditioning reduces entropy and that initial battery level is finite and known to both sides and hence $H(S_1) = 0$, (4.40) follows from $Y_i \rightarrow X_i \rightarrow \hat{S}_i$ and also from the fact that $Y_i, \hat{S}_i$ are independent of W, Y^{i-1}, S^{i-1} given X_i, i.e., $W, Y^{i-1}, S^{i-1} \rightarrow X_i \rightarrow Y_i, \hat{S}_i$. Finally, (4.41) follows from conditioning reduces entropy and (4.43) is due to the fact that the energy for the input sequence X_i is maintained by the energy arrivals E_i and hence $\frac{1}{n}\sum_{i=1}^{n} E[X_i] \leq P_{avg}$. By Fano's inequality, $H(W|Y^n, S^{n+1})$ goes to zero as $n \rightarrow \infty$ and hence completing the proof.

4.8.4 Proof of Theorem 4.4

We start the proof with the converse part and assume that the energy arrival sequence E^n is available at both the transmitter and the receiver non-causally. Note that non-causal knowledge of energy arrivals is stronger than the original system assumptions, yielding an upper bound for the rate achievable under them. First,

define $\mathcal{F}(E^n)$ as the support set of the X^n sequence defined by the battery dynamics:

$$\mathcal{F}_n(E^n) \triangleq \{p(x^n) \text{ with supoort } x_i \leq s_i,\ s_{i+1} = \min\{s_i - x_i + E_i, E_{max}\},\ s_1 = E_{max}\} \tag{4.44}$$

The code is generated based on the non-causal knowledge of the energy arrivals: For any given E^n sequence, the codewords are constrained to lie in the set $\mathcal{F}_n(E^n)$. Note that this is equivalent to causal conditioning for the code symbol energy at each channel use. We have the following inequalities:

$$\begin{aligned} nR - H(W|Y^n, E^n) &= I(W; Y^n, E^n) && (4.45)\\ &\leq I(X^n; Y^n|E^n) && (4.46)\\ &\leq \sup_{p(x^n)\in\mathcal{F}_n(E^n)} I(X^n; Y^n|E^n) && (4.47) \end{aligned}$$

where (4.46) follows from the data processing inequality and the fact that message W is independent of the energy arrivals E^n. Taking the limit as n tends to infinity and using Fano's inequality, we reach the following inequality:

$$R \leq \liminf_{n\to\infty} \frac{1}{n} \sup_{p(x^n)\in\mathcal{F}(E^n)} I(X^n; Y^n|E^n) \tag{4.48}$$

Now, define $C_n = \sup_{p(x^n)\in\mathcal{F}(E^n)} I(X^n; Y^n|E^n)$. We next show that C_n is a sub-additive sequence. Note the following relation:

$$\mathcal{F}_{n+m}(E^{n+m}) \subseteq \{p(x^{n+m}) : p(x_1^n) \in \mathcal{F}_n(E^n), p(x_{n+1}^{n+m}) \in \mathcal{F}_m(E_{n+1}^{n+m})\} \tag{4.49}$$

where (4.49) follows from the fact that in the definition of $\mathcal{F}_n(E^n)$ in (4.44), initial battery energy is E_{max}. Define the set on the right hand side of (4.49) as $\tilde{\mathcal{F}}(E^{n+m})$. We reach the following inequalities:

$$C_{n+m} = \sup_{p(x^{n+m})\in\mathcal{F}(E^{n+m})} I(X^{n+m};Y^{n+m}|E^{n+m}) \tag{4.50}$$

$$\leq \sup_{p(x^{n+m})\in\tilde{\mathcal{F}}(E^{n+m})} I(X^{n+m};Y^{n+m}|E^{n+m}) \tag{4.51}$$

$$\leq \sup_{p(x^{n})\in\mathcal{F}(E^{n})} I(X^{n};Y^{n}|E^{n}) + \sup_{p(x^{m})\in\mathcal{F}(E_{n+1}^{n+m})} I(X^{m};Y^{m}|E_{n+1}^{n+m}) \tag{4.52}$$

$$= C_n + C_m \tag{4.53}$$

where (4.51) follows from the relation in (4.49) and (4.52) is due to the fact that $p(x^n)$ and $p(x_{n+1}^{n+m})$ could be independently selected in $\tilde{\mathcal{F}}(E^{n+m})$. Finally, (4.53) follows from the fact that E_i is i.i.d. and hence $C_m = \sup_{p(x^m)\in\mathcal{F}(E_{n+1}^{n+m})} I(X^m;Y^m|E_{n+1}^{n+m})$ is independent of the time index n. By Fekete's lemma, we have

$$\lim\inf_{n\to\infty} \frac{1}{n}C_n = \inf_n \frac{C_n}{n} = \lim_{n\to\infty}\frac{1}{n}C_n \tag{4.54}$$

We now show that the rate $R = \lim_{n\to\infty}\frac{C_n}{n}$ is achievable with non-causal knowledge of the energy arrivals. Fix n and consider all possible $E^n = e^n$ sequences. Find $\sup_{p(x^n)\in\mathcal{F}_n(e^n)} I(X^n;Y^n|e^n)$ for all e^n. Then, we perform the encoding over blocks of n channel uses and insert zero symbols $o(n)$ channel uses so that the battery returns to the full energy state. That is, each block is of length $n+o(n)$ and consider k such blocks: the ith block consists of n code symbols generated from the

distribution that achieves $\sup_{p(x^n)\in\mathcal{F}_n(e_{(i-1)(n+o(n))+1}^{(i-1)(n+o(n))+n})} I(X^n;Y^n)$ and they are followed by $o(n)$ zero symbols. Since $e_{(i-1)(n+o(n))+1}^{(i-1)(n+o(n))+n}$ are independent for all i, we conclude that as the number of blocks k grows to infinity, by multiplexing over different codebooks as in [65], the rate $\sup_{p(x^n)\in\mathcal{F}_n(E^n)} I(X^n;Y^n|E^n)$ is achieved provided that the initial full battery state is guaranteed at the beginning of each block. However, by selecting $o(n)$ such that $o(n)\to\infty$ as $n\to\infty$, (e.g., $o(n)=\log(n)$), we conclude that

$$\lim_{n\to\infty}\frac{C_n}{n+o(n)} \tag{4.55}$$

is indeed achievable. This proves that $\lim_{n\to\infty}\frac{C_n}{n}$ is achievable. Note that [81] uses a similar achievable scheme when the energy arrivals are deterministic. However, the waiting time is finite in that case as the energy arrivals are deterministic and battery is finite.

We have just shown that $\lim_{n\to\infty}\frac{C_n}{n}$ is the capacity with non-causal knowledge of energy arrivals. To complete the proof, we prove that in the above achievable scheme, only causal knowledge of the energy arrivals is sufficient. In other words, we prove the following equality:

$$\sup_{p(x^n)\in\mathcal{F}(E^n)} I(X^n;Y^n|E^n) = \sup_{p(x_i|s_i)} I(X^n;Y^n|E^n) \tag{4.56}$$

To this end, we express the objective as:

$$
\begin{aligned}
I(X^n;Y^n|E^n) &= H(Y^n|E^n) - H(Y^n|X^n,E^n) \\
&= \sum_{i=1}^{n} H(Y_i|Y^{i-1},E^n) - H(Y_i|Y^{i-1},X^n,E^n) && (4.57)\\
&\leq \sum_{i=1}^{n} H(Y_i|Y^{i-1},E^{i-1}) - H(Y_i|X^i,E^{i-1}) && (4.58)\\
&= \sum_{i=1}^{n} H(Y_i|Y^{i-1},E^{i-1}) - H(Y_i|X_i,S_i) && (4.59)
\end{aligned}
$$

where (4.58) follows from conditioning reduces entropy and the fact that channel is DMC, i.e., $p(y_i|x^i,y^{i-1}) = p(y_i|x_i)$ with $x_i \leq s_i = f(x^{i-1},e^{i-1})$; (4.59) also follows from the fact that $s_i = f(x^{i-1},e^{i-1})$, a deterministic function. Next, we show that it suffices to consider input distributions in the form of $p(x_i|s_i)$ to maximize (4.59).

Let us fix $p(x_i|x^{i-1},e^{i-1})$ for $i = 1,\ldots,n-1$ and maximize the objective over $p(x_n|x^{n-1},e^{n-1})$. Note that fixing $p(x_i|x^{i-1},e^{i-1})$ for $i = 1,\ldots,n-1$ fixes $H(Y_i|Y^{i-1},E^{i-1})$ and $H(Y_i|X_i,S_i)$ for $i = 1,\ldots,n-1$ and $p(s_i)$ for $i = 1,\ldots,n$. The remaining term, $H(Y_n|Y^{n-1},E^{n-1}) - H(Y_n|X_n,S_n)$, is a function of $p(x_n|x^{n-1},e^{n-1})$. In particular, $H(Y_n|X_n,S_n)$ is just a function of $p(x_n|s_n)$ when $p(s_n)$ is fixed. Hence, it suffices to show that $H(Y_n|Y^{n-1},E^{n-1})$ is maximized by distributions of the form $p(x_i|s_i)$. To this end, we note that for any given $p(x^{n-1}|e^{n-1})$, $Y^{n-1} = y^{n-1}$ and $E^{n-1} = e^{n-1}$, a distribution is generated on x^{n-1}, denoted as $p(x^{n-1}|y^{n-1},e^{n-1})$, with the support set $\mathcal{F}_{n-1}(e^{n-1})$. We have:

$$
p(y_n|y^{n-1},e^{n-1}) = \sum_{x^n,s_n} p(y_n|x_n)p(x_n|s_n,x^{n-1},e^{n-1})p(x^{n-1}|y^{n-1},e^{n-1}) \qquad (4.60)
$$

In addition, the next battery energy level distribution is:

$$p(s_{n+1}) = \sum_{x^n, e^n} p(s_{n+1}|x_n, s_n, e_n) p(x_n|s_n, x^{n-1}, e^{n-1}) p(x^{n-1}, e^n) \tag{4.61}$$

where $p(s_{n+1}|x_n, s_n, e_n) = 1$ if and only if $s_{n+1} = \min\{s_n - x_n + e_n, E_{max}\}$ and 0 otherwise.

We select $p(x_n|s_n, x^{n-1}, e^{n-1})$ as in the following

$$\hat{p}(x_n|s_n, x^{n-1}, e^{n-1}) = p(x_n|s_n) = \sum_{x^{n-1}, e^{n-1}} p(x_n|s_n, x^{n-1}, e^{n-1}) p(x^{n-1}, e^{n-1}) \tag{4.62}$$

As $H(Y_n|Y^{n-1}, E^{n-1})$ is a concave function of $p(y_n|y^{n-1}, e^{n-1})$, we deduce from (4.60) and by Jensen's inequality that it yields higher $H(Y_n|Y^{n-1}, E^{n-1})$ value. Moreover, this selection $\hat{p}(x_n|s_n, x^{n-1}, e^{n-1})$ does not change the remaining energy distribution $p(s_{n+1})$ in view of (4.61). In particular, $p(x^{n-1}, y^{n-1}, e^n) = p(e_n) p(x^{n-1}, y^{n-1}, e^{n-1})$ Since this is true for any n, we prove that $p(x_i|s_i)$ is sufficient for the optimization problem on the left hand side of (4.56).

To conclude, we have shown that even under non-causal knowledge of E^n, the rate $R = \inf_n \frac{C_n}{n}$ is the highest achievable rate and it can be achieved by an encoding scheme that determines the channel input x_i as a stochastic function of only the battery state s_i. This result and its proof could be viewed as an extension of the coding theorem in [65].

We remark that the energy harvesting channel with deterministic energy arrivals and no side information considered in [81] is a special case of the current

problem. In view of Theorem 4.4, encoding based on the current battery state s_i is sufficient for achieving the capacity when energy arrivals are deterministic.

4.8.5 Proof of Corollary 4.2

In order to prove Corollary 4.2, it suffices to prove the following inequality:

$$\sup_{p(x_i|s_i)} I(X^n;Y^n|E^n) \geq \sup_{p(x_i|s_i)} \sum_{i=1}^{n} I(X_i;Y_i|S_i) \tag{4.63}$$

We first observe from (4.59) that whenever $p(x_i|x^{i-1},e^{i-1}) = p(x_i|s_i)$:

$$I(X^n;Y^n|E^n) = \sum_{i=1}^{n} H(Y_i|Y^{i-1},E^{i-1}) - H(Y_i|X_i,S_i) \tag{4.64}$$

Hence, it suffices to prove:

$$\sup_{p(x_i|s_i)} \sum_{i=1}^{n} H(Y_i|Y^{i-1},E^{i-1}) - H(Y_i|X_i,S_i) \geq \sup_{p(x_i|s_i)} \sum_{i=1}^{n} I(X_i;Y_i|S_i) \tag{4.65}$$

We note that since $X_i = f_i(S_i)$, the following Markov chain holds:

$$Y^{i-1}, E^{i-1} \leftrightarrow S_i \leftrightarrow X_i \leftrightarrow Y_i \tag{4.66}$$

Then, we have the following inequality due to the data processing inequality:

$$H(Y_i|Y^{i-1},E^{i-1}) \geq H(Y_i|S_i) \tag{4.67}$$

This proves the desired result in (4.65).

Chapter 5

Secrecy in Gaussian Energy Harvesting Channel

5.1 Introduction

In this chapter, we consider the Gaussian wiretap channel [21, 22, 87] which consists of a transmitter, a legitimate user and an eavesdropper as shown in Figure 5.1. In the Gaussian wiretap channel, each link is a memoryless additive white Gaussian noise (AWGN) channel. The goal of the transmitter is to have secure communication with the legitimate user while keeping the eavesdropper ignorant of this communication as much as possible.

Since the Gaussian wiretap channel is degraded, its rate-equivocation region is known in a single-letter form due to [21] under an average power constraint. In particular, under an average power constraint, Gaussian input with full power attains both the secrecy capacity and the capacity of the channel between the transmitter and the legitimate user, providing the entire rate-equivocation region [22]. One important implication of this result is that the transmitter and the legitimate user do not compromise from their communication rate in order to maximize the equivocation of their communication at the eavesdropper. In other words, there is no trade-off between the rate and the equivocation for the average power constrained Gaussian wiretap channel.

In this chapter, we start by considering the Gaussian wiretap channel with

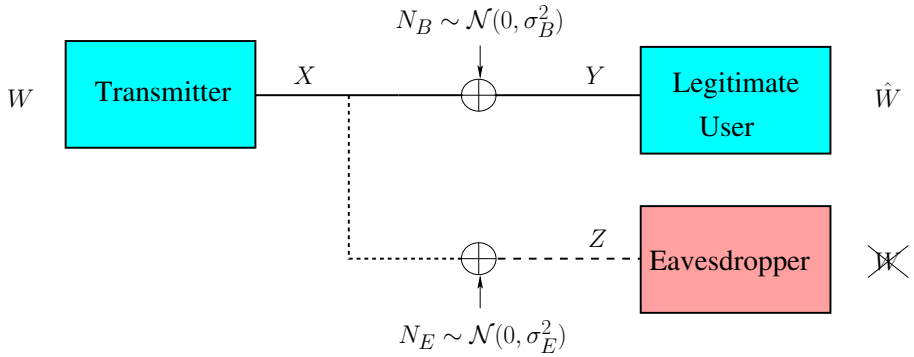

Figure 5.1: The Gaussian wiretap channel.

a static amplitude constraint. Similar to the average power constrained case, here also, we can use the existing single-letter description for the rate-equivocation region of the Gaussian wiretap channel due to [21]. However, unlike the average power constrained case, here, due to the peak power constraint, the corresponding optimization problems are harder to solve explicitly. For example, the entropy-power inequality, which is the key tool to obtain the rate-equivocation region under an average power constraint [22], does not provide a tight result for the rate-equivocation region under a peak power constraint.

We circumvent difficulties arising from the existence of a peak power constraint by using the methodology originally devised by [5, 6], and later, extended further by [7, 26, 58–60, 62, 63, 88]. First, we consider the single-letter description of the rate-equivocation region under a peak power constraint, and obtain necessary and sufficient conditions for the optimal input distribution. Next, we prove by contradiction that the optimal input distribution should be discrete with finite support. We provide numerical results which highlight an important difference between the peak power constrained and the average power constrained cases. As mentioned,

in the average power constrained case, both the secrecy capacity and the capacity are simultaneously achieved by the same input distribution (Gaussian distribution with full power). On the other hand, our numerical results demonstrate that under a peak power constraint, in general, the secrecy capacity and the capacity are not achieved by the same distribution. In other words, under a peak power constraint, in general, there is a trade-off between the rate and its equivocation, in the sense that, when we want to maximize the equivocation, we may need to compromise from the rate; and conversely, when we want to maximize the rate, we may need to compromise from its equivocation.

Next, we study the conditions under which a binary input distribution is optimal in the amplitude constrained Gaussian wiretap channel. By adapting the steps in [88] for the Gaussian wiretap channel, we show that if $A \leq 1.05$, the rate-equivocation region boundary is achieved by the symmetric binary distribution. In other words, there is no trade-off between the rate and its equivocation if the amplitude constraint is sufficiently small.

Then, we extend the optimality of discrete input distributions to the case when an additional variance constraint is imposed on the input. To this end, we provide a modified contradiction argument that uses the optimality conditions of the equivalent amplitude unconstrained optimization problem. In particular, we start with the KKT optimality conditions of the amplitude and variance constrained problem and show, using analyticity and the identity theorem, that these KKT conditions are equivalent to the KKT conditions of the amplitude unconstrained and variance constrained problem. The unique solution of the amplitude unconstrained

and variance constrained problem is known to be a Gaussian distribution. Since the Gaussian distribution is not amplitude constrained, this yields a contradiction. We present this modified contradiction argument in Appendix 5.5.3 for the single user AWGN channel, and adapt it in the text for the Gaussian wiretap channel.

Finally, we investigate the role of stochastic energy arrivals in the Gaussian wiretap channel, by considering an energy harvesting Gaussian wiretap channel with zero energy storage at the transmitter. In this system, the code symbols of the channel input obey stochastic amplitude constraints which are observed by the transmitter causally. This establishes a connection between the problem of data transmission with an energy harvesting transmitter and the problem of data transmission over state-dependent channels. Viewing the available energy at the transmitter as a channel state, the setting becomes a state-dependent wiretap channel with causal state information at the transmitter only.

A sequence of works about wiretap channel with state information have appeared in the literature [89–92]. However, none of them considered the wiretap channel with causal information at the transmitter only. Since the energy replenishes at the transmitter side independently in time, the energy at each channel use is a state that is available at the transmitter only. We first prove that single-letter Shannon strategies span the entire rate-equivocation region of the Gaussian wiretap channel under stochastic amplitude constraints. Then, we find the boundary of the rate-equivocation region using the single-letter expressions in terms of Shannon strategy. However, corresponding optimization problems are challenging to solve explicitly: The links of the constructed wiretap channel are not additive noise chan-

nels and the inputs are amplitude constrained. In this case, we provide numerically verifiable necessary and sufficient optimality conditions for the input distribution. Our numerical results show, for the cases that we considered, that the optimal input distributions are discrete with finite support.

5.2 Gaussian Wiretap Channel with Amplitude and Variance Constraints

The Gaussian wiretap channel is defined by

$$Y_i = X_i + N_{B_i}, \qquad i = 1, \ldots, n \tag{5.1}$$

$$Z_i = X_i + N_{E_i}, \qquad i = 1, \ldots, n \tag{5.2}$$

where X_i, Y_i, Z_i denote the channel input, the legitimate user's observation and the eavesdropper's observation, respectively. N_{B_i} and N_{E_i} are i.i.d. zero-mean Gaussian random variables with variances σ_B^2 and σ_E^2, respectively, where $\sigma_B^2 < \sigma_E^2$. We assume that there is an amplitude constraint on the channel input X_i as

$$|X_i| \leq A, \qquad i = 1, \ldots, n \tag{5.3}$$

An $(n, 2^{nR})$ code for the Gaussian wiretap channel with peak power constraint consists of a message set $W \in \mathcal{W} = \{1, \ldots, 2^{nR}\}$, an encoder at the transmitter $f_n : \mathcal{W} \to \mathbb{R}^n$ satisfying the peak power constraint in (5.3), and a decoder at the legitimate user $g_n : \mathbb{R}^n \to \mathcal{W}$. Equivocation of a code is measured by the normalized

conditional entropy $(1/n)H(W|Z^n)$, where W is a uniformly distributed random variable over $\mathcal{W}$. Probability of error for a code is defined as $P_e^n = \Pr[g_n(f_n(W)) \neq W]$. A rate-equivocation pair (R, R_e) is said to be achievable if there exists an $(n, 2^{nR})$ code satisfying $\lim_{n\to\infty} P_e^n = 0$, and

$$R_e \leq \lim_{n\to\infty} \frac{1}{n} H(W|Z^n) \tag{5.4}$$

The rate-equivocation region consists of all achievable rate-equivocation pairs, and is denoted by $\mathcal{C}$. A rate R is said to be perfectly secure if we have $R_e = R$, i.e., if there exists an $(n, 2^{nR})$ code satisfying $\lim_{n\to\infty}(1/n)I(W; Z^n) = 0$. Supremum of such rates is defined to be the secrecy capacity and denoted by C_s.

Since the Gaussian wiretap channel is stochastically degraded, its entire rate-equivocation region $\mathcal{C}$ can be expressed in a single-letter form by using the result of [21].

Theorem 5.1 *The rate-equivocation region of the Gaussian wiretap channel with a peak power constraint is given by the union of the rate-equivocation pairs* (R, R_e) *satisfying*

$$R \leq I(X; Y) \tag{5.5}$$

$$R_e \leq I(X; Y) - I(X; Z) \tag{5.6}$$

for some input distribution $F_X \in \Omega$, where the feasible set Ω is given by

$$\Omega \triangleq \left\{ F_X : \int_{-A}^{A} dF_X(x) = 1 \right\} \tag{5.7}$$

Since the rate-equivocation region $\mathcal{C}$ is convex due to time-sharing, it can be characterized by finding the tangent lines to the region $\mathcal{C}$, which are given by the solutions of

$$\max_{F_X \in \Omega} \; g_\mu(F_X) = \max_{F_X \in \Omega} \; \mu I(X;Y) + I(X;Y) - I(X;Z) \tag{5.8}$$

for all $\mu \geq 0$.

For the amplitude constrained Gaussian wiretap channel, our main result is to show that the maximizer distribution for (5.8) is discrete with finite support.

Theorem 5.2 *Let F_X^* be the maximizer of the optimization problem in (5.8) with a support set $\mathcal{S}_{F_X^*}$. The support set $\mathcal{S}_{F_X^*}$ is a finite set.*

Theorem 5.2 implies that the secrecy capacity C_s is also achieved by a discrete distribution with finite support, as stated in the following corollary.

Corollary 5.1 *Let F_X^* be the distribution that attains the secrecy capacity of the Gaussian wiretap channel with a peak power constraint. The support set $\mathcal{S}_{F_X^*}$ is a finite set.*

In the next two subsections, we first prove Corollary 5.1, and then, by using the proof of Corollary 5.1, we prove Theorem 5.2.

5.2.1 Proof of Corollary 5.1

The proof follows from the convexity of the optimization problem [93] and hence the fact that derivation of an equivalent necessary and sufficient optimality condition in terms of equivocation density is possible [5, 6]. Then, we provide a contradiction argument to prove that a support set with infinite points cannot be optimal under an amplitude constrained input. We start by noting that the secrecy capacity of the Gaussian wiretap channel with peak power constraint is given by

$$C_s = \max_{F_X \in \Omega} g_0(F_X) = \max_{F_X \in \Omega} I(X;Y) - I(X;Z) \tag{5.9}$$

where the objective function $g_0(F_X)$ is a strictly concave functional of the input distribution F_X due to the assumption $\sigma_B^2 < \sigma_E^2$ [93]. Moreover, the feasible set Ω is convex and sequentially compact with respect to the Levy metric [5]. Thus, (5.9) is a convex optimization problem with a unique solution.

Next, we obtain the necessary and sufficient conditions that the optimal distribution F_X^* of the optimization problem in (5.9) should satisfy. To this end, we introduce some notation which will be frequently used throughout the chapter. Since both channels are AWGN, the output densities for Y and Z exist for any input distribution F_X, and are given by

$$p_Y(y;F_X) = \int_{-A}^{A} \phi_B(y-x) dF_X(x), \qquad y \in \mathbb{R} \tag{5.10}$$

$$p_Z(z;F_X) = \int_{-A}^{A} \phi_E(z-x) dF_X(x), \qquad z \in \mathbb{R} \tag{5.11}$$

where $\phi_B(y), \phi_E(z)$ are zero-mean Gaussian densities with variances σ_B^2 and σ_E^2, respectively.

We define the equivocation density $r_e(x; F_X)$ as

$$r_e(x; F_X) = i_B(x; F_X) - i_E(x; F_X) \tag{5.12}$$

where $i_B(x; F_X)$ and $i_E(x; F_X)$ are the mutual information densities for the main channel and the wiretapper's channel

$$i_B(x; F_X) = -\phi_B(x) * \log\left(p_Y(x; F_X)\right) - \frac{1}{2}\log\left(2\pi e\sigma_B^2\right) \tag{5.13}$$

$$i_E(x; F_X) = -\phi_E(x) * \log\left(p_Z(x; F_X)\right) - \frac{1}{2}\log\left(2\pi e\sigma_E^2\right) \tag{5.14}$$

where $*$ denotes the convolution. We note that the convolutions in (5.13) and (5.14) follow from the symmetry of the Gaussian density function. The mutual information and the mutual information density are related through

$$I(X;Y) = \int_{-A}^{A} i_B(x; F_X) dF_X(x) \tag{5.15}$$

$$I(X;Z) = \int_{-A}^{A} i_E(x; F_X) dF_X(x) \tag{5.16}$$

Since the Gaussian wiretap channel is stochastically degraded, without loss of generality, we can assume $Z = Y + Z_D$ for some zero-mean Gaussian random variable Z_D with variance $\sigma_D^2 = \sigma_E^2 - \sigma_B^2$. We denote the density of Z_D by $\phi_D(x)$ which leads to the identity $\phi_E = \phi_B * \phi_D$. Using this identity in conjunction with (5.13)-(5.14),

the equivocation density $r_e(x; F_X)$ in (5.12) can be expressed as

$$r_e(x; F_X) = \frac{1}{2} \log \left(\frac{\sigma_E^2}{\sigma_B^2} \right) - \phi_B(x) * [\log (p_Y(x; F_X)) - \phi_D(x) * \log (p_Z(x; F_X))] \tag{5.17}$$

Now, we are ready to obtain the necessary and sufficient conditions for the optimal distribution of the optimization problem in (5.9). To this end, we first note that the objective function $g_0(F_X)$ in (5.9) is Frechet differentiable and the derivative of $g_0(F_X)$ at F_{X_0} in the direction of F_X is given by:

$$\begin{aligned} &\lim_{\theta \to 0} \frac{1}{\theta} \left[g_0(\theta F_X + (1-\theta) F_{X_0}) - g_0(F_{X_0}) \right] \\ &\qquad = \int_{\mathbb{R}} (p_Y(y; F_{X_0}) - p_Y(y; F_X)) \log (p_Y(y; F_{X_0}))\, dy \\ &\qquad\quad - \int_{\mathbb{R}} (p_Z(z; F_{X_0}) - p_Z(z; F_X)) \log (p_Z(z; F_{X_0}))\, dz \end{aligned} \tag{5.18}$$

which, using the equivocation density in (5.17), is expressed as

$$\lim_{\theta \to 0} \frac{1}{\theta} \left[g_0(\theta F_{X_0} + (1-\theta) F_X) - g_0(F_X) \right] = \int_{-A}^{A} r_e(x; F_{X_0}) dF_X(x) - g_0(F_{X_0}) \tag{5.19}$$

Due to the linearity of the derivative operation, the Frechet derivative of $g_0(F_X)$ in (5.18) is the difference of Frechet derivatives of $I(X;Y)$ and $I(X;Z)$. Explicit derivations of the Frechet derivatives of individual mutual information terms can be found in [5, Proof of Proposition 1] and [6, Lemma on p. 29].

In view of the concavity of the objective functional in (5.9) with respect to

the input distribution F_X, steps analogous to [5, Corollary 1] yield the following necessary and sufficient conditions for the optimality of the distribution F_X^*:

$$r_e(x; F_X^*) \leq C_s, \qquad \forall x \in [-A, A] \tag{5.20}$$

$$r_e(x; F_X^*) = C_s, \qquad \forall x \in \mathcal{S}_{F_X^*} \tag{5.21}$$

where the secrecy capacity C_s is expressed as

$$C_s = I_B(F_X^*) - I_E(F_X^*) = h_Y(F_X^*) - h_Z(F_X^*) + \frac{1}{2}\log\left(\frac{\sigma_E^2}{\sigma_B^2}\right) \tag{5.22}$$

where $I_B(F_X^*)$ and $I_E(F_X^*)$ are the mutual information for Bob (between X and Y) and Eve (between X and Z), respectively, generated by the input distribution F_X^*. Similarly, $h_Y(F_X^*)$ and $h_Z(F_X^*)$ are the differential entropies of Y and Z, respectively, generated by the input distribution F_X^*. We note that (5.20)-(5.21) are equivalent to the Kuhn-Tucker conditions for the functional optimization problem in (5.9). Due to the concavity of the objective in (5.9), non-negativity of the Frecehet derivative in (5.18) in every direction is necessary and sufficient, c.f. [5, Proposition 1]. This, in turn, is equivalent to (5.20)-(5.21) by [5, Corollary 1].

We now prove by contradiction that the support set $\mathcal{S}_{F_X^*}$ of the optimal distribution is a finite set. To reach a contradiction, we use the optimality conditions given by (5.20)-(5.21). To this end, we note that both $i_B(x; F_X)$ and $i_E(x; F_X)$ have analytic extensions over the whole complex plane $\mathbb{C}$ [5]. Since $\phi_B(z)$, $\phi_E(z)$ have analytic extensions for all $z \in \mathbb{C}$, the following functions of a complex variable are

well defined and analytic for all $z \in \mathbb{C}$:

$$i_B(z; F_X) = -\int_{-\infty}^{\infty} \phi_B(z-\tau) \log\left(p_Y(\tau; F_X)\right) d\tau - \frac{1}{2}\log\left(2\pi e \sigma_B^2\right) \tag{5.23}$$

$$i_E(z; F_X) = -\int_{-\infty}^{\infty} \phi_E(z-\tau) \log\left(p_Z(\tau; F_X)\right) d\tau - \frac{1}{2}\log\left(2\pi e \sigma_E^2\right) \tag{5.24}$$

Therefore, the equivocation density has the analytic extension $r_e(z; F_X) = i_B(z; F_X) - i_E(z; F_X)$ for $z \in \mathbb{C}$. Now, let us assume that $\mathcal{S}_{F_X^*}$ has infinite number of elements. In view of the optimality condition (5.21), analyticity of $r_e(z; F_X)$ over all $\mathbb{C}$ and the identity theorem for complex numbers along with Bolzano-Weierstrass theorem, if $\mathcal{S}_{F_X^*}$ has infinite number of elements, we should have $r_e(z; F_X^*) = C_s$ for all $z \in \mathbb{C}$, which, in turn, implies

$$r_e(x; F_X^*) = C_s, \qquad \forall x \in \mathbb{R} \tag{5.25}$$

Next, we show that (5.25) results in a contradiction. To this end, we first state the following result from [26].

Lemma 5.1 ([26, Corollary 9]) *Let Z be a Gaussian random variable and $P_Z(z)$ be the corresponding probability density function. Suppose $g(z)$ is a continuous function such that $|g(z)| \leq \alpha + \beta|z|^2$ for some $\alpha, \beta > 0$. If $P_Z(z) * g(z)$ is the zero function, then $g(z)$ is also the zero function.*

Next, we rearrange (5.25) by using (5.17) to get

$$\int_{\mathbb{R}} \phi_B(y-x)v(y)dy = 0, \qquad \forall x \in \mathbb{R} \tag{5.26}$$

where $v(y)$ and c are defined as

$$v(y) = c + \log\left(p_Y(y; F_X^*)\right) - \int_{\mathbb{R}} \phi_D(\tau) \log\left(p_Z(y-\tau; F_X^*)\right) d\tau \tag{5.27}$$

$$c = h_Y(F_X^*) - h_Z(F_X^*) \tag{5.28}$$

Note that $c < 0$ for any nontrivial input distribution F_X^*. This follows from the stochastic degradedness of the channel, i.e., $Z = Y + Z_D$ for some zero-mean Gaussian random variable Z_D with variance $\sigma_D^2 = \sigma_E^2 - \sigma_B^2$. Hence $h(Z) > h(Z|Z_D) = h(Y)$ by the fact that conditioning reduces entropy, and this proves $c < 0$. Note that $h_Y(F_X^*)$ and $h_Z(F_X^*)$ are representations of $h(Y)$ and $h(Z)$, respectively.

Next, we show that if (5.26) holds, we should have $v(y) = 0, \forall y \in \mathbb{R}$. To this end, we note that since $p_Y(y; F_X^*) = \int_{-A}^{A} \phi_B(y-x) dF_X^*(x)$, Jensen's inequality implies

$$\frac{1}{\sqrt{2\pi\sigma_B^2}} \geq p_Y(y; F_X^*) \geq \frac{1}{\sqrt{2\pi\sigma_B^2}} e^{-\frac{1}{2\sigma_B^2}\int_{-A}^{A}(y-x)^2 dF_X^*(x)} \tag{5.29}$$

which, in turn, implies $|\log\left(p_Y(y; F_X^*)\right)| \leq \alpha y^2 + \beta$ for some $\alpha, \beta > 0$. Similarly, we can show that $|\log\left(p_Z(y; F_X^*)\right)| \leq \kappa y^2 + \gamma$ for some $\kappa, \gamma > 0$. Consequently, we have $|v(y)| \leq \eta y^2 + \zeta$ for some $\eta, \zeta > 0$, which, in conjunction with (5.26) and by

Lemma 5.1, implies that $v(y) = 0$ for all $y \in \mathbb{R}$.

Now, we show that we cannot have $v(y) = 0, \forall y \in \mathbb{R}$, and therefore, reach a contradiction. In particular, we show that there exists y' such that $v(y) < 0, \forall y \geq y'$. To this end, we note that $c < 0$ and introduce the following lemma.

Lemma 5.2 *There exists sufficiently large y' such that $\forall y \geq y'$, we have*

$$\int_{\mathbb{R}} \phi_D(\tau) \log \left(p_Z(y - \tau; F_X^*) \right) d\tau \geq \log \left(p_Y(y; F_X^*) \right) \tag{5.30}$$

We provide the proof of Lemma 5.2 in Appendix 5.5.1.

Lemma 5.2 and the fact that $c < 0$ imply that $v(y) < 0, \forall y \geq y'$, which, in turn, implies that (5.26) cannot hold. This, in turn, implies that $\mathcal{S}_{F_X^*}$ cannot have infinite number of elements. This completes the proof of Corollary 5.1.

5.2.2 Proof of Theorem 5.2

In this section, we extend our analysis in the previous section to the entire rate-equivocation region. This extension entails generalizing the contradiction argument in the proof of Corollary 5.1 to the case when an additional mutual information term is present in the objective function. We start by noting that the rate-equivocation region can be characterized by solving the following optimization problem

$$\max_{F_X \in \Omega} g_\mu(F_X) = \max_{F_X \in \Omega} \mu I(X;Y) + I(X;Y) - I(X;Z) \tag{5.31}$$

for all $\mu \geq 0$. Since the objective function $g_\mu(F_X)$ in (5.31) is strictly concave, and the feasible set Ω is convex and sequentially compact with respect to the Levy metric, the optimization problem in (5.31) has a unique maximizer. We denote the optimal input distribution for (5.31) as F_X^* which depends on the value of μ.

Now, we obtain the necessary and sufficient conditions for the optimal distribution of the optimization problem in (5.31). To this end, we note that $g_\mu(F_X)$ is Frechet differentiable, and its derivative at F_{X_0} in the direction of F_X is given as

$$\lim_{\theta \to 0} \frac{1}{\theta} \left[g_\mu(\theta F_X + (1-\theta) F_{X_0}) - g_\mu(F_{X_0}) \right] = \int_{-A}^{A} \left[\mu i_B(x; F_{X_0}) + r_e(x; F_{X_0}) \right] dF_X(x) - g_\mu(F_{X_0}) \tag{5.32}$$

Using similar arguments to those in [5], the necessary and sufficient conditions for the optimal distribution of the optimization problem in (5.31) can be obtained as follows

$$\mu i_B(x; F_X^*) + r_e(x; F_X^*) \leq (\mu+1) I_B(F_X^*) - I_E(F_X^*), \qquad \forall x \in [-A, A] \tag{5.33}$$

$$\mu i_B(x; F_X^*) + r_e(x; F_X^*) = (\mu+1) I_B(F_X^*) - I_E(F_X^*), \qquad \forall x \in \mathcal{S}_{F_X^*} \tag{5.34}$$

where $I_B(F_X^*)$ and $I_E(F_X^*)$ are the mutual information for Bob (between X and Y) and Eve (between X and Z), respectively, generated by the input distribution F_X^*. Similarly, $i_B(x; F_X^*)$ and $i_E(x; F_X^*)$ are the corresponding mutual information densities generated by F_X^*.

Now, we show that the optimal input distribution F_X^* should have finite sup-

port. Similar to the proof of Corollary 5.1, here also, we prove the finiteness of the support set by contradiction and using the optimality conditions in (5.33)-(5.34).

Let us assume that $\mathcal{S}_{F_X^*}$ has infinite number of elements. Under this assumption, (5.34), analyticity of $i_B(z;F_X^*)$ and $r_e(z;F_X^*)$ over all $\mathbb{C}$ and the identity theorem for complex numbers imply that $\mu i_B(z;F_X^*)+r_e(z;F_X^*)=(\mu+1)I_B(F_X^*)-I_E(F_X^*)$ over all $\mathbb{C}$, which, in turn, implies that

$$\mu i_B(x;F_X^*)+r_e(x;F_X^*)=(\mu+1)I_B(F_X^*)-I_E(F_X^*), \qquad \forall x\in\mathbb{R} \tag{5.35}$$

Next, we show that (5.35) results in a contradiction. To this end, we first rearrange (5.35) to obtain

$$\int_{\mathbb{R}}\phi_B(y-x)\hat{v}(y)dy=0 \tag{5.36}$$

where $\hat{v}(y)$ and $\hat{c}$ are given by

$$\hat{v}(y)=\hat{c}+(\mu+1)\log\left(p_Y(y;F_X^*)\right)-\int_{\mathbb{R}}\phi_D(\tau)\log\left(p_Z(y-\tau;F_X^*)\right)d\tau \tag{5.37}$$

$$\hat{c}=(\mu+1)h_Y(F_X^*)-h_Z(F_X^*) \tag{5.38}$$

We note that the expressions in (5.37)-(5.38) differ from the ones in (5.27)-(5.28) for the secrecy capacity in the additional terms factored by μ; hence, the negativity of $\hat{c}$ is not immediately ensured. Therefore, we take an alternative route for the proof. By using similar arguments to those we provided in the proof of Corollary 5.1, one

can show that $|\hat{v}(y)| \leq \eta y^2 + \zeta$ for some $\eta, \zeta > 0$. By Lemma 5.1, this implies that if (5.36) holds, we should have $\hat{v}(y) = 0, \forall y \in \mathbb{R}$. Next, we show that we cannot have $\hat{v}(y) = 0, \forall y \in \mathbb{R}$. Using Lemma 5.2 and the fact that $h_Y(F_X^*) - h_Z(F_X^*) < 0$ in (5.37), we get

$$\hat{v}(y) - \mu\big(h_Y(F_X^*) + \log\left(p_Y(y; F_X^*)\right)\big) < 0, \qquad \forall y \geq y' \tag{5.39}$$

Hence, if $\hat{v}(y) = 0, \forall y \in \mathbb{R}$ holds, due to (5.39), we should have

$$h_Y(F_X^*) + \log\left(p_Y(y; F_X^*)\right) > 0, \qquad \forall y \geq y' \tag{5.40}$$

which implies

$$p_Y(y; F_X^*) \geq e^{-h_Y(F_X^*)}, \qquad \forall y \geq y' \tag{5.41}$$

However, since $p_Y(y; F_X^*)$ is a density function, it has to vanish as $y \to \infty$, and (5.41) cannot hold. Hence, we reach a contradiction; implying that the optimal input distribution should have a finite support set. This completes the proof of Theorem 5.2.

5.2.3 Numerical Results for the Amplitude Constrained Case

In this section, we provide numerical illustrations for the secrecy capacity and the rate-equivocation region of the Gaussian wiretap channel under a peak power con-

straint.

We first consider how the secrecy capacity changes with respect to the amplitude constraint A for $\sigma_B^2 = 1$ and $\sigma_E^2 = 2$. We provide a plot of the equivocation density for an optimal input distribution in Figure 5.2 for $A = 2.6$. We numerically calculated that for these parameters the optimal input distribution is quaternary located at $x = \pm 0.64$ and $x = \pm 2.6$ with probability masses 0.2496 at $x = \pm 0.64$ and 0.2504 at $x = \pm 2.6$. We observe that the equivocation density is less than or equal to the secrecy capacity and it is equal to the secrecy capacity at the mass points; verifying the optimality conditions in (5.20)-(5.21).

Next, we observe in Figure 5.3 that the rates of increase of the amplitude and variance constrained capacities with respect to SNR follow the same asymptote. A similar observation was made by Smith [5] for the capacities without secrecy constraint. Moreover, in Figure 5.3, we also plot the difference $C_B - C_E$ where C_B and C_E are the legitimate user's and the eavesdropper's capacities, respectively. This difference is, in general, a lower bound for the secrecy capacity C_s. We observe that, for small values of A, $C_B - C_E$ and C_s are identical[1]. However, as A increases, $C_B - C_E$ and C_s become different. We note that $I(X;Y)$, $I(X;Z)$ and the difference $I(X;Y) - I(X;Z)$ are concave in the input distribution. Hence, one may be tempted to conclude that if the same input distribution maximizes both $I(X;Y)$ and $I(X;Z)$, then it should also maximize the difference $I(X;Y) - I(X;Z)$. However, this observation holds if the capacity achieving input distribution is within the interior of the feasible set; but not on the boundary, see also [93, Theorem 3]. For the

[1]We will investigate this analytically in Section 5.2.4.

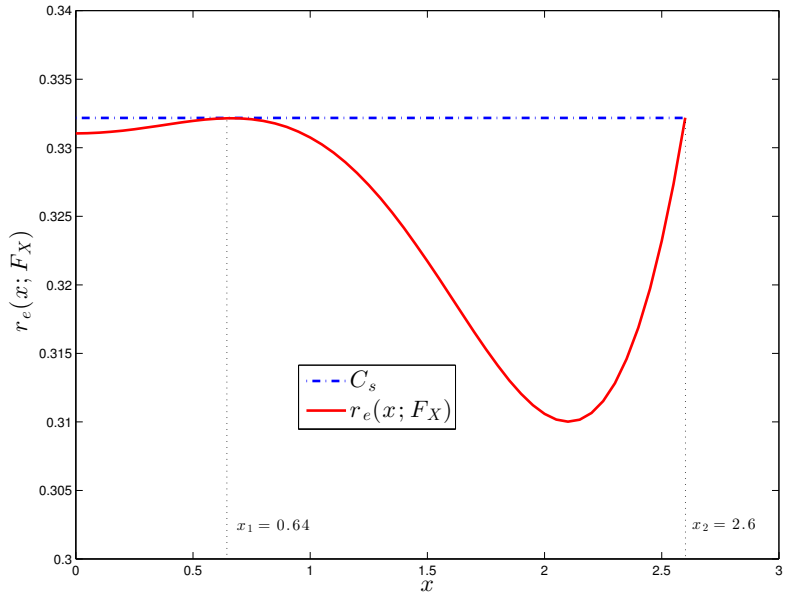

Figure 5.2: Illustration of the equivocation density yielded by the optimal input distribution when $\sigma_B^2 = 1$, $\sigma_E^2 = 2$ and $A = 2.6$.

average power constrained case, Gaussian distribution maximizes both $I(X;Y)$ and $I(X;Z)$ and as the Gaussian distribution is not on the boundary of the feasible set, it also maximizes the difference $I(X;Y) - I(X;Z)$. However, for the peak power constrained case, discrete distributions are extreme distributions, lying out of the interior of the space of input distributions. Therefore, even if both $I(X;Y)$ and $I(X;Z)$ are maximized by the same discrete distribution, $I(X;Y) - I(X;Z)$ may be maximized by a different input distribution. As a specific example, when $A = 1.5$ and hence $A^2 = 2.25$, while both $I(X;Y)$ and $I(X;Z)$ are maximized by the same binary distribution with equal probability masses at $\pm A$, $I(X;Y) - I(X;Z)$ is maximized by a ternary distribution with mass points at $\pm A$ and 0 with probabilities 0.399, 0.399 and 0.202, respectively. This explains the difference between C_s and

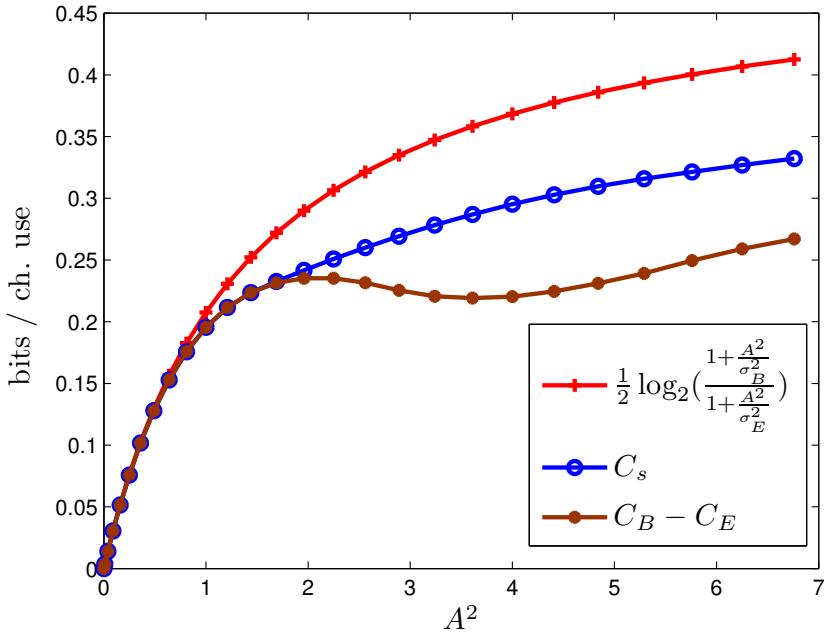

Figure 5.3: The secrecy capacity for $\sigma_B^2 = 1$ and $\sigma_E^2 = 2$ versus the square of the amplitude constraint A.

$C_B - C_E$ at $A^2 = 2.25$ in Figure 5.3.

In Figure 5.4, we plot the entire rate-equivocation region of the wiretap channel when $\sigma_B^2 = 1$ and $\sigma_E^2 = 1.6$ for two different values of A. When $A = 1$, it is clear from Figure 5.4 that both the secrecy capacity and the capacity can be attained simultaneously. In particular, for $A = 1$, the binary input distribution located at $\pm A$ with equal probabilities achieves both the capacity and the secrecy capacity. In fact, for $A = 1$, the binary distribution at $\pm A$ with equal probabilities maximizes $I(X;Y)$, $I(X;Z)$ and $I(X;Y)-I(X;Z)$. That is, the optimal input distributions for the secrecy capacity and the capacity are identical. This implies that, when $A = 1$, the transmitter can communicate with the legitimate user at the capacity while achieving the maximum equivocation at the same time. On the other hand, when

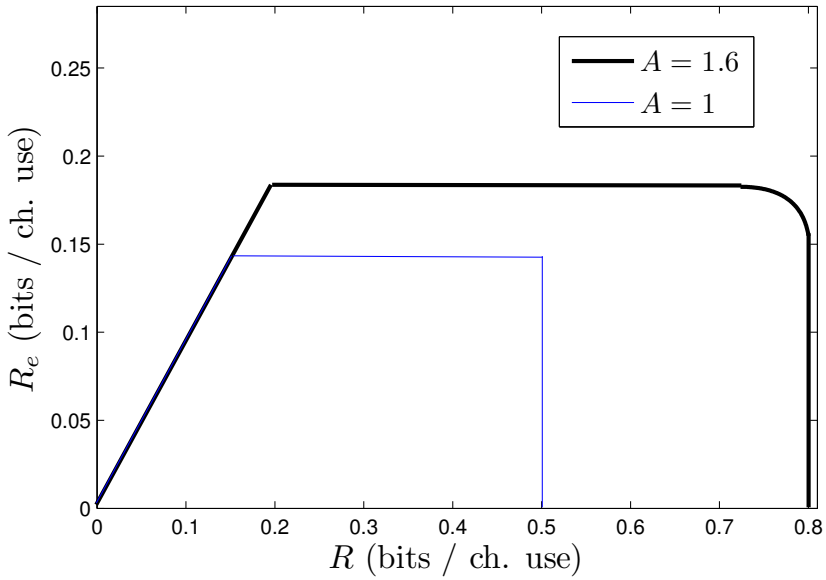

Figure 5.4: The rate-equivocation regions for $\sigma_B^2 = 1$ and $\sigma_E^2 = 1.6$ under amplitude constraints $A = 1$ and $A = 1.6$.

$A = 1.6$, the secrecy capacity and the capacity cannot be achieved simultaneously. In particular, for $A = 1.6$, the binary input distribution located at $\pm A$ with equal probabilities achieves the capacity, while a ternary distribution located at $x = \pm A$ and $x = 0$ with probability masses 0.358 at $\pm A$ and 0.284 at 0 achieves the secrecy capacity, i.e., the optimal input distributions for the secrecy capacity and the capacity are different. In other words, there is a trade-off between the rate and the equivocation in the sense that, to increase the communication rate, we should compromise from the equivocation of this communication, and to increase the achieved equivocation, we should compromise from the communication rate. This result is in contrast with the average power constrained case, where irrespective of the average power constraint, both the secrecy capacity and the capacity can be simultaneously achieved by a Gaussian distribution with full power.

5.2.4 On the Optimality of Symmetric Binary Distribution

We have seen that in the peak power constrained case, there may be a trade-off between the secrecy capacity and the capacity. However, the numerical results in Section 5.2.3 indicate that if the amplitude constraint is sufficiently small, binary distribution achieves both the secrecy capacity and the capacity simultaneously. In this section, we will quantify this observation by extending the result in [88] to the wiretap channel setting.

We first note that the optimal input distributions that solve (5.8) are always symmetric around the origin as stated in the following lemma, which is proved in Appendix 5.5.2.

Lemma 5.3 *The solution of (5.8) is symmetric around the origin.*

Moreover, there are always non-zero probability mass points at $-A$ and $+A$ when $\mu = \infty$, i.e., when the objective function is $I(X;Y)$; see also [64]. A possible proof for this follows from the I-MMSE relation [94, 95], since $I(X;Y)$ is monotone increasing function of the snr. Therefore, if the amplitude constraint is not satisfied with equality, there is always room for improvement. On the other hand, it is not clear that the mutual information difference $I(X;Y) - I(X;Z)$ is always monotone increasing with the snr and hence the inclusion of $+A$ and $-A$ in the support set of the optimal input distribution for all $\mu > 0$ is inconclusive. However, we observed in our numerical studies that $+A$ and $-A$ points are always included. A mathematical proof for this remains an open problem.

Next, we will follow steps analogous to those in [88]. We first note that by

using the I-MMSE relation in [94, 95], when $\sigma_B^2 = 1$ we can express the mutual information difference as:

$$I(X;Y) - I(X;Z) = \int_{\frac{1}{\sigma_E^2}}^{1} \text{mmse}(X|\sqrt{\gamma}X + N)d\gamma \tag{5.42}$$

where $\text{mmse}(X|\sqrt{\gamma}X+N)$ is the minimum mean squared error for the input X given the noisy observation $\sqrt{\gamma}X + N$ where N is a zero-mean unit-variance Gaussian noise independent of X. Note that $\text{mmse}(X|\sqrt{\gamma}X + N)$ is a functional of the input distribution F_X. In [96], it is shown that the least favorable (MMSE maximizing) input distribution is the symmetric binary distribution $\frac{1}{2}\delta_{-A}+\frac{1}{2}\delta_A$ if $|X| \leq A \leq 1.05$ and $\gamma \leq 1$. Therefore, as in [88], the integrand on the right hand side of (5.42) is always maximized by this binary input distribution for the range $\gamma \in (\frac{1}{\sigma_E^2}, 1)$. This implies that $I(X;Y)$ and $I(X;Y) - I(X;Z)$ are both maximized by the symmetric binary distribution located at $\pm A$ if $A \leq 1.05$.

Theorem 5.3 *If $A \leq 1.05$, the entire rate-equivocation region boundary is achieved by the symmetric binary input distribution $\frac{1}{2}\delta_{-A} + \frac{1}{2}\delta_A$.*

Theorem 5.3 implies that for sufficiently small amplitude constraints, binary distribution is optimal for the secrecy capacity. As we increase the amplitude constraint, optimal distribution changes. Let A_c be the critical maximum amplitude constraint for which the secrecy capacity achieving input distribution is binary. One can numerically calculate A_c for specified $\sigma_B^2 = 1$ and $\sigma_E^2 > 1$ values. In [64], $A = 1.67$ is calculated as the maximum amplitude constraint for which the legitimate user's capacity is achieved by the binary distribution. Accordingly, as

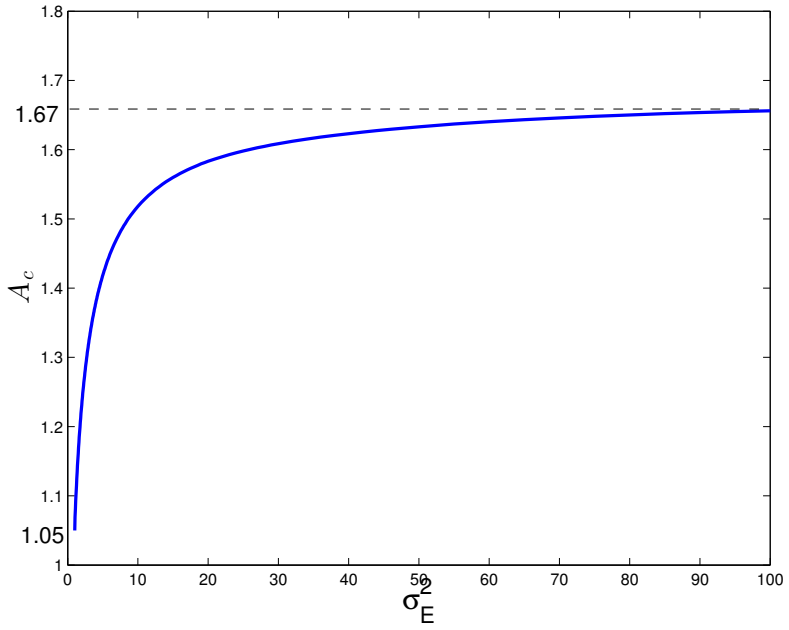

Figure 5.5: Critical amplitude A_c where the optimal distribution switches from binary to ternary with respect to σ_E^2.

$\sigma_E^2 \to \infty$, A_c approaches 1.67. On the other extreme, as $\sigma_E^2 \to 1$, the critical amplitude constraint approaches $A_c = 1.05$ due to the relation in (5.42) and the fact that the MMSE maximizer distribution transitions from binary to ternary at $A = 1.05$ as calculated in [96]. In Figure 5.5, we plot A_c with respect to σ_E^2. The range of A_c is [1.05, 1.67]. A_c monotonically increases from 1.05 to 1.67 as the noise variance of the eavesdropper σ_E^2 increases from 1 to ∞, when $\sigma_B^2 = 1$.

5.2.5 The Case of Amplitude and Variance Constraints

In this section, we generalize the discreteness result for the optimal input distribution when a variance constraint is present in addition to an amplitude constraint. In the AWGN channel with amplitude and variance constraints, the proof of discrete-

ness follows from the fact that if the optimal input distribution F_X^* has infinitely many points in its support set, then it has to be a Gaussian distribution, contradicting the fact that the input is amplitude constrained [5, 6, 26]. This fact is proved in [5, 6, 26] by the observation (after using properties of Schwartz functions) that the output density $p_Y(y; F_X^*)$ has to be Gaussian distributed if the support set of F_X^* has infinitely many points. In the Gaussian wiretap channel setting under amplitude and variance constraints, proving that $p_Y(y; F_X^*)$ and $p_Z(z; F_X^*)$ have to be both Gaussian distributed if the support of the optimal input distribution F_X^* has infinitely many elements is not straightforward using the properties of Schwartz functions. Therefore, we need an alternative approach to prove the fact that the optimal input distribution is still discrete under amplitude and variance constraints in the Gaussian wiretap channel. To this end, we devise in Appendix 5.5.3 a modified argument for the discreteness proof in [5, 6, 26] for the AWGN channel with amplitude and variance constraints. In the following, we show that this modified argument is more suitable for our purposes as it easily generalizes to the wiretap channel with amplitude and variance constraints.

We now generalize Theorem 5.2 and Corollary 5.1 for the case when we have both amplitude and variance constraints by establishing parallels to the modified proof method presented in Appendix 5.5.3. Let the variance constraint be P. The new feasible set for the input distribution is

$$\Omega_{A,P} = \left\{ F_X : \int_{-A}^{A} dF_X(x) = 1, \quad \int_{-A}^{A} x^2 dF_X(x) \leq P \right\} \tag{5.43}$$

We start with considering the secrecy capacity, C_s:

$$C_s = \max_{F_X \in \Omega_{A,P}} I(X;Y) - I(X;Z) \tag{5.44}$$

In view of [5, Proposition 3] and the strict concavity of the mutual information difference $I(X;Y) - I(X;Z)$ along with the compactness of $\Omega_{A,P}$, the necessary and sufficient conditions in (5.20)-(5.21) take the following new form

$$r_e(x;F_X^*) - \lambda x^2 \leq C_s - \lambda E[X^2], \qquad \forall x \in [-A, A] \tag{5.45}$$

$$r_e(x;F_X^*) - \lambda x^2 = C_s - \lambda E[X^2], \qquad \forall x \in \mathcal{S}_{F_X^*} \tag{5.46}$$

$$\lambda \left(E[X^2] - P \right) = 0 \tag{5.47}$$

for some $\lambda \geq 0$. We note that if the variance constraint is not tight for the optimal distribution F_X^*, then $\lambda = 0$. In this case, F_X^* is the optimal distribution under the amplitude constraint only, which has already been proven in Corollary 5.1 to be discrete with finite support. Therefore, we assume, without loss of generality, that $\lambda > 0$ and (5.45)-(5.47) reduce to:

$$r_e(x;F_X^*) - \lambda x^2 \leq C_s - \lambda P, \qquad \forall x \in [-A, A] \tag{5.48}$$

$$r_e(x;F_X^*) - \lambda x^2 = C_s - \lambda P, \qquad \forall x \in \mathcal{S}_{F_X^*} \tag{5.49}$$

$$E[X^2] = P \tag{5.50}$$

Next, we prove by contradiction that the input distribution F_X^* that satisfies (5.48)-

(5.50) must be a discrete distribution with finite support. Assume that $\mathcal{S}_{F_X^*}$ has infinite number of elements. In view of (5.48)-(5.50), analyticity of $r_e(z; F_X)$ and z^2 over $\mathbb{C}$ and the identity theorem for complex numbers, we have

$$r_e(x; F_X^*) - \lambda x^2 = C_s - \lambda P, \qquad \forall x \in \mathbb{R} \tag{5.51}$$

$$E[X^2] = P \tag{5.52}$$

We can show by substitution that (5.51)-(5.52) are satisfied when $\lambda = \frac{\log(e)}{2}\left(\frac{1}{\sigma_B^2+P} - \frac{1}{\sigma_E^2+P}\right)$ and F_X is selected as the Gaussian distribution with zero-mean and variance P, i.e., $F_X(x) = \int_{-\infty}^{x} \frac{1}{\sqrt{2\pi P}} e^{-\frac{y^2}{2P}} dy$. In this case, $C_s = \frac{1}{2}\log\left(1+\frac{P}{\sigma_B^2}\right) - \frac{1}{2}\log\left(1+\frac{P}{\sigma_E^2}\right)$. We claim that (5.51)-(5.52) cannot have another solution. To prove this claim, we note that (5.51)-(5.52) are independent of the amplitude constraint A and therefore are valid for any A, in particular for $A \to \infty$. That is, (5.51)-(5.52) are also the KKT conditions for the amplitude unconstrained problem (c.f. Appendix 5.5.3):

$$\max_{E[X^2] \le P} I(X;Y) - I(X;Z) \tag{5.53}$$

It is well-known by [22] using the entropy power inequality or alternatively by [95] using the I-MMSE relation that the unique solution of (5.53) is the Gaussian input distribution with zero-mean and variance P. We conclude that whenever (5.45)-(5.47) have a solution F_X^* with a support set of infinitely many points, it is a Gaussian distribution. However, since Gaussian distribution does not satisfy the amplitude

constraint, the optimal input distribution F_X^* that achieves the secrecy capacity C_s cannot have infinitely many mass points, and must be a discrete distribution with finite support.

We can extend this contradiction argument for the entire rate-equivocation region. Consider the optimization problem for determining the boundary point of the rate-equivocation region with slope $\mu \geq 0$:

$$\max_{F_X \in \Omega_{A,P}} (\mu+1)I(X;Y) - I(X;Z) \tag{5.54}$$

Note that if the variance constraint is not tight, i.e., $E[X^2] < P$, the problem again reduces to the case where only the amplitude constraint is present, in which case the optimal input distribution is discrete with finite support by Theorem 5.2. Hence, we assume without loss of generality that the variance constraint is tight and the necessary and sufficient optimality conditions for (5.54) are:

$$\mu i_B(x;F_X^*) + r_e(x;F_X^*) - \lambda x^2 \leq (\mu+1)I_B(F_X^*) - I_E(F_X^*) - \lambda P, \ \forall x \in [-A, A] \tag{5.55}$$

$$\mu i_B(x;F_X^*) + r_e(x;F_X^*) - \lambda x^2 \leq (\mu+1)I_B(F_X^*) - I_E(F_X^*) - \lambda P, \ \forall x \in \mathcal{S}_{F_X^*} \tag{5.56}$$

$$E[X^2] = P \tag{5.57}$$

Next, we prove by contradiction that the input distribution F_X^* that satisfies (5.55)-(5.57) must be a discrete distribution with finite support. Assume that $\mathcal{S}_{F_X^*}$ has infinite number of elements. In view of (5.55)-(5.57), analyticity of $i_B(z;F_X)$, $r_e(z;F_X)$

and z^2 over $\mathbb{C}$ and the identity theorem for complex numbers, we have

$$\mu i_B(x;F_X^*) + r_e(x;F_X^*) - \lambda x^2 = (\mu+1)I_B(F_X^*) - I_E(F_X^*) - \lambda P,\ \forall x \in \mathbb{R} \quad (5.58)$$

$$E[X^2] = P \quad (5.59)$$

It is easy to verify by substitution that (5.58)-(5.59) are satisfied when $\lambda = \frac{\log(e)}{2}\left(\frac{\mu+1}{\sigma_B^2+P} - \frac{1}{\sigma_E^2+P}\right)$ and F_X is selected as the Gaussian distribution with zero-mean and variance P. In this case, $I_B(F_X^*) = \frac{1}{2}\log\left(1+\frac{P}{\sigma_B^2}\right)$ and $I_E(F_X^*) = \frac{1}{2}\log\left(1+\frac{P}{\sigma_E^2}\right)$. Moreover, as in the secrecy capacity case, (5.58)-(5.59) cannot have another solution since (5.58)-(5.59) are independent of the amplitude constraint A and therefore are valid for $A \to \infty$. That is, (5.58)-(5.59) are also the KKT conditions for the amplitude unconstrained problem

$$\max_{E[X^2]\leq P} (\mu+1)I(X;Y) - I(X;Z) \quad (5.60)$$

It is known from [22] and [95] that for all $\mu \geq 0$ the unique solution of (5.60) is also the Gaussian input distribution with zero-mean and variance P. This causes a contradiction since Gaussian input distribution is not amplitude constrained. Therefore, F_X^* is discrete with finite support. The two parts in this section prove the following theorem.

Theorem 5.4 *Let F_X^* be the distribution that attains the secrecy capacity of the Gaussian wiretap channel with peak and average power constraints. The support set $\mathcal{S}_{F_X^*}$ is a finite set. More generally, the support set of distributions that attain*

the boundary of the entire rate-equivocation region under amplitude and variance constraints are finite sets.

We now provide an illustration for the effect of the variance constraint on the secrecy capacity achieving input distribution. Let $\sigma_B^2 = 1$, $\sigma_E^2 = 2$ and $A = 1$. If the variance constraint is $P \geq 1$, it is inactive for any input distribution, i.e., the problem reduces to the one with amplitude constraint only. In this case, in view of Theorem 5.3, the optimal distribution is the symmetric binary distribution $\frac{1}{2}\delta_{-A} + \frac{1}{2}\delta_A$. We now impose a variance constraint $P = 0.8$. Clearly, in this case, the symmetric binary distribution at $\pm A$ is not feasible. We numerically find that the symmetric ternary distribution $0.4\delta_{-A} + 0.2\delta_0 + 0.4\delta_A$ is optimal in this case and the corresponding Lagrange multiplier is $\lambda = 0.116753$. We provide the plot of the KKT condition in Figure 5.6 where we observe that $r_e(x; F_X^*) - \lambda x^2$ always lies below $C_s - \lambda P$ with equality on the support set.

5.3 Gaussian Energy Harvesting Wiretap Channel with Zero Energy Storage

5.3.1 System Model and Main Results

In this section, we investigate the role of stochastic energy arrivals in the Gaussian wiretap channel as shown in Figure 5.1. The energy required to transmit code symbols is maintained by an i.i.d. energy arrival process E_i and there is no battery to save unused energy. The transmitter observes the energy arrival causally. For

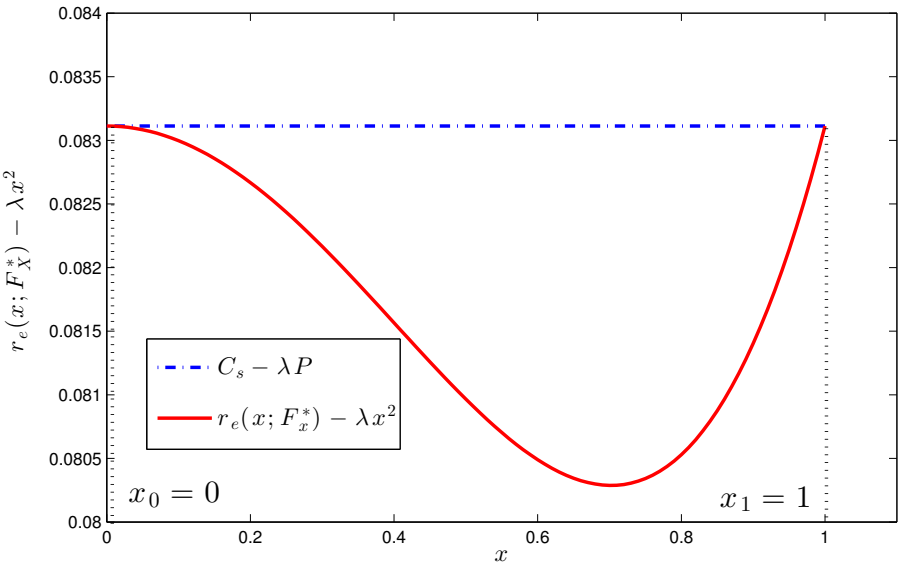

Figure 5.6: The KKT conditions for $\sigma_B^2=1$, $\sigma_E^2=2$, $A=1$ and $P=0.8$.

convenience, we assume that the energy arrivals E_i take one of two values $\mathcal{E}=\{e_1,e_2\}$ with probabilities p_1 and p_2, respectively. Consequently, there is a stochastic amplitude constraint on the channel input X_i as

$$|X_i|\leq\sqrt{E_i},\quad i=1,\ldots,n \tag{5.61}$$

and the transmitter observes the arrived energy causally.

An $(n,2^{nR})$ code for the Gaussian wiretap channel with stochastic amplitude constraints and causal information of energy arrivals consists of a message set $W\in\mathcal{W}=\{1,\ldots,2^{nR}\}$, a sequence of encoders at the transmitter $f_i:\mathcal{W}\times\mathcal{E}^i\to\mathbb{R}^i$ satisfying the constraint in (5.61), i.e., $|f_i(w,E_1,E_2,\ldots,E_i)|\leq\sqrt{E_i}$ for $i=1,2,\ldots,n$, and a decoder at the legitimate user $g_n:\mathbb{R}^n\to\mathcal{W}$. Equivocation of a code is measured by the normalized conditional entropy $(1/n)H(W|Z^n)$, where W is a uniformly

distributed random variable over $\mathcal{W}$. Probability of error for a code is defined as $P_e^n = \Pr[g_n(f_n(W)) \neq W]$. A rate-equivocation pair (R, R_e) is said to be achievable if there exists an $(n, 2^{nR})$ code satisfying $\lim_{n\to\infty} P_e^n = 0$ and (5.4).

We first show that Shannon strategies are sufficient to cover the rate-equivocation region in the following theorem. We provide the proof in Appendix 5.5.4.

Theorem 5.5 *The rate-equivocation region $\mathcal{C}$ of the Gaussian wiretap channel with an energy harvesting transmitter and zero energy storage is the union of the rate-equivocation pairs (R, R_e) satisfying*

$$R \leq I(T_1, T_2; Y) \tag{5.62}$$

$$R_e \leq I(T_1, T_2; Y) - I(T_1, T_2; Z) \tag{5.63}$$

for some input distribution $F_{T_1,T_2}(t_1, t_2) \in \Omega$.

As the rate-equivocation region $\mathcal{C}$ is convex due to time-sharing, it can be characterized by its supporting hyperplanes, that is, we solve the following problem

$$\max_{F_{T_1,T_2}\in\Omega} g_\mu(F_{T_1,T_2}) = \max_{F_{T_1,T_2}\in\Omega} (\mu+1)I(T_1, T_2; Y) - I(T_1, T_2; Z) \tag{5.64}$$

for all $\mu \geq 0$. In particular, the secrecy capacity of the extended input wiretap channel is given by

$$C_s = \max_{F_{T_1,T_2}\in\Omega} g_0(F_{T_1,T_2}) = \max_{F_{T_1,T_2}\in\Omega} I(T_1, T_2; Y) - I(T_1, T_2; Z) \tag{5.65}$$

where the objective function $g_0(F_{T_1,T_2})$ is a strictly concave functional of the input distribution F_{T_1,T_2} due to the assumption $\sigma_B^2 < \sigma_E^2$ and resulting degradedness of the wiretap channel. Moreover, the feasible set Ω is convex and sequentially compact with respect to the Levy-Prokhorov metric. Thus, (5.65) is a convex optimization problem with a unique solution.

Next, we obtain the necessary and sufficient conditions that the optimal distribution $F^*_{T_1,T_2}$ of the optimization problem in (5.65) should satisfy. To this end, we introduce some notation next. We note that the output densities for Y and Z exist for any input distribution F_{T_1,T_2}, and are given by

$$p_Y(y; F_{T_1,T_2}) = \int_{-\sqrt{e_1}}^{\sqrt{e_1}} \int_{-\sqrt{e_2}}^{\sqrt{e_2}} \left(p_1\phi_B(y-t_1) + p_2\phi_B(y-t_2)\right) dF_{T_1,T_2} \tag{5.66}$$

$$p_Z(z; F_{T_1,T_2}) = \int_{-\sqrt{e_1}}^{\sqrt{e_1}} \int_{-\sqrt{e_2}}^{\sqrt{e_2}} \left(p_1\phi_E(z-t_1) + p_2\phi_E(z-t_2)\right) dF_{T_1,T_2} \tag{5.67}$$

where $\phi_B(y), \phi_E(z)$ are zero-mean Gaussian densities with variances σ_B^2 and σ_E^2, respectively.

The equivocation density $r_e(t_1, t_2; F_{T_1,T_2})$ is

$$r_e(t_1, t_2; F_{T_1,T_2}) = i_B(t_1, t_2; F_{T_1,T_2}) - i_E(t_1, t_2; F_{T_1,T_2}) \tag{5.68}$$

where $i_B(t_1, t_2; F_{T_1,T_2})$ and $i_E(t_1, t_2; F_{T_1,T_2})$ are the mutual information densities for the main channel and the wiretapper's channel

$$i_B(t_1, t_2; F_{T_1,T_2}) = \int_{\mathbb{R}} p_B(y|t_1, t_2) \log\left(\frac{p_B(y|t_1, t_2)}{p_Y(y; F_{T_1,T_2})}\right) dy \tag{5.69}$$

$$i_E(t_1,t_2;F_{T_1,T_2}) = \int_{\mathbb{R}} p_E(z|t_1,t_2)\log\left(\frac{p_E(z|t_1,t_2)}{p_Z(z;F_{T_1,T_2})}\right)dz \tag{5.70}$$

We note that mutual information and mutual information density are related through

$$I(X;Y) = \int_{-\sqrt{e_1}}^{\sqrt{e_1}}\int_{-\sqrt{e_2}}^{\sqrt{e_2}} i_B(t_1,t_2;F_{T_1,T_2})dF_{T_1,T_2}(t_1,t_2) \tag{5.71}$$

$$I(X;Z) = \int_{-\sqrt{e_1}}^{\sqrt{e_1}}\int_{-\sqrt{e_2}}^{\sqrt{e_2}} i_E(t_1,t_2;F_{T_1,T_2})dF_{T_1,T_2}(t_1,t_2) \tag{5.72}$$

Since the Gaussian wiretap channel is stochastically degraded, without loss of generality, we can assume $Z = Y + Z_D$ for some zero-mean Gaussian random variable Z_D with variance $\sigma_D^2 = \sigma_E^2 - \sigma_B^2$. We denote the density of Z_D by $\phi_D(x)$ which leads to the identity $\phi_E = \phi_B * \phi_D$.

Now, we are ready to obtain the necessary and sufficient conditions for the optimal distribution of the optimization problem in (5.65). To this end, first, we note that the objective function $g_0(F_{T_1,T_2})$ in (5.65) is Frechet differentiable and the derivative of $g_0(F_{T_1,T_2})$ at $F^0_{T_1,T_2}$ in the direction of F_{T_1,T_2} is expressed using the equivocation density as [58]

$$\begin{aligned}&\lim_{\theta\to 0}\frac{1}{\theta}\left[g_0(\theta F_{T_1,T_2} + (1-\theta)F^0_{T_1,T_2}) - g_0(F^0_{T_1,T_2})\right]\\ &\quad= \int_{-\sqrt{e_1}}^{\sqrt{e_1}}\int_{-\sqrt{e_2}}^{\sqrt{e_2}} r_e(t_1,t_2;F^0_{T_1,T_2})dF_{T_1,T_2} - g_0(F^0_{T_1,T_2})\end{aligned} \tag{5.73}$$

Following similar arguments to those in Section 5.2, the necessary and sufficient Kuhn-Tucker conditions for the optimal distribution $F^*_{T_1,T_2}$ maximizing (5.65) can be obtained from (5.73) as follows:

Theorem 5.6 *$F^*_{T_1,T_2}$ achieves the secrecy capacity in (5.65) if and only if the following conditions are satisfied:*

$$r_e(t_1,t_2;F^*_{T_1,T_2}) \le C_s, \quad t_1 \in [-\sqrt{e_1},\sqrt{e_2}], t_2 \in [-\sqrt{e_2},\sqrt{e_2}] \tag{5.74}$$

$$r_e(t_1,t_2;F^*_{T_1,T_2}) = C_s, \quad (t_1,t_2) \in \mathcal{S}_{F^*_{T_1,T_2}} \tag{5.75}$$

where C_s is the secrecy capacity.

Similarly, since the objective function $g_\mu(F_{T_1,T_2})$ in (5.64) is strictly concave, and the feasible set Ω is convex and sequentially compact with respect to the Levy-Prokhorov metric, the optimization problem in (5.64) has a unique maximizer, which we denote as $F^*_{T_1,T_2}$. Following the same steps we followed in Section 5.2, the necessary and sufficient conditions for the optimal distribution of the optimization problem in (5.64) can be obtained as follows:

Theorem 5.7 *$F^*_{T_1,T_2}$ is an optimal input distribution for (5.64) if and only if the following conditions are satisfied: For all $t_1 \in [-\sqrt{e_1},\sqrt{e_1}]$, $t_2 \in [-\sqrt{e_2},\sqrt{e_2}]$:*

$$\mu i_B(t_1,t_2;F^*_{T_1,T_2}) + r_e(t_1,t_2;F^*_{T_1,T_2}) \le (\mu+1)I_B(F^*_{T_1,T_2}) - I_E(F^*_{T_1,T_2}) \tag{5.76}$$

For $(t_1,t_2) \in \mathcal{S}_{F^*_{T_1,T_2}}$:

$$\mu i_B(t_1,t_2;F^*_{T_1,T_2}) + r_e(t_1,t_2;F^*_{T_1,T_2}) = (\mu+1)I_B(F^*_{T_1,T_2}) - I_E(F^*_{T_1,T_2}) \tag{5.77}$$

where $I_B(F^*_{T_1,T_2})$ and $I_E(F^*_{T_1,T_2})$ are $I(T_1,T_2;Y)$ and $I(T_1,T_2;Z)$ evaluated at $F^*_{T_1,T_2}$,

respectively.

5.3.2 Numerical Results

In this section, we provide numerical illustrations for the secrecy capacity and the rate-equivocation region of the Gaussian wiretap channel with an energy harvesting transmitter of zero energy storage. We first illustrate in Figure 5.7 that the necessary and sufficient optimality conditions in Theorem 5.6 are numerically verifiable in the sense we discussed after Theorem 3.1. In particular, we provide a plot of the equivocation density in Figure 5.7 where parameters of the channel are $\sigma_B^2 = 1$ and $\sigma_E^2 = 2$, $e_1 = 2.25$, $e_2 = 0.25$, $p_1 = 0.6$. The input distribution is set as quaternary located at $(t_1, t_2) = (0.75, 0.5)$, $(t_1, t_2) = (-0.75, -0.5)$, $(t_1, t_2) = (1.5, 0.5)$ and $(t_1, t_2) = (-1.5, -0.5)$ with probability masses 0.0635, 0.0635, 0.4365 and 0.4365, respectively. The plot shows the range $t_1 \in [-1.5, 1.5]$ and $t_2 \in [0, 0.5]$ and the remaining range is obtained by symmetry with respect to origin. We observe that the equivocation density satisfies the optimality conditions in (5.74)-(5.75). Therefore, we conclude that this input distribution is optimal.

Next, we consider a binary on-off energy arrival process at the transmitter with $e_1 > 0$, $e_2 = 0$, and probabilities p_{on}, $1 - p_{on}$, respectively. In Figure 5.8, we plot the secrecy capacity as the non-zero energy arrival e_1 increases. We also plot the secrecy capacity when energy state information (ESI) is available at the transmitter, legitimate user and eavesdropper. The secrecy capacity in this case is equal to the

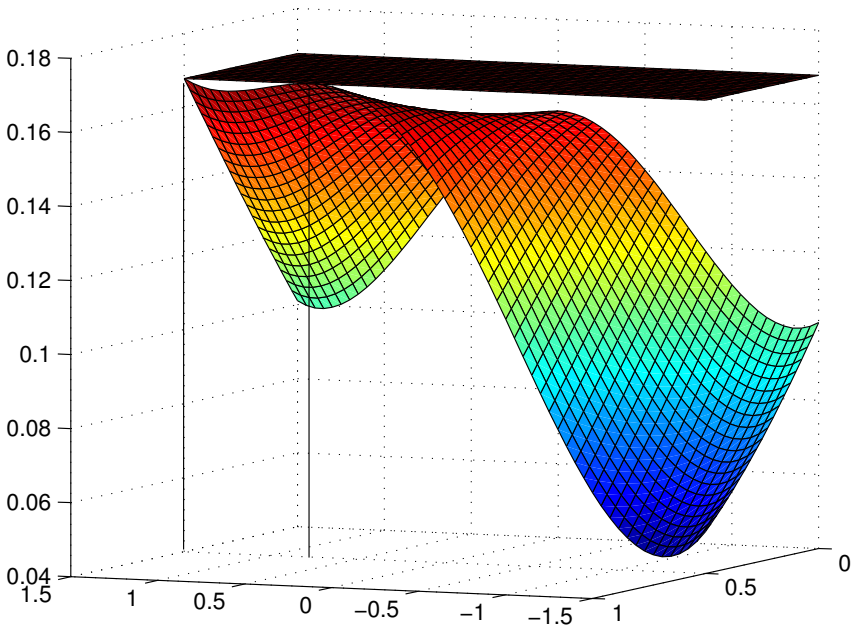

Figure 5.7: Illustration of the equivocation density corresponding to the optimal input distribution when $\sigma_B^2 = 1$, $\sigma_E^2 = 2$, $e_1 = 2.25$, $e_2 = 0.25$, $p_1 = 0.6$.

average of amplitude constrained secrecy capacity over the energy arrivals, i.e., it is

$$p_{on}\left(\max_{|X|\leq\sqrt{e_1}} I(X;Y) - I(X;Z)\right) \tag{5.78}$$

Moreover, we compare them with the secrecy capacity of the Gaussian wiretap channel with an infinite capacity battery energy harvesting transmitter, which is equal to the secrecy capacity of the Gaussian wiretap channel with average power constraint $p_{on}e_1$, i.e., it is

$$\frac{1}{2}\log\left(\frac{1+\frac{p_{on}e_1}{\sigma_B^2}}{1+\frac{p_{on}e_1}{\sigma_E^2}}\right) \tag{5.79}$$

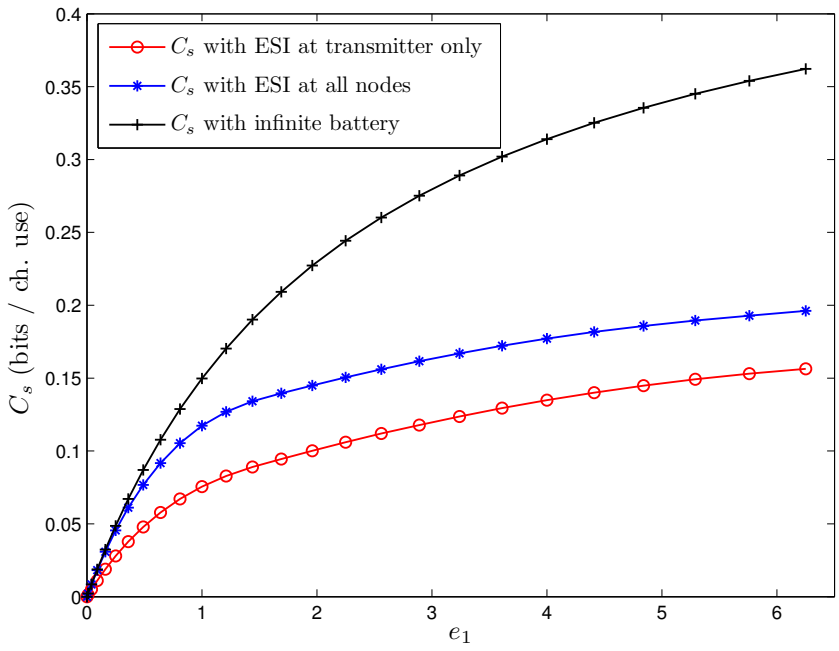

Figure 5.8: Comparison of the secrecy capacity of the extended input wiretap channel with the secrecy capacities when ESI is available at all nodes and when the transmitter has an infinite battery. $\sigma_B^2 = 1$ and $\sigma_E^2 = 2$.

We observe in Figure 5.8 that the secrecy capacity with an infinite capacity battery is significantly higher than the secrecy capacity corresponding to the other cases.

Next, we plot the secrecy capacity with respect to the probability of energy arrival p_{on}. We set $e_1 = 2.25$ and plot in Figure 5.9 the secrecy capacity of the Gaussian wiretap channel along with the secrecy capacity with ESI at all nodes and the secrecy capacity with an infinite battery transmitter. We observe that the secrecy capacity achieving distribution for $p_{on} = 1$ is ternary located at $\pm\sqrt{e_1}$ and 0 with masses 0.399 and 0.202, respectively. However, the optimal distribution changes as p_{on} is varied. In particular, we observe that symmetric binary distribution at $\pm\sqrt{e_1}$ is optimal for sufficiently small p_{on}.

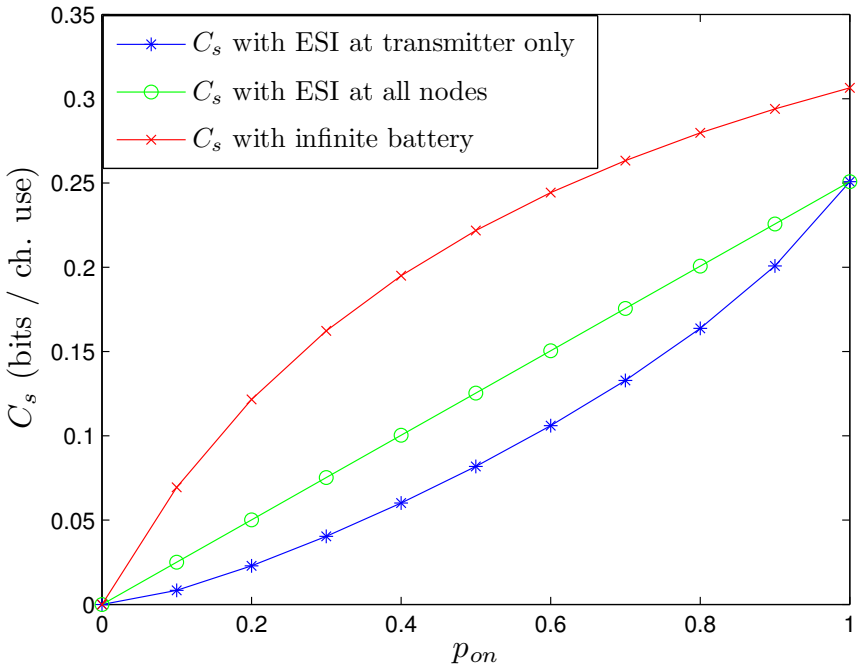

Figure 5.9: Variation of the secrecy capacities under different assumptions with respect to p_{on} when $e_1 = 2.25$.

Finally, in Figure 5.10, we plot the entire rate-equivocation region of the wire-tap channel when $\sigma_B^2 = 1$ and $\sigma_E^2 = 2$ for two different values of e_1 when $e_2 = 0$. When $e_1 = 1.44$, both the secrecy capacity and the capacity can be attained simultaneously. In particular, for $e_1 = 1.44$, the binary input distribution located at $\pm\sqrt{e_1}$ achieves both the capacity and the secrecy capacity, i.e., the optimal input distributions for the secrecy capacity and the capacity are identical. On the other hand, when $e_1 = 2.89$, the secrecy capacity and the capacity cannot be achieved simultaneously. In particular, for $e_1 = 2.89$, the binary input distribution located at $\pm\sqrt{e_1}$ achieves the capacity, while a ternary distribution located at $\pm\sqrt{e_1}$ and 0 with probability masses 0.357 at $\pm\sqrt{e_1}$ and 0.286 at 0 achieves the secrecy capacity, i.e., the optimal input distributions for the secrecy capacity and the capacity are

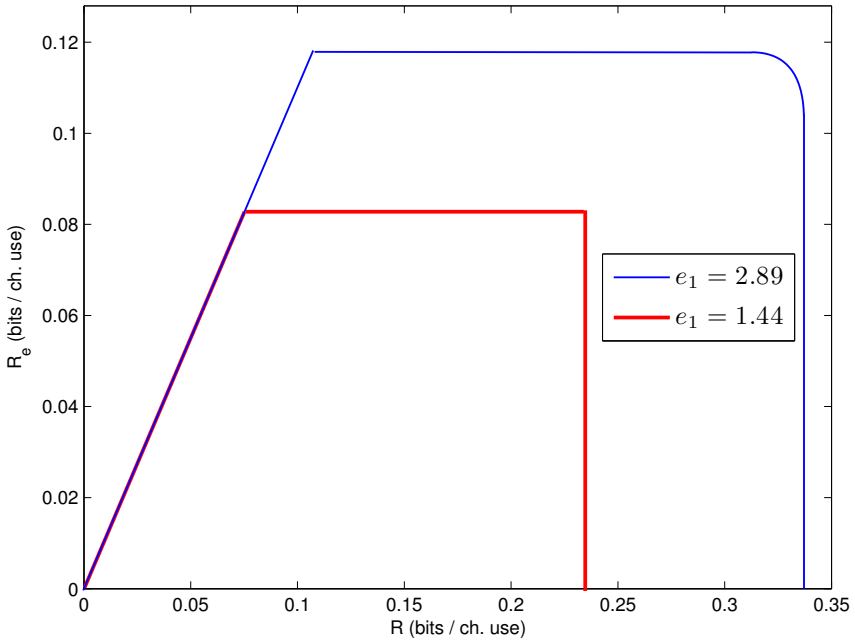

Figure 5.10: The rate-equivocation regions for $\sigma_B^2 = 1$ and $\sigma_E^2 = 2$ under on-off energy arrivals with $p_{on} = 0.6$ and $e_1 = 2.89$ and $e_1 = 1.44$.

different. In other words, there is trade-off between the rate and the equivocation in the sense that, to increase the communication rate, we should compromise from the equivocation of this communication, and to increase the achieved equivocation, we should compromise from the communication rate.

5.4 Conclusion

In this chapter, we studied the Gaussian wiretap channel with an energy harvesting transmitter of zero energy storage. First, we considered static amplitude constraints on the input of the Gaussian wiretap channel. We showed that the boundary of the entire rate-equivocation region is achieved by discrete input distributions that have finite support. We proved this result by using the methodology in [5, 6] for our

setting. An interesting aspect that our result reveals is that, unlike the average power constrained Gaussian wiretap channel, under a peak power constraint, the secrecy capacity and the capacity cannot be obtained simultaneously in general, i.e., there is a trade-off between the rate and the equivocation for the peak power constrained case. In the special case $A \leq 1.05$, we showed that the secrecy capacity and the capacity are achieved simultaneously by a symmetric binary distribution at $\pm A$. Finally, we extended the discreteness result for the case when we have both amplitude and variance constraints. Next, we considered stochastic amplitude constraints on the input of the Gaussian wiretap channel. We first proved that single-letter Shannon strategies span the entire rate-equivocation region. We observed in our numerical results that the boundary of the rate-equivocation region is achieved by discrete input distributions.

5.5 Appendix

5.5.1 Proof of Lemma 5.2

We first note that $p_Z(y) > \phi_E(|y| + A)$. We divide the integral into the following two regions $(-\infty, y]$, (y, ∞) and apply this bound to obtain

$$\begin{aligned}\int_{\mathbb{R}} \phi_D(\tau) \log\left(p_Z(y-\tau)\right) d\tau \geq &- \int_{-\infty}^{y} \phi_D(\tau) \frac{\log(e)(y-\tau+A)^2}{2\sigma_E^2} d\tau \\ &- \int_{y}^{\infty} \phi_D(\tau) \frac{\log(e)(\tau-y+A)^2}{2\sigma_E^2} d\tau + \log\left(\frac{1}{\sqrt{2\pi\sigma_E^2}}\right)\end{aligned} \tag{5.80}$$

Rearranging this bound, we get

$$\int_{\mathbb{R}} \phi_D(\tau) \log\left(p_Z(y-\tau)\right) d\tau \geq \log\left(\frac{1}{\sqrt{2\pi\sigma_E^2}}\right) - \log(e) \int_{-\infty}^{\infty} \phi_D(\tau) \frac{(y-\tau)^2 + A^2}{2\sigma_E^2} d\tau$$
$$- \frac{A}{\sigma_E^2} \log(e) \left(\int_y^{\infty} (\tau - y)\phi_D(\tau) d\tau + \int_{-\infty}^{y} (y-\tau)\phi_D(\tau) d\tau \right) \quad (5.81)$$
$$= \log\left(\frac{1}{\sqrt{2\pi\sigma_E^2}}\right) - \frac{\log(e)}{2\sigma_E^2}\left(y^2 + A^2 + \sigma_E^2 - \sigma_B^2\right) - \frac{A\log(e)}{\sigma_E^2} b(y) \quad (5.82)$$

where

$$b(y) = \int_y^{\infty} (\tau - y)\phi_D(\tau) d\tau + \int_{-\infty}^{y} (y-\tau)\phi_D(\tau) d\tau \quad (5.83)$$
$$= y\left(1 - 2Q\left(\frac{y}{\sigma_D}\right)\right) + \frac{2\sigma_D}{\sqrt{2\pi}} e^{-\frac{y^2}{2\sigma_D^2}} \quad (5.84)$$

where $\sigma_D^2 = \sigma_E^2 - \sigma_B^2$ and $Q(x) = \frac{1}{\sqrt{2\pi}} \int_x^{\infty} e^{-\frac{t^2}{2}} dt$. We note that $b(y) \in o(y^2)$, i.e., $\frac{b(y)}{y^2} \to 0$ as $y \to \infty$ due to the fact that $Q(x) \leq 1$ and $e^{-y^2} \leq 1$.

On the other hand, we have $p_Y(y) \leq \phi_B(y - A)$ for $y > A$. Therefore,

$$\log\left(p_Y(y)\right) \leq \log\left(\frac{1}{\sqrt{2\pi\sigma_B^2}}\right) - \frac{(y-A)^2}{2\sigma_B^2}\log(e), \qquad y > A \quad (5.85)$$

Consequently, in order to prove the asserted inequality in (5.30), it suffices to show that there exists y' sufficiently large such that for all $y > y'$

$$\log\left(\frac{1}{\sqrt{2\pi\sigma_B^2}}\right) - \frac{(y-A)^2}{2\sigma_B^2}\log(e) \leq \log\left(\frac{1}{\sqrt{2\pi\sigma_E^2}}\right) - \frac{(y^2 + A^2 + \sigma_E^2 - \sigma_B^2)}{2\sigma_E^2}\log(e)$$
$$- \frac{A\log(e)}{\sigma_E^2} b(y) \quad (5.86)$$

As $b(y) \in o(y^2)$, (5.86) is equivalent to

$$-\frac{y^2}{\sigma_B^2} \leq -\frac{y^2}{\sigma_E^2} + o(y^2) \tag{5.87}$$

Since $\sigma_B^2 < \sigma_E^2$, (5.87), and hence (5.86), is true for $y > y'$ for sufficiently large y'. This completes the proof of Lemma 5.2.

5.5.2 Proof of Lemma 5.3

The claim follows from the fact that the Gaussian density is symmetric around the origin and since both channels are additive noise channels, flipping the input distribution around the origin yields the same mutual informations and secrecy rate. Moreover, the objective $g_\mu(F_X) = (\mu+1)I_{F_X}(X;Y) - I_{F_X}(X;Z)$ is strictly concave with the input distribution. By [64, Proposition 1] (see also [6, Lemma on page 44]), we get the desired result.

5.5.3 A Modified Proof for the AWGN Channel

In this section, we present a modified version of the discreteness proof in [5, 6] for the AWGN channel under amplitude and variance constraints. Our proof method closely follows the one in [5, 6], but it takes a short-cut by directly relating the amplitude and variance constrained problem to the amplitude unconstrained but variance constrained problem. This is more readily generalizable to the Gaussian wiretap channel as done in Section 5.2.5.

Consider the AWGN channel:

$$Y = X + N \tag{5.88}$$

where N is Gaussian with zero-mean and unit-variance. The channel capacity C of the AWGN channel under amplitude constraint A and variance constraint P is

$$C = \max_{F_X \in \Omega_{A,P}} I(X;Y) \tag{5.89}$$

where the feasible set of input distributions $\Omega_{A,P}$ is:

$$\Omega_{A,P} = \left\{ F_X : \int_{-A}^{A} dF_X(x) = 1, \quad \int_{-A}^{A} x^2 dF_X(x) \leq P \right\} \tag{5.90}$$

By the Lagrangian theorem, $F_X^* \in \Omega_{A,P}$ is optimal if and only if there exists $\lambda \geq 0$ such that F_X^* is the unique solution of the following optimization problem:

$$\max_{F_X \in \Omega_A} I(X;Y) - \lambda E[X^2] \tag{5.91}$$

where $\Omega_A = \left\{ F_X : \int_{-A}^{A} dF_X(x) = 1 \right\}$.

Since the objective function in (5.91) is strictly concave in the input distribution, the directional derivative of the objective function with respect to F_X gives us the following necessary and sufficient conditions that the optimal input distribution

F_X^* should satisfy [5, 6, 26]

$$i(x;F_X^*) - \lambda x^2 \leq C - \lambda E[X^2], \qquad \forall x \in [-A, A] \tag{5.92}$$

$$i(x;F_X^*) - \lambda x^2 = C - \lambda E[X^2], \qquad \forall x \in \mathcal{S}_{F_X^*} \tag{5.93}$$

$$\lambda \left(E[X^2] - P \right) = 0 \tag{5.94}$$

We will show the discreteness of the optimal input distribution satisfying the KKT conditions in (5.92)-(5.94) by contradiction. To this end, we first note that when the second moment constraint in (5.94) is not active, i.e., when $\lambda = 0$, the problem reduces to the AWGN channel with only an amplitude constraint, for which we know that the optimal input distribution is discrete. Hence, from now on, we will focus on the case where the second moment constraint in (5.94) is active, i.e., $E\left[X^2\right] = P$. When this equality is satisfied, we can rewrite the KKT conditions in (5.92)-(5.94) as follows:

$$i(x;F_X^*) - \lambda x^2 \leq C - \lambda P, \qquad \forall x \in [-A, A] \tag{5.95}$$

$$i(x;F_X^*) - \lambda x^2 = C - \lambda P, \qquad \forall x \in \mathcal{S}_{F_X^*} \tag{5.96}$$

$$E[X^2] = P \tag{5.97}$$

Now, we prove that the optimal input distribution satisfying (5.95)-(5.97) should be discrete by contradiction. To this end, we assume that the support set $\mathcal{S}_{F_X^*}$ includes infinitely many points. In view of the analyticity of $i(z;F_X^*)$ and z^2

over all complex numbers $\mathbb{C}$, this assumption implies that we should have

$$i(x; F_X^*) - \lambda x^2 = C - \lambda P, \qquad \forall x \in \mathbb{R} \tag{5.98}$$

$$E[X^2] = P \tag{5.99}$$

for the optimal input distribution. We can verify by substitution that (5.98)-(5.99) are satisfied when $\lambda = \frac{\log(e)}{2(1+P)}$ and F_X is selected as the cumulative distribution function corresponding to the Gaussian density with zero-mean and variance P, i.e., $F_X(x) = \int_{-\infty}^{x} \frac{1}{\sqrt{2\pi P}} e^{-\frac{y^2}{2P}} dy$. In this case, $C = \frac{1}{2}\log(1+P)$.

Next, we claim that (5.98)-(5.99) cannot have another solution. To prove this claim, we note that (5.98)-(5.99) is independent of the amplitude constraint A and therefore is valid for any A and in particular $A \to \infty$. That is, (5.98)-(5.99) are also the KKT conditions for the amplitude unconstrained problem, i.e.,

$$\max_{E[X^2] \leq P} I(X;Y) \tag{5.100}$$

It is well known (see, e.g., [54]) that the unique optimal input distribution for (5.100) is Gaussian with zero-mean and variance P and the optimal value for (5.100) is $\frac{1}{2}\log(1+P)$. Consequently, (5.98)-(5.99) have a unique solution, which is $\lambda = \frac{\log(e)}{2(1+P)}$ and F_X is Gaussian with zero-mean and variance P. However, this causes a contradiction in view of the assumption that the input is amplitude constrained. Therefore, F_X^* is a discrete distribution with finite support.

5.5.4 Proof of Theorem 5.5

For achievability, we use an extended input alphabet to transform the discrete memoryless wiretap channel with causal state information to a discrete memoryless wiretap channel without any state. In particular, a codeword in the extended channel is (T_1^n, T_2^n) where $|T_{mi}| \leq \sqrt{e_m}$ for all $i = 1, \ldots, n$ and $m = 1, 2$. At the ith time, if $S_i = m$ then the transmitter puts T_{mi} to the channel. This corresponds to n-channel uses of the discrete memoryless wiretap channel characterized by:

$$p(y, z|t_1, t_2) = p_B(y|t_1, t_2)p_E(z|t_1, t_2) \tag{5.101}$$

where $p_B(y|t_1, t_2) = p_1\phi_B(y - t_1) + p_2\phi_B(y - t_2)$ and $p_E(z|t_1, t_2) = p_1\phi_E(z - t_1) + p_2\phi_E(z - t_2)$. This yields the stochastically degraded wiretap channel $(T_1, T_2) - Y - Z$. Using Wyner's result [21], we conclude that the claimed (R, R_e) pairs are achievable.

To prove the converse, we define the following auxiliary random variables: $U_i = W, E^{i-1}, Z_{i+1}^n$ for $i = 1, \ldots, n$. Note that we have the Markov chain: $U_i -$

$X_i, E_i - Y_i - Z_i$. Let $\epsilon_n = H(W|Y^n)$:

$$
\begin{aligned}
nR_e &= H(W|Z^n) && (5.102)\\
&\leq \sum_{i=1}^{n} I(W;Y_i|Y^{i-1},Z_{i+1}^n) - I(W;Z_i|Y^{i-1},Z_{i+1}^n) + \epsilon_n && (5.103)\\
&\leq \sum_{i=1}^{n} I(W,Y^{i-1},Z_{i+1}^n;Y_i) - I(W,Y^{i-1},Z_{i+1}^n;Z_i) + \epsilon_n && (5.104)\\
&\leq \sum_{i=1}^{n} I(W,Y^{i-1},E^{i-1},Z_{i+1}^n;Y_i) - I(W,Y^{i-1},E^{i-1},Z_{i+1}^n;Z_i) + \epsilon_n && (5.105)\\
&= \sum_{i=1}^{n} I(W,Y^{i-1},E^{i-1},X^{i-1},Z_{i+1}^n;Y_i) - I(W,Y^{i-1},E^{i-1},X^{i-1},Z_{i+1}^n;Z_i) + \epsilon_n \\
& && (5.106)\\
&= \sum_{i=1}^{n} I(W,E^{i-1},X^{i-1},Z_{i+1}^n;Y_i) - I(W,E^{i-1},X^{i-1}Z_{i+1}^n;Z_i) + \epsilon_n && (5.107)\\
&= \sum_{i=1}^{n} I(W,E^{i-1},Z_{i+1}^n;Y_i) - I(W,E^{i-1},Z_{i+1}^n;Z_i) + \epsilon_n && (5.108)\\
&= \sum_{i=1}^{n} I(U_i;Y_i) - I(U_i;Z_i) + \epsilon_n && (5.109)
\end{aligned}
$$

where (5.104)-(5.105) follow from the degradedness of the wiretap channel; (5.106) follows from $X_i = f(W, E^i)$; (5.107) follows from the Markov chain $Y^{i-1} - X^{i-1}E^{i-1} - WZ_{i+1}^n Y_i Z_i$ and (5.108) follows from $X_i = f(W, E^i)$.

Next, we consider the rate:

$$
\begin{aligned}
nR &\leq \sum_{i=1}^{n} I(W;Y_i|Y^{i-1}) + \epsilon_n && (5.110)\\
&\leq \sum_{i=1}^{n} I(W,E^{i-1},Y^{i-1},Z_{i+1}^n;Y_i) + \epsilon_n && (5.111)
\end{aligned}
$$

$$= \sum_{i=1}^{n} I(W, E^{i-1}, X^{i-1}, Y^{i-1}, Z_{i+1}^{n}; Y_i) + \epsilon_n \tag{5.112}$$

$$= \sum_{i=1}^{n} I(W, E^{i-1}, X^{i-1}, Z_{i+1}^{n}; Y_i) + \epsilon_n \tag{5.113}$$

$$= \sum_{i=1}^{n} I(W, E^{i-1}, Z_{i+1}^{n}; Y_i) + \epsilon_n \tag{5.114}$$

where (5.111) follows from nonneagtivity of mutual information; (5.112) follows from the Markov chain $Y^{i-1} - X^{i-1}E^{i-1} - WZ_{i+1}^{n}Y_iZ_i$ and (5.113) follows from $X_i = f(W, E^i)$. In addition, $X_i = f(W, E^i)$ satisfies $|X_i| \leq \sqrt{E_i}$. By Fano's inequality, $\epsilon_n \to 0$ as $n \to \infty$. Note that we can equivalently write $X_i = f(U_i, E_i)$ as providing the extra information of Z_{i+1}^{n} in the computation of X_i provides an upper bound for the case when only W and E^i are used to compute X_i. This proves that the following region is an outer bound:

$$R_e \leq I(U;Y) - I(U;Z) \tag{5.115}$$

$$R \leq I(U;Y) \tag{5.116}$$

with $X = f(U, E)$ and union over all (U, X) satisfying $U - X, E - Y, Z$ and $|f(U, E = e_m)| \leq \sqrt{e_m}$ for $m = 1, 2$. It is an easy exercise to show that for any $p(u)$ and $f(U, E)$, there exist extended inputs (T_1, T_2) such that $I(T_1, T_2; Y) = I(U; Y)$ [97] and by degradedness we have $I(T_1, T_2; Z) = I(U; Z)$. This completes the proof.

Chapter 6

Transmission Scheduling for Energy Harvesting Transmitters over a Single User Channel

6.1 Introduction

In this chapter, we consider data transmission scheduling for energy harvesting transmitters. In such a scenario, incremental energy is harvested by the transmitter during the course of data transmission from random energy sources. As such, energy becomes available for packet transmission at random times and in random amounts. In addition, the wireless communication channel fluctuates randomly due to fading. These together lead to a need for designing new transmission strategies that can best take advantage of and adapt to the random energy arrivals as well as channel variations in time.

The simplest system model for which this setting leads to new design insights is a wireless link with a rechargeable transmitter, which we consider here. The incoming energy can be stored in the battery of the rechargeable transmitter for future use. However, this battery has finite storage capacity and the transmission policy needs to guarantee that there is sufficient battery space for each energy arrival, otherwise incoming energy cannot be saved and will be wasted. In this setting, we find optimal offline and online transmission schemes that adapt the instantaneous

transmit power to the variations in the energy and fade levels.

There has been recent research effort on understanding data transmission with an energy harvesting transmitter that has a rechargeable battery [10–12, 14, 15, 23, 98]. Additionally, an earlier line of research considered the problem of energy management in communications satellites [16, 17]. In this chapter, we obtain optimal transmission policies to maximize the throughput and minimize the transmission completion time, under channel fluctuations and energy variations, in a continuous time model, combining and generalizing the related literature from various different perspectives.

In particular, we consider two related optimization problems. The first problem is the maximization of the number of bits (or throughput) transmitted by a deadline T. The second problem is the minimization of the time (or delay) by which the transmission of B bits is completed. We solve the first problem under deterministic (offline) and stochastic (online) settings, and we solve the second problem in the deterministic setting. We start the analysis by considering the first problem in a static channel under offline knowledge. The solution calls for a new algorithm, termed *directional water-filling*. Taking into account the causality constraints on the energy usage, i.e., the energy can be saved and used in the future, the algorithm allows energy flow only to the right. In the algorithmic implementation of the solution, we utilize *right permeable taps* at each energy arrival point. This solution serves as a building block for the fading case. Specifically, we show that a directional water-filling algorithm that adapts to both energy arrivals and channel fade levels is optimal. Next, we consider the second problem, i.e., the minimization of the time by

which transmission of B bits is completed. We use the solution of the first problem to solve this second problem. This is accomplished by mapping the first problem to the second problem by means of the *maximum departure curve*. This completes the identification of the optimal offline policies in the fading channel.

Next, we address online scheduling for maximum throughput by the deadline T in a setting where fading level changes and energy arrives as random processes in time. Assuming statistical knowledge and causal information of the energy and fading variations, we solve for the optimal online power policy by using dynamic programming [42, 43]. To reduce the complexity required by the dynamic programming solution, we propose simple online algorithms that perform near-optimal. Finally, we provide a thorough numerical study of the proposed algorithms under various system settings.

6.2 System Model

We consider a single user fading channel with additive Gaussian noise and causal channel state information (CSI) feedback as shown in Figure 6.1. The transmitter has two queues, the data queue where data packets are stored, and an energy queue where the arriving (harvested) energy is stored. The energy queue, i.e., the battery, can store at most E_{max} units of energy, which is used only for transmission, i.e., energy required for processing is not considered.

The received signal y is given by $y = \sqrt{h}x + n$, where h is the (squared) fading, x is the channel input, and n is a Gaussian random noise with zero-mean and unit-

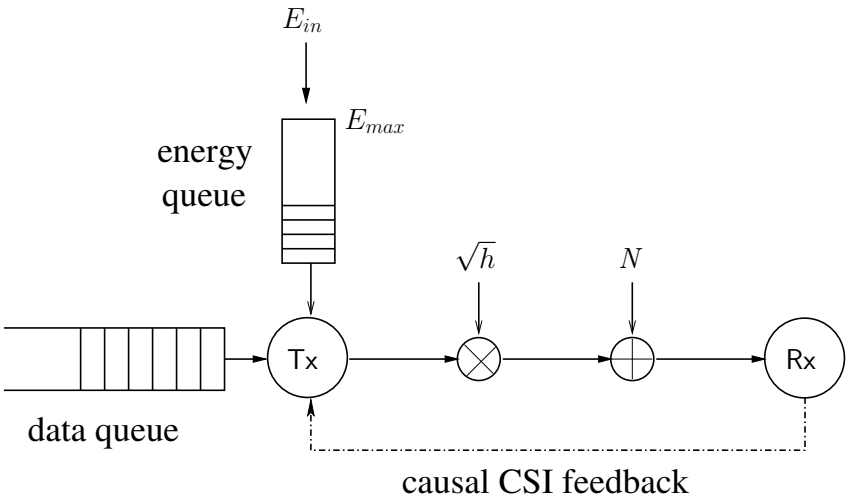

Figure 6.1: Additive Gaussian fading channel with an energy harvesting transmitter and causal channel state information (CSI) feedback.

variance. Whenever an input signal x is transmitted with power p in an epoch of duration L, $\frac{L}{2}\log(1+hp)$ bits of data is served out from the backlog with the cost of Lp units of energy depletion from the energy queue. This follows from the Gaussian channel capacity formula. The bandwidth is sufficiently wide so that L can take small values and we approximate the slotted system to a continuous time system. Hence, we say that if at time t the transmit power of the signal is $x^2(t) = p(t)$, the instantaneous rate $r(t)$ in bits per channel use is

$$r(t) = \frac{1}{2}\log\left(1 + h(t)p(t)\right) \tag{6.1}$$

Following a model similar to [99], we assume that the fading level h and energy arrivals are stochastic processes in time that are marked by Poisson counting processes with rates λ_h and λ_e, respectively. Therefore, changes in fading level and energy arrivals occur in countable time instants, which are indexed respectively as

$t_1^f, t_2^f, \ldots, t_n^f, \ldots$ and $t_1^e, t_2^e, \ldots, t_n^e, \ldots$ with the convention that $t_1^e = t_1^f = 0$. By the Poisson property, the inter-occurrence times $t_i^f - t_{i-1}^f$ and $t_j^e - t_{j-1}^e$ are exponentially distributed with means $1/\lambda_f$ and $1/\lambda_e$, respectively. The fading level in $[0, t_1^f)$ is h_1, in $[t_1^f, t_2^f)$ is h_2, and so on. Similarly, E_i units of energy arrives at time t_i^e, and E_0 units of energy is available at time 0. Hence $\{(t_i^e, E_i)\}_{i=0}^{\infty}$ and $\{(t_i^f, h_i)\}_{i=1}^{\infty}$ completely define the events that take place during the course of data transmission. This model is shown in Figure 6.2. The incoming energy is first buffered in the battery before it is used in data transmission, and the transmitter is allowed to use the battery energy only. Accordingly, we assume $E_i \leq E_{max}$ for all i as otherwise excess energy cannot be accommodated in the battery anyway.

In the sequel, we will refer to a change in the channel fading level or in the energy level as an *event* and the time interval between two consecutive events as an *epoch*. More precisely, epoch i is defined as the time interval $[t_i, t_{i+1})$ where t_i and t_{i+1} are the times at which successive events happen and the length of the epoch is $L_i = t_{i+1} - t_i$. Naturally, energy arrival information is causally available to the transmitter. Moreover, by virtue of the causal feedback link, perfect information of the channel fade level is available to the transmitter. Therefore, at time t all $\{E_i\}$ and $\{h_j\}$ such that $t_i^e < t$ and $t_j^f < t$ are known perfectly by the transmitter.

A power management policy is denoted as $p(t)$ for $t \in [0, T]$. There are two constraints on $p(t)$, due to energy arrivals at random times and also due to finite battery storage capacity. Since energy that has not arrived yet cannot be used at the current time, there is a causality constraint on the power management policy

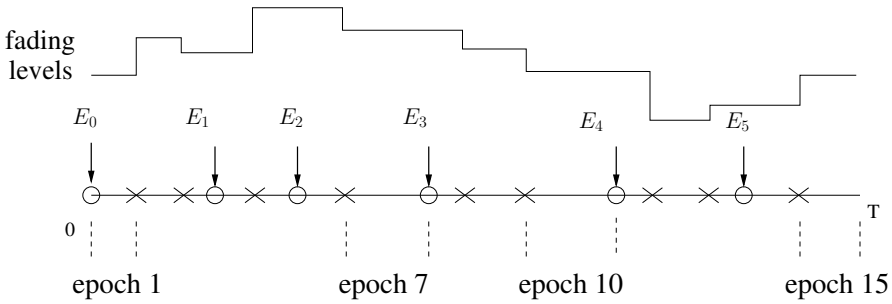

Figure 6.2: The system model and epochs under channel fading.

as:

$$\int_0^{t_i^e} p(u)du \leq \sum_{j=0}^{i-1} E_j, \quad \forall i \tag{6.2}$$

where the limit of the integral t_i^e should be interpreted as ${t_i}^e - \epsilon$, for small enough ϵ. Moreover, due to the finite battery storage capacity, we need to make sure that energy level in the battery never exceeds E_{max}. Since energy arrives at certain time points, it is sufficient to ensure that the energy level in the battery never exceeds E_{max} at the times of energy arrivals. Let $d(t) = \max\{t_i^e : t_i^e \leq t\}$. Then,

$$\sum_{j=0}^{d(t)} E_j - \int_0^t p(u)du \leq E_{max}, \quad \forall t \in [0, T] \tag{6.3}$$

We emphasize that our system model is continuous rather than slotted. In slotted models, e.g., [11, 16, 98], the energy input-output relationship is written for an entire slot. Such models allow energies larger than E_{max} to enter the battery and be used for transmission in a given single slot. Our continuous system model prohibits such occurrences.

Our ultimate goal is to develop an online algorithm that determines the transmit power as a function of time using the causal knowledge of the system, e.g., the instantaneous energy state and fading CSI. We will start our development by considering the optimal offline policy.

6.3 Maximizing Throughput in a Static Channel

In this section, we consider maximizing the number of bits delivered by a deadline T, in a non-fading channel with offline knowledge of energy arrivals which occur at times $\{t_1, t_2, \ldots, t_N\}$ in amounts $\{E_1, E_2, \ldots, E_N\}$. The epoch lengths are $L_i = t_i - t_{i-1}$ for $i = 1, \ldots, N$ with $t_0 = 0$, and $L_{N+1} = T - t_N$. There are a total of $N+1$ epochs. The optimization is subject to causality constraints on the harvested energy, and the finite storage constraint on the rechargeable battery. This problem was solved in [23] using a geometric framework. Here, we provide the formulation for completeness and provide an alternative algorithmic solution which will serve as the building block for the solution for the fading channel presented in the next section.

First, we note that the transmit power must be kept constant in each epoch [14, 15, 23], due to the concavity of rate in power. Let us denote the power in epoch i by p_i. The causality constraints in (6.2) reduce to the following constraints on p_i,

$$\sum_{i=1}^{\ell} L_i p_i \leq \sum_{i=0}^{\ell-1} E_i, \quad \ell = 1, \ldots, N+1 \tag{6.4}$$

Moreover, since the energy level in the battery is the highest at instants when energy arrives, the battery capacity constraints in (6.3) reduce to a countable number of

constraints, as follows

$$\sum_{i=0}^{\ell} E_i - \sum_{i=1}^{\ell} L_i p_i \leq E_{max}, \quad \ell = 1, \ldots, N \tag{6.5}$$

Note that since $E_0 > 0$, there is no incentive to make $p_i = 0$ for any i. Hence, $p_i > 0$ is necessary for optimality.

The optimization problem is:

$$\max_{p_i \geq 0} \quad \sum_{i=1}^{N+1} \frac{L_i}{2} \log(1 + p_i) \tag{6.6}$$

$$\text{s.t.} \quad \sum_{i=1}^{\ell} L_i p_i \leq \sum_{i=0}^{\ell-1} E_i, \quad \ell = 1, \ldots, N+1 \tag{6.7}$$

$$\sum_{i=0}^{\ell} E_i - \sum_{i=1}^{\ell} L_i p_i \leq E_{max}, \quad \ell = 1, \ldots, N \tag{6.8}$$

We note that the constraint in (6.7) must be satisfied with equality for $\ell = N + 1$, otherwise, we can always increase some p_i without conflicting any other constraints, increasing the resulting number of bits transmitted.

Note that the objective function in (6.6) is concave in the vector of powers since it is a sum of log functions, which are concave themselves. In addition, the constraint set is convex as it is composed of linear constraints. Hence, the above optimization problem is a convex optimization problem, and has a unique maximizer. We define

the following Lagrangian function [100] for any $\lambda_i \geq 0$ and $\mu_i \geq 0$,

$$\mathcal{L} = \sum_{i=1}^{N+1} \frac{L_i}{2} \log(1+p_i) - \sum_{j=1}^{N+1} \lambda_j \left(\sum_{i=1}^{j} L_i p_i - \sum_{i=0}^{j-1} E_i \right) - \sum_{j=1}^{N} \mu_j \left(\sum_{i=0}^{j} E_i - \sum_{i=1}^{j} L_i p_i - E_{max} \right) \tag{6.9}$$

Lagrange multipliers $\{\lambda_i\}$ are associated with constraints in (6.7) and $\{\mu_i\}$ are associated with (6.8). Additional complimentary slackness conditions are as follows,

$$\lambda_j \left(\sum_{i=1}^{j} L_i p_i - \sum_{i=0}^{j-1} E_i \right) = 0, \quad j = 1, \ldots, N \tag{6.10}$$

$$\mu_j \left(\sum_{i=0}^{j} E_i - \sum_{i=1}^{j} L_i p_i - E_{max} \right) = 0, \quad j = 1, \ldots, N \tag{6.11}$$

In (6.10), $j = N+1$ is not included since this constraint is in fact satisfied with equality, because otherwise the objective function can be increased by increasing some p_i. Note also that as $p_i > 0$, we did not include any slackness conditions for p_i.

We apply the KKT optimality conditions to this Lagrangian to obtain the optimal power levels p_i^* in terms of the Lagrange multipliers as,

$$p_i^* = \frac{1}{\left(\sum_{j=i}^{N+1} \lambda_j - \sum_{j=i}^{N} \mu_j \right)} - 1, \quad i = 1, \ldots, N \tag{6.12}$$

and $p_{N+1}^* = \frac{1}{\lambda_{N+1}} - 1$. Note that p_i^* that satisfy $\sum_{i=1}^{N+1} L_i p_i^* = \sum_{i=0}^{N} E_i$ is unique.

Based on the expression for p_i^* in terms of the Lagrange multipliers in (6.12), we have the following observation on the structure of the optimal power allocation

scheme. We provide the proof in Appendix 6.9.1.

Theorem 6.1 *When $E_{max} = \infty$, the optimal power levels is a monotonically increasing sequence: $p_{i+1}^* \geq p_i^*$. Moreover, if for some ℓ, $\sum_{i=1}^{\ell} L_i p_i^* < \sum_{i=0}^{\ell-1} E_i$, then $p_\ell^* = p_{\ell+1}^*$.*

The monotonicity in Theorem 6.1 is a result of the fact that energy may be spread from the current time to the future for optimal operation. Whenever a constraint in (6.7) is not satisfied with equality, it means that some energy is available for use but is not used in the current epoch and is transferred to future epochs. Hence, the optimal power allocation is such that, if some energy is transferred to future epochs, then the power level must remain the same. However, if the optimal power level changes from epoch i to $i+1$, then this change should be in the form of an increase and no energy is transferred for future use. That is, the corresponding constraint in (6.7) is satisfied with equality.

If E_{max} is finite, then its effect on the optimal power allocation is observed through μ_i in (6.12). In particular, if the constraints in (6.8) are satisfied without equality, then optimal p_i^* are still monotonically increasing since $\mu_i = 0$. However, as $E_i \leq E_{max}$ for all i, the constraint with the same index in (6.7) is satisfied without equality whenever a constraint in (6.8) is satisfied with equality. Therefore, a non-zero μ_i and a zero λ_i appear in p_i^* in (6.12). This implies that the monotonicity of p_i^* may no longer hold. E_{max} constraint restricts power levels to take the same value in adjacent epochs as it constrains the energy that can be transferred from current epoch to the future epochs. Indeed, from constraints in (6.8), the energy

that can be transferred from current, say the ith, or previous epochs, to future epochs is $E_{max} - E_i$. Hence, the power levels are equalized only to the extent that E_{max} constraint allows.

6.3.1 Directional Water-Filling Algorithm

We interpret the observed properties of the optimal power allocation scheme as a *directional water-filling* scheme. We note that if E units of water (energy) is filled into a rectangle of bottom size L, then the water level is $\frac{E}{L}$. Another key ingredient of the directional water-filling algorithm is the concept of a *right permeable* tap, which permits transfer of water (energy) only from left to right.

Consider the two epoch system. Assume E_{max} is sufficiently large. If $\frac{E_0}{L_1} > \frac{E_1}{L_2}$, then some energy is transferred from epoch 1 to epoch 2 so that the levels are equalized. This is shown in the top figure in Figure 6.3. However, if $\frac{E_0}{L_1} < \frac{E_1}{L_2}$, no energy can flow from right to left. This is due to the causality of energy usage, i.e., energy cannot be used before it is harvested. Therefore, as shown in the middle figure in Figure 6.3, the water levels are not equalized. We implement this using *right permeable* taps, which let water (energy) flow only from left to right.

We note that the finite E_{max} case can be incorporated into the energy-water analogy as a constraint on the amount of energy that can be transferred from the past to the future. If the equalizing water level requires more than $E_{max} - E_i$ amount of energy to be transferred, then only $E_{max} - E_i$ can be transferred. Because, otherwise, the energy level in the next epoch exceeds E_{max} causing overflow of energy, which

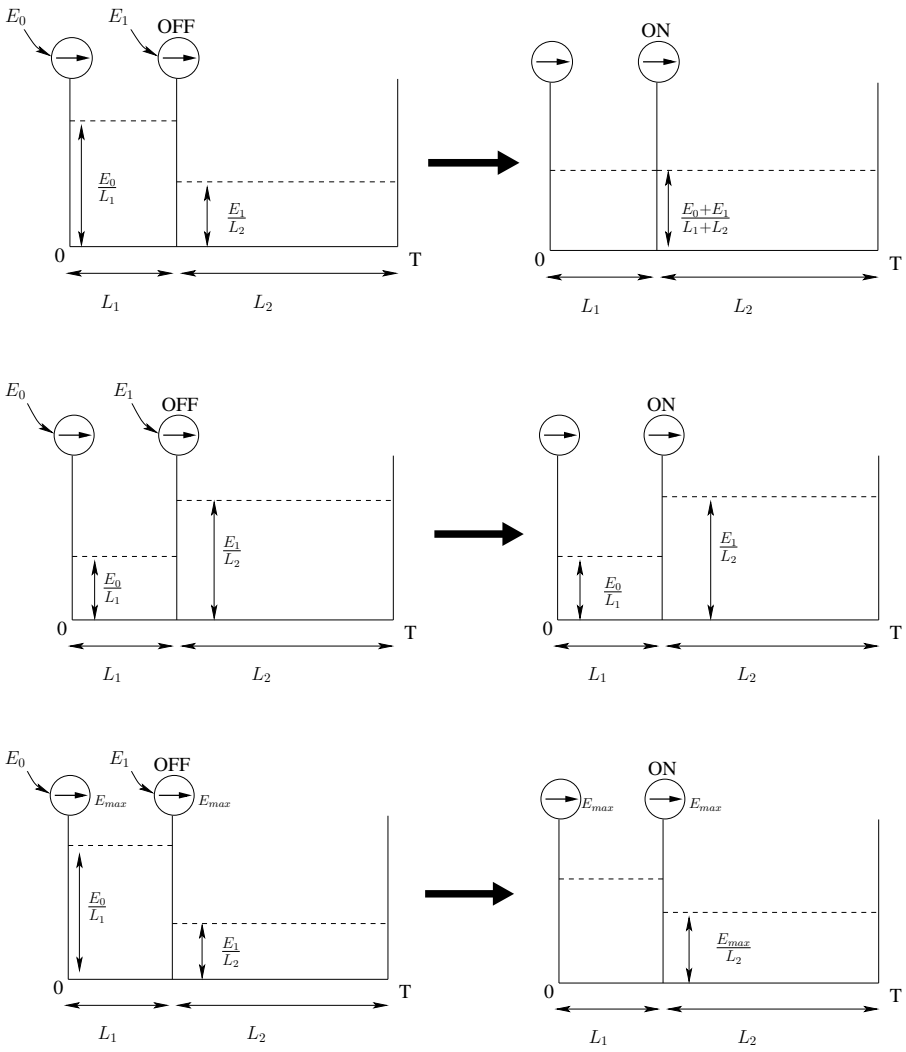

Figure 6.3: Directional water-filling with right permeable taps in a two-epoch setting.

results in inefficiencies. More specifically, when the right permeable tap in between the two epochs of the example in bottom figure in Figure 6.3 is turned on, only $E_{max} - E_1$ amount of energy transfer is allowed from epoch 1 to epoch 2.

6.4 Maximizing Throughput in a Fading Channel

We now solve for the offline policy for the fading channel utilizing the insights obtained in the previous section. The channel state changes M times and energy arrives N times in the duration $[0, T)$. Hence, we have $M + N + 1$ epochs. Our goal is again to maximize the number of bits transmitted by the deadline T. Similar to the non-fading case, the optimal power management strategy is such that the transmit power is constant in each event epoch. Therefore, let us again denote the transmit power in epoch i by p_i, for $i = 1, \ldots, M + N + 1$. We define $E_{in}(i)$ as the energy which arrives in epoch i. Hence, $E_{in}(i) = E_j$ for some j if event i is an energy arrival and $E_{in}(i) = 0$ if event i is a fade level change. Also, $E_{in}(1) = E_0$. Similar to the non-fading case, we have causality constraints due to energy arrivals and an E_{max} constraint due to finite battery size. Hence, the optimization problem in this fading case becomes:

$$\max_{p_i \geq 0} \quad \sum_{i=1}^{M+N+1} \frac{L_i}{2} \log\left(1 + h_i p_i\right) \tag{6.13}$$

$$\text{s.t.} \quad \sum_{i=1}^{\ell} L_i p_i \leq \sum_{i=1}^{\ell} E_{in}(i), \quad \forall \ell \tag{6.14}$$

$$\sum_{i=1}^{\ell} E_{in}(i) - \sum_{i=1}^{\ell} L_i p_i \leq E_{max}, \quad \forall \ell \tag{6.15}$$

Note that, as in the non-fading case, the constraint in (6.14) for $\ell = M + N + 1$ must be satisfied with equality, since otherwise, we can always increase one of p_i to increase the throughput.

As in the non-fading case, the objective function in (6.13) is concave and the

constraints are convex. The optimization problem has a unique optimal solution. We define the Lagrangian for any λ_i, μ_i and η_i as,

$$\mathcal{L} = \sum_{i=1}^{M+N+1} \frac{L_i}{2} \log\left(1 + h_i p_i\right) - \sum_{j=1}^{M+N+1} \lambda_j \left(\sum_{i=1}^{j} L_i p_i - \sum_{i=1}^{j} E_{in}(i) \right) - \sum_{j=1}^{M+N+1} \mu_j \left(\sum_{i=1}^{j} E_{in}(i) - \sum_{i=1}^{j} L_i p_i - E_{max} \right) + \sum_{i=1}^{M+N+1} \eta_i p_i \tag{6.16}$$

Note that we have not employed the Lagrange multipliers $\{\eta_i\}$ in the non-fading case, since in that case, we need to have all $p_i > 0$. However, in the fading case, some of the optimal powers can be zero depending on the channel fading state. Associated complimentary slackness conditions are,

$$\lambda_j \left(\sum_{i=1}^{j} L_i p_i - \sum_{i=1}^{j} E_{in}(i) \right) = 0, \quad \forall j \tag{6.17}$$

$$\mu_j \left(\sum_{i=1}^{j} E_{in}(i) - \sum_{i=1}^{j} L_i p_i - E_{max} \right) = 0, \quad \forall j \tag{6.18}$$

$$\eta_j p_j = 0, \quad \forall j \tag{6.19}$$

It follows that the optimal powers are given by

$$p_i^* = \left[\nu_i - \frac{1}{h_i} \right]^+ \tag{6.20}$$

where the water level in epoch i, ν_i, is

$$\nu_i = \frac{1}{\sum_{j=i}^{M+N+1} \lambda_j - \sum_{j=i}^{M+N+1} \mu_j} \tag{6.21}$$

We have the following observation for the fading case. We provide the proof in Appendix 6.9.2

Theorem 6.2 *When $E_{max} = \infty$, for any epoch i, the optimum water level ν_i is monotonically increasing: $\nu_{i+1} \geq \nu_i$. Moreover, if some energy is transferred from epoch i to $i+1$, then $\nu_i = \nu_{i+1}$.*

As in the non-fading case, the effect of finite E_{max} is observed via the Lagrange multipliers μ_i. In particular, whenever E_{max} constraint is satisfied with equality, the monotonicity of the water level no longer holds. E_{max} constrains the amount of energy that can be transferred from one epoch to the next. Specifically, the transferred energy cannot be larger than $E_{max} - E_{in}(i)$. Note that this constraint is trivially satisfied for those epochs with $E_{in}(i) = 0$ because $E_{in}(i) < E_{max}$ and hence the water level in between two energy arrivals must be equalized. However, the next water level may be higher or lower depending on the new arriving energy amount.

6.4.1 Directional Water-Filling Algorithm

The directional water-filling algorithm in the fading channel requires walls at the points of energy arrival, with right permeable water taps in each wall which allows at most E_{max} amount of water to flow. No walls are required to separate the epochs due to changes in the fading level. The water levels when each right permeable tap is turned on will be found by the directional water-filling algorithm. Optimal power allocation p_i^* is then calculated by plugging the resulting water levels into (6.20). An example run of the algorithm is shown in Figure 6.4, for a case of 12 epochs.

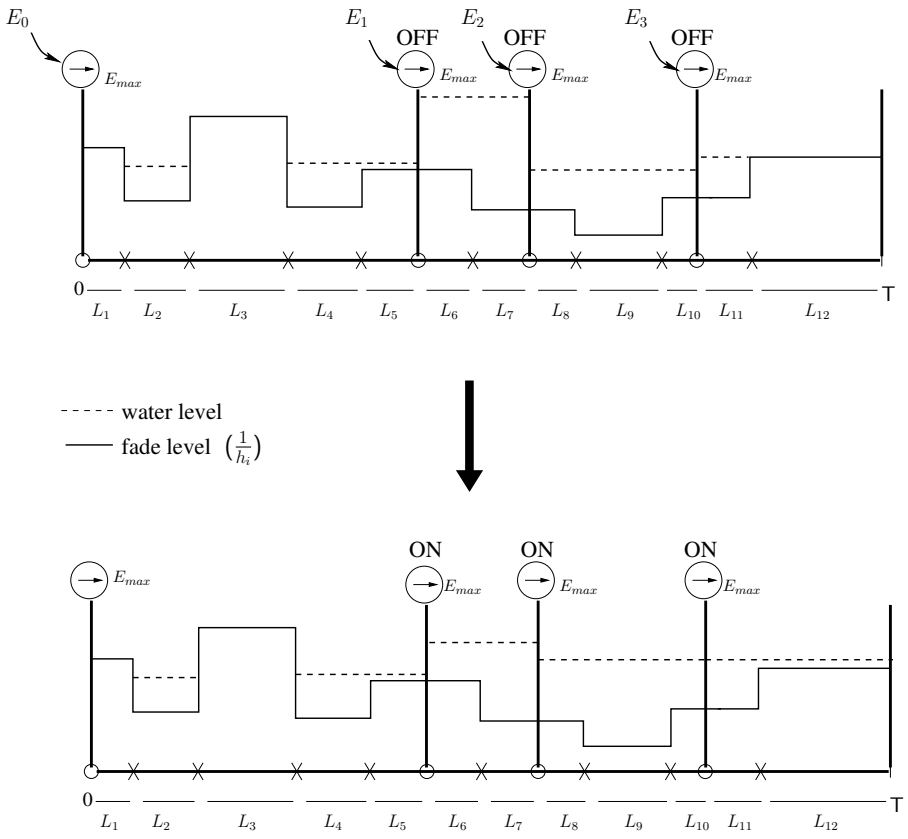

Figure 6.4: Directional water-filling with right permeable taps in a fading channel.

Three energy arrivals occur during the course of the transmission, in addition to the energy available at time $t = 0$. We observe that the energy level equalizes in epochs 2, 4, 5, while no power is transmitted in epochs 1 and 3, since the channel gains in these epochs are too low (i.e., $\frac{1}{h_i}$ too high). The energy arriving at the beginning of epoch 6 cannot flow left due to causality constraints, which are enforced by right permeable taps, which allow energy flow only to the right. We observe that the energy equalizes between epochs 8 through 12, however, the excess energy in epochs 6 and 7 cannot flow right, due to the E_{max} constraint enforced by the right permeable tap between epochs 7 and 8.

6.5 Transmission Completion Time Minimization in Fading Channel

In contrast to the infinite backlog assumption of the previous sections, we now assume that the transmitter has B bits to be communicated to the receiver in the energy harvesting and fading channel setting. Our objective now is to minimize the time necessary to transmit these B bits. This problem is called the transmission completion time minimization problem. In [14, 15], this problem is formulated and solved for an energy harvesting system in a non-fading environment. In [23], the problem is solved when there is an E_{max} constraint on the energy buffer (battery) by identifying its connection to its throughput optimization counterpart. Here, our goal is to address this problem in a fading channel, by using the directional water-filling approach we have developed so far.

The transmission completion time minimization problem can be stated as,

$$\min \quad T \tag{6.22}$$

$$\text{s.t.} \quad \sum_{i=1}^{N} \frac{L_i}{2} \log\left(1 + h_i p_i\right) = B \tag{6.23}$$

$$\sum_{i=1}^{\ell} L_i p_i \leq \sum_{i=1}^{\ell} E_{in}(i), \quad \ell = 1, \ldots, N \tag{6.24}$$

$$\sum_{i=1}^{\ell} E_{in}(i) - \sum_{i=1}^{\ell} L_i p_i \leq E_{max}, \quad \ell = 1, \ldots, N \tag{6.25}$$

where $N \triangleq N(T)$ is the number of epochs in the interval $[0, T]$. The solution will be a generalization of the results in [14, 15, 23] for the fading case. To this end, we introduce the maximum departure curve. This maximum departure curve function will map the transmission completion time minimization problem of this section to

the throughput maximization problem of the previous sections.

6.5.1 Maximum Departure Curve

Given a deadline T, define the maximum departure curve $D(T)$ for a given sequence of energy arrivals and channel fading states as,

$$D(T) = \max \sum_{i=1}^{N(T)} \frac{L_i}{2} \log\left(1 + h_i p_i\right) \tag{6.26}$$

where $N(T)$ is the number of epochs in the interval $[0, T]$. The maximization in (6.26) is subject to the energy causality and maximum battery storage capacity constraints in (6.24) and (6.25). The maximum departure function $D(T)$ represents the maximum number of bits that can be served out of the backlog by the deadline T given the energy arrival and fading sequences. This is exactly the solution of the problem studied in the previous sections. Some characteristics of the maximum departure curve are stated in the following lemma. We provide the proof in Appendix 6.9.3.

Lemma 6.1 *The maximum departure curve $D(T)$ is a monotonically increasing and continuous function of T. $D(T)$ is not differentiable at $\{t_i^e\}$ and $\{t_i^f\}$.*

The continuity and monotonicity of $D(T)$ implies that the inverse function of $D(T)$ exists, and that for a closed interval $[a, b]$, $D^{-1}([a, b])$ is also a closed interval. Since $D(T)$ is obtained by the directional water-filling algorithm, the derivative of $D(T)$ has the interpretation of the rate of energy transfer from past into the future

at time T, i.e., it is the measure of the tendency of water to flow right. The non-differentiabilities at energy arrival and fading change points are compatible with this interpretation.

We can visualize the result of Lemma 6.1 by considering a few simple examples. As the simplest example, consider the non-fading channel ($h = 1$) with E_0 units of energy available at the transmitter (i.e., no energy arrivals). Then, the optimal transmission scheme is a constant transmit power scheme, and hence, we have,

$$D(T) = \frac{T}{2} \log \left(1 + \frac{E_0}{T} \right) \tag{6.27}$$

It is clear that this is a continuous, monotonically increasing function, whose derivative at $T = 0$ (at the time of energy arrival) is unbounded.

Next, we consider a two epoch case where E_1 arrives at T_1 and fading level is constant (and also $h = 1$). We assume E_0 and E_1 are both smaller than E_{max} and $E_0 + E_1 > E_{max}$. After some algebra, $D(T)$ can shown to be expressed as,

$$D(t) = \begin{cases} \frac{t}{2} \log \left(1 + \frac{E_0}{t} \right), & 0 < t < T_1 \\ \frac{T_1}{2} \log \left(1 + \frac{E_0}{T_1} \right) + \frac{t-T_1}{2} \log \left(1 + \frac{E_1}{t-T_1} \right), & T_1 \leq t \leq T_2 \\ \frac{t}{2} \log \left(1 + \frac{E_0+E_1}{t} \right), & T_2 < t < T_3 \\ \frac{T_3}{2} \log \left(1 + \frac{E_0+E_1-E_{max}}{T_3} \right) + \frac{t-T_3}{2} \log \left(1 + \frac{E_{max}}{t-T_3} \right), & T_3 < t < \infty \end{cases} \tag{6.28}$$

where $T_2 = \frac{E_1 T_1}{E_0} + T_1$, $T_3 = \frac{T_1(E_0+E_1)}{E_0+E_1-E_{max}}$. In this E_{max} constrained case, the asymptote of $D(T)$ as $T \to \infty$ is strictly smaller than that in $E_{max} = \infty$ case.

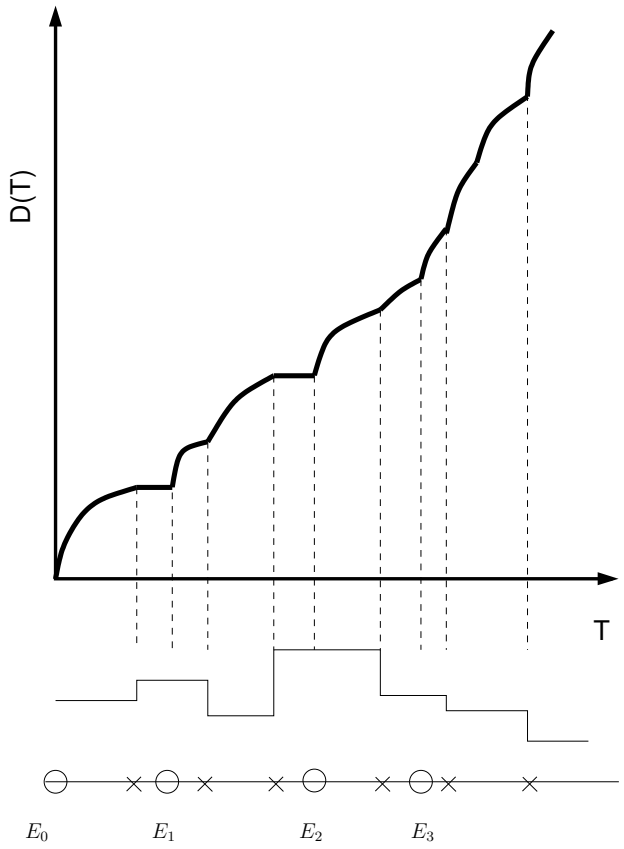

Figure 6.5: The general form of the maximum departure curve.

In the most general case where we have multiple energy arrivals and channel state changes, these basic properties will follow. An example case is shown in Figure 6.5. Note that there may be discontinuities in $D'(T)$ due to other reasons than fading level changes and energy arrivals, such as the E_{max} constraint.

6.5.2 Solution of the Transmission Completion Time Minimization Problem in a Fading Channel

We now solve the transmission completion time minimization problem stated in (6.22)-(6.25). Minimization of the time to complete the transmission of B bits

available at the transmitter is closely related with the maximization of the number of bits that can be sent by a deadline. In fact, if the maximum number of bits that can be sent by T is less than B, then it is not possible to complete the transmission of B bits by T. As we state formally below, if T^* is the minimal time to complete the transmission of B bits, then necessarily $B = D(T^*)$. This argument provides a characterization for T^* in terms of the maximum departure curve, as stated in the following theorem. We provide the proof in Appendix 6.9.4

Theorem 6.3 *The minimum transmission completion time T^* to transmit B bits is $T^* = \min\{t \in \mathcal{M}_B\}$ where $\mathcal{M}_B = \{t : B = D(t)\}$.*

6.6 Online Transmission Policies

In this section, we will study scheduling in the given setting with online, i.e., causal, information of the events. In particular, we consider the maximization of the number of bits sent by deadline T given only causal information of the energy arrivals and channel fade levels at the transmitter side as in Figure 6.1.

We assume that the energy arrival is a compound Poisson process with a density function f_e. Hence, N_e is a Poisson random variable with mean $\lambda_e T$. The channel fade level is a stochastic process marked with a Poisson process of rate λ_f. Thus, N_f is Poisson with mean $\lambda_f T$. The channel takes independent values with probability density f_h at each marked time and remains constant in between two marked points.

6.6.1 Optimal Online Policy

The states of the system are fade level h and battery energy e. An online policy is denoted as $g(e, h, t)$ which denotes the transmit power decided by the transmitter at time t given the states e and h. We call a policy admissible if g is nonnegative, $g(0, h, t) = 0$ for all h and $t \in [0, T]$ and $e(T) = 0$. That is, we impose an infinite cost if the remaining energy in the battery is non-zero after the deadline. Hence, admissible policies guarantee that no transmission can occur if the battery energy is zero and energy left in the battery at the time of the deadline is zero so that resources are used fully by the deadline. The throughput $J_g(e, h, t)$ is the expected number of bits sent by the time t under the policy g

$$J_g(e, h, t) = E\left[\int_0^t \frac{1}{2}\log\left(1 + h(\tau)g(e, h, \tau)\right) d\tau\right] \tag{6.29}$$

Then, the value function is the supremum over all admissible policies g

$$J(e, h, t) = \sup_g J_g \tag{6.30}$$

Therefore, the optimal online policy $g^*(e, h, t)$ is such that $J(e, h, t = 0) = J_{g^*}$, i.e., it solves the following problem

$$\max_g E\left[\int_0^T \frac{1}{2}\log\left(1 + h(\tau)g(e, h, \tau)\right) d\tau\right] \tag{6.31}$$

In order to solve (6.31), we first consider δ-skeleton of the random processes [42]. For sufficiently small δ, we quantize the time by δ and have the following:

$$\max_{g} E\left[\int_0^T \frac{1}{2}\log\left(1+h(\tau)g(e,h,\tau)\right)d\tau\right] =$$
$$\max_{g(e,h,T-\delta)}\left(\frac{\delta}{2}\log\left(1+h(T-\delta)g(e,h,T-\delta)\right)+J(e-\delta g(e,h,T-\delta),h,T)\right) \quad (6.32)$$

Then, we can recursively solve (6.32) to obtain $g^*(e,h,t=T-k\delta)$ for $k=1,2,\ldots,\lfloor\frac{T}{\delta}\rfloor$. This procedure is the dynamic programming solution for continuous time and the outcome is the optimal online policy [42, 43]. After solving for $g^*(e,h,t)$, the transmitter records this function as a look-up table and at each time t, it receives feedback $h(t)$, observes the battery energy $e(t)$ and transmits with power $g^*(e(t),h(t),t)$.

6.6.2 Other Online Policies

Due to the *curse of dimensionality* inherent in the dynamic programming solution, it is natural to forgo performance in lieu of less complex online policies. In this subsection, we propose several suboptimal transmission policies that can somewhat mimic the offline optimal algorithms while being computationally simpler and requiring less statistical knowledge. In particular, we resort to event-based online policies which react to a change in fading level or an energy arrival. Whenever an event is detected, the online policy decides on a new power level. Note that the transmission is subject to availability of energy and the E_{max} constraint.

- **Constant Water Level Policy:** The constant water level policy makes on-

line decisions for the transmit power whenever a change in fading level is observed through the causal feedback. Assuming that the knowledge of the average recharge rate P is available to the transmitter and that fading density f_h is known, the policy calculates h_0 that solves the following equation.

$$\int_{h_0}^{\infty} \left(\frac{1}{h_0} - \frac{1}{h} \right) f_h(h) dh = P \tag{6.33}$$

Whenever a change in the fading level occurs, the policy decides on the following power level $p_i = \left(\frac{1}{h_0} - \frac{1}{h_i} \right)^+$. If the energy in the battery is nonzero, transmission with p_i is allowed, otherwise the transmitter becomes silent.

Note that this power control policy is the same as the capacity achieving power control policy in a stationary fading channel [65] with an average power constraint equal to the average recharge rate. In [12], this policy is proved to be stability optimal in the sense that all data queues with stabilizable arrival rates can be stabilized by policies in this form where the power budget is $P - \epsilon$ for some $\epsilon > 0$ sufficiently small. However, for the time constrained setting, this policy is strictly suboptimal as will be verified in the numerical results section. This policy requires the transmitter to know the mean value of the energy arrival process and the full statistics of the channel fading. A channel state information (CSI) feedback is required from the receiver to the transmitter at the times of events only.

- **Energy Adaptive Water-Filling:** Another reduced complexity event-based

policy is obtained by adapting the water level to the energy level in each event. Again the fading statistics is assumed to be known. Whenever an event occurs, the policy determines a new power level. In particular, the cutoff fade level h_0 is calculated at each energy arrival time as the solution of the following equation

$$\int_{h_0}^{\infty} \left(\frac{1}{h_0} - \frac{1}{h} \right) f(h) dh = E_{current} \tag{6.34}$$

where $E_{current}$ is the energy level at the time of the event. Then, the transmission power level is determined similarly as $p_i = \left(\frac{1}{h_0} - \frac{1}{h} \right)^+$. This policy requires transmitter to know the fading statistics. A CSI feedback is required from the receiver to the transmitter at the times of changes in the channel state.

- **Time-Energy Adaptive Water-Filling:** A variant of the energy adaptive water filling policy is obtained by adapting the power to the energy level and the remaining time to the deadline. The cutoff fade level h_0 is calculated at each energy arrival time as the solution of the following equation.

$$\int_{h_0}^{\infty} \left(\frac{1}{h_0} - \frac{1}{h} \right) f(h) dh = \frac{E_{current}}{T - s_i} \tag{6.35}$$

Then, the transmission power level is determined as $p_i = \left(\frac{1}{h_0} - \frac{1}{h} \right)^+$.

6.7 Numerical Results

We consider a fading additive Gaussian channel with bandwidth W where the instantaneous rate is

$$r(t) = W \log\left(1 + h(t)p(t)\right) \tag{6.36}$$

$h(t)$ is the channel SNR, i.e., the actual channel gain divided by the noise power spectral density multiplied by the bandwidth, and $p(t)$ is the transmit power at time t. Bandwidth is chosen as $W = 1$ MHz for the simulations.

We will examine the deadline constrained throughput performances of the optimal offline policy, optimal online policy, and other proposed sub-optimal online policies. In particular, we compare the optimal performance with the proposed sub-optimal online policies which are based on water-filling [65]. The proposed sub-optimal online policies use the fading distribution, and react only to the new energy arrivals and fading level changes. These event-based algorithms require less feedback and less computation, however, the fact that they react only to the changes in the fading level and new energy arrivals is a shortcoming of these policies. Since the system is deadline constrained, the policies need to take the remaining time into account yet the proposed policies do not do this optimally. We will simulate these policies under various different settings and we will observe that the proposed sub-optimal policies may perform very well in some cases while not as well in some others.

We perform all simulations for 1000 randomly generated realizations of the channel fade pattern and $\delta = 0.001$ is taken for the calculation of the optimal online policy. The rates of Poisson mark processes for energy arrival and channel fading λ_e and λ_f are assumed to be 1. The unit of λ_e is J/sec and that of λ_f is 1/sec. Hence, the mean value of the density function f_e is also the average recharge rate and the mean value of f_h is the average fading level. The changes in the fading level occur relatively slowly with respect to the symbol duration.

f_e is set as a non-negative uniform random variable with mean P, and as the energy arrival is assumed to be smaller than E_{max}, we have $2P < E_{max}$. Selection of the E_{max} constraint is just for illustration. In real life, sensors may have batteries of E_{max} on the order of kJ but the battery feeds all circuits in the system. Here, we assume a fictitious battery that carries energy for only communication purposes. Hence, E_{max} on the order of 1 J will be considered. We will examine different fading distributions f_h. In particular, Nakagami distribution with different shape parameter m will be considered. We implement the specified fading by sampling its probability density function with sufficiently large number of points.

In order to assess the performance, we find an upper bound on the performances of the policies by first assuming that the channel fading levels and energy arrivals in the $[0, T]$ interval are known non-causally, and that the total energy that will arrive in $[0, T]$ is available at the transmitter at time $t = 0$. Then, for the water level p_w that is obtained by spreading the total energy to the interval $[0, T]$, with

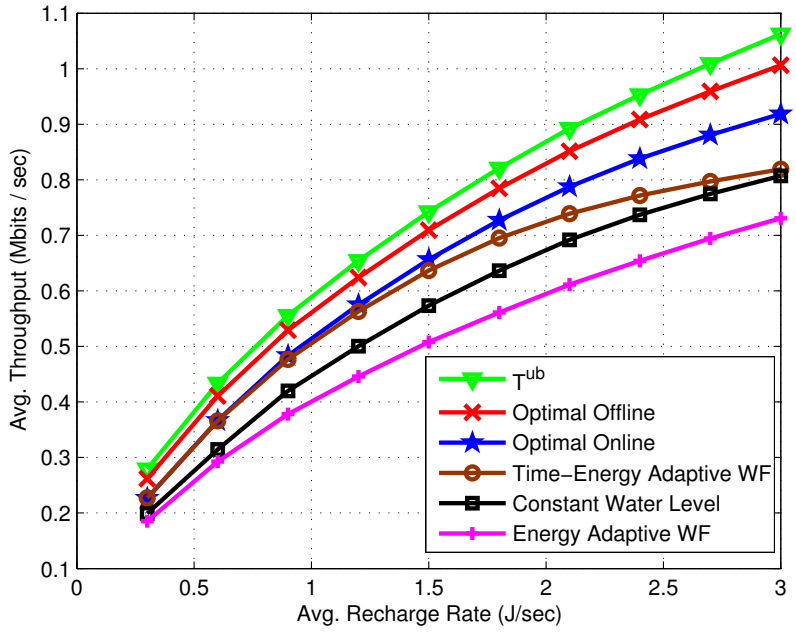

Figure 6.6: Performances of the policies for various energy arrival rates under unit-mean Rayleigh fading, $T = 10$ sec and $E_{max} = 10$ J.

the corresponding fading levels, yield the throughput T^{ub} defined in the following

$$T^{ub} = \frac{W}{T} \sum_{i=1}^{K} l_i \frac{1}{2} \log \left(1 + h_i \left(p_w - \frac{1}{h_i} \right)^+ \right) \tag{6.37}$$

as an upper bound for the average throughput in the $[0, T]$ interval; here l_i denotes the duration of the fade level in the ith epoch. Even the offline optimal policy has a smaller average throughput than T^{ub} as the causality constraint does not allow energies to be spread evenly into the entire interval.

We start with examining the average throughput of the system under Rayleigh fading with SNR= 0 dB and deadline $T = 10$ sec, $E_{max} = 10$ J as depicted in Figure 6.6. We observe that time-energy adaptive water-filling policy performs quite close

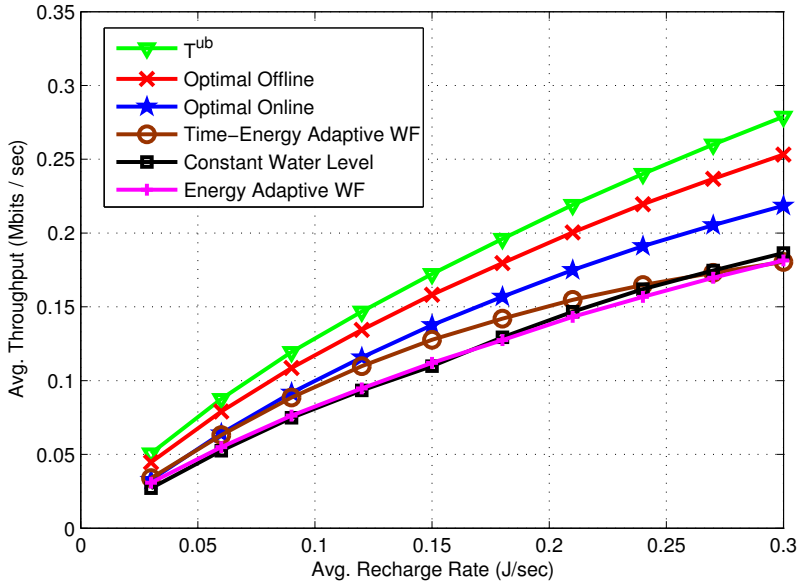

Figure 6.7: Performances of the policies for various average recharge rates under unit-mean Rayleigh fading, $T = 10$ sec and $E_{max} = 1$ J.

to the optimal online policy in the low recharge rate regime. It can be a viable policy to spread the incoming energy when the recharge rate is low; however, its performance saturates as the recharge rate is increased. In this case the incoming energy cannot be easily accommodated and more and more energy is lost due to overflows. Similar trends can be found in Figure 6.7 under very low recharge rate regime in the same setting with only difference being the battery capacity $E_{max} = 1$ J. Next, we examine the setting with $T = 10$ sec, $E_{max} = 10$ J under Nakagami fading of $m = 3$ (average SNR= 5 dB) and we observe similar performances as in the previous cases in Figure 6.8. As a common behavior in these settings, energy adaptive water-filling performs poorer with respect to the constant water level and time-energy adaptive water-filling schemes.

Finally, we examine the policies under different deadline constraints and present

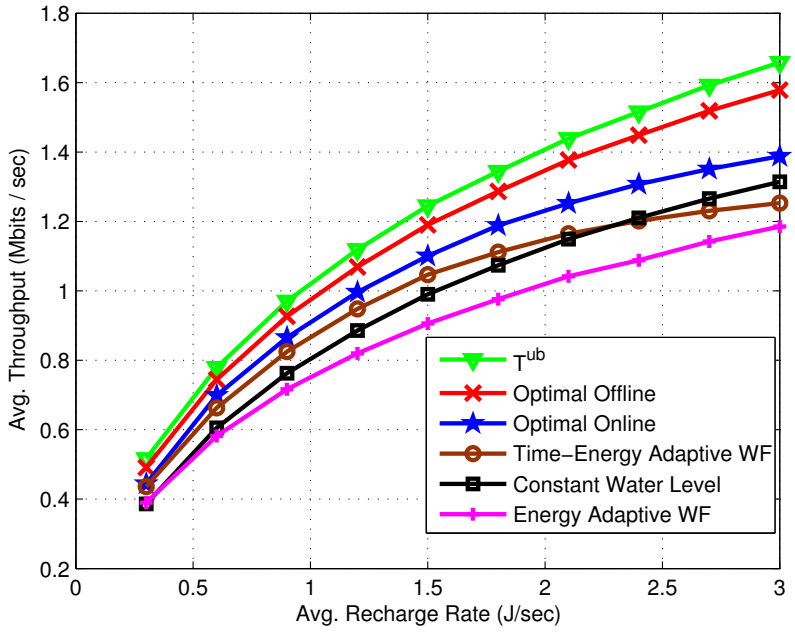

Figure 6.8: Performances of the policies for different energy recharge rates under Nakagami fading with $m = 3$, $T = 10$ sec and $E_{max} = 10$ J.

the plots for Nakagami fading distribution with $m = 5$ in Figure 6.9. A remarkable result is that as the deadline is increased, stability optimal [12] constant water level policy approaches the optimal online policy. We conclude that the time-awareness of the optimal online policy has less and less importance as the deadline constraint becomes looser. We also observe that the throughput of the energy-adaptive water-filling policy is roughly a constant regardless of the deadline. Moreover, the time-energy adaptive policy performs worse as T is increased because energies are spread to very long intervals rendering the transmit power very small and hence energy accumulates in the battery. This leads to significant energy overflows since the battery capacity is limited, and the performance degrades.

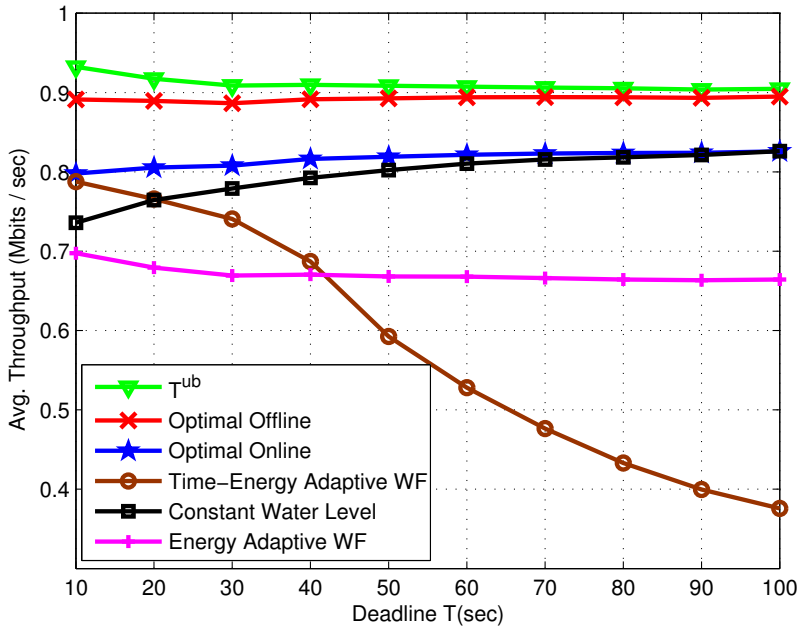

Figure 6.9: Performances of the policies with respect to deadline T under Nakagami fading distribution with $m = 5$ and average recharge rate $P = 0.5$ J/sec and $E_{max} = 10$ J.

6.8 Conclusion

In this chapter, we developed optimal energy management schemes for energy harvesting systems operating in fading channels, with finite capacity rechargeable batteries. We considered two related problems under offline knowledge of the events: maximizing the number of bits sent by a deadline, and minimizing the time it takes to send a given amount of data. We solved the first problem using a directional water-filling approach. We solved the second problem by mapping it to the first problem via the maximum departure curve function. Finally, we solved for throughput optimal policy for the deadline constrained setting under online knowledge of the events using dynamic programming in continuous time. Our numerical results

show the performances of these algorithms under offline and online knowledge.

6.9 Appendix

6.9.1 Proof of Theorem 6.1

Since $E_{max} = \infty$, constraints in (6.8) are satisfied without equality and $\mu_i = 0$ for all i by slackness conditions in (6.11). From (6.12), since $\lambda_i \geq 0$, optimum p_i^* are monotonically increasing: $p_{i+1}^* \geq p_i^*$. Moreover, if for some ℓ, $\sum_{i=1}^{\ell} L_i p_i^* < \sum_{i=0}^{\ell-1} E_i$, then $\lambda_\ell = 0$, which means $p_\ell^* = p_{\ell+1}^*$.

6.9.2 Proof of Theorem 6.2

$E_{max} = \infty$ assumption results in $\mu_i = 0$ for all i. From (6.21), and since $\lambda_i \geq 0$, we have $\nu_{i+1} \geq \nu_i$. If energy is transferred from the ith epoch to the $i+1$st epoch, then the ith constraint in (6.14) is satisfied without equality. This implies, by slackness conditions in (6.17), that for those i, we have $\lambda_i = 0$. Hence, by (6.21), $\nu_i = \nu_{i+1}$. In particular, $\nu_i = \nu_j$ for all epochs i and j that are in between two consecutive energy arrivals as there is no wall between these epochs and injected energy freely spreads into these epochs.

6.9.3 Proof of Lemma 6.1

The monotonicity follows because as the deadline is increased, we can transmit at least as many bits as we could with the smaller deadline. The continuity follows by observing that, if no new energy arrives or fading state changes, there is no reason to

have a discontinuity. When new energy arrives, since the number of bits that can be transmitted with a finite amount of energy is finite, the number of bits transmitted will not have any jumps. Similarly, if the fading level changes, due to the continuity of the log function, $D(T)$ will be continuous.

For the non-differentiable points, assume that at $t = t_i^e$, an energy in the amount of E_i arrives. There exists a small enough increment from t_i^e that the water level on the right is higher than the water level on the left. The right permeable taps will not allow this water to flow to left. Then, the $D(T)$ is in the following form:

$$D(t_i^e + \Delta) = D(t_i^e) + \frac{\Delta}{2} \log\left(1 + \frac{E_i h}{\Delta}\right) \tag{6.38}$$

Thus, the right derivative of $D(T)$ at $t = t_i^e$, becomes arbitrarily large. Hence, $D(T)$ is not differentiable at t_i^e. At $t = t_i^f$, the fade level changes from h_i to h_{i+1}. As t is increased, water level decreases unless new energy arrives. The change in the water level is proportional to $\frac{1}{h_{i+1}}$ for $t > t_i^f$ and is proportional to $\frac{1}{h_i}$ for $t < t_i^f$. Hence, at $t = t_i^f$, $D(T)$ is not differentiable.

6.9.4 Proof of Theorem 6.3

For t such that $D(t) < B$, $T^* > t$ since the maximum number of bits that can be served by t is $D(t)$ and it is less than B. Hence, B bits cannot be completed by t. Conversely, for t such that $D(t) > B$, $T^* < t$ because B bits can be completed by t. Hence, $D(T^*) = B$ is a necessary condition. As $D(T)$ is continuous, the set

$\{t : B = D(t)\}$ is a closed set. Hence, $\min\{t : B = D(t)\}$ exists and is unique. By the definition of T^*, we have $T^* = \min\{t : B = D(t)\}$.

Chapter 7

Scheduling over Gaussian Broadcast Channels with an Energy Harvesting Transmitter

7.1 Introduction

In this chapter, we consider a broadcast channel with an energy harvesting transmitter with a *finite capacity battery* and M receivers as shown in Figure 7.1. $M+1$ queues at the transmitter are: M data queues that store the data destined to the receivers and an energy queue (battery) that stores the harvested energy. The energy queue has a finite capacity and can store at most E_{max} units of energy. As shown in Figure 7.2, the energy arrives (is harvested) at times s_k in amounts E_k. E_0 is the initial energy available in the battery at time zero. Saving energy for future use is advantageous, however, finite battery capacity constrains this capability, and thus necessitates avoiding energy overflows. We focus on the optimal offline policy that minimizes the time, T, required to transmit B_m bits to receiver m, for $m = 1, \ldots, M$. The transmission policy is subject to the causality of energy arrivals as well as the finite battery capacity constraint.

In [24], we show, under the assumption of an infinite-sized battery, that the time sequence of the optimal total power in a broadcast channel increases monotonically as in the single user case in [14, 15]. Moreover, in [24], we prove that there

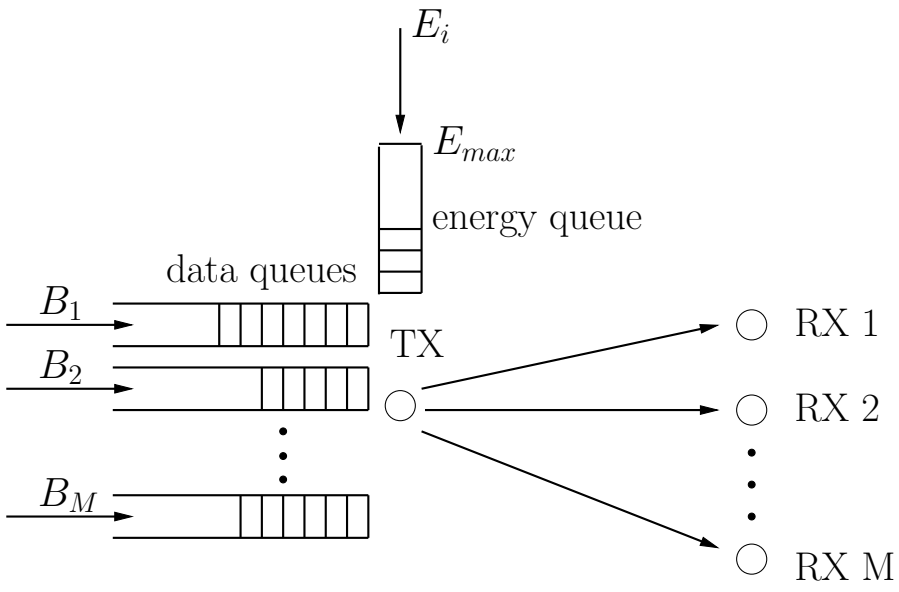

Figure 7.1: M-user broadcast channel with an energy harvesting transmitter and a finite capacity battery.

exists a *cut-off* power level for the power shares of the strong and weak users; strong user's power share is always less than or equal to this cut-off level and when it is strictly less than this cut-off level, weak user's power share is zero. The structure of the optimal policy in [24] is contingent upon the infinite capacity battery. In particular, when a large amount of energy is harvested, the development in [24] assumes that some portion of this harvested energy can always be saved for future use. However, when the battery capacity is finite, energy may overflow in such cases. Therefore, the added challenge in the finite capacity battery case is to accommodate every bit of the incoming energy by carefully managing the transmission power and users' power shares according to the times and amounts of the harvested energy.

We find that as in [24], the determination of the total transmit power can be separated from the determination of the shares of the users without losing optimality.

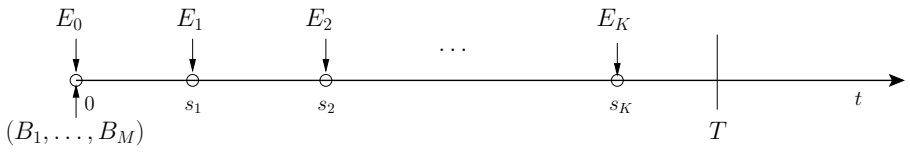

Figure 7.2: Energies arrive at time instants s_k in amounts E_k.

We first obtain the structural properties of the optimal policy by means of a dual problem, namely, the maximization of the region of bits served for the receivers by a fixed time T, i.e., the *maximum departure region.* We show that, similar to the battery unlimited case, we have a *cut-off* property in the optimal power shares. However, different from the battery unlimited case, the transmit power is not monotonically increasing.

We formulate the battery-unconstrained problem in [24] in the rate domain. However, when there is a battery capacity constraint, the resulting no-energy-overflow constraint gives a non-convex constraint for the optimization problem in the rate domain. Therefore, we formulate the problem in the power domain. We show that the total power in each epoch must be the same as the total power in the single user channel, which, in turn, can be found by the directional water-filling algorithm developed in Chapter 6. We then find the optimal shares of the users from the total power in closed form via a single-variable optimization problem, completing the characterization of the optimal solution of the dual problem. We then use the structure of this dual problem, in particular the *cut-off* property and the optimality of directional water-filling to solve the transmission completion time minimization problem. Finally, we provide numerical illustrations and performance comparisons for the optimal offline policy.

7.2 System Model and Problem Formulation

As shown in Figures 7.1 and 7.2, the transmitter has M data queues each having B_m bits destined to the mth receiver, and an energy queue of finite capacity E_{max}. The initial energy available in the battery at time zero is E_0 and energy arrivals occur at times $\{s_1, s_2, \ldots\}$ in amounts $\{E_1, E_2, \ldots\}$. We call the time interval between two consecutive energy arrivals an *epoch*. The epoch lengths are $\ell_i = s_i - s_{i-1}$ with $s_0 = 0$. We assume that $E_i \leq E_{max}$ for all i.

The physical layer is modeled as an AWGN broadcast channel, with received signals

$$Y_m = X + Z_m, \qquad m = 1, \ldots, M \tag{7.1}$$

where X is the transmit signal, and Z_m is a Gaussian noise with zero-mean and variance σ_m^2, and without loss of generality $\sigma_1^2 \leq \sigma_2^2 \leq \ldots \leq \sigma_M^2$. Therefore, the first user is the strongest and the Mth user is the weakest user in our broadcast channel. The capacity region for the M-user AWGN broadcast channel is the set of rate vectors $(r_1, \ldots, r_M)$ [54]:

$$r_m = \frac{1}{2}\log_2\left(1 + \frac{\alpha_m P}{\sum_{j<m}\alpha_j P + \sigma_m^2}\right), \qquad m = 1, \ldots, M \tag{7.2}$$

where $\alpha_m \geq 0$ and $\sum_m \alpha_m = 1$.

Our goal is to select a transmission policy that minimizes the time, T, by which all of the bits are delivered to their intended receivers. The transmitter adapts its

transmit power and the portions of the total transmit power used to transmit signals to the M users according to the available energy level and the remaining number of bits. The energy consumed must satisfy the causality constraints, i.e., at any given time t, the total amount of energy consumed up to time t must be less than or equal to the total amount of energy harvested up to time t.

Let us denote the transmit power at time t as $P(t)$ for $t \in [0, T]$. The transmission policy in a broadcast channel is comprised of the total power $P(t)$ and the portion of the total transmit power $\alpha_m(t)$ that is allocated for user m, $m = 1, \ldots, M$. As $\sum_{m=1}^{M} \alpha_m(t) = 1$, the transmission policy is represented by $\alpha_m(t)$, $m = 1, \ldots, M-1$ and $\alpha_M(t) = 1 - \sum_{m=1}^{M-1} \alpha_m(t)$. For the special case of $M = 2$, we denote the strong user's power share without a subscript as $\alpha(t)$.

The total energy consumed by the transmitter up to time t can be expressed as $\int_0^t P(\tau)d\tau$. Note that because of the finite battery capacity constraint, at any time t, if the unconsumed energy is greater than E_{max}, only E_{max} can be stored in the battery and the rest of the energy overflows and hence is wasted. This may happen only at the instants of energy arrival. Therefore, the total removed energy from the battery at s_k, $E_r(s_k)$, including the consumed part and the wasted part, can be expressed recursively for $k = 1, 2, \ldots$ as

$$E_r(s_k^+) = \max \left\{ E_r(s_{k-1}^+) + \int_{s_{k-1}}^{s_k} P(\tau)d\tau, \left(\sum_{j=0}^{k} E_j - E_{max} \right)^+ \right\} \tag{7.3}$$

where $(x)^+ = \max\{0, x\}$, and s_k^+ should be interpreted as $s_k + \epsilon$ for arbitrarily small $\epsilon > 0$. In addition, $E_r(s_0) = 0$. We can extend the definition of E_r for the times

$t \neq s_k$ as:

$$E_r(t) = E_r(s^+_{h_+(t)}) + \int_{s_{h_+(t)}}^{t} P(\tau)d\tau \tag{7.4}$$

where $h_+(t) = \max\{i : s_i \leq t\}$. As the transmitter cannot utilize the energy that has not arrived yet, the transmission policy is subject to an energy causality constraint. The removed energy $E_r(t)$ cannot exceed the total energy arrival during the communication. This constraint is mathematically stated as follows:

$$E_r(t) \leq \sum_{i=0}^{h_-(t)} E_i, \qquad \forall t \in [0, T] \tag{7.5}$$

where $h_-(t) = \max\{i : s_i < t\}$. As the energies arrive at discrete times, the causality constraint reduces to inequalities that have to be satisfied at the times of energy arrivals:

$$E_r(s^+_{k-1}) + \int_{s_{k-1}}^{s_k} P(\tau)d\tau \leq \sum_{i=0}^{k-1} E_i, \quad \forall k \tag{7.6}$$

An illustration of $E_r(t)$ and the causality constraint is shown in Figure 7.3. The upper curve in Figure 7.3 represents the total energy arrived and the lower curve is obtained by subtracting E_{max} from the upper curve. The causality constraint imposes $E_r(t)$ to remain below the upper curve. Moreover, $E_r(t)$ always remains above the lower curve by definitions in (7.3) and (7.4). Therefore, $E_r(t)$ always lies in between these two curves. In the particular $E_r(t)$ shown in Figure 7.3, the energy in the battery exceeds E_{max} at the time of the third energy arrival at s_3 and some

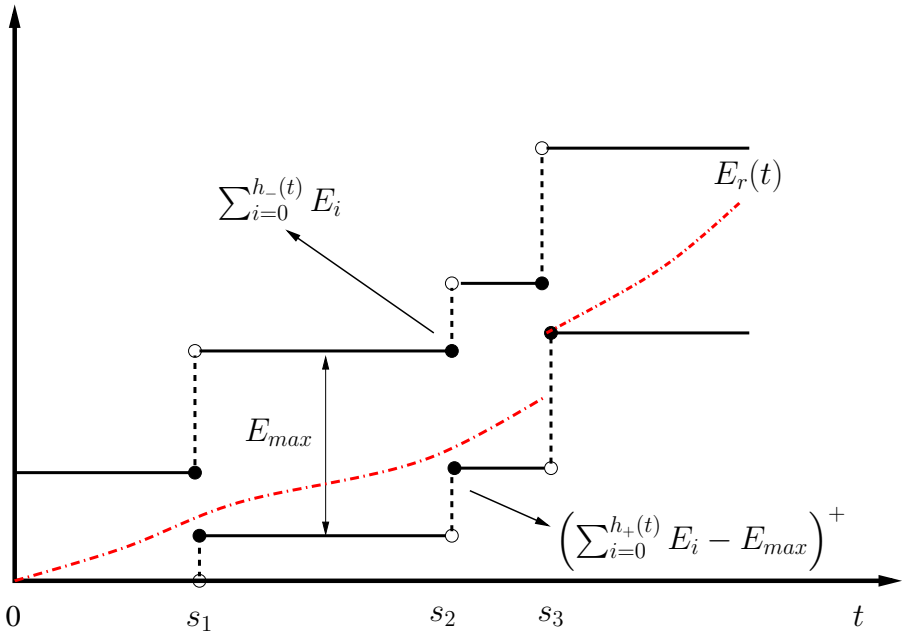

Figure 7.3: The total removed energy curve $E_r(t)$. The jump at s_3 represents an energy overflow because of the finite battery capacity limit.

energy is removed from the battery without being utilized for data transmission. After s_3, energy removal from the battery continues due to data transmission and hence the removal curve approaches the total energy arrival curve indicating that the battery energy is decreasing.

As observed in Figure 7.3, some energy is lost due to energy overflow if $E_r(t)$ intersects the lower curve at the vertically rising parts at the energy arrival instants. Therefore, a transmission policy guarantees no-energy-overflow if the following constraint is satisfied:

$$\int_0^t P(\tau)d\tau \geq \left(\sum_{i=0}^{h_+(t)} E_i - E_{max}\right)^+, \quad \forall t \in [0,T] \tag{7.7}$$

The constraint in (7.7) imposes that at least $\sum_{i=0}^{k} E_i - E_{max}$ amount of energy

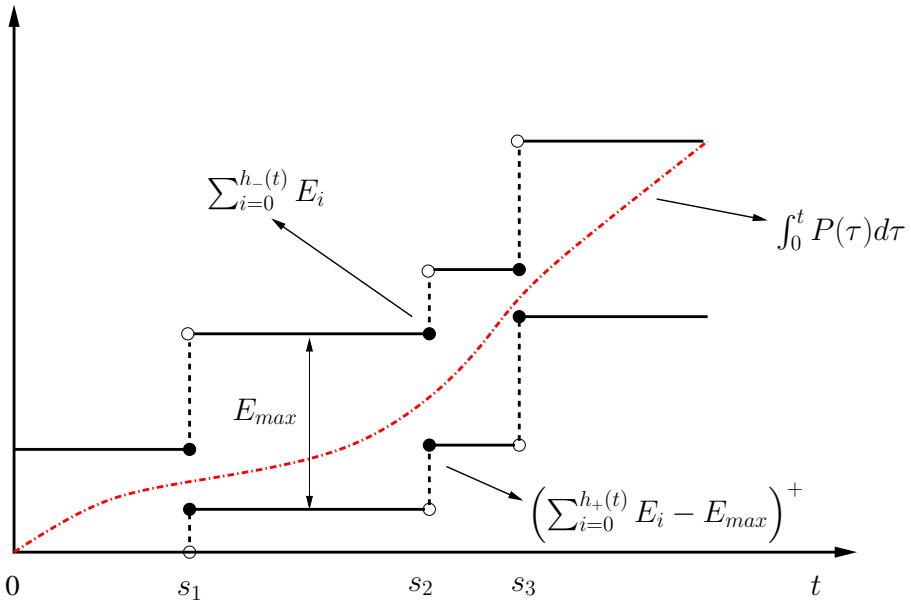

Figure 7.4: Graphical representation of energy causality and no-energy-overflow constraints.

has been consumed by the time the kth energy arrives so that the battery can accommodate E_k at time s_k. If a policy satisfies (7.7), the max in (7.3) always yields the first term in it. Therefore, the causality constraint in (7.6) is simplified to the following:

$$\int_0^t P(\tau)d\tau \leq \sum_{i=0}^{h_-(t)} E_i, \quad \forall t \in [0, T] \tag{7.8}$$

This is depicted in Figure 7.4 in which the total energy curve of the policy does not intersect the lower curve at the vertically rising parts (at the energy arrival instants) and thus no energy is removed from the battery due to energy overflows. Hence, the causality constraint reduces to the condition that the total energy arrival curve must lie below the upper curve in Figure 7.4.

Instead of directly finding the optimal policy that minimizes the transmission completion time, we start by solving the dual problem of finding the *maximum departure region*, the largest region of number of bits that the transmitter can deliver to each user by a fixed time T. Solving the dual problem enables us to identify the properties of an optimal policy in the original problem.

7.3 The Dual Problem

In this section, we consider the dual problem of determining the *maximum departure region* which is the set of number of bits that can be delivered to the receivers by a fixed deadline T.

Definition 7.1 *For any fixed transmission duration T, the maximum departure region, denoted as $\mathcal{D}(T)$, is the union of $\mathcal{R}(B_1, \ldots, B_M) = \{(b_1, \ldots, b_M) : 0 \leq b_1 \leq B_1; \ldots; 0 \leq b_M \leq B_M\}$ where $(B_1, \ldots, B_M)$ is the total number of bits sent by some power allocation policy $P(t)$ and $\alpha_m(t)$, $m = 1, \ldots, M$, that satisfy the energy causality (7.8) and no-energy-overflow (7.7) conditions.*

The departure region of any policy that causes energy overflows can be dominated by a policy that does not allow energy overflows. Hence, in the definition of $\mathcal{D}(T)$, we restrict the policies to satisfy the no-energy-overflow condition in (7.7). We refer to any policy that satisfies the energy causality and no-energy-overflow conditions as *feasible*. We call a feasible policy *optimal* if it achieves the boundary of $\mathcal{D}(T)$.

The transmission rates remain constant between energy harvests under any optimal policy (c.f. Lemma 1 in [24] and Lemma 2 in [14, 15]). Therefore, in the sequel, we restrict ourselves to the policies in which the powers and the power shares remain constant between any two consecutive energy arrivals. Let K denote the number of energy arrivals in $(0, T)$ yielding $K + 1$ epochs, with $s_0 = 0$ and $s_{K+1} = T$. We represent the transmission policy by $(M+1)(K+1)$ variables P_k and α_{mk}, for $m = 1, \ldots, M$, and $k = 1, \ldots, K + 1$. P_k and α_{mk} denote, respectively, the total power allocated and the corresponding power share of user m over the duration $[s_{k-1}, s_k)$. The causality constraint in (7.8) reduces to the following constraints on P_i:

$$\sum_{i=1}^{k} P_i \ell_i \leq \sum_{i=0}^{k-1} E_i, \qquad k = 1, \ldots, K + 1 \tag{7.9}$$

and the no-energy-overflow condition in (7.7) reduces to:

$$\sum_{i=1}^{k} P_i \ell_i \geq \left(\sum_{i=0}^{k} E_i - E_{max} \right)^+, \qquad k = 1, \ldots, K \tag{7.10}$$

An important property of $\mathcal{D}(T)$ is stated next [101]. The proof is provided in Appendix 7.7.1.

Lemma 7.1 *$\mathcal{D}(T)$ is a convex region.*

Since $\mathcal{D}(T)$ is a convex region[1] its boundary is uniquely characterized by the supporting hyperplanes [102]. Therefore, in order to characterize the boundary of

[1]In fact, it is a strictly convex region due to the strict concavity of the log function. In a strictly convex region, no two points on the boundary of $\mathcal{D}(T)$ lie on the same hyperplane.

$\mathcal{D}(T)$, we consider all possible supporting hyperplanes to the maximum departure region and solve the following optimization problem for all $\mu_1, \ldots, \mu_M \geq 0$,

$$\begin{aligned} \max_{\{P_i, \boldsymbol{\alpha}_i\}} \quad & \mu_1 \sum_{i=1}^{K+1} r_1(\boldsymbol{\alpha}_i, P_i)\ell_i + \ldots + \mu_M \sum_{i=1}^{K+1} r_M(\boldsymbol{\alpha}_i, P_i)\ell_i \\ \text{s.t.} \quad & \sum_{i=1}^{k} P_i \ell_i \leq \sum_{i=0}^{k-1} E_i, \qquad k = 1, \ldots, K+1 \\ & \sum_{i=1}^{k} P_i \ell_i \geq \left(\sum_{i=0}^{k} E_i - E_{max} \right)^+, \qquad k = 1, \ldots, K \end{aligned} \tag{7.11}$$

where $\mu_1, \ldots, \mu_M \geq 0$ are the weights of the number of departed bits, and $r_m(\boldsymbol{\alpha}_i, P_i)$ is the rate allocated for the mth user at epoch i:

$$r_m(\boldsymbol{\alpha}_i, P_i) = \frac{1}{2} \log_2 \left(1 + \frac{\alpha_{mi} P_i}{\sum_{j<m} \alpha_{ji} P_i + \sigma_m^2} \right) \tag{7.12}$$

Therefore, $\sum_{i=1}^{K+1} r_m(\boldsymbol{\alpha}_i, P_i)\ell_i$ is the total number of bits served for user m in the $[0, T]$ interval.

The problem in (7.11) is not a convex problem as the variables α_{mi} and P_i appear in a product form, causing the objective function to be a non-concave function of the variables $\boldsymbol{\alpha}_i$ and P_i. Even though the objective function is concave with respect to P_i for any given $\boldsymbol{\alpha}_i$, since the optimal α_is depend on the powers, we cannot immediately conclude that the objective function is concave in powers. We solve (7.11) in two steps. We first optimize (7.11) with respect to α_i for a given fixed set of powers. We show that when optimal α_is, which are functions of the powers, are inserted back into (7.11), we obtain an objective function which is concave in

powers, and this leads to a convex overall problem. In [101], we solved the problem in (7.11) for $M = 2$ in the rate domain. The difficulty of working in the rate domain is that the feasible set of the problem becomes non-convex under the constraints due to finite capacity battery; see the discussion around [101, eqn. (24)]. We overcome this issue here by casting the problem in terms of powers.

Assume that P_i are given at each epoch i. We solve the following problem in each epoch i:

$$\max_{\boldsymbol{\alpha}_i} \quad \mu_1 r_1(\boldsymbol{\alpha}_i, P_i) + \ldots + \mu_M r_M(\boldsymbol{\alpha}_i, P_i) \tag{7.13}$$

Let us define the result of the optimization problem in (7.13) as a function of P:

$$f(P) \triangleq \max_{\boldsymbol{\alpha}} \mu_1 r_1(\boldsymbol{\alpha}, P) + \ldots + \mu_M r_M(\boldsymbol{\alpha}, P) \tag{7.14}$$

We have the following lemma whose proof is provided in Appendix 7.7.2.

Lemma 7.2 *$f(P)$ is a strictly concave function of P and the derivative of $f(P)$ is continuous.*

Then, the problem in (7.11) can be written as a problem only in terms of P_i as follows:

$$\begin{aligned} \max_{\mathbf{P}} \quad & \sum_{i=1}^{K+1} f(P_i)\ell_i \\ \text{s.t.} \quad & \sum_{i=1}^{k} P_i\ell_i \leq \sum_{i=0}^{k-1} E_i, \qquad k=1,\ldots,K+1 \\ & \sum_{i=1}^{k} P_i\ell_i \geq \left(\sum_{i=0}^{k} E_i - E_{max}\right)^+, \qquad k=1,\ldots,K \end{aligned} \tag{7.15}$$

The problem in (7.15) is a convex optimization problem. The objective function is strictly concave by Lemma 7.2 and the feasible set is a convex set. In the next lemma, we state a key structural property of the optimal policy. The proof is provided in Appendix 7.7.3.

Lemma 7.3 *Optimal total transmit power sequence P_i^*, $i=1,\ldots,K+1$, is independent of the values of $\mu_1,\ldots,\mu_M$. In particular, it is the same as the single user optimal transmit power sequence, i.e., it is the same as the solution for $\mu_1>0$ and $\mu_m=0$, $m=2,\ldots,M$.*

Therefore, irrespective of the values of $\mu_1,\ldots,\mu_M$, the unique total power allocation can be found by the directional water-filling algorithm in Chapter 6. An alternative algorithm for solving the same problem is provided in [23], which uses the feasible energy tunnel approach. The structures of these two alternative algorithms, as well as the one in [14, 15] for the unconstrained battery case, are determined only by the strict concavity of the rate-power relation. We obtained the same structure in the broadcast channel here due to the strict concavity of $f(P)$ in P, which is

stated and proved in Lemma 7.2.

Once the optimal *total* transmit powers, P_i^*, are determined, the optimal power shares of the users can be determined by solving the problem in (7.13) in terms of $\boldsymbol{\alpha}_i$, by using the analysis presented in the proof of Lemma 7.2 in Appendix 7.7.2. In particular, splitting the total power among M users requires a *cut-off* power structure. Whenever $\mu_j \leq \mu_l$ for any $1 \leq l < j \leq M$, i.e., whenever a degraded user has a smaller weight, the solution of (7.13) is such that $r_{ji}^* = 0$ for any value of P_i. This is because, the allocated rate of a degraded user j can be transferred to a stronger user l [54], and doing so yields a higher weighted sum of rates if $\mu_j < \mu_l$ (see also Appendix 7.7.2). Hence, we remove the users j where $\mu_j \leq \mu_l$ and $1 \leq l < j \leq M$. The remaining $R \leq M$ users are such that $\sigma_1^2 \leq \sigma_2^2 \leq \ldots \leq \sigma_R^2$ with $\mu_1 < \mu_2 < \ldots < \mu_R$. Using a first order differential analysis (see Appendix 7.7.2), the optimal cut-off power levels for the remaining R users must satisfy the following equations for $m = 1, \ldots, R-1$:

$$P_{cm} = \max \left\{ \left(\frac{\mu_m \sigma_{\bar{m}}^2 - \mu_{\bar{m}} \sigma_m^2}{\mu_{\bar{m}} - \mu_m} \right)^+, P_{c(m-1)} \right\} \tag{7.16}$$

where $\bar{m}$ is the smallest user index with $P_{c\bar{m}} > P_{cm}$. By convention, we have $P_{c0} = 0$, $P_{cR} = \infty$. We note that P_{cm} and $\bar{m}$ in (7.16) can be recursively calculated. We immediately observe that for $m = R-1$, $\bar{m} = R$ and $P_{cm} = P_{c(R-1)}$ for

$m = u_1^*, \ldots, R-1$ where:

$$P_{c(R-1)} = \max_{k \in [1:R-1]} \left(\frac{\mu_k \sigma_R^2 - \mu_R \sigma_k^2}{\mu_R - \mu_k} \right)^+ \tag{7.17}$$

$$u_1^* = \arg \max_{k \in [1:R-1]} \left(\frac{\mu_k \sigma_R^2 - \mu_R \sigma_k^2}{\mu_R - \mu_k} \right)^+ \tag{7.18}$$

Similarly, we find P_{cm} for $m = u_1^* - 1$ by replacing R with u_1^* in (7.17). $P_{cm} = P_{c(u_1^*-1)}$ and $\bar{m} = u_1^*$ for $m = u_2^*, \ldots, u_1^* - 1$ where u_2^* is calculated as in (7.18) by replacing R with u_1^*. We continue until we reach $u_j^* = 1$ for some j. We can verify that P_{cm} calculated this way satisfies the conditions in (7.16); therefore, this procedure determines the desired cut-off power levels.

We show the structure of optimally splitting the total power among the users in Figure 7.5. The top portion of the total power is allocated to the user with the worst channel and the power below it is interference for this user. The bottom portion of the total power is allocated to the user with the best channel and this user experiences no interference. We note that the cut-off power levels are independent of the varying total power levels in epochs or the E_{max} constraint.

As a specific example, for the two-user case ($M = 2$), the single cut-off power level is

$$P_c = \left(\frac{\mu_1 \sigma_2^2 - \mu_2 \sigma_1^2}{\mu_2 - \mu_1} \right)^+ \tag{7.19}$$

If the optimal total power level in the ith epoch, P_i^*, is smaller than the cut-off power level P_c, then only the stronger user's data is transmitted. If $P_i^* \geq P_c$, then

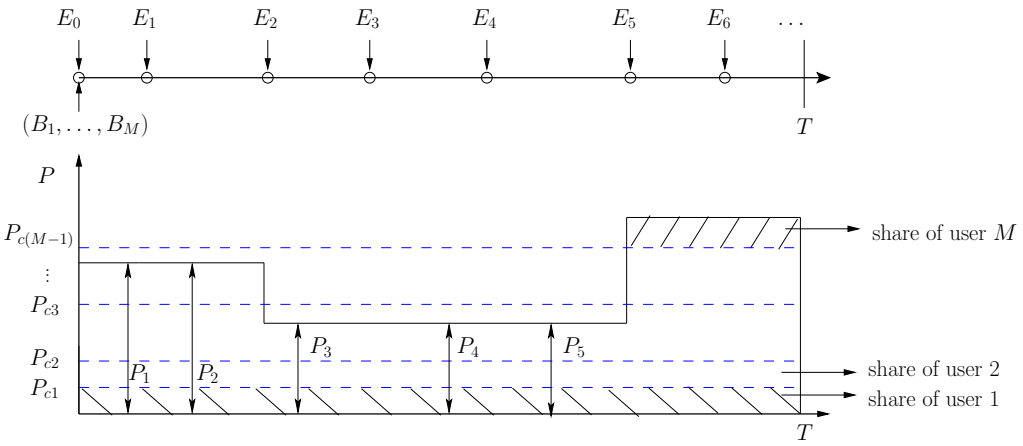

Figure 7.5: Optimally splitting the total power for M users.

the strong user's power share is P_c and the weak user's power share is the remainder of the power in that epoch. From Lemma 7.3, the optimal policies that achieve the boundary of $\mathcal{D}(T)$ have a common *total* transmit power and from Lemma 7.2 its splitting between the two users depends on μ_1, μ_2 through μ_2/μ_1 as reflected in the cut-off power in (7.19). For different values of μ_1, μ_2, the optimal policy achieves different boundary points on $\mathcal{D}(T)$. Varying the values of μ_1, μ_2 traces the boundary of $\mathcal{D}(T)$.

7.4 Minimum Transmission Completion Time

In this section, our goal is to minimize the transmission completion time given $(B_1, \ldots, B_M)$:

$$\begin{aligned} \min_{\mathbf{P}} \quad & T \\ \text{s.t.} \quad & \sum_{i=1}^{k} P_i \ell_i \leq \sum_{i=1}^{k-1} E_i, \quad k = 1, \ldots, K+1 \\ & \sum_{i=1}^{k} P_i \ell_i \geq \left(\sum_{i=0}^{k} E_i - E_{max} \right)^+, \ k = 1, \ldots, K \\ & \sum_{i=1}^{K+1} \frac{1}{2} \log_2 \left(1 + \frac{\alpha_m^*(P_i) P_i}{\sum_{j<m} \alpha_j^*(P_i) P_i + \sigma_m^2} \right) \ell_i = B_m, \ \forall m \end{aligned} \tag{7.20}$$

where $K = K(T)$ is the number of energy arrivals over $(0, T)$, and $l_{K(T)+1} = T - s_{K(T)}$. Since $K(T)$ depends on T, the optimization problem in (7.20) is not convex in general.

We observe that (7.20) is the dual problem of finding the maximum departure region for fixed T in (7.11) in the sense that, if the minimum transmission completion time for $(B_1, \ldots, B_M)$ is T, then $(B_1, \ldots, B_M)$ must lie on the boundary of $\mathcal{D}(T)$, and the optimal policies in both problems must be the same. In the following, we provide an algorithm to minimize the transmission completion time for given $(B_1, \ldots, B_M)$, by using the properties we developed for the optimal policy for the dual problem in the previous section. We first start with the $M = 2$ user case.

(B_1, B_2) must lie on the boundary of $\mathcal{D}(T_{min})$. Hence, without losing optimality we restrict our attention to the policies which allocate the total transmit

power by directional water-filling and have the cut-off power structure. As the initial step, we suppose that the transmitter transmits only to the stronger user with an arbitrary P_c and find the transmission completion time for the stronger user by $T_1 = \frac{B_1}{\frac{1}{2}\log_2(1+P_c)}$. For this fixed T_1, we run the directional water-filling algorithm and find the total power allocation $P_1, P_2, \ldots, P_{K(T_1)+1}$ with the deadline T_1. The number of bits transmitted to the stronger user is

$$D_1(T_1, P_c) = \sum_{i=1}^{K(T_1)+1} \frac{1}{2}\log_2\left(1 + P_i - [P_i - P_c]^+\right)\ell_i \tag{7.21}$$

We allocate the remaining power $[P_i - P_c]^+$ to the weaker user and calculate the total bits departed from the weaker user's queue by deadline T_1 as

$$D_2(T_1, P_c) = \sum_{i=1}^{K(T_1)+1} \frac{1}{2}\log_2\left(1 + \frac{[P_i - P_c]^+}{P_c + \sigma^2}\right)\ell_i \tag{7.22}$$

$D_2(T_1, P_c)$ is monotonically decreasing with P_c for fixed T_1. In fact, $D_2(T_1, P_c)$ takes its maximum value at $P_c = 0$ and as P_c is increased, the achievable bit departure pairs travel on the boundary of $\mathcal{D}(T_1)$ from one extreme to the other.

We divide the bit departure plane into 5 regions as shown in Figure 7.6. The regions are bordered by the constant B_1, B_2 lines and the $\mathcal{D}(T_{min})$ curve. Region ① is $D_1 \leq B_1$ and $D_2 \leq B_2$. Regions ② and ③ combined represent the north-west part, i.e., $D_1 \leq B_1$ and $D_2 \geq B_2$. The border between regions 2 and 3 is the $\mathcal{D}(T_{min})$ curve. Region ⑤ is bordered by the constant B_1 line and the $\mathcal{D}(T_{min})$ curve. The rest of the first quadrant is region ④. We start the problem with the knowledge of

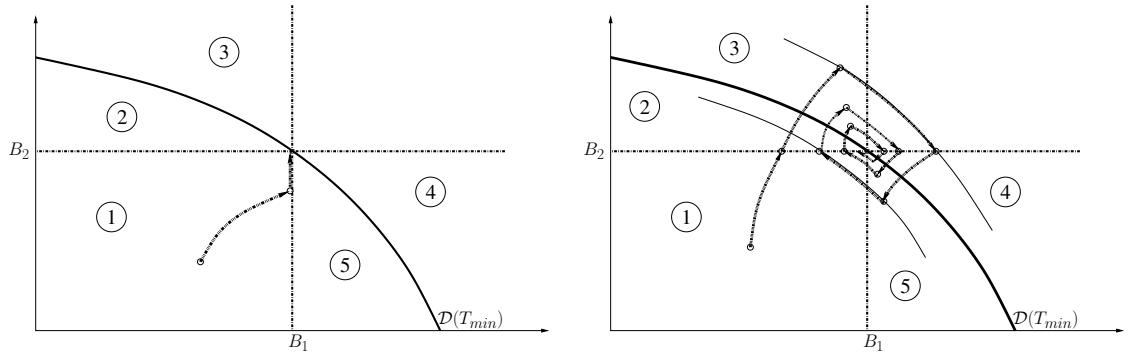

(a) If the algorithm starts in region ① and hits $D_1(T_1, P_c) = B_1$, then the trajectory does not deviate from the constant B_1 line.

(b) If $D_1(T_1, P_c) < B_1$ and $D_2(T_1, P_c) = B_2$ is achieved, then a bisection algorithm converges to the desired (B_1, B_2) point yielding the minimum T.

Figure 7.6: The possible trajectories followed during the operation of the algorithm.

(B_1, B_2). While we know that (B_1, B_2) must lie on the boundary of $\mathcal{D}(T_{min})$, we do not know $\mathcal{D}(T_{min})$ or T_{min}. We want to find T_{min} and the policy that achieves it.

After the initial step, we have $D_1(T_1, P_c) \leq B_1$ since $P_i < P_c$ may occur in some epochs. Hence, the initial operating point lies in one of regions ①, ②, ③. If the operating point lies in the interior of region ①, it implies that (B_1, B_2) transmission cannot be completed by T_1. Therefore, we decrease P_c, obtain $T_1 = \frac{B_1}{\frac{1}{2}\log_2(1+P_c)}$, and repeat the procedure, until we leave this region. If the operating point hits the B_1 line, i.e., $D_1\left(\frac{B_1}{\frac{1}{2}\log_2(1+P_c)}, P_c\right) = B_1$, while $D_2\left(\frac{B_1}{\frac{1}{2}\log_2(1+P_c)}, P_c\right) < B_2$, as shown in Figure 7.6(a), then $P_c < P_i$ for all epochs i. Even if we further decrease P_c to increase D_2, we always have $D_1\left(\frac{B_1}{\frac{1}{2}\log_2(1+P_c)}, P_c\right) = B_1$ in view of the update rule of T_1 as $T_1 = \frac{B_1}{\frac{1}{2}\log_2(1+P_c)}$. Hence, similar to the algorithm for the unlimited battery case in [24], we apply bisection only on P_c and approach $D_2\left(\frac{B_1}{\frac{1}{2}\log_2(1+P_c)}, P_c\right) = B_2$ sufficiently. For the final value of P_c, $T_{min} = \frac{B_1}{\frac{1}{2}\log_2(1+P_c)}$.

Then, we consider the scenario when the operating point enters into region

② or ③, i.e., $D_2\left(\frac{B_1}{\frac{1}{2}\log_2(1+P_c)}, P_c\right) > B_2$ while $D_1\left(\frac{B_1}{\frac{1}{2}\log_2(1+P_c)}, P_c\right) \leq B_1$. For this scenario, we fix T_1 and increase P_c such that $D_2(T_1, P_c) = B_2$. This brings us to the horizontal B_2 line, as shown in Figure 7.6(b). Depending on the updated D_1 under this policy, the operating point lies either on the left or on the right of the (B_1, B_2) point. If we end up at $D_1(T_1, P_c) < B_1$, then $T_1 < T_{min}$. We decrease P_c, and set $T_1 = \frac{B_1}{\frac{1}{2}\log(1+P_c)}$. Another round of directional water-filing results $D_2 > B_2$, and brings the operating point back into region ② and ③. If we end up at $D_1(T_1, P_c) > B_1$, it implies $T_1 > T_{min}$. Then, we fix P_c and decrease T_1 only. By doing this, we decrease D_1 and D_2 at the same time and this brings the operating point back to the horizontal B_2 line, which in turn brings us back to one of the previously considered cases depending on whether $D_1(T_1, P_c)$ is greater or smaller than B_1.

For all of the above cases, we carefully control the step size when we do the adjustment of P_c and T_1, to make sure that the operating point gets closer to the (B_1, B_2) point at each step. In particular, we update T and P_c using a bisection method. Starting with arbitrary step sizes, we halve the step size each time the update sign is changed, i.e., if an increase is required while previous update was a decrease, then step size is halved. Convergence is guaranteed due to monotonicity and continuity of $D_1(T_1, P_c)$ and $D_2(T_1, P_c)$ [103].

The algorithm naturally generalizes for an M-user broadcast channel. Initially, we suppose that the transmitter transmits only to user 1 with an arbitrary P_{c1} and find the transmission completion time for the strongest user by $T_1 = \frac{B_1}{\frac{1}{2}\log_2(1+P_{c1})}$. For

this fixed T_1, we run the directional water-filling algorithm and find the total power allocation $P_1, P_2, \ldots, P_{K(T_1)+1}$ with the deadline T_1. The number of bits transmitted to user 1 is $D_1(T_1, P_{c1})$. We allocate the remaining power $[P_i - P_{c1}]^+$ to the second user and calculate the total bits departed from the second user's queue by deadline T_1, $D_2(T_1, P_{c1})$, as in (7.22). If $D_2(T_1, P_{c1}) > B_2$, then B_2 bits can be served for user 2. We find the corresponding cut-off power level P_{c2}. We continue finding the remaining cut-off power levels P_{cm} until some power level becomes infeasible, i.e., some user cannot be served by T_1. In this case, we decrease P_{c1} and recalculate T_1. Otherwise, $(B_2, \ldots, B_M)$ bits can be served by T_1. In this case, we fix T_1 and increase P_{c1}. We apply the bisection method and update the step sizes according to whether an increase or decrease is required and whether previous update was an increase or a decrease. The convergence is again guaranteed due to the monotonicity and continuity of the number of bits served for each user [103].

7.5 Numerical Results

We consider a band-limited AWGN broadcast channel with $M = 3$ users. The bandwidth is $B_W = 1$ MHz and the noise power spectral density is $N_0 = 10^{-19}$ W/Hz. We assume that the path losses between the transmitter and the receivers

are 100 dB, 105 dB and 110 dB.

$$r_1 = B_W \log_2\left(1 + \frac{\alpha_1 P h_1}{N_0 B_W}\right)$$
$$= \log_2\left(1 + \frac{\alpha_1 P}{10^{-3}}\right) \text{Mbps} \tag{7.23}$$
$$r_2 = B_W \log_2\left(1 + \frac{\alpha_2 P h_2}{\alpha_1 P h_2 + N_0 B_W}\right)$$
$$= \log_2\left(1 + \frac{\alpha_2 P}{\alpha_1 P + 10^{-2.5}}\right) \text{Mbps} \tag{7.24}$$
$$r_3 = B_W \log_2\left(1 + \frac{(1-\alpha_1-\alpha_2) P h_3}{(\alpha_1+\alpha_2) P h_3 + N_0 B_W}\right)$$
$$= \log_2\left(1 + \frac{(1-\alpha_1-\alpha_2) P}{(\alpha_1+\alpha_2) P + 10^{-2}}\right) \text{Mbps} \tag{7.25}$$

7.5.1 Deterministic Energy Arrivals

In this subsection, we illustrate the optimal offline policy in a deterministic energy arrival sequence setting. In particular, we assume that at times $\mathbf{t} = [0, 2, 5, 8, 9, 12]$ s, energies with the amounts $\mathbf{E} = [8, 3, 6, 9, 8, 9]$ mJ are harvested. The battery capacity is $E_{max} = 10$ mJ.

We first study the two-user broadcast channel by removing the third user, i.e., setting $B_3 = 0$. We find the maximum departure region of the two-user broadcast channel $\mathcal{D}(T)$ for $T = 10, 12, 13, 14, 16$ s, and plot them in Figure 7.7. These regions are obtained by first finding the total power sequence and then varying the cut-off power level P_c. In particular, $P_c = 0$ implies all the power is allocated to user 2 while $P_c = \max_i P_i$ implies that all the power is allocated to user 1. Note that the maximum departure regions are strictly convex for all T and monotone in T. We

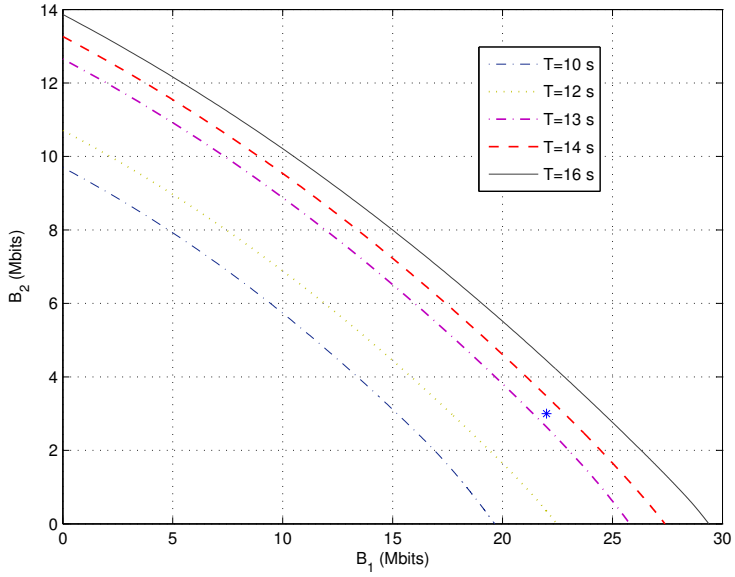

Figure 7.7: The maximum departure region $\mathcal{D}(T)$ for different T.

observe that the gap between the regions for different T increases in the passage from $T = 12$ s to $T = 13$ s since an energy arrival occurs at $t = 12$ s.

We next consider the same energy arrival sequence with $(B_1, B_2) = (22, 3)$ Mbits. We have the optimal transmission policy as shown in Figure 7.8. In this example, optimal transmit rates are $\mathbf{r}_1 = [1.6438, 1.6554, 1.6554, 1.6554]$ Mbps and $\mathbf{r}_2 = [0, 0.9358, 0.2827, 0.8877]$ Mbps, with durations $\mathbf{l} = [8, 1, 3, 1.35]$ s. Initial energy in the battery and the first two energy arrivals are spread till $t = 8$ s. However, only 2 mJ energy can flow from the time interval $[8, 9]$ to $[9, 12]$ as $E_{max} = 10$ mJ constrains the energy flow. This, in turn, breaks the monotonicity in the total transmit power. In the optimal policy, $P_c = 2.15$ mW is found, while in the first three epochs the transmit power is allocated as 2.125 mW. Therefore, only the stronger user's data is transmitted in the first three epochs. In the remaining

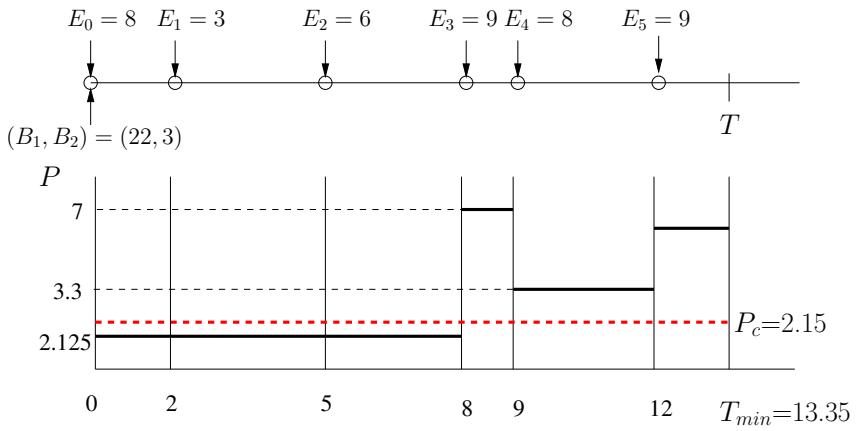

Figure 7.8: Illustration of the optimal policy for $M = 2$.

epochs, both users' data are transmitted simultaneously with transmit power $P_4 = 7$ mW in $[8, 9]$ s, $P_5 = 3.33$ mW in $[9, 12]$ s and $P_6 = 6.66$ mW in $[12, 13.35]$ s. Note that $(22, 3)$ Mbits point (marked with *) in Figure 7.7 is not included in $\mathcal{D}(T)$ at $T = 13$ s while it is strictly included in $\mathcal{D}(T)$ at $T = 14$ s.

Finally, we consider the same energy arrival sequence with $(B_1, B_2, B_3) = (15, 4, 1.75)$ Mbits and the optimal policy is shown in Figure 7.9. In this example, optimal cut-off power levels are $P_{c1} = 0.97$ mW and $P_{c2} = 1.79$ mW; and optimal transmit rates are $\mathbf{r}_1 = [0.9783, 0.9783, 0.9783]$ Mbps, $\mathbf{r}_2 = [0.2610, 0.2610, 0.2610]$ Mbps and $\mathbf{r}_3 = [0.0404, 0.5280, 0.1409]$ Mbps with durations $\mathbf{l} = [8, 1, 6.33]$ s. In the optimal total power sequence, 2 mJ energy is transferred from $[8, 9]$ s to [9,12] s and about 1 mJ of this transferred energy is further transferred to the last epoch. We calculate the cut-off power levels as $P_{c1} = 0.97$ mW and $P_{c2} = 1.79$ mW. The bits of all three users are always transmitted throughout the communication. The transmission is finished by $T = 15.33$ s.

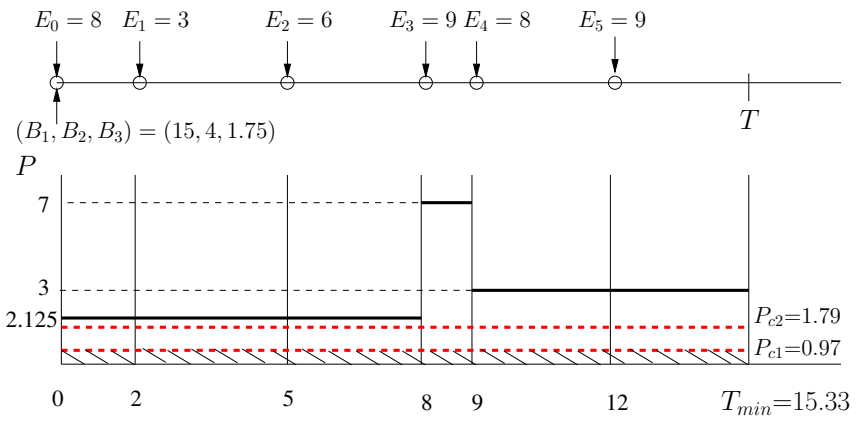

Figure 7.9: Illustration of the optimal policy for $M = 3$.

7.5.2 Stochastic Energy Arrivals

In this subsection, we consider stochastic energy arrivals in the two-user case, i.e., we set $B_3 = 0$. We compare the performance of the optimal offline policy with those of three suboptimal policies which require no offline knowledge of the energy arrivals.

- **Constant Power Constant Share (CPCS) Policy**

  This policy transmits with constant power equal to the average recharge rate, $P = \mathbb{E}[E]$, whenever the battery energy is non-zero and the transmitter is silent otherwise. If the battery energy exceeds E_{max} at the energy arrival instants, then excess energy overflows. In addition, the strong user's power share is constant whenever the transmitter is non-silent. In particular, the constant power share α^* is found from:

$$\frac{B_1}{B_2} = \frac{\log_2\left(1 + \frac{\alpha\mathbb{E}[E]}{\sigma_1^2}\right)}{\log_2\left(1 + \frac{(1-\alpha)\mathbb{E}[E]}{\alpha\mathbb{E}[E]+\sigma_2^2}\right)} \tag{7.26}$$

Note that CPCS does not require offline or online knowledge of the energy arrivals. It only requires the mean of the energy arrival process, $\mathbb{E}[E]$.

- **Energy Adaptive Power Constant Share (EACS) Policy**

  This policy transmits with power equal to the instantaneous energy value at each energy arrival instant, $P_i = E_{current}$. If the battery energy exceeds E_{max} at the energy arrival instants, then excess energy overflows. Moreover, the power share of the stronger user is set constant equal to that found in (7.26) throughout the duration in which the transmitter is not silent and both users' data queues are non-empty. Whenever one data queue becomes empty, no power is allocated for that user.

- **Energy Adaptive Power Dynamic Share (EADS) Policy**

  This policy transmits with power equal to the instantaneous energy value at each energy arrival instant, $P_i = E_{current}$. If the battery energy exceeds E_{max} at the energy arrival instants, then excess energy overflows. The strong user's power share α_i^* is updated dynamically whenever an energy arrival occurs according to:

$$\frac{B_{1i}}{B_{2i}} = \frac{\log_2\left(1+\frac{\alpha_i P_i}{\sigma_1^2}\right)}{\log_2\left(1+\frac{(1-\alpha_i)P_i}{\alpha_i P_i+\sigma_2^2}\right)} \tag{7.27}$$

  where B_{1i} and B_{2i} are the number of bits of user 1 and user 2, respectively, at the beginning of epoch i. Note that EADS requires online knowledge of the energy arrival process as well as the remaining data backlog.

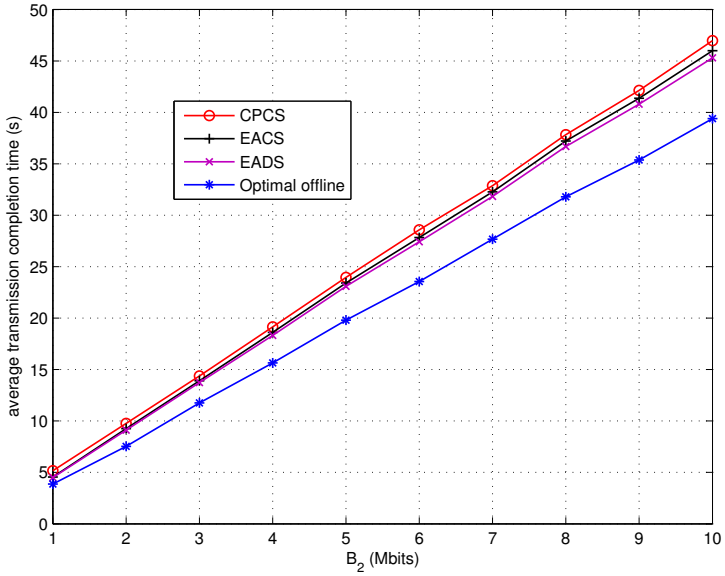

Figure 7.10: Average transmission completion time versus B_2 when $\rho = 1.6$, $P_{avg} = 1$ mJ/s and $E_{max} = 4$ mJ.

In the simulations, we consider a compound Poisson energy arrival process. The average inter-arrival time is 1 s and the arriving energy is a random variable which is distributed uniformly in $[0, 2P_{avg}]$ mJ, where $P_{avg} \leq \frac{E_{max}}{2}$ is the average recharge rate. The performance metric of the policies is the average transmission completion time over 1000 realizations of the stochastic energy arrival process. We first set the $\rho = \frac{B_1}{B_2}$ ratio constant, i.e., $B_1 = \rho B_2$. We plot the performances for $E_{max} = 4$ mJ, $\rho = 1.6$ and $P_{avg} = 1$ mJ/s with varying B_2 in Figure 7.10. We observe the increase in the average transmission completion times of the policies with the number of bits. It is notable that energy adaptive policies complete the transmission faster with respect to CPCS policy. We also observe that EADS yields smaller transmission completion time on average compared to EACS; therefore, dynamically varying the power shares of the users yields better performance compared to keeping

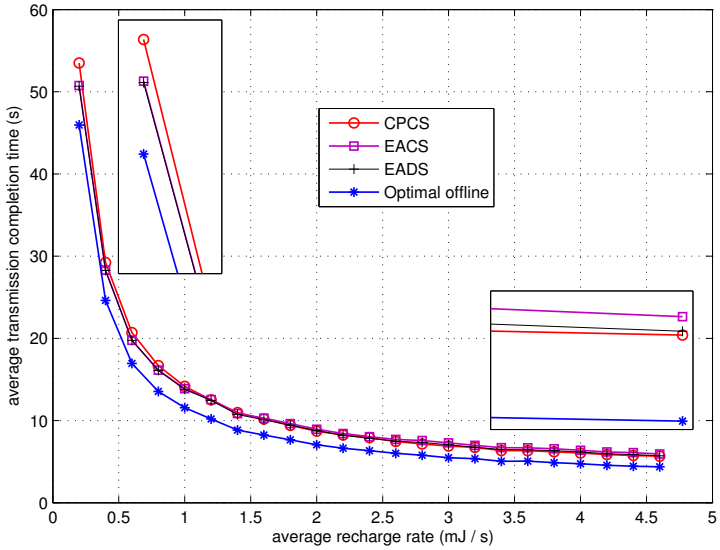

Figure 7.11: Average transmission completion time versus average recharge rate when $B_1 = 8$ Mbits, $B_2 = 5$ Mbits and $E_{max} = 10$ mJ.

the power shares constant. Next, we plot the average transmission completion time with respect to the average recharge rate for $B_1 = 8$ Mbits, $B_2 = 5$ Mbits and $E_{max} = 10$ mJ in Figure 7.11. We observe that in the small recharge rate regime, CPCS performs worse while it performs better in the high recharge rate regime compared to energy adaptive schemes. In both plots, we observe that offline knowledge of the energy arrivals yields a significant performance gain with respect to the other policies.

7.6 Conclusion

In this chapter, we considered the transmission completion time minimization problem in an M-user broadcast channel where the transmitter harvests energy from nature and saves it in a battery of finite capacity. We characterized the structural

properties of the optimal policy by means of the dual problem of maximizing the weighted sum of bits served for each user by a fixed deadline. We found that the total power allocation is the same as the single user power allocation, which is found by the directional water-filling algorithm. Moreover, there exist $M-1$ cut-off power levels that determine the power shares of the users throughout the transmission. This structure enabled us to develop an optimal offline algorithm which uses directional water-filling iteratively.

7.7 Appendix

7.7.1 Proof of Lemma 7.1

Assume that (B_1, B_2) and (B_1', B_2') are two points that can be achieved by some policies $\{(r_{1i}, r_{2i})\}_{i=1}^{K+1}$ and $\{(r_{1i}', r_{2i}')\}_{i=1}^{K+1}$, respectively, that satisfy the energy causality constraint in (7.9) and the no-energy-overflow constraint in (7.10) such that

$$(B_1, B_2) = \Big(\sum_{i=1}^{K+1} r_{1i}\ell_i, \sum_{i=1}^{K+1} r_{2i}\ell_i \Big) \tag{7.28}$$

$$(B_1', B_2') = \Big(\sum_{i=1}^{K+1} r_{1i}'\ell_i, \sum_{i=1}^{K+1} r_{2i}'\ell_i \Big) \tag{7.29}$$

We will show that there exists a policy that achieves $(\lambda B_1 + \bar{\lambda} B_1', \lambda B_2 + \bar{\lambda} B_2')$ where $\bar{\lambda} = 1 - \lambda$.

It is well-known that minimum power necessary to achieve the rate pairs (r_1, r_2)

in the AWGN channel is (see e.g. [24]):

$$P = 2^{2(r_1+r_2)} + (\sigma^2 - 1)2^{2r_2} - \sigma^2 \tag{7.30}$$

$$\triangleq g(r_1, r_2) \tag{7.31}$$

By the convexity of $g(r_1, r_2)$ in (7.31), we have

$$g(\lambda r_1 + \bar{\lambda} r_1', \lambda r_2 + \bar{\lambda} r_2') \leq \lambda g(r_1, r_2) + \bar{\lambda} g(r_1', r_2') \tag{7.32}$$

Hence, transmission of convex combination of (B_1, B_2) and (B_1', B_2') requires less energy than the convex combination of the energies required to transmit them separately. Therefore, the rate allocation $\{\lambda r_{1i} + \bar{\lambda} r_{1i}', \lambda r_{2i} + \bar{\lambda} r_{2i}'\}_{i=1}^{K+1}$ may not satisfy the no-energy-overflow constraints in (7.10), though, it achieves $(\lambda B_1 + \bar{\lambda} B_1', \lambda B_2 + \bar{\lambda} B_2')$ in the $[0, T]$ interval. If this is the case, we can always increase the energy consumption so that we get a new policy that achieves the desired point while satisfying the no-energy-overflow and causality constraints. Let us define the new policy $\{(r_{1i}'', r_{2i}'')\}$ as $r_{1i}'' \geq \lambda r_{1i} + \bar{\lambda} r_{1i}'$ and $r_{2i}'' \geq \lambda r_{2i} + \bar{\lambda} r_{2i}'$ for all i so that we have

$$g(r_{1i}'', r_{2i}'') = \lambda g(r_{1i}, r_{2i}) + \bar{\lambda} g(r_{1i}', r_{2i}') \tag{7.33}$$

Since $g(r_1, r_2)$ is strictly monotone and continuous in r_1, r_2, one can always find $\{r_{1i}'', r_{2i}''\}_{i=1}^{K+1}$ as desired.

Clearly $\{(r_{1i}'', r_{2i}'')\}$ satisfies the energy causality and no-energy-overflow condi-

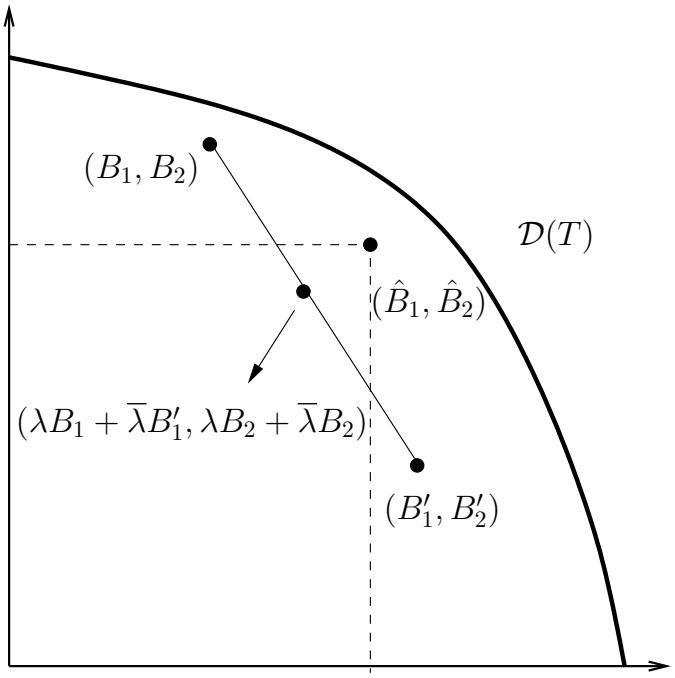

Figure 7.12: The maximum departure region $\mathcal{D}(T)$ is a convex region.

tions and the resulting operating point $(\hat{B}_1, \hat{B}_2)$ is such that

$$\hat{B}_1 \geq \lambda B_1 + \overline{\lambda} B_1' \tag{7.34}$$

$$\hat{B}_2 \geq \lambda B_2 + \overline{\lambda} B_2' \tag{7.35}$$

Hence, any convex combination of (B_1, B_2) and (B_1', B_2') can be achieved by some policy that obeys energy causality and no-energy-overflow constraints. This proves the convexity of $\mathcal{D}(T)$. We illustrate the main steps of this proof in Figure 7.12.

7.7.2 Proof of Lemma 7.2

For $M = 2$ and given P_i, the problem in (7.13) is a single-variable optimization problem and it has a unique solution α_i^*. We define a function $\alpha^*(P) : \mathbf{R}^+ \to [0, 1]$

which denotes the solution of the problem in (7.13) for $P_i = P$. Using the derivative of the objective function in (7.13) with respect to α for fixed P, we obtain $\alpha^*(P)$ as follows: If $\frac{\mu_2}{\mu_1} \leq 1$ then $\alpha^*(P) = 1$ for all P. If $\frac{\mu_2}{\mu_1} \geq \frac{\sigma_2^2}{\sigma_1^2}$, then $\alpha^*(P) = 0$ for all P. For $1 < \frac{\mu_2}{\mu_1} < \frac{\sigma_2^2}{\sigma_1^2}$, we have

$$\alpha^*(P) = \begin{cases} 1, & 0 \leq P \leq \frac{\mu_1\sigma_2^2 - \mu_2\sigma_1^2}{\mu_2 - \mu_1} \\ \frac{1}{P}\frac{\mu_1\sigma^2 - \mu_2\sigma_1^2}{\mu_2 - \mu_1}, & P \geq \frac{\mu_1\sigma_2^2 - \mu_2\sigma_1^2}{\mu_2 - \mu_1} \end{cases} \tag{7.36}$$

In the extreme cases, the lemma trivially holds. When $\frac{\mu_2}{\mu_1} < 1$, we have $\alpha^*(P) = 1$ and when $\frac{\mu_2}{\mu_1} > \frac{\sigma_2^2}{\sigma_1^2}$, we have $\alpha^*(P) = 0$ for all P. Consequently, in these extreme cases, all the power is allocated for either user 1 or user 2 and no data is transmitted for the other user. As the single user rate-power relation is logarithmic, which is strictly concave, the lemma holds.

Now, we consider the range $1 < \frac{\mu_2}{\mu_1} < \frac{\sigma_2^2}{\sigma_1^2}$. From (7.36), for $0 \leq P \leq \frac{\mu_1\sigma_2^2 - \mu_2\sigma_1^2}{\mu_2 - \mu_1}$, we have

$$f(P) = \frac{\mu_1}{2}\log_2\left(1 + \frac{P}{\sigma_1^2}\right) \tag{7.37}$$

Therefore, $f(P)$ is strictly concave in this range with the strict monotone decreasing derivative

$$\frac{df(P)}{dP} = \frac{\mu_1}{2\ln(2)(\sigma_1^2 + P)}, \quad 0 \leq P \leq \frac{\mu_1\sigma_2^2 - \mu_2\sigma_1^2}{\mu_2 - \mu_1} \tag{7.38}$$

Using the expression of $\alpha^*(P)$ for the range $P \geq \frac{\mu_1\sigma_2^2 - \mu_2\sigma_1^2}{\mu_2 - \mu_1}$, $f(P)$ in this range

becomes

$$f(P) = \frac{\mu_1}{2}\log_2\left(\frac{\mu_1(\sigma_2^2-\sigma_1^2)}{\sigma_1^2(\mu_2-\mu_1)}\right) + \frac{\mu_2}{2}\log_2\left(\frac{\mu_2-\mu_1}{\mu_2(\sigma_2^2-\sigma_1^2)}(P+\sigma_2^2)\right) \tag{7.39}$$

$f(P)$ is strictly concave in this range, as well. The derivative in this range is

$$\frac{df(P)}{dP} = \frac{\mu_2}{2\ln(2)(P+\sigma_2^2)}, \quad P \geq \frac{\mu_1\sigma_2^2-\mu_2\sigma_1^2}{\mu_2-\mu_1} \tag{7.40}$$

Note that $\frac{df(P)}{dP}$ in different ranges in (7.38) and (7.40) are continuous and monotone decreasing. Evaluating the derivatives in (7.38) and (7.40) at $P = \frac{\mu_1\sigma_2^2-\mu_2\sigma_1^2}{\mu_2-\mu_1}$, we observe that $\frac{df(P)}{dP}$ is continuous at this point and for all P. Therefore, $f(P)$ is strictly concave for all P and its derivative is continuous everywhere in the non-negative real line for any $\mu_1, \mu_2 \geq 0$.

For the general M-user case, whenever $\mu_j \leq \mu_l$ for any $1 \leq l < j \leq M$, i.e., whenever a degraded user has a smaller coefficient, that user is allocated no power for any value of P, i.e., $\alpha_j^* = 0$ for such users. Note that for $1 \leq l < j \leq M$, if user l achieves R_l and user j achieves R_j, then user l can achieve $R_l + R_j$ [54]. Since $\mu_j < \mu_l$, we have $\mu_l R_l + \mu_j R_j < \mu_l(R_l + R_j)$, i.e., allocating all available rate to user l yields a larger weighted sum of rates. Hence, we remove user j whenever $\mu_j \leq \mu_l$ for any $1 \leq l < j \leq M$. The remaining $R \leq M$ users are such that $\sigma_1^2 \leq \sigma_2^2 \leq \ldots \leq \sigma_R^2$ with $\mu_1 < \mu_2 < \ldots < \mu_R$. One can show using a first order differential analysis (see

also [24]) that for given P, $f(P) = \mu_1 r_1^*(P) + \ldots + \mu_M r_M^*(P)$ where

$$r_1^*(P) = \frac{1}{2}\log\left(1 + \frac{\min\{P, P_{c1}\}}{\sigma_1^2}\right) \tag{7.41}$$

$$r_2^*(P) = \frac{1}{2}\log\left(1 + \frac{\min\{(P - P_{c1})^+, P_{c2} - P_{c1}\}}{P_{c1} + \sigma_2^2}\right) \tag{7.42}$$

$$\vdots$$

$$r_R^*(P) = \frac{1}{2}\log\left(1 + \frac{(P - P_{c(R-1)})^+}{P_{c(R-1)} + \sigma_R^2}\right) \tag{7.43}$$

and where the cut-off power levels satisfy [24, Appendix B]

$$P_{cm} = \max\left\{\left(\frac{\mu_m\sigma_{\bar{m}}^2 - \mu_{\bar{m}}\sigma_m^2}{\mu_{\bar{m}} - \mu_m}\right)^+, P_{c(m-1)}\right\} \tag{7.44}$$

for $m = 1, \ldots, R-1$ and $\bar{m}$ is the smallest user index with $P_{c\bar{m}} > P_{cm}$. By convention, $P_{c0} = 0$, $P_{cR} = \infty$. Note that $P_{c0} \le P_{c1} \le \ldots \le P_{c(R-1)} \le P_{cR}$. As $r_m(P)$ is continuous and differentiable, so is $f(P)$. Taking the first derivative of $f(P)$ with respect to P, we have

$$\frac{df(P)}{dP} = \begin{cases} \frac{\mu_1}{2\ln(2)(P+\sigma_1^2)}, & P \le P_{c1} \\ \frac{\mu_2}{2\ln(2)(P+\sigma_2^2)}, & P_{c1} < P \le P_{c2} \\ \quad\vdots & \quad\vdots \\ \frac{\mu_R}{2\ln(2)(P+\sigma_R^2)}, & P_{c(R-1)} < P \end{cases} \tag{7.45}$$

As in the two-user case, we observe that $\frac{df(P)}{dP}$ is continuous and monotone decreasing in each disjoint interval $(P_{c(m-1)}, P_{cm})$. Evaluating $\frac{df(P)}{dP}$ in (7.45) at $P = P_{cm}$, and

using the expression for P_{cm} in (7.44), we observe that $\frac{df(P)}{dP}$ is continuous at these points and hence for all P, and $\frac{df(P)}{dP}$ is monotone decreasing. Consequently, $f(P)$ is strictly concave for all P, for any $\mu_1, \ldots, \mu_M \geq 0$.

7.7.3 Proof of Lemma 7.3

We write the Lagrangian function as:

$$\begin{aligned}\mathcal{L} = &\sum_{i=1}^{K+1} f(P_i)\ell_i - \sum_{k=1}^{K+1} \lambda_k \left(\sum_{i=1}^{k} P_i \ell_i - \sum_{i=0}^{k-1} E_i \right) \\ &- \sum_{k=1}^{K} \eta_k \left(\left(\sum_{i=0}^{k} E_i - E_{max} \right)^+ - \sum_{i=1}^{k} P_i \ell_i \right)\end{aligned} \tag{7.46}$$

Note that $P_i > 0$, for all i, therefore in the Lagrangian we do not include slackness variables for P_i. Taking the derivatives of $\mathcal{L}$ in (7.46) with respect to P_i, and setting them to zero, we have

$$\frac{df(P_i)}{dP_i} = \sum_{k=i}^{K+1} \lambda_k - \sum_{k=i}^{K} \eta_k, \qquad i = 1, \ldots, K+1 \tag{7.47}$$

Additional complimentary slackness conditions are

$$\lambda_k \left(\sum_{i=1}^{k} P_i \ell_i - \sum_{i=0}^{k-1} E_i \right) = 0, \quad k = 1, \ldots, K \tag{7.48}$$

$$\eta_k \left(\left(\sum_{i=0}^{k} E_i - E_{max} \right)^+ - \sum_{i=1}^{k} P_i \ell_i \right) = 0, \quad k = 1, \ldots, K \tag{7.49}$$

The optimal total power sequence P_i^* is the solution of (7.47) with the complimentary slackness conditions in (7.48), (7.49) and with the equality condition that no energy is left unused in the battery at time T. The Lagrangian multipliers λ_k and η_k are unique as the objective function in (7.15) is strictly concave and the constraint set is convex.

From the KKT optimality conditions in (7.47), we have

$$P_i = \left(\frac{df}{dP_i}\right)^{-1} \left(\sum_{k=i}^{K+1} \lambda_k - \sum_{k=i}^{K} \eta_k\right) \tag{7.50}$$

Since the derivative of $\frac{df}{dP}$ is strictly monotonically decreasing and continuous by Lemma 7.2, it has a well-defined inverse, which is also strictly monotonically decreasing and continuous. The Lagrange multipliers λ_i and η_i are uniquely determined by the complimentary slackness conditions as well as the following equality condition: $\sum_{i=1}^{K+1} P_i \ell_i = \sum_{i=0}^{K} E_i$. Therefore, the optimum total power allocation is unique.

We have $\lambda_i = 0$ and $\eta_i = 0$, if the energy causality constraint and the no-energy-overflow constraint are satisfied with strict inequality, respectively. Whenever a no-energy-overflow constraint is satisfied with equality, i.e., $\eta_i > 0$, a strict decrease in P_i^* is observed in view of (7.50). This is due to the fact that the inverse mapping of the derivative is monotonically decreasing and the argument of the inverse in (7.50) is also decreasing. Similarly, whenever an energy causality constraint is satisfied with equality, i.e., $\lambda_i > 0$, a strict increase in P_i^* is observed in view of (7.50). Thus, equality of energy causality constraints leads to an increase

while that of no-energy-overflow constraint leads to a decrease in the total power. Imposing the energy constraint at time T as an equality, we get exactly the optimal power allocation policy in the single user E_{max} constrained average throughput maximization problem in [23, 39], i.e., in the special case of $\mu_1 > 0$ and $\mu_m = 0$, for $m = 2, \ldots, M$. Moreover, this characterization is the same for any $\mu_1, \ldots, \mu_M \geq 0$ because the strict concavity of $f(P)$ in Lemma 7.2 holds for any $\mu_1, \ldots, \mu_M \geq 0$.

Chapter 8

Scheduling over Parallel and Fading Gaussian Broadcast Channels with an Energy Harvesting Transmitter

8.1 Introduction

In this chapter, we extend the offline optimal scheduling in energy harvesting communication systems to the parallel and fading broadcast channels as shown in Figures 8.1 and 8.2. Data for the two receivers are backlogged at the transmitter buffers while arriving energy is stored in a finite-capacity battery. Service is provided to the data buffers with the cost of energy depletion from the energy buffer, i.e., the battery. As the users utilize the common resources, which are the harvested energy and the wireless communication medium, there is a trade-off between the performances of the users. In Chapter 7, we characterize this trade-off by obtaining the maximum departure region by a deadline T and determine the optimal offline policies that achieve the boundary of the maximum departure region. In both scenarios, the transmitter has to adapt its transmission power with respect to the available energy and also avoid possible energy overflows due to the finite-capacity battery.

We first consider offline scheduling for energy harvesting transmitters over parallel broadcast channels. In this case, the time sequence of the power allocation and the splitting to two users are simultaneously determined for each parallel channel.

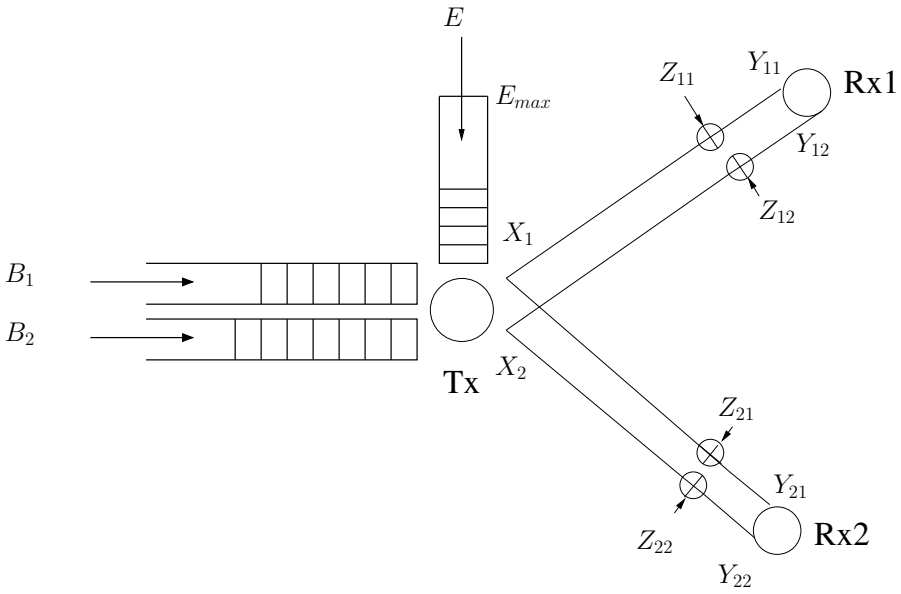

Figure 8.1: The two-user parallel broadcast channel with energy harvesting transmitter.

We show that the optimal total transmit power policy that achieves the boundary of the maximum departure region is the same as the optimal policy for the non-fading scalar broadcast channel, which does not depend on the priorities of the users, and therefore is the same as the optimal policy for the non-fading scalar single user channel. The optimal policy is found by the directional water-filling algorithm in Chapter 6.

Next, we consider offline scheduling for energy harvesting transmitters over fading broadcast channels. As the fading levels and strength order of the users vary throughout the communication, the power allocation is determined according to the joint fading variations of the users. We show that in the optimal policy that achieves the boundary of the maximum departure region, energy allocation in each epoch is determined by a directional water-filling algorithm that is specific to the

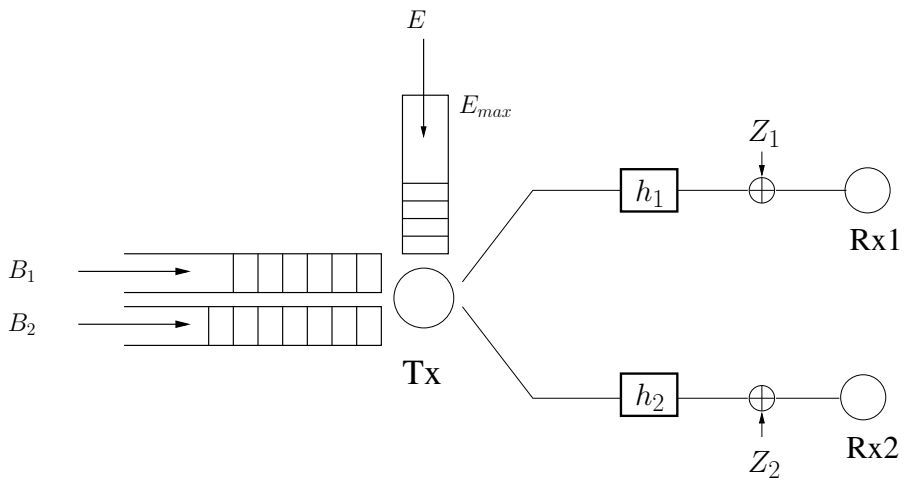

Figure 8.2: The energy harvesting transmitter in a fading broadcast channel.

fading broadcast channel (c.f. Chapter 6). In particular, water level in between two energy arrivals is calculated by using the water-filling scheme described in [48] or the greedy power allocation in [49]. If the water level is higher on the right, no energy is transferred; otherwise some energy is transferred to the future. Unlike the case of parallel broadcast channels, in the case of fading broadcast channels, the total transmit power policies achieving different points on the boundary of the maximum departure region depend on the priorities of the users. Finally, we numerically examine the resulting maximum departure regions for parallel and fading broadcast channels in a deterministic setting.

8.2 The Channel and Energy Models

We consider two different channel models, namely parallel broadcast channels and fading broadcast channels. Although the treatment of these two channel models in traditional systems with non-rechargeable batteries subject to average power con-

straints are equivalent [48, 49], the extra dimension created due to the battery energy variations at the transmitter leads to significant differences between these two channel models in the context of offline broadcast scheduling. In the following, we provide the details of these two channel models as well as the energy model.

8.2.1 The Parallel Broadcast Channel Model

In a two-user parallel broadcast channel, one transmitter sends data to two receivers over independent parallel channels. The model is depicted in Figure 8.1. We consider the case where there are two parallel channels only. The generalization to more than two parallel channels is straightforward, and left out for brevity and clarity of presentation.

The received signals at the two receivers are

$$Y_{1i} = X_i + Z_{1i}, \qquad i = 1, 2 \tag{8.1}$$

$$Y_{2i} = X_i + Z_{2i}, \qquad i = 1, 2 \tag{8.2}$$

where X_i is the signal transmitted in the ith parallel channel, and Z_{1i} and Z_{2i} are Gaussian noises with variances σ_{1i}^2 and σ_{2i}^2, respectively. If $\sigma_{1i}^2 \leq \sigma_{2i}^2$ for all i, or $\sigma_{2i}^2 \leq \sigma_{1i}^2$ for all i, then the overall channel is degraded in favor of user 1 or user 2, respectively, and hence the problem reduces to the scheduling problem over a scalar non-fading broadcast channel as in Chapter 7. Therefore, we consider the case $\sigma_{11}^2 < \sigma_{21}^2$ and $\sigma_{12}^2 > \sigma_{22}^2$ where the overall broadcast channel is not degraded.

Assuming that the transmitter transmits with power P, the achievable rate

region for this two-user parallel broadcast channel is [49, 54]

$$R_1 \leq \frac{1}{2}\log_2\left(1+\frac{\alpha_1\beta P}{\sigma_{11}^2}\right)+\frac{1}{2}\log_2\left(1+\frac{\alpha_2(1-\beta)P}{(1-\alpha_2)(1-\beta)P+\sigma_{12}^2}\right) \tag{8.3}$$

$$R_2 \leq \frac{1}{2}\log_2\left(1+\frac{(1-\alpha_2)(1-\beta)P}{\sigma_{22}^2}\right)+\frac{1}{2}\log_2\left(1+\frac{(1-\alpha_1)\beta P}{\alpha_1\beta P+\sigma_{21}^2}\right) \tag{8.4}$$

where βP is the power allocated to the first parallel channel, and $(1-\beta)P$ is the power allocated to the second parallel channel, α_1 and α_2 are the fractions of powers spent for the message transmitted to user 1 in each parallel channel. Note that even though the overall channel is not degraded, there is no constraint on the sum rate in the expressions that define the capacity region in (8.3)-(8.4) since individual channels are degraded. By varying $\alpha_1 \in [0,1]$, $\alpha_2 \in [0,1]$ and $\beta \in [0,1]$, we obtain a family of achievable regions and their union is the capacity region. Any operating point on the boundary of the capacity region is fully characterized by solving for the power allocation policy that maximizes $\mu_1 R_1 + \mu_2 R_2$ for some (μ_1, μ_2). For any μ_1, μ_2, there exist P^*, α_1^*, α_2^* and β^* that achieve the corresponding point on the boundary of the capacity region [48, 49].

8.2.2 The Fading Broadcast Channel Model

The fading broadcast channel model is depicted in Figure 8.2. The received signals at the two receivers are

$$Y_1 = \sqrt{h_1}X + Z_1 \tag{8.5}$$

$$Y_2 = \sqrt{h_2}X + Z_2 \tag{8.6}$$

where X is the transmit signal, Z_1, Z_2 are Gaussian noises with zero-mean and variances σ_1^2 and σ_2^2, respectively, and h_1, h_2 are the (squared) fading coefficients[1] for receivers 1 and 2, respectively. As in [48], we combine the effects of fading and noise power, and obtain an equivalent broadcast channel by letting $n_1 = \frac{\sigma_1^2}{h_1}$ and $n_2 = \frac{\sigma_2^2}{h_2}$. If the channel fade levels are constant at h_1, h_2, and the transmitter transmits with power P, the resulting broadcast channel capacity region is [54]:

$$R_1 \leq \frac{1}{2}\log_2\left(1 + \frac{\alpha P}{(1-\alpha)P\mathbf{1}(n_1 > n_2) + n_1}\right) \tag{8.7}$$

$$R_2 \leq \frac{1}{2}\log_2\left(1 + \frac{(1-\alpha)P}{\alpha P\mathbf{1}(n_2 > n_1) + n_2}\right) \tag{8.8}$$

where α is the fraction of the power spent for the message transmitted to user 1, and $\mathbf{1}(x > y)$ is the indicator function for the event $x > y$. We call the receiver which observes smaller combined noise power the stronger receiver and the other one the weaker receiver. That is, receiver 1 is the stronger user if $n_1 < n_2$ and receiver 2 is

[1] We note that the model can be generalized to a broadcast channel with conventional complex baseband fading coefficients after proper scalings that are inconsequential for our analysis.

the stronger user if $n_2 < n_1$. Note that changes in the fading levels of the channels during the communication session causes time variation in the strength order of the receivers.

8.2.3 Energy and Power-Rate Models

In two-user energy harvesting parallel and fading broadcast channels, the transmitter has three queues as in Figures 8.1 and 8.2: two data queues where data packets for the two receivers are stored, and an energy queue where the arriving (harvested) energy is stored. The energy queue, i.e., the battery, can store at most E_{max} units of energy, which is used for transmission only, i.e., energy required for processing is not considered.

We consider an offline setting where the changes that occur in the energy levels throughout the communication session are known by the transmitter a priori. In the fading broadcast channel, the changes in the fade levels are also known by the transmitter a priori. Performance of any transmission policy with a priori knowledge provides an upper bound for that of a real time system. In the fading broadcast channel, the fading and energy levels change at discrete time instants $t_1^f, t_2^f, \ldots, t_n^f, \ldots$ and $t_1^e, t_2^e, \ldots, t_n^e, \ldots$, respectively, as shown in Figure 8.3. Note that a change in the fading level means any change in the joint fading state (h_1, h_2). We define an epoch as a time interval in which no energy arrival or channel fade level change occurs as shown in Figure 8.3. An epoch in the parallel broadcast channels scenario is the time interval between two energy harvests as the channel gains do

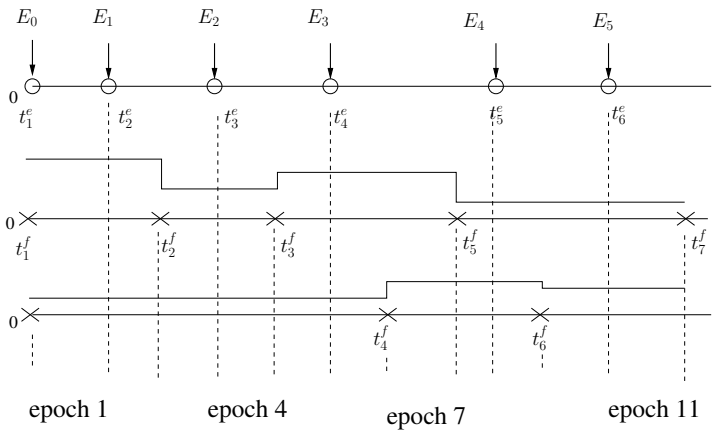

Figure 8.3: The energy arrivals, channel variations and epochs.

not vary. In the fading broadcast channel, we extend the definition of energy arrival sequence for the time instants at which a fading change occurs. In particular, the input energy for epoch i is denoted as E_{i-1} and it is equal to the amount of incoming energy if the epoch starts with an energy arrival; if epoch i starts with a variation in the fading level without an energy arrival, $E_{i-1} = 0$. Finally, we let ℓ_i denote the length of the ith epoch.

Whenever an input signal x is transmitted with power p in an epoch of duration ℓ in which the channel fades are constant at the levels h_1 and h_2, $R_1\ell$ and $R_2\ell$ bits of data are served out from the backlogs of receivers 1 and 2 at the transmitter, with the cost of $p\ell$ units of energy depletion from the energy queue. Here, (R_1, R_2) is the rate allocation for this epoch. (R_1, R_2) must reside in the corresponding capacity region. In particular, for the parallel channels scenario, (R_1, R_2) must satisfy (8.3) and (8.4), and in the fading broadcast channel scenario, (R_1, R_2) must reside in the capacity region of the two-user AWGN broadcast channel $\mathcal{C}_{n_1,n_2}(P)$, indexed by the noise variances n_1 and n_2, which vary during the communication session. Extending this

for continuous time, if at time t the transmit power is $P(t)$ and the noise variances are $n_1(t) = \sigma_1^2/h_1(t)$ and $n_2(t) = \sigma_2^2/h_2(t)$, the instantaneous rate pairs $(R_1(t), R_2(t))$ reside in the corresponding capacity region, i.e., $(R_1(t), R_2(t)) \in \mathcal{C}_{n_1(t),n_2(t)}(P(t))$.

The transmission policy in the parallel broadcast channel is comprised of $P(t)$, the total power, $\beta(t) \in [0,1]$, the power share of the 1st parallel channel, and $\alpha_1(t) \in [0,1]$ and $\alpha_2(t) \in [0,1]$, the power shares of user 1 in the 1st and 2nd parallel channels, respectively. In fading broadcast channels, transmission policy is comprised of the total power $P(t)$ and the portion of the total transmit power $\alpha(t) \in [0,1]$ that is allocated for user 1. Therefore, in parallel and fading broadcast channels, the total energy consumed by the transmitter up to time t can be expressed as $\int_0^t P(\tau)d\tau$. Due to the finiteness of the battery capacity, at any time t, if the unconsumed energy is greater than E_{max}, only E_{max} can be stored in the battery and the rest of the energy is wasted due to energy overflow. This may happen only at the instants of energy arrivals. Therefore, the total removed energy from the battery at s_k, $E_r(s_k)$, including the consumed part and the wasted part, can be expressed recursively as

$$E_r(s_k^+) = \max\left\{E_r(s_{k-1}^+) + \int_{s_{k-1}}^{s_k} P(\tau)d\tau, \left(\sum_{j=0}^{k} E_j - E_{max}\right)^+\right\}, \quad k = 1, 2, \ldots \tag{8.9}$$

where $(x)^+ = \max\{0, x\}$, and s_k^+ should be interpreted as $s_k + \epsilon$ for arbitrarily small $\epsilon > 0$. In addition, $E_r(s_0) = 0$. We can extend the definition of E_r for the times

$t \neq s_k$ as:

$$E_r(t) = E_r(s^+_{d_+(t)}) + \int_{s_{d_+(t)}}^{t} P(\tau)d\tau \tag{8.10}$$

where $d_+(t) = \max\{i : s_i \leq t\}$. As the transmitter cannot utilize the energy that has not arrived yet, the transmission policy is subject to an energy causality constraint. The removed energy $E_r(t)$ cannot exceed the total energy arrival during the communication. This constraint is mathematically stated as follows:

$$E_r(t) \leq \sum_{i=0}^{d_-(t)} E_i, \qquad \forall t \in [0, T] \tag{8.11}$$

where $d_-(t) = \max\{i : s_i < t\}$. As the energies arrive at discrete times, the causality constraint reduces to inequalities that have to be satisfied at the times of energy arrivals:

$$E_r(s^+_{k-1}) + \int_{s_{k-1}}^{s_k} P(\tau)d\tau \leq \sum_{i=0}^{k-1} E_i, \quad \forall k \tag{8.12}$$

A transmission policy guarantees no-energy-overflow if the following constraint is satisfied:

$$\int_0^t P(\tau)d\tau \geq \left(\sum_{i=0}^{d_+(t)} E_i - E_{max} \right)^+, \quad \forall t \in [0, T] \tag{8.13}$$

The constraint in (8.13) imposes that at least $\sum_{i=0}^{k} E_i - E_{max}$ amount of energy has been consumed (including both the data transmission and the energy overflow) by

the time the kth energy arrives so that the battery can accommodate E_k at time s_k. If a policy satisfies (8.13), the max in (8.9) always yields the first term in it. Therefore, the causality constraint in (8.12) reduces to the following:

$$\int_0^t P(\tau)d\tau \leq \sum_{i=0}^{d_-(t)} E_i, \quad \forall k \tag{8.14}$$

8.3 The Maximum Departure Region

In both parallel and fading broadcast channels, the performances of user 1 and user 2 are strongly coupled as they are yielded by the utilization of the common resources, which are the harvested energy and the shared wireless communication channel. In this section, we characterize the trade-off between the performances of user 1 and user 2 by finding the region of bits sent for receivers 1 and 2 in the interval $[0, T]$ with offline knowledge of energy and fading variations. The number of bits sent for users 1 and 2 are:

$$B_1 = \int_0^T R_1(\tau)d\tau \tag{8.15}$$

$$B_2 = \int_0^T R_2(\tau)d\tau \tag{8.16}$$

The instantaneous rates $R_1(t)$ and $R_2(t)$ are determined as a function of the instantaneous power policy $P(t)$ as described in power-rate model in Section 8.2.3. For any fixed transmission duration T, the maximum departure region, denoted as $\mathcal{D}(T)$, is defined identically as in Definition 7.6. We have the following lemma, the

proof of which can be carried out following the proof of Lemma 7.1 and hence is skipped for brevity.

Lemma 8.1 *For both parallel and fading broadcast channels, $\mathcal{D}(T)$ is a convex region.*

We note that a transmission policy that violates the no-energy-overflow condition is always strictly inside $\mathcal{D}(T)$; therefore, without losing optimality we restrict the feasible set to the policies that allow no energy overflows. In the following, we call any policy that satisfies energy causality and no-energy-overflow conditions *feasible*. We call a feasible policy *optimal* if it achieves the boundary of $\mathcal{D}(T)$.

8.3.1 $\mathcal{D}(T)$ for Parallel Broadcast Channels

In parallel broadcast channels, the instantaneous rates $r_1(t)$ and $r_2(t)$ allocated for users 1 and 2 are determined as a function of the instantaneous power, $P(t)$, power share of the 1st channel, $\beta(t)$, and the power shares of user 1 in the ith channel, $\alpha_i(t)$, $i = 1, 2$, via (8.3) and (8.4). The instantaneous power, $P(t)$, is subject to the energy causality and no-energy-overflow conditions as in (8.14) and (8.13), respectively. We let N denote the number of energy arrivals in the $[0, T]$ interval.

Due to the convexity of $\mathcal{D}(T)$ in Lemma 8.1 and the convex power-rate relation, an optimal policy should remain constant in any epoch (c.f. Lemma 1 in [24] and Lemma 2 in [14, 15]). Therefore, we consider a power policy as a sequence of powers allocated for each epoch $\{p_i\}_{i=1}^{N+1}$ with the 1st channel's share $\{\beta_i\}_{i=1}^{N+1}$, the power share of user 1 in each channel $\{(\alpha_{i1}, \alpha_{i2})\}_{i=1}^{N+1}$. Then, the energy causality and no-

energy-overflow conditions in (8.14) and (8.13) reduce to the following constraints, respectively, which are described by a finite sequence of powers:

$$\sum_{i=1}^{k} p_i \ell_i \leq \sum_{i=0}^{k-1} E_i, \quad k = 1, \ldots, N+1 \tag{8.17}$$

$$\sum_{i=1}^{k} p_i \ell_i \geq \left(\sum_{i=0}^{k} E_i - E_{max} \right)^+, \quad k = 1, \ldots, N \tag{8.18}$$

Here (8.17) is due to the energy causality constraint in (8.14) and (8.18) is due to the no-energy-overflow condition in (8.13). We define the following functions:

$$r_1(\alpha_1, \alpha_2, \beta, p) = \frac{1}{2} \log_2 \left(1 + \frac{\alpha_1 \beta p}{\sigma_{11}^2} \right) + \frac{1}{2} \log_2 \left(1 + \frac{\alpha_2 (1-\beta) p}{(1-\alpha_2)(1-\beta)p + \sigma_{12}^2} \right) \tag{8.19}$$

$$r_2(\alpha_1, \alpha_2, \beta, p) = \frac{1}{2} \log_2 \left(1 + \frac{(1-\alpha_1)\beta p}{\alpha_1 \beta p + \sigma_{21}^2} \right) + \frac{1}{2} \log_2 \left(1 + \frac{(1-\alpha_2)(1-\beta)p}{\sigma_{22}^2} \right) \tag{8.20}$$

which are the rates achieved by users 1 and 2, respectively, if p is allocated to the channels with the first parallel channel's share βp, and user 1's power share (α_1, α_2) in each channel. By Lemma 8.1, any point on the boundary of the maximum departure region $\mathcal{D}(T)$ can be characterized by solving the following optimization

problem:

$$\begin{aligned}
\max_{\boldsymbol{\alpha}_1,\boldsymbol{\alpha}_2,\boldsymbol{\beta},\mathbf{P}} \quad & \mu_1 \sum_{i=1}^{N+1} r_1(\alpha_{1i},\alpha_{2i},\beta_i,p_i)\ell_i + \mu_2 \sum_{i=1}^{N+1} r_2(\alpha_{1i},\alpha_{2i},\beta_i,p_i)\ell_i \\
\text{s.t.} \quad & \sum_{i=1}^{k} p_i\ell_i \le \sum_{i=0}^{k-1} E_i, \qquad \forall k \\
& \sum_{i=1}^{k} p_i\ell_i \ge \left(\sum_{i=0}^{k} E_i - E_{max}\right)^+, \qquad \forall k \\
& 0 \le \alpha_{ik} \le 1, \qquad 0 \le \beta_i \le 1, \qquad p_k \ge 0, \qquad i = 1,2, \ \forall k
\end{aligned} \tag{8.21}$$

In (8.21), $\boldsymbol{\alpha}_1, \boldsymbol{\alpha}_2, \boldsymbol{\beta}, \mathbf{P}$ collectively denote the vector of total powers and power shares for the parallel channels and users. The optimization problem (8.21) is not a convex problem as the variables p_i, β_i, α_{1i} and α_{2i} appear in product forms in the expression of $r_i(\alpha_1, \alpha_2, \beta, p)$, causing it to be non-concave in α_i, p and β jointly. However, for any given $\alpha_1, \alpha_2, \beta$ we note that $\mu_1 r_1(\alpha_1, \alpha_2, \beta, p) + \mu_2 r_2(\alpha_1, \alpha_2, \beta, p)$ is concave with respect to p. Using this property, we solve (8.21) in two steps. We optimize over $\alpha_{1i}, \alpha_{2i}, \beta_i$ first and then over the total power p_i. The details of the optimal policy are presented in Section 8.4.

8.3.2 $\mathcal{D}(T)$ for Fading Broadcast Channels

In fading broadcast channels, the instantaneous rates $r_1(t)$ and $r_2(t)$ allocated for users 1 and 2 are determined as a function of the instantaneous power, $P(t)$ and the power share of user 1, $\alpha(t)$, via (8.7) and (8.8). The instantaneous power, $P(t)$, is subject to the energy causality and no-energy-overflow conditions as in (8.14) and (8.13), respectively. We let N denote the number of energy arrivals and K denote

the number of changes in the joint fading level in the $[0, T]$ interval. We assume that fading variations and energy arrivals occur at distinct time instants so that the number of epochs in $[0, T]$ interval is $N + K + 1$. If an energy arrival and a fading variation occur at the same instant, the number of epochs is less than $N + K + 1$.

Due to the convexity of $\mathcal{D}(T)$ in Lemma 8.1 and the convex power-rate relation, an optimal policy should remain constant in any epoch (c.f. Lemma 1 in [24] and Lemma 2 in [14, 15]). Therefore, the policy is a sequence of powers $\{p_i\}_{i=1}^{N+K+1}$ and user 1's power share $\{\alpha_i\}_{i=1}^{N+K+1}$. The sequence of noise variances of the equivalent broadcast channels is $\{(n_{1i}, n_{2i})\}_{i=1}^{N+K+1}$. Then, the causality and no-energy-overflow conditions in (8.14) and (8.13) reduce to the following constraints, respectively, which are described by a finite sequence of powers:

$$\sum_{i=1}^{k} p_i \ell_i \leq \sum_{i=0}^{k-1} E_i, \quad k = 1, \ldots, N + K + 1 \tag{8.22}$$

$$\sum_{i=1}^{k} p_i \ell_i \geq \left(\sum_{i=0}^{k} E_i - E_{max} \right)^+, \quad k = 1, \ldots, N + K \tag{8.23}$$

Here (8.22) is due to the energy causality constraint in (8.14) and (8.23) is due to the no-energy-overflow condition in (8.13). We define the following functions:

$$r_1(n_1, n_2, \alpha, p) = \frac{1}{2} \log_2 \left(1 + \frac{\alpha p}{(1-\alpha) p \mathbf{1}(n_1 > n_2) + n_1} \right) \tag{8.24}$$

$$r_2(n_1, n_2, \alpha, p) = \frac{1}{2} \log_2 \left(1 + \frac{(1-\alpha) p}{\alpha p \mathbf{1}(n_2 > n_1) + n_2} \right) \tag{8.25}$$

which are the rates achieved by users 1 and 2, respectively, in the fading broadcast channel when power is p and power share of user 1 is α. By Lemma 8.1, any point

on the boundary of $\mathcal{D}(T)$ can be characterized by solving the following optimization problem for some $\mu_1, \mu_2 \geq 0$:

$$\begin{aligned}
\max_{\mathbf{P},\boldsymbol{\alpha}} \quad & \mu_1 \sum_{i=1}^{N+K+1} r_1(n_{1i}, n_{2i}, \alpha_i, p_i)\ell_i + \mu_2 \sum_{i=1}^{N+K+1} r_2(n_{1i}, n_{2i}, \alpha_i, p_i)\ell_i \\
\text{s.t.} \quad & \sum_{i=1}^{k} p_i \ell_i \leq \sum_{i=0}^{k-1} E_i, \qquad \forall k \\
& \sum_{i=1}^{k} p_i \ell_i \geq \left(\sum_{i=0}^{k} E_i - E_{max} \right)^+, \qquad \forall k \\
& 0 \leq \alpha_k \leq 1, \qquad p_k \geq 0, \qquad \forall k
\end{aligned} \tag{8.26}$$

where $\mathbf{P}, \boldsymbol{\alpha}$ denote the vector of total powers and the power shares of user 1, respectively. The optimization problem in (8.26) is not a convex problem as the variables p_i, α_i appear in a product form in the expression of $r_i(n_1, n_2, \alpha, p)$, causing it to be non-concave in α_i and p_i jointly. However, $\mu_1 r_1(n_1, n_2, \alpha, p) + \mu_2 r_2(n_1, n_2, \alpha, p)$ is concave with respect to p for any given α. We will solve (8.26) using this property. The details of the optimal policy for the fading broadcast channel is presented in Section 8.5.

8.4 Optimal Policy for Parallel Broadcast Channels

The optimization problem in (8.21) can be cast as a sequence of optimization problems of the following form given the power p:

$$\begin{aligned} &\max_{\alpha_1,\alpha_2,\beta} \ \mu_1 r_1(\alpha_1,\alpha_2,\beta,p) + \mu_2 r_2(\alpha_1,\alpha_2,\beta,p) \\ &\text{s.t.} \quad 0 \le \alpha_1,\alpha_2,\beta \le 1 \end{aligned} \tag{8.27}$$

Note that given β and p, optimal α_1 and α_2 can be separately calculated. In particular, (8.27) is solved at $\alpha_1 = \alpha_1^*(\beta,p)$ and $\alpha_2 = \alpha_2^*(\beta,p)$. If $\frac{\mu_2}{\mu_1} \le 1$, $\alpha_1^*(\beta,p) = 1$ while if $\frac{\mu_2}{\mu_1} \ge \frac{\sigma_{21}^2}{\sigma_{11}^2}$, $\alpha_1^*(\beta,p) = 0$ for all β. On the other hand, if $1 < \frac{\mu_2}{\mu_1} < \frac{\sigma_{21}^2}{\sigma_{11}^2}$, we have

$$\alpha_1^*(\beta,p) = \begin{cases} 1, & 0 \le \beta p \le \frac{\mu_2\sigma_{11}^2 - \mu_1\sigma_{21}^2}{\mu_1 - \mu_2} \\ \frac{1}{\beta p}\frac{\mu_2\sigma_{11}^2 - \mu_1\sigma_{21}^2}{\mu_1 - \mu_2}, & \beta p \ge \frac{\mu_2\sigma_{11}^2 - \mu_1\sigma_{21}^2}{\mu_1 - \mu_2} \end{cases} \tag{8.28}$$

Similarly, if $\frac{\mu_1}{\mu_2} \le 1$, $\alpha_2^*(\beta,p) = 0$ while if $\frac{\mu_1}{\mu_2} \ge \frac{\sigma_{12}^2}{\sigma_{22}^2}$ then $\alpha_2^*(\beta,p) = 1$ for all β. If $1 < \frac{\mu_1}{\mu_2} < \frac{\sigma_{12}^2}{\sigma_{22}^2}$,

$$\alpha_2^*(\beta,p) = \begin{cases} 0, & 0 \le (1-\beta)p \le \frac{\mu_1\sigma_{22}^2 - \mu_2\sigma_{12}^2}{\mu_2 - \mu_1} \\ 1 - \frac{1}{(1-\beta)p}\frac{\mu_1\sigma_{22}^2 - \mu_2\sigma_{12}^2}{\mu_2 - \mu_1}, & (1-\beta)p \ge \frac{\mu_1\sigma_{22}^2 - \mu_2\sigma_{12}^2}{\mu_2 - \mu_1} \end{cases} \tag{8.29}$$

Hence, (8.27) is equivalent to the following given p:

$$\max_{0\le\beta\le 1} \ \mu_1 r_1^*(\beta,p) + \mu_2 r_2^*(\beta,p) \tag{8.30}$$

where $r_1^*(\beta,p) = r_1(\alpha_1^*(\beta,p),\alpha_2^*(\beta,p),\beta,p)$ and $r_2^*(\beta,p) = r_2(\alpha_1^*(\beta,p),\alpha_2^*(\beta,p),\beta,p)$. Note that in view of Lemma 7.2, the objective function in (8.30) is strictly concave with respect to the two power levels $p_1 = \beta p$ and $p_2 = (1-\beta)p$ allocated to the two parallel channels. This, in turn, implies that the objective function in (8.30) is strictly concave with respect to β. The solution of (8.30) has a water-filling interpretation. Working on the optimal α_1 and α_2 in (8.28) and (8.29), one can show that

$$\beta^* p = \max_{u\in\{1,2\}} \left(\mu_u \lambda - \sigma_{u1}^2\right)^+ \tag{8.31}$$

$$(1-\beta^*)p = \max_{u\in\{1,2\}} \left(\mu_u \lambda - \sigma_{u2}^2\right)^+ \tag{8.32}$$

where λ is the water level and β^* is the optimizer of (8.30). The water level λ is found by a greedy power allocation algorithm [48, 49]. Power is incrementally allocated to the parallel channel that yields the maximum increase in the objective function in (8.30): For small power values, only a single parallel channel is allocated power. As the power is further increased, both parallel channels are allocated power. In the extreme cases, only single users are allocated power and the power is split over the parallel channels by single user water-filling: If $\frac{\mu_2}{\mu_1} \leq \frac{\sigma_{22}^2}{\sigma_{12}^2}$, then all the power is allocated to user 1; if $\frac{\mu_2}{\mu_1} \geq \frac{\sigma_{21}^2}{\sigma_{11}^2}$, then all the power is allocated for user 2. The outcome of the optimization problem depends on the power p. Let us define

$$g(p) = \max_{0\leq\beta\leq 1} \mu_1 r_1^*(\beta,p) + \mu_2 r_2^*(\beta,p) \tag{8.33}$$

We have the following lemma whose proof is provided in Appendix 8.8.1:

Lemma 8.2 *$g(p)$ is monotone increasing, strictly concave function of p.*

Then, the optimization problem in (8.21) is equivalently stated as an optimization problem only in terms of p_i as follows:

$$\begin{aligned}
\max_{\mathbf{p}} \quad & \sum_{i=1}^{N+1} g(p_i)\ell_i \\
\text{s.t.} \quad & \sum_{i=1}^{k} p_i\ell_i \leq \sum_{i=0}^{k-1} E_i, \qquad \forall k \\
& \sum_{i=1}^{k} p_i\ell_i \geq \left(\sum_{i=0}^{k} E_i - E_{max}\right)^+, \qquad \forall k \\
& p_k \geq 0, \qquad \forall k
\end{aligned} \tag{8.34}$$

The optimization problem in (8.34) is a convex optimization problem. The objective function is strictly concave by Lemma 8.2 and the feasible set is a convex set.

Following the steps for finding the optimal policy in non-fading scalar broadcast channels, and as the objective function in (8.34) is concave, we obtain an important characteristic of optimal policies that achieve the boundary of $\mathcal{D}(T)$ of parallel broadcast channels.

Lemma 8.3 *For any point on the boundary of $\mathcal{D}(T)$ of parallel broadcast channels, the optimal total transmit power allocation sequence is the same as the optimal single user power allocation policy in the scalar case.*

With Lemma 8.3 and the preceding findings, we obtain the full structure of a point on the boundary of the maximum departure region $\mathcal{D}(T)$. We first calculate the

total power allocated for each receiver using the tightest curve approach in [14, 15] if $E_{max} = \infty$, or the feasible tunnel approach in [23] or the directional water-filling algorithm in [39] if E_{max} is finite. As a result, we get the sequence of total powers allocated at each time epoch, $\{p_i^*\}_{i=1}^{N+1}$. Then, we divide each p_i^* as $p_{i1}^* = \beta_i^* p$ and $p_{i2}^* = (1 - \beta_i^*)p$ allocated to the two parallel broadcast channels by means of the water-filling solution described in (8.31)-(8.32). With this, we get the power shares for each parallel channel p_{i1}^* and p_{i2}^* as well as the corresponding power shares of user 1 in each parallel channel $\alpha_1^*(p_{i1}^*)$ and $\alpha_2^*(p_{i2}^*)$. Then, (B_1^*, B_2^*) point that corresponds to the priority coefficients μ_1 and μ_2 is

$$B_1^* = \sum_{i=1}^{N+1} \frac{1}{2} \log \left(1 + \frac{\alpha_1^*(p_{i1}^*) p_{i1}^*}{\sigma_{11}^2} \right) \ell_i + \frac{1}{2} \log \left(1 + \frac{\alpha_2^*(p_{i2}^*) p_{i2}^*}{(1 - \alpha_2^*(p_{i2}^*)) p_{i2}^* + \sigma_{12}^2} \right) \ell_i \quad (8.35)$$

$$B_2^* = \sum_{i=1}^{N+1} \frac{1}{2} \log \left(1 + \frac{(1 - \alpha_2^*(p_{i2}^*)) p_{i2}^*}{\sigma_{22}^2} \right) \ell_i + \frac{1}{2} \log \left(1 + \frac{(1 - \alpha_1^*(p_{i1}^*)) p_{i1}^*}{\alpha_1^*(p_{i1}^*) p_{i1}^* + \sigma_{21}^2} \right) \ell_i \quad (8.36)$$

8.5 Optimal Policy for Fading Broadcast Channels

We now consider the fading broadcast channel. In order to solve (8.26), we first optimize the cost function in the ith epoch over α_i for a given total transmit power p_i. Consider the single-variable optimization problem in α for a given p:

$$\max_{0 \le \alpha \le 1} \ \mu_1 r_1(n_1, n_2, \alpha, p) + \mu_2 r_2(n_1, n_2, \alpha, p) \quad (8.37)$$

The optimal solution of (8.37) is denoted by $\alpha = \alpha^*(n_1, n_2, p)$. Assume $n_1 < n_2$ and let $\mu = \mu_2/\mu_1$. If $1 < \mu < \frac{n_2}{n_1}$, $\alpha^*(n_1, n_2, p)$ is expressed as:

$$\alpha^*(n_1, n_2, p) = \begin{cases} 1, & 0 \le p \le \frac{\mu n_1 - n_2}{1-\mu} \\ \frac{1}{p}\frac{\mu n_1 - n_2}{1-\mu}, & p \ge \frac{\mu n_1 - n_2}{1-\mu} \end{cases} \tag{8.38}$$

In the extreme cases, $\alpha^*(n_1, n_2, p) = 1$ if $\mu \le 1$ and $\alpha^*(n_1, n_2, p) = 0$ if $\mu \ge \frac{n_2}{n_1}$. If the order of noises is the other way, i.e., if $n_2 < n_1$, by changing the definition of μ as $\mu = \frac{\mu_1}{\mu_2}$,

$$\alpha^*(n_1, n_2, p) = \begin{cases} 0, & 0 \le p \le \frac{\mu n_2 - n_1}{1-\mu} \\ 1 - \frac{1}{p}\frac{\mu n_1 - n_2}{1-\mu}, & p \ge \frac{\mu n_2 - n_1}{1-\mu} \end{cases} \tag{8.39}$$

We define

$$h(n_1, n_2, p) \triangleq \mu_1 r_1(n_1, n_2, \alpha^*, p) + \mu_2 r_2(n_1, n_2, \alpha^*, p)$$

We have the following due to Lemma 7.2.

Lemma 8.4 *$h(n_1, n_2, p)$ is monotone increasing, strictly concave function of p given n_1 and n_2.*

In particular, $h(n_1, n_2, p)$ has a continuous monotone decreasing first derivative: for $n_1 < n_2$, whenever $\alpha^*(n_1, n_2, p) = 1$, the derivative is $\frac{\mu_1}{p+n_1}$ and otherwise, it is $\frac{\mu_2}{p+n_2}$. Similarly, if $n_2 < n_1$, whenever $\alpha^*(n_1, n_2, p) = 0$, the derivative is $\frac{\mu_2}{p+n_2}$ and otherwise, it is $\frac{\mu_1}{p+n_1}$. Hence, by first optimizing over α_i in (8.26), we obtain the

following convex optimization problem over the total power sequence $\{p_i\}$:

$$\begin{aligned}
\max_{\mathbf{P}} \quad & \sum_{i=1}^{N+K+1} h(n_{1i}, n_{2i}, p_i)\ell_i \\
\text{s.t.} \quad & \sum_{i=1}^{k} p_i \ell_i \leq \sum_{i=0}^{k-1} E_i, \qquad \forall k \\
& \sum_{i=1}^{k} p_i \ell_i \geq \left(\sum_{i=0}^{k} E_i - E_{max} \right)^+, \qquad \forall k \\
& p_k \geq 0, \qquad \forall k
\end{aligned} \tag{8.40}$$

The optimization problem in (8.40), and hence the one in (8.26), has a unique optimal solution.

We define the Lagrangian for the problem in (8.40) as,

$$\begin{aligned}
\mathcal{L} = & \sum_{i=1}^{N+K+1} h(n_{1i}, n_{2i}, p_i)\ell_i - \sum_{j=1}^{N+K+1} \lambda_j \left(\sum_{i=1}^{j} p_i \ell_i - \sum_{i=0}^{j-1} E_i \right) \\
& - \sum_{j=1}^{N+K+1} \kappa_j \left(\left(\sum_{i=0}^{j} E_i - E_{max} \right)^+ - \sum_{i=1}^{j} p_i \ell_i \right) + \sum_{i=1}^{N+K+1} \eta_i p_i
\end{aligned} \tag{8.41}$$

The first order condition on the Lagrangian is

$$\frac{d}{dp_i} h(n_{1i}, n_{2i}, p_i) = \sum_{j=i}^{N+K+1} \lambda_j - \sum_{j=i}^{N+K+1} \kappa_j - \eta_i \tag{8.42}$$

The complimentary slackness conditions are:

$$\lambda_j \left(\sum_{i=1}^{j} p_i \ell_i - \sum_{i=0}^{j-1} E_i \right) = 0, \quad \forall j \tag{8.43}$$

$$\kappa_j \left(\left(\sum_{i=0}^{j} E_i - E_{max} \right)^+ - \sum_{i=1}^{j} p_i \ell_i \right) = 0, \quad \forall j \tag{8.44}$$

$$\eta_j p_j = 0, \quad \forall j \tag{8.45}$$

It follows that the optimal total power in epoch i is given by

$$p_i^* = \mu_{u_i} \left[\nu_i - \frac{1}{\mu_{u_i} h_{u_i}} \right]^+ \tag{8.46}$$

where the water level in epoch i, ν_i, is

$$\nu_i = \frac{1}{\sum_{j=i}^{N+K+1} \lambda_j - \sum_{j=i}^{N+K+1} \kappa_j} \tag{8.47}$$

The index u_i is uniquely determined by the given μ_1, μ_2, n_1, n_2 and E_i. In particular, u_i is 1 if the derivative of $h(n_1, n_2, p)$ at the allocated power p_i^* in (8.46) is $\frac{\mu_1}{p+n_1}$ and it is 2 otherwise. For $\frac{\mu_2}{\mu_1} \leq \min_i\{\frac{n_{1i}}{n_{2i}}, \frac{n_{2i}}{n_{1i}}\}$, $u_i = 1$ for all i and all the power is allocated to the first user only. If $\frac{\mu_2}{\mu_1} \geq \max_i\{\frac{n_{1i}}{n_{2i}}, \frac{n_{2i}}{n_{1i}}\}$, $u_i = 2$ for all i and all the power is allocated to the second user. For the remaining values of $\frac{\mu_2}{\mu_1}$, both users may be allocated power in some epoch.

Note that the slackness variables λ_i and κ_i are zero in between two energy harvesting instants as the energy causality and no-energy-overflow constraints are never violated except possibly at the energy arriving instants. Therefore, the water

level ν_i is the same for all epochs in between two energy harvesting instants. When $E_{max} = \infty$, for any epoch i, the optimum water level ν_i is monotonically increasing, i.e., $\nu_{i+1} \geq \nu_i$ as $\kappa_j = 0$ in this case. If some energy is transferred from epoch i to $i+1$, then $\nu_i = \nu_{i+1}$.

For finite E_{max} case, the solution is found by a directional water-filling algorithm [39], which we describe next. The directional water-filling algorithm requires walls at the points of energy arrival, with right permeable water taps in each wall which allows at most E_{max} amount of water to flow, as shown in Figure 8.4. First, the taps are kept off and transfer from one epoch to the other is not allowed. Each incoming energy E_i is spread in the time interval till the next energy arrival time and the water level is calculated. The main difficulty arises due to the fact that the index u_i is not known a priori. If a sequence of u_i is assumed, the resulting water levels and power allocation should be compatible with (8.39) and there exists a unique u_i^* sequence that is compatible with (8.39). The resulting water levels ν_i can be found by the water-filling algorithm in [48] or the greedy water-filling algorithm in [49]. The water levels when each right permeable tap is turned on will be found allowing at most $E_{max} - E_i$ amount of energy transfer from the past epochs to the epochs which start with arrival of E_i provided that the initial water level in epoch $i-1$ is higher than that in epoch i. This is due to the fact that the slackness variable κ_i is not active if energy transfer from past to the future is less than $E_{max} - E_i$. If κ_i is not active, water level ν_i in the past should be less than or equal to the water level ν_j in the future. As $\lambda_i = 0$ if an energy arrival does not occur at epoch i, we conclude that the incoming energy should be spread till the time next energy

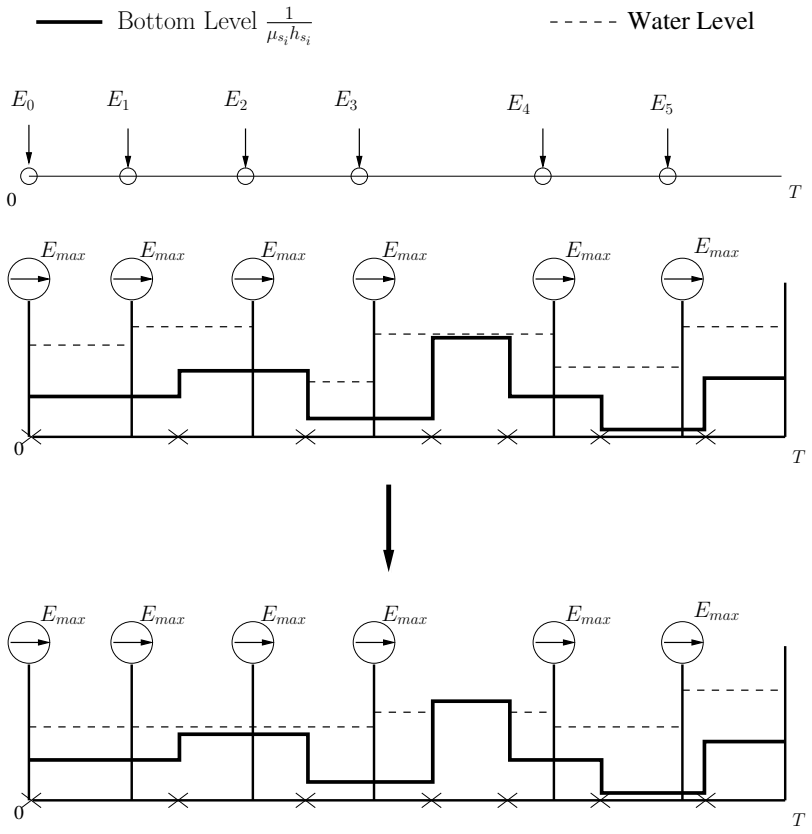

Figure 8.4: Directional water-filling algorithm.

arrives. Optimal power allocation p_i^* is then calculated by plugging the resulting water levels into (8.46). We note that the water level is scaled by different priority coefficients μ_{u_i} to yield the energy consumed at each epoch. Individual power shares are then found via (8.39). The optimal solution is unique unless $n_{1i} = n_{2i}$ for some epoch i. If $n_{1i} = n_{2i}$ for some epoch i, the optimal policy when $\mu_1 = \mu_2$ is any policy formed by time-sharing between giving strict priority to one of the users at that epoch. In this case, the sum throughput optimal points of $\mathcal{D}(T)$ form a line.

An example run of the algorithm is shown in Figure 8.4, for a case of 12 epochs. Five energy arrivals occur during the communication session, in addition to the energy available at time $t = 0$. We observe that the water level equalizes in

epochs 1, 2, 3, 4, 5. No power is transmitted in epoch 7, since $\frac{1}{\mu_{u_i} h_{u_i}}$ is too high. The energy arriving at the beginning of epoch 6 cannot flow left due to energy causality constraints, which are ensured by right permeable taps. We observe that the excess energy in epochs 6, 7 and 8 cannot flow right, due to the E_{max} constraint at the beginning of epoch 9.

We remark here that the optimal policy strongly depends on the priority coefficients μ_1, μ_2 of the users in contrast to the non-fading and parallel broadcast channels in which the optimal total power sequence is independent of μ_1 and μ_2. In particular, the bottom level of the directional water-filling is determined by the particular values of μ_1 and μ_2. If the user priorities are identical, i.e., $\mu_1 = \mu_2$, then the optimal policy is equal to the single user transmission policy for the user with the best channel at each epoch. The power allocation is found by applying the directional water-filling algorithm in [39] by selecting the bottom level in Figure 8.4 as $\frac{1}{\max\{h_{1i},h_{2i}\}}$.

We finally remark that our analysis can be extended for the case in which the transmitter sends messages over parallel broadcast channels with time-varying channel gains. For given channel gains, the share variables α_1,α_2 and β are defined as in (8.19)-(8.20) and after optimizing the weighted sum of rates over the share variables as in (8.37) we obtain a strictly concave function of power due to Lemma 8.4. Using similar convex optimization tools, we conclude that the solution is unique and it is found by a generalized directional water-filling algorithm.

8.6 Numerical Results

In this section, we provide numerical results for the maximum departure region over parallel and fading broadcast channels. We start with parallel channels and then consider fading broadcast channels.

8.6.1 Parallel Broadcast Channels

We consider a band-limited two-user AWGN broadcast channel with two parallel channels operating with a bandwidth of $W = 1$ MHz and under noise power spectral density $N_0 = 10^{-19}$ W/Hz. In the first channel, the path loss between the transmitter and receiver 1 is $c_{11} = 100$ dB and between the transmitter and receiver 2 is $c_{21} = 105$ dB. We have

$$r_{11} = W \log_2 \left(1 + \frac{\alpha_1 c_{11} \beta P 10^{-3}}{N_0 W}\right) = \log_2 \left(1 + \frac{\alpha_1 \beta P}{n_{11}}\right) \text{Mbps} \tag{8.48}$$

and

$$r_{21} = W \log_2 \left(1 + \frac{(1-\alpha_1) c_{21} \beta P 10^{-3}}{\alpha_1 c_{21} \beta P 10^{-3} + N_0 W}\right) = \log_2 \left(1 + \frac{(1-\alpha_1)\beta P}{\alpha_1 \beta P + n_{21}}\right) \text{Mbps} \tag{8.49}$$

where $n_{11} = 1$ and $n_{21} = 10^{0.5}$. The second parallel channel has path loss coefficients $c_{12} = 107$ dB and $c_{22} = 103$ dB and the resulting rate expressions are

$$r_{12} = \log_2 \left(1 + \frac{\alpha_2 (1-\beta) P}{(1-\alpha_2)(1-\beta)P + n_{12}} \right) \text{Mbps} \tag{8.50}$$

$$r_{22} = \log_2 \left(1 + \frac{(1-\alpha_2)(1-\beta) P}{n_{22}} \right) \text{Mbps} \tag{8.51}$$

where $n_{12} = 10^{0.7}$ and $n_{22} = 10^{0.3}$.

We assume that the battery capacity is $E_{max} = 10$ mJ and the energy arrivals occur at time instants $t_1^e = 2$ s, $t_2^e = 5$ s, $t_3^e = 8$ s, $t_4^e = 9$ s, $t_5^e = 12$ s with amounts $E_1 = 3$ mJ, $E_2 = 6$ mJ, $E_3 = 9$ mJ, $E_4 = 8$ mJ, $E_5 = 9$ mJ. The battery energy at time $t = 0$ s is $E_0 = 8$ mJ. We show the optimal total transmit power sequences for $T = 10$ s, $T = 12$ s, $T = 14$ s and $T = 16$ s in Figure 8.5. Initial energy in the battery and the first two energy arrivals are spread till $t = 8$ s. However, at most 2 mJ energy can flow from the time interval $[8, 9]$ s to the future as the finite battery constrains the energy flow. For example, for $T = 10$ s, only 0.5 mJ energy is transfered from $[8, 9]$ s interval while for $T = 12$ s, 2 mJ limit is hit and the power in $[8, 9]$ s is kept at 7 mJ (which leads to 7 mW power in that interval). Similarly, at most 1 mJ energy can flow from $[9, 12]$ s interval to the future. This leads to a non-monotonic total transmit power sequence as opposed to the $E_{max} = \infty$ case. We plot the resulting maximum departure regions in Figure 8.6. Note that the maximum departure regions are strictly convex for all T and monotone in T. We observe that the gap between the regions for different T increases in the passage from $T = 12$ s to $T = 14$ s since an energy arrival occurs at $t = 12$ s. This is

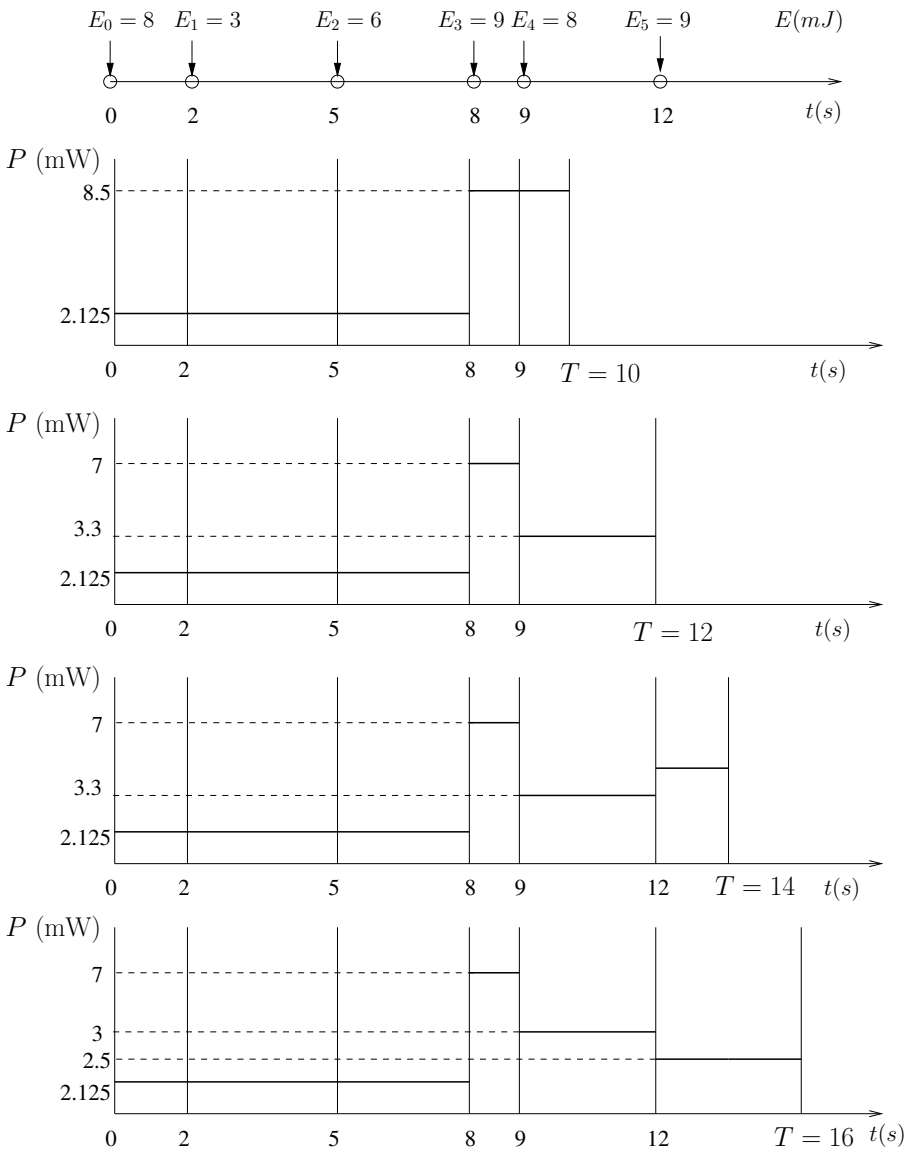

Figure 8.5: Illustration of the optimal transmission policy for $T = 10$ s, $T = 12$ s, $T = 14$ s and $T = 16$ s.

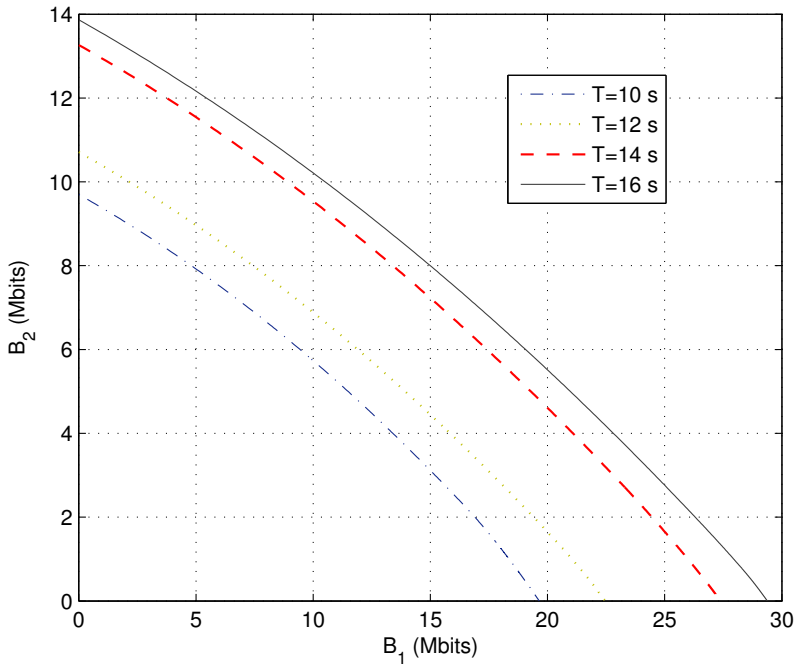

Figure 8.6: The maximum departure region for non-fading channel under the given energy arrivals for various T.

reminiscent of the fact that in a single user energy harvesting system, the rate of increase of the maximum departure curve is infinite at energy harvesting instants as observed in [39].

8.6.2 Fading Broadcast Channels

We consider a band-limited AWGN broadcast channel with bandwidth $W = 1$ MHz and noise power spectral density $N_0 = 10^{-19}$ W/Hz. The path loss between the transmitter and receiver 1 is $c_1 = 100$ dB and between the transmitter and receiver 2, is $c_2 = 105$ dB. In addition, the channel fading coefficients h_1 and h_2 vary during

the transmission. We have

$$r_1 = W \log_2 \left(1 + \frac{\alpha c_1 h_1 P 10^{-3}}{(1-\alpha) c_1 h_1 P 10^{-3} \mathbf{1}(c_1 h_1 < c_2 h_2) + N_0 W} \right) \tag{8.52}$$

$$= \log_2 \left(1 + \frac{\alpha P}{(1-\alpha) P \mathbf{1}(c_1 h_1 < c_2 h_2) + n_1} \right) \text{Mbps} \tag{8.53}$$

and similarly

$$r_2 = \log_2 \left(1 + \frac{(1-\alpha) P}{\alpha P \mathbf{1}(c_1 h_1 > c_2 h_2) + n_2} \right) \text{Mbps} \tag{8.54}$$

where $n_1 = \frac{1}{h_1}$ and $n_2 = \frac{10^{0.5}}{h_2}$. The fading profile, $\mathbf{h}_i = (h_{1i}, h_{2i})$ where i is the time index and both entries are in dB, is $\mathbf{h}_1 = (7, 4)$, $\mathbf{h}_2 = (7, 2)$, $\mathbf{h}_3 = (2, 2)$, $\mathbf{h}_4 = (-1, 3)$, $\mathbf{h}_5 = (-1, 8)$, $\mathbf{h}_6 = (1, 13)$, $\mathbf{h}_7 = (1, 8)$, $\mathbf{h}_8 = (3, 8)$ and $\mathbf{h}_9 = (5, 7)$ at time instants $t_1^f = 0$ s, $t_2^f = 1$ s, $t_3^f = 3$ s, $t_4^f = 4$ s, $t_5^f = 7$ s, $t_6^f = 8$ s, $t_7^f = 10$ s, $t_8^f = 11$ s. We show the energy and fading profiles in Figure 8.7. In particular, the fading profiles in Figure 8.7 are the inverted overall channel gains of the users, i.e., the path loss times fading coefficients.

We plot the maximum departure region corresponding to the given energy and channel profiles for $T = 14$ s in Figure 8.8. There are four critical points of the maximum departure region, A, B, C and D, as indicated in Figure 8.8. At point A, all the power is allocated for the transmission of user 1 and no data is transmitted for user 2; point D is vice versa. At points B and C, the priorities of the users are equal, i.e., $\mu = \frac{\mu_2}{\mu_1} = 1$. For the points to the left of B, $\mu \geq 1$ and for the points to the right of C, $\mu \leq 1$. The total power allocation at points A and D are found

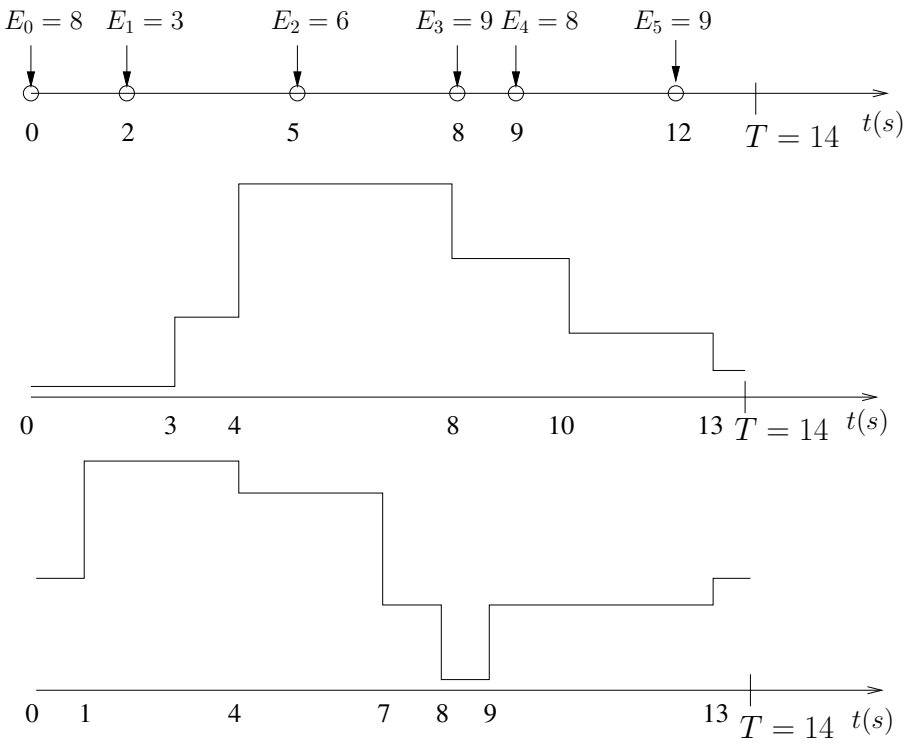

Figure 8.7: The energy and fading profiles.

by single user directional water-filling in [39] with the bottom level selected as $\frac{1}{c_1 h_{1i}}$ and $\frac{1}{c_2 h_{2i}}$, respectively. Moreover, the total power allocation at the sum throughput optimal policies (points B and C) is found by single user directional water-filling with the bottom level selected as $\frac{1}{\max\{c_1 h_{1i}, c_2 h_{2i}\}}$. In Figure 8.9, we show the total power allocation of the sum throughput optimal policies corresponding to the time-sharing between points B and C in Figure 8.8. Note that the total power allocation is not affected by the choice of the index u_i at epochs i in which $c_1 h_{1i} = c_2 h_{2i}$. As $c_1 h_{1i} = c_2 h_{2i}$ holds for some i, time sharing between these users in these epochs does not violate optimality for $\mu = 1$. Therefore, the boundary of the maximum departure region includes a line segment with a slope of $-45°$. We remark that if $h_{1i} \neq h_{2i}$ for all i, the boundary of the maximum departure region does not include a

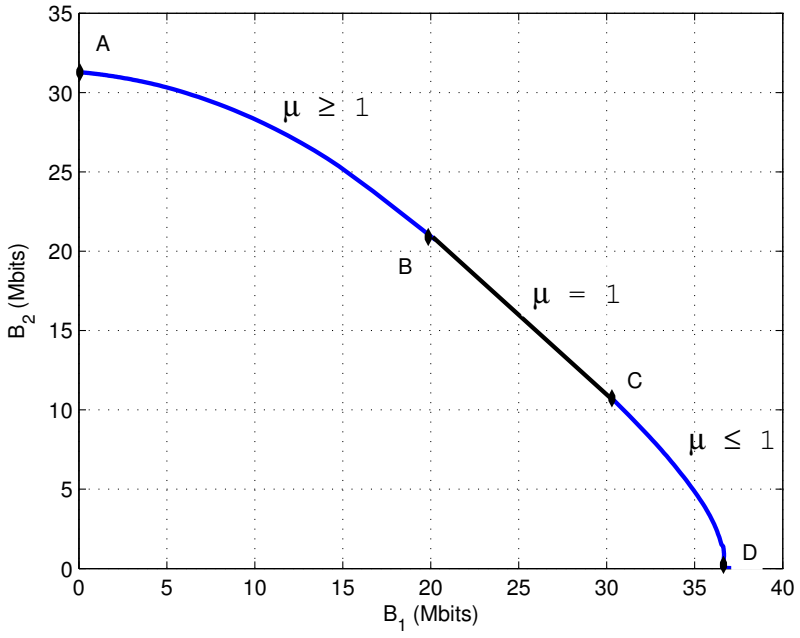

Figure 8.8: The maximum departure region for the given energy arrival and channel fade sequence and $T = 14$ s.

line segment, i.e., it is strictly convex. In an ergodic setting with continuous fading distributions, under some mild conditions, the probability that $c_1 h_{1i} = c_2 h_{2i}$ for some i is zero and therefore the ergodic capacity region is strictly convex [48].

8.7 Conclusion

In this chapter, we considered communication over parallel and fading broadcast channels with an energy harvesting rechargeable transmitter that has a finite-capacity battery. We characterized the region of bit departures by a deadline T in an offline setting where changes in the energy and fading levels are known a priori at the transmitter. For parallel broadcast channels, we showed that the optimal total power allocation sequence is the same as that for the non-fading broadcast channel,

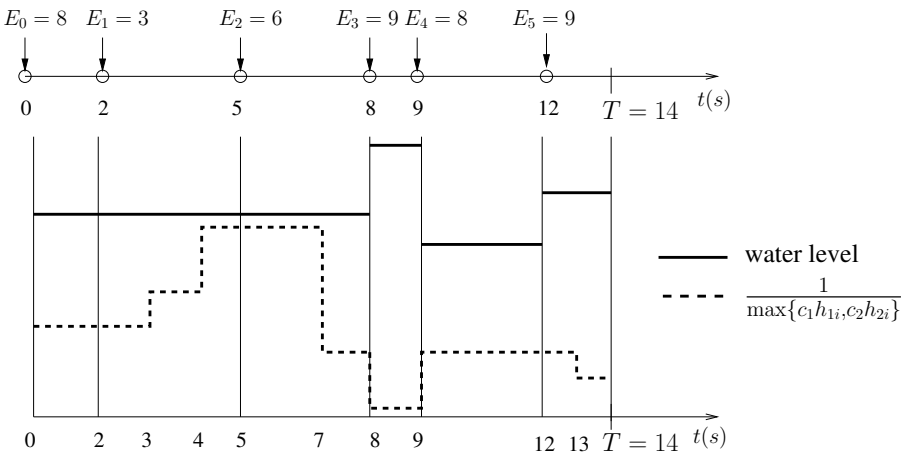

Figure 8.9: At points B and C in Figure 8.8, data is transmitted only for the user with the best channel and the total power sequence is found by single user directional water-filling when the bottom level is selected as $\frac{1}{\max\{h_{1i}, h_{2i}\}}$.

which does not depend on the priorities of the users and equals the single user optimal power allocation policy. The total power is split for the parallel channels in each interval separately. For fading broadcast channels, in contrast with non-fading broadcast channels, we showed that the optimal power allocation policy strongly depends on the priorities of the users and it is found by a specific directional water-filling algorithm. Finally, we provided illustrations for the maximum departure region for both parallel and fading broadcast channels.

8.8 Appendix

8.8.1 Proof of Lemma 8.2

Continuity of $g(p)$ follows from the continuity of g_1 and g_2. In order to prove that $g(p)$ is strictly concave, we need to show the following

$$g(\lambda p_1 + (1-\lambda)p_2) > \lambda g(p_1) + (1-\lambda)g(p_2) \tag{8.55}$$

for all $0 < \lambda < 1$.

We define the following functions for each parallel channel:

$$g_1(p) \triangleq \max_{0\le\alpha\le 1} \frac{\mu_1}{2}\log_2\left(1+\frac{\alpha p}{\sigma_{11}^2}\right) + \frac{\mu_2}{2}\log_2\left(1+\frac{(1-\alpha)p}{\alpha p+\sigma_{21}^2}\right) \tag{8.56}$$

$$g_2(p) \triangleq \max_{0\le\alpha\le 1} \frac{\mu_1}{2}\log_2\left(1+\frac{\alpha p}{(1-\alpha)p+\sigma_{12}^2}\right) + \frac{\mu_2}{2}\log_2\left(1+\frac{(1-\alpha)p}{\sigma_{22}^2}\right) \tag{8.57}$$

We first note that both $g_1(p)$ and $g_2(p)$ are continuous, strictly concave functions of p due to Lemma 2 in [44].

$g(p)$ in Lemma 8.2 can be expressed in terms of $g_1(p)$ and $g_2(p)$ as follows:

$$g(p) = \max_{0\le\beta\le 1} g_1(\beta p) + g_2((1-\beta)p) \tag{8.58}$$

Therefore, for any $0 \le \beta \le 1$, we have

$$g(p) \ge g_1(\beta p) + g_2((1-\beta)p) \tag{8.59}$$

We now prove the strict concavity. Let p_1 and p_2 be given. Let β_1 be the solution of (8.58) when $p = p_1$ and β_2 be the solution when $p = p_2$. Then,

$$g(p_1) = g_1(\beta_1 p_1) + g_2((1-\beta_1)p_1) \tag{8.60}$$

$$g(p_2) = g_1(\beta_2 p_2) + g_2((1-\beta_2)p_2) \tag{8.61}$$

For any $0 < \lambda < 1$, we have

$$\begin{aligned}
&g(\lambda p_1 + (1-\lambda)p_2) \\
&\geq g_1(\lambda\beta_1 p_1 + (1-\lambda)\beta_2 p_2) + g_2(\lambda(1-\beta_1)p_1 + (1-\lambda)(1-\beta_2)p_2) && (8.62)\\
&> \lambda g_1(\beta_1 p_1) + (1-\lambda) g_1(\beta_2 p_2) + \lambda g_2((1-\beta_1)p_1) + (1-\lambda) g_2((1-\beta_2)p_2) && (8.63)\\
&= \lambda g(p_1) + (1-\lambda) g(p_2) && (8.64)
\end{aligned}$$

The inequality in (8.62) is by evaluating (8.59) for $p = \lambda p_1 + (1-\lambda)p_2$ and $\beta = \frac{\lambda\beta_1 p_1 + (1-\lambda)\beta_2 p_2}{\lambda p_1 + (1-\lambda)p_2}$. (8.63) is due to the concavity of $g_1(p)$ and $g_2(p)$ and (8.64) is a rearrangement of (8.63). This proves the strict concavity of $g(p)$.

Chapter 9

Conclusions

In this dissertation, we used information theoretic and scheduling theoretic approaches to obtain fundamental limits of communication with energy harvesting devices.

In Chapter 2, we established the capacity of the AWGN channel under stochastic energy harvesting where an unlimited sized battery buffers energy between an uncontrolled recharge process and the transmitter. This nature of the energy arrivals yields an unprecedented power constraint on each code symbol. We showed that communication can be performed at the capacity of the average power constrained AWGN channel. We first presented a save-and-transmit scheme in which data transmission occurs in two phases. In the first phase energy is collected and in the second phase data is transmitted. Next, we provided an alternative best-effort-transmit scheme that achieves the capacity without utilizing an initial saving phase. Finally, we extended our model to time varying recharge rates in large time scales. We obtained optimal offline power management for maximum average throughput.

In Chapter 3, we considered the capacity of the AWGN channel with an energy harvesting transmitter of zero energy storage. The energy arrivals impose amplitude constraints on the code symbol at each channel use. In this model, energy arrival is a state attached to the channel and therefore, channel capacity is achieved by

Shannon strategies. We determined numerically verifiable necessary and sufficient optimality conditions for the input distribution and our numerical results showed that optimal input distributions have finite support. Next, we extended our analysis to an additive Gaussian multiple access channel where multiple users with energy harvesting transmitters of zero energy storage communicate with a single receiver. We investigated the achievable rate region under static and stochastic amplitude constraints on the users' channel inputs. In the static amplitude constrained MAC, we proved that capacity achieving input distributions have finite support. In the stochastic amplitude constrained MAC, we numerically studied necessary optimality conditions for the optimal Shannon strategies. Finally, we considered state amplification in a single user AWGN channel with energy harvesting transmitters. We characterized the trade-off region between entropy reduction Δ of the energy arrivals and the message transmission rate R in a communication system with an energy harvesting transmitter with zero or unlimited energy storage. In the zero energy storage case, Shannon strategies achieve the boundary of the region and we obtained necessary and sufficient optimality conditions for the optimal input distribution. In the unlimited battery case, we showed that the optimal trade-off region is expressed explicitly in a simple form and its boundary is achieved by a combination of best-effort-transmit and block Markov encoding schemes.

In Chapter 4, we considered the case of finite battery in energy harvesting channel. As a first step, we provided an overview of approaches for the finite battery case. Next, we proposed a timing based achievable scheme in a noiseless channel with $E_{max} > 1$. Then, we focused on the case of side information at the receiver. We

determined the capacity of an energy harvesting channel with an energy harvesting transmitter and battery state information available at the receiver side. This is an instance of a finite-state channel and the channel output feedback does not increase the capacity. We stated the capacity as maximum directed mutual information from the input to the output and the battery state. We identified sufficient conditions for the channel to have stationary input distributions as optimal distributions. We also derived a single-letter capacity expression for this channel with battery state information at both sides and infinite-sized battery at the transmitter. Then, we determined the capacity of an energy harvesting channel with energy arrival side information at the receiver side. We first found an n-letter capacity expression and showed that the optimal coding is based on only current battery state s_i. Next, we showed that the capacity is expressed as maximum directed information between the input and the output and proved that the channel output feedback does not increase the capacity.

In Chapter 5, we studied the Gaussian wiretap channel with energy harvesting transmitters. First, we considered static amplitude and average power constraints. We showed that the boundary of the entire rate-equivocation region is achieved by discrete input distributions that have finite support. An interesting aspect that our result reveals is that, unlike the average power constrained Gaussian wiretap channel, under an amplitude constraint, the secrecy capacity and the capacity cannot be obtained simultaneously in general, i.e., there is a trade-off between the rate and the equivocation for the amplitude constrained case. In the special case $A \leq 1.05$, we show that the secrecy capacity and the capacity are achieved simultaneously by

a symmetric binary distribution. Finally, we extended the discreteness result for the case when we have both amplitude and variance constraints. Next, we studied the Gaussian wiretap channel with an energy harvesting transmitter of zero energy storage. We first proved that single-letter Shannon strategies span the entire rate-equivocation region. Next, we obtained necessary and sufficient optimality conditions for optimal input distributions that achieve the boundary of the entire rate-equivocation region. We observed in our numerical results that the optimal input distributions have finite support and in general the secrecy capacity and the capacity cannot be obtained simultaneously, i.e., there is a trade-off between the rate and the equivocation.

In the remaining parts of the dissertation, we focused on optimal transmission scheduling for energy harvesting transmitters. In Chapter 6, we developed optimal transmission schemes for energy harvesting systems operating in fading channels, with finite capacity rechargeable batteries. We considered two related problems under offline knowledge of the events: maximizing the number of bits sent by a deadline, and minimizing the time it takes to send a given amount of data. We solved the first problem using a directional water-filling approach. We solved the second problem by mapping it to the first problem via the maximum departure curve function. Additionally, we solved for the throughput optimal policy for the deadline constrained setting under online knowledge of the events using dynamic programming.

In Chapter 7, we considered the transmission completion time minimization problem in an M-user broadcast channel where the transmitter harvests energy from

nature and saves it in a battery of finite capacity. We characterized the structural properties of the optimal policy by means of the dual problem of maximizing the weighted sum of bits served for each user by a fixed deadline. We found that the total power allocation is the same as the single user power allocation, which is found by the directional water-filling algorithm. Moreover, there exist $M-1$ cut-off power levels that determine the power shares of the users throughout the transmission. This structure enabled us to develop an optimal offline algorithm which uses directional water-filling iteratively.

In Chapter 8, we considered communication over parallel and fading broadcast channels with an energy harvesting rechargeable transmitter that has a finite-capacity battery. We characterized the maximum departure region by a deadline T in an offline setting. For parallel broadcast channels, we showed that the optimal total power allocation sequence is the same as that for the non-fading broadcast channel, which does not depend on the priorities of the users and equals the single user optimal power allocation policy. The total power is split for the parallel channels in each interval separately. For fading broadcast channels, in contrast with non-fading broadcast channels, we showed that the optimal power allocation policy strongly depends on the priorities of the users and it is found by a specific directional water-filling algorithm.

Bibliography

[1] J. A. Paradiso and T. Starner. Energy scavenging for mobile and wireless electronics. *IEEE Pervasive Computing*, pages 18–27, January 2005.

[2] V. Raghunathan, S. Ganeriwal, and M. Srivastava. Emerging techniques for long-lived wireless sensor networks. *IEEE Commun. Magazine*, 44(4):108–114, April 2006.

[3] S. Sudevalayam and P. Kulkarni. Energy harvesting sensor nodes: Survey and implications. *IEEE Communication Surveys & Tutorials*, 13(3):443–461, Third Quarter 2011.

[4] C. E. Shannon. A mathematical theory of communication. *Bell System Tech. Journal*, 27(3):379–423, July, October 1948.

[5] J. G. Smith. The information capacity of amplitude and variance-constrained scalar Gaussian channels. *Information and Control*, 18:203–219, April 1971.

[6] J. G. Smith. *On the information capacity of peak and average power constrained Gaussian channels*. PhD thesis, Univ. California, Berkeley, CA, USA, 1969.

[7] S. Shamai and I. Bar-David. The capacity of average and peak-power-limited quadrature Gaussian channels. *IEEE Trans. on Inform. Theory*, 41(4):1060–1071, July 1995.

[8] O. Ozel and S. Ulukus. Information theoretic analysis of an energy harvesting communication system. In *Workshop on Green Wireless (W-GREEN) at IEEE PIMRC*, September 2010.

[9] O. Ozel and S. Ulukus. Achieving AWGN capacity under stochastic energy harvesting. *IEEE Trans. on Inform. Theory*, 58(10):6471–6483, October 2012.

[10] J. Lei, R. Yates, and L. Greenstein. A generic model for optimizing single-hop transmission policy of replenishable sensors. *IEEE Trans. on Wireless Commun.*, 8(2):547–551, February 2009.

[11] M. Gatzianas, L. Georgiadis, and L. Tassiulas. Control of wireless networks with rechargeable batteries. *IEEE Trans. on Wireless Commun.*, 9(2):581–593, February 2010.

[12] V. Sharma, U. Mukherji, V. Joseph, and S. Gupta. Optimal energy management policies for energy harvesting sensor nodes. *IEEE Trans. on Wireless Commun.*, 9(4):1326–1336, April 2010.

[13] V. Sharma, U. Mukherji, and V. Joseph. Efficient energy management policies for networks with energy harvesting sensor nodes. In *Allerton Conference*, September 2008.

[14] J. Yang and S. Ulukus. Transmission completion time minimization in an energy harvesting system. In *CISS*, March 2010.

[15] J. Yang and S. Ulukus. Optimal packet scheduling in an energy harvesting

communication system. *IEEE Trans. on Commun.*, 60(1):220–230, January 2012.

[16] A. Fu, E. Modiano, and J. N. Tsitsiklis. Optimal energy allocation and admission control for communications sattelites. *IEEE/ACM Trans. on Networking*, 11(3):488–500, June 2003.

[17] A. Fu, E. Modiano, and J. N. Tsitsiklis. Optimal transmission scheduling over a fading channel with energy and deadline constraints. *IEEE Trans. on Wireless Commun.*, 5(3):630–641, March 2006.

[18] C. E. Shannon. Channels with side information at the transmitter. *IBM Jour. of Research and Development*, 2(4), October 1958.

[19] A. Sutivong, M. Chiang, T. M. Cover, and Y.-H. Kim. Channel capacity and state estimation for state-dependent Gaussian channels. *IEEE Trans. on Inform. Theory*, 51(4):1486–1495, April 2005.

[20] Y.-H. Kim, A. Sutivong, and T. M. Cover. State amplification. *IEEE Trans. on Inform. Theory*, 54(5):1850–1859, April 2008.

[21] A. Wyner. The wire-tap channel. *Bell Sys. Tech. Journal*, 54(8):1355–1387, October 1975.

[22] S. K. Leung-Yan-Cheung and M. Hellman. The Gaussian wire-tap channel. *IEEE Trans. on Inform. Theory*, 24(4):451–456, July 1978.

[23] K. Tutuncuoglu and A. Yener. Optimum transmission policies for battery limited energy harvesting nodes. *IEEE Trans. on Wireless Commun.*, 11(3):1180–1189, March 2012.

[24] J. Yang, O. Ozel, and S. Ulukus. Broadcasting with an energy harvesting rechargeable transmitter. *IEEE Trans. on Wireless Commun.*, 11(2):571–583, February 2012.

[25] O. Ozel and S. Ulukus. AWGN channel under time-varying amplitude constraints with causal information at the transmitter. In *Asilomar Conference*, November 2011.

[26] T. H. Chan, S. Hranilovic, and F. Kschischang. Capacity-achieving probability measure for conditionally Gaussian channels with bounded inputs. *IEEE Trans. on Inform. Theory*, 51:2073–2088, June 2005.

[27] O. Ozel and S. Ulukus. On the capacity region of the Gaussian MAC with batteryless energy harvesting transmitters. In *IEEE Globecom*, December 2012.

[28] O. Ozel and S. Ulukus. Energy state amplification in energy harvesting communication systems. In *IEEE ISIT*, July 2012.

[29] W. Mao and B. Hassibi. On the capacity of a communication system with energy harvesting and a limited battery. In *IEEE ISIT*, July 2013.

[30] K. Tutuncuoglu, O. Ozel, A. Yener, and S. Ulukus. Binary energy harvesting channel with finite energy storage. In *IEEE ISIT*, July 2013.

[31] K. Tutuncuoglu, O. Ozel, A. Yener, and S. Ulukus. Improved capacity bounds for the binary energy harvesting channel. In *IEEE ISIT*, June 2014.

[32] K. Tutuncuoglu, O. Ozel, A. Yener, and S. Ulukus. The binary energy harvesting channel with a unit sized battery. *IEEE Trans. on Inform. Theory.* Submitted, August 2014. Available at arXiv:1408.6504.

[33] D. M. Arnold, H.-A. Loeliger, P. O. Vontobel, A. Kavcic, and W. Zeng. Simulation-based computation of information rates for channels with memory. *IEEE Trans. on Inform. Theory*, 52(8):3498–3508, August 2006.

[34] O. Ozel, K. Tutuncuoglu, S. Ulukus, and A. Yener. Capacity of the discrete memoryless energy harvesting channel with side information. In *IEEE ISIT*, June 2014.

[35] O. Ozel, K. Tutuncuoglu, S. Ulukus, and A. Yener. Capacity of the energy harvesting channel with energy arrival information at the receiver. In *IEEE ITW*, November 2014.

[36] O. Ozel, E. Ekrem, and S. Ulukus. Gaussian wiretap channel with an amplitude constraint. In *IEEE ITW*, September 2012.

[37] O. Ozel, E. Ekrem, and S. Ulukus. Gaussian wiretap channel with amplitude and variance consraints. *IEEE Trans. on Inform. Theory.* Submitted, December 2013.

[38] O. Ozel, E. Ekrem, and S. Ulukus. Gaussian wiretap channel with a batteryless energy harvesting transmitter. In *IEEE ITW*, September 2012.

[39] O. Ozel, K. Tutuncuoglu, J. Yang, S. Ulukus, and A. Yener. Transmission with energy harvesting nodes in fading wireless channels: Optimal policies. *IEEE Jour. on Selected Areas in Commun.*, 29(8):1732–1743, September 2011.

[40] O. Ozel, K. Tutuncuoglu, S. Ulukus, and A. Yener. Resource management for fading wireless channels with energy harvesting nodes. In *IEEE INFOCOM*, April 2011.

[41] O. Ozel, K. Tutuncuoglu, S. Ulukus, and A. Yener. Adaptive transmission policies for energy harvesting wireless nodes in fading channels. In *CISS*, March 2011.

[42] M. Zafer and E. Modiano. Continuous time optimal rate control for delay constrained data transmission. In *Allerton Conference*, September 2005.

[43] D. P. Bertsekas. *Dynamic Programming and Optimal Control*. Athena Scientific, 2007.

[44] O. Ozel, J. Yang, and S. Ulukus. Optimal broadcast scheduling for an energy harvesting rechargeable transmitter with a finite capacity battery. *IEEE Trans. on Wireless Commun.*, 11(6):2193–2203, June 2012.

[45] O. Ozel, J. Yang, and S. Ulukus. Optimal transmission schemes for parallel and fading Gaussian broadcast channels with an energy harvesting rechargeable transmitter. *Elsevier Computer Communications*, 36(12):1360–1371, July 2013.

[46] O. Ozel, J. Yang, and S. Ulukus. Optimal transmission policies over vector Gaussian broadcast channels with energy harvesting transmitters. In *Asilomar Conference*, November 2011.

[47] O. Ozel, J. Yang, and S. Ulukus. Optimal scheduling over fading broadcast channels with an energy harvesting transmitter. In *IEEE CAMSAP*, December 2011.

[48] L. Li and A. Goldsmith. Capacity and optimal resource allocation for fading broadcast channels-part I. *IEEE Trans. on Inform. Theory*, 47(3):1083–1102, March 2001.

[49] D. N. C. Tse. Optimal power allocation for parallel Gaussian broadcast channels. *Technical Report*, 1997. Available at www.eecs.berkeley.edu/∼dtse/broadcast2.pdf.

[50] R. Rajesh, V. Sharma, and P. Viswanath. Capacity of Gaussian channels with energy harvesting and processing cost. *IEEE Trans. on Inform. Theory*, 60(5):2563–2575, May 2014.

[51] S. Verdu and T. S. Han. A general formula for channel capacity. *IEEE Trans. on Inform. Theory*, 40(4):1147–1157, July 1994.

[52] G. Grimmet and D. Stirzaker. *Probability and Random Processes*. Oxford University Press, 2001.

[53] G. H. Cai. Strong laws for weigthed sums of i.i.d random variables. *Electronic*

Research Announcements of the American Mathematical Society, 12:29–36, March 2008.

[54] T. M. Cover and J. Thomas. *Elements of Information Theory*. John Wiley and Sons Inc., 2006.

[55] G. Caire and S. Shamai. On the capacity of some channels with channel state information. *IEEE Trans. on Inform. Theory*, 45(6):2007–2019, September 1999.

[56] E. Jorswieck and H. Boche. *Majorization and Matrix Monotone Functions in Wireless Communication*. Now Publishers Inc., 2007.

[57] M. Zafer and E. Modiano. A calculus approach to energy-efficient data transmission with quality-of-service constraints. *IEEE/ACM Trans. on Networking*, 17(3):898–911, June 2009.

[58] I. Abu-Faycal, M. Trott, and S. Shamai. The capacity of discrete-time memoryless Rayleigh fading channels. *IEEE Trans. on Inform. Theory*, 47(4):1290–1301, May 2001.

[59] M. C. Gursoy, H. V. Poor, and S. Verdu. The noncoherent Ricean fading channel part-I: Structure of the capacity achieving input. *IEEE Trans. on Wireless Commun.*, 4(5):2193–2206, September 2005.

[60] J. Huang and S. Meyn. Characterization and computation of optimal distributions for channel coding. *IEEE Trans. on Inform. Theory*, 51(7):2336–2351, July 2005.

[61] J. Singh, O. Dabeer, and U. Madhow. Transceiver design with low-precision analog-to-digital conversion: An information-theoretic perspective. *IEEE Trans. on Commun.*, 57(12):3629–3639, December 2009.

[62] L. Zhang and D. Guo. Capacity of Gaussian channels with duty cycle and power constraints. In *IEEE ISIT*, July 2011.

[63] A. Tchamkerten. On the discreteness of capacity achieving distributions. *IEEE Trans. on Inform. Theory*, 50(11):2273–2278, November 2004.

[64] N. Sharma and S. Shamai. Transition points in the capacity-achieving distribution for the peak-power limited AWGN and free-space optical intensity channels. *Prob. of Inform. Trans.*, 46(4):283–299, 2010.

[65] A. Goldsmith and P. Varaiya. Capacity of fading channels with channel side information. *IEEE Trans. on Inform. Theory*, 43(6):1986–1992, November 1997.

[66] S. Verdu. Capacity region of Gaussian CDMA channels: The symbol-synchronous case. In *Allerton Conference*, October 1986.

[67] B. Mamandipoor, K. Moshksar, and A. K. Khandani. On the sum-capacity of Gaussian MAC with peak constraint. In *IEEE ISIT*, July 2012.

[68] G. Keshet, Y. Steinberg, and N. Merhav. *Channel Coding in the Presence of Side Information*. Now Publishers Inc., 2007.

[69] S. A. Jafar. Capacity with causal and non-causal side information- a unified view. *IEEE Trans. on Inform. Theory*, 52(12):5468–5474, December 2006.

[70] S. Sigurjonsson and Y.-H. Kim. On multiple user channels with state information at the transmitters. In *IEEE ISIT*, September 2005.

[71] A. Lapidoth and Y. Steinberg. The multiple access channel with two independent states each known causally to one encoder. In *IEEE ISIT*, June 2010.

[72] M. Li, O. Simeone, and A. Yener. Multiple access channels with states causally known at the transmitters. *IEEE Trans. on Inform. Theory*, 59(3):1394–1404, March 2013.

[73] W. Zhang, S. Vedantam, and U. Mitra. A constrained channel coding approach to joint communication and channel estimation. In *IEEE ISIT*, July 2008.

[74] C. Choudhuri, Y.-H. Kim, and U. Mitra. Capacity-distortion trade-off in channels with state. In *Allerton Conference*, September 2010.

[75] C. Choudhuri, Y.-H. Kim, and U. Mitra. Causal state amplification. In *IEEE ISIT*, July 2011.

[76] N. Merhav and S. Shamai. Information rates subjected to state masking. *IEEE Trans. on Inform. Theory*, 54(6):2254–2261, June 2007.

[77] K. Tutuncuoglu, O. Ozel, S. Ulukus, and A. Yener. State amplification and state masking for the binary energy harvesting channel. In *IEEE ITW*, November 2014.

[78] H. Permuter, T. Weissman, and A. Goldsmith. Finite state channels with time-invariant deterministic feedback. *IEEE Trans. on Inform. Theory*, 55(2):644–662, February 2009.

[79] J. Chen and T. Berger. The capacity of finite-state Markov channels with feedback. *IEEE Trans. on Inform. Theory*, 51(3):780–798, March 2005.

[80] Y. Dong and A. Ozgur. Approximate capacity of energy harvesting communication with finite battery. In *IEEE ISIT*, June 2014.

[81] V. Jog and V. Anantharam. An energy harvesting AWGN channel with a finite battery. In *IEEE ISIT*, June 2014.

[82] I. Naiss and H. Permuter. Extension of the Blahut-Arimoto algorithm for maximizing directed information. *IEEE Trans. on Inform. Theory*, 59(1):204–223, January 2013.

[83] S. Tatikonda and S. Mitter. Capacity of channels with feedback. *IEEE Trans. on Inform. Theory*, 55(1):323–349, January 2009.

[84] P. K. Deekshith, V. Sharma, and R. Rajesh. AWGN channel capacity of energy harvesting transmitters with a finite energy buffer. Available at arXiv:1307.4505.

[85] J. Massey. Causality, feedback and directed mutual information. In *IEEE ISITA*, November 1990.

[86] S. Tatikonda. *Control under Communication Constraints*. PhD thesis, MIT, Cambridge, MA, USA, 2000.

[87] I. Csiszár and J. Körner. Broadcast channels with confidential messages. *IEEE Trans. on Inform. Theory*, 24(3):339–348, May 1978.

[88] M. Raginsky. On the information capacity of Gaussian channels under small peak power constraints. In *Allerton Conference*, September 2008.

[89] C. Mitrpant, A. J. Han Vick, and Y. Luo. An achievable region for the wiretap channel with side information. *IEEE Trans. on Inform.Theory*, 52(5):2181–2190, May 2006.

[90] W. Liu and B. Chen. Wiretap channel with two-sided state information. In *Asilomar Conference*, November 2007.

[91] Y. Chen and A. J. Han Vick. Wiretap channel with side information. *IEEE Trans. on Inform. Theory*, 54(1):395–402, January 2008.

[92] Y.-K. Chia and A. El Gamal. Wiretap channel with causal state information. In *IEEE ISIT*, June 2010.

[93] M. van Dijk. On a special class of broadcast channels with confidential messages. *IEEE Trans. on Inform. Theory*, 43(2):712–714, March 1997.

[94] D. Guo, S. Verdu, and S. Shamai. Mutual information and minimum mean-square error in Gaussian channels. *IEEE Trans. on Inform. Theory*, 51(4):1261–1282, April 2005.

[95] D. Guo, Y. Wu, S. Verdu, and S. Shamai. Estimation in Gaussian noise: Properties of minimum mean-square error. *IEEE Trans. on Inform. Theory*, 57(4):2371–2385, April 2011.

[96] G. Casella and W. E. Strawderman. Estimating a bounded normal mean. *Annals of Statistics*, 9(4):870–878, 1981.

[97] A. El Gamal and Y.-H. Kim. *Network information theory*. Cambridge University Press, 2011.

[98] C. K. Ho and R. Zhang. Optimal energy allocation for wireless communications with energy harvesting constraints. *IEEE Trans. on Signal Proc.*, 60(9):4808–4818, September 2012.

[99] E. Uysal-Biyikoglu and A. El Gamal. On adaptive transmission for energy efficiency in wireless data networks. *IEEE Trans. on Inform. Theory*, 50(12):3081–3094, December 2004.

[100] D. P. Bertsekas. *Convex Analysis and Optimization*. Athena Scientific, 2003.

[101] O. Ozel, J. Yang, and S. Ulukus. Broadcasting with a battery limited energy harvesting rechargeable transmitter. In *IEEE WiOpt*, May 2011.

[102] S. Boyd and L. Vandenberghe. *Convex Optimization*. Cambridge University Press, United Kingdom, 2004.

[103] R. L. Burden and J. D. Faires. *Numerical Analysis*. Thomson Brooks/Cole, 2005.